

Life Science Journal

Life Science Journal

Marsland Press

PO Box 180432, Richmond Hill, New York 11418, USA

Website:
<http://www.sciencepub.net>

Emails:
editor@sciencepub.net
sciencepub@gmail.com

Phone: (347) 321-7172

Life Science Journal 2012 Volume 9, Number 1, Part 2 ISSN:1097-8135



Volume 9, Number 1, Part 2 March 25, 2012 ISSN:1097-8135

Life Science Journal



MARSLAND PRESS
Multidisciplinary Academic Journal Publisher

Websites:
<http://www.lifesciencesite.com>
<http://www.sciencepub.net>

Emails:
lifesciencej@gmail.com
editor@sciencepub.net

Life Science Journal

Acta Zhengzhou University Oversea Version
(Life Sci J)

Life Science Journal, the Acta Zhengzhou University Oversea Version, is an international journal with the purpose to enhance our natural and scientific knowledge dissemination in the world under the free publication principle. The journal is calling for papers from all who are associated with Zhengzhou University-home and abroad. Any valuable papers or reports that are related to life science - in their broadest sense - are welcome. Other academic articles that are less relevant but are of high quality will also be considered and published. Papers submitted could be reviews, objective descriptions, research reports, opinions/debates, news, letters, and other types of writings. Let's work together to disseminate our research results and our opinions.

Editor-in-Chief: Shen, Changyu, Ph.D., Professor, Chinese Academy of Sciences

Associate Editors-in-Chief: Ma, Hongbao; Cherng, Shen; Xin, Shijun

Editorial Boards: Aghdam, Hashemi; An, Xiuli; Chandra, Avinash; Chen, George; Dong, Ziming; Duan, Guangcai; Edmondson, Jingjing; Gao, Danying; Huang, Shuan-Yu; Li, Xinhua; Li, Yuhua; Lindley, Mark; Liu, Hua; Liu, Hongmin; Ma, Margret; Qi, Yuanming; Sabyasachi Chatterjee; Shang, Fude; Shi, Lifeng; Song, Chunpeng; Sun, Yingpu; Wang, Lidong; Wen, Jianguo; Xu, Cunshuan; Xu, Yuming; Xue, Changgui; Zaki, Mona; Zhang, Jianying; Zhang, Kehao; Zhang, Shengjun; Zhang, Xueguo; Zhang, Zhan; Zhang, Zhao; Zhu, Huaijie

Introductions to Authors

1. General Information

- (1) Goals:** As an international journal published both in print and on internet, **Life Science Journal** is dedicated to the dissemination of fundamental knowledge in all areas of nature and science. The main purpose of **Life Science Journal** is to enhance our knowledge spreading in the world under the free publication principle. It publishes full-length papers (original contributions), reviews, rapid communications, and any debates and opinions in all the fields of nature and science.
- (2) What to Do:** The **Life Science Journal** provides a place for discussion of scientific news, research, theory, philosophy, profession and technology - that will drive scientific progress. Research reports and regular manuscripts that contain new and significant information of general interest are welcome.
- (3) Who:** All people are welcome to submit manuscripts in life science fields. Papers of other fields are also considered.
- (4) Copyright and Responsibility of Authors to their Articles:** When the manuscript(s) is submitted to the journal, the authors agree the following: All the authors have participated sufficiently in this work; The article is not published elsewhere; Authors are responsibility on the contents of the article; The journal and author(s) have same right for the copyright of the article and either of the journal or author(s) can use it by anyway without noting the other party.
- (5) Publication Costs:** US\$500 per article to defray costs of the publication will be paid by the authors when it is received. Extra expense for color reproduction of figures will be paid by authors (estimate of cost will be provided by the publisher for the author's approval).
- (6) Advertisements:** The price will be calculated as US\$400/page, i.e. US\$200/a half page, US\$100/a quarter page, etc. Any size of the advertisement is welcome.

2. Manuscript Preparation

Each manuscript is suggested to include the following components but authors can do their own ways:

- (1) Title:** including the complete article title; each author's full name; institution(s) with which each author is affiliated,

with city, state/province, zip code, and country; and the name, complete mailing address, telephone number, facsimile number (if available), and at least one email address for author(s). **(2) Abstract:** including Background, Materials and Methods, Results, and Discussions. **(3) Key Words.** **(4) Introduction.** **(5) Materials and Methods.** **(6) Results.** **(7) Discussions.** **(8) Acknowledgments.** **(9) References.**

3. Manuscripts Submission

- (1) Submission Methods:** Submission through email (editor@sciencepub.net) is encouraged.
- (2) Software:** The Microsoft Word file will be preferred.
- (3) Font:** Normal, Times New Roman, 10 pt, single space.
- (4) Indent:** Type 2 space in the beginning of each new paragraph.
- (5) Manuscript:** Don't use "Footnote" or "Header and Footer".
- (6) Email:** At least one author's email must be put under title.
- (7) Title:** Use Title Case in the title and subtitles, e.g. "**Debt and Agency Costs**".
- (8) Figures and Tables:** Use full word of figure and table, e.g. "**Figure 1. Annual Income of Different Groups**", **Table 1. Annual Increase of Investment**".
- (9) References:** Cite references by "last name, year", e.g. "(Smith, 2003)". References should include all the authors' last names and initials, title, journal, year, volume, issue, and pages etc.

Reference Examples:

Journal Article: Hacker J, Hentschel U, Dobrindt U. Prokaryotic chromosomes and disease. *Science* 2003;301(34):790-3. **Book:** Berkowitz BA, Katzung BG. Basic and clinical evaluation of new drugs. In: Katzung BG, ed. Basic and clinical pharmacology. Appleton & Lance Publisher. Norwalk, Connecticut, USA. 1995:60-9.

- (10) Submission Address:** editor@sciencepub.net, Marsland Press, PO Box 180432, Richmond Hill, New York 11418, USA, 347-321-7172.

Marsland Press / Zhengzhou University
PO Box 180432, Richmond Hill, New York 11418, USA
<http://www.lifesciencesite.com>; <http://www.sciencepub.net>
lifesciencej@gmail.com; editor@sciencepub.net
© 2005-2012 Marsland Press / Zhengzhou University

CONTENTS

23	Genetic Variation among Nine Egyptian Gecko Species (Reptilia: Gekkonidae) Based on RAPD-PCR Ramadan A. M. Ali	154-162
24	Role of Diffusion Tensor Imaging in Characterization and Preoperative Planning of Brain Neoplasms Mohsen Gomaa and Yosra abdel zaher	163-176
25	Detection of Genotoxicity of Phenolic Antioxidants, Butylated hydroxyanisole and tert-butylhydroquinone in Multiple Mouse Organs by the Alkaline Comet Assay Ramadan, A.M. Ali, Takayoshi Suzuki	177-183
26	Natural Cases of Rickets in Baraki Goat Kids Mona.S. Zaki, Awadalla. I.M, Mohamed. M.I, Iman. M. Zytaun, Sami Shalaby, Nagwa Atta, and Suzan.O. Mostafa.	184-188
27	Clinical and laboratory approach for the identification of the risk for tumour lysis syndrome in children with acute lymphoblastic leukemia. Hesham A. Abdel-Baset, Eman Nasr Eldin, Azza A. Eltayeb, Almontaser M. Hussein.	189-195
28	Application of chitosan for wound repair in dogs. Inas, N.El-Husseiny and Kawkab, A. Ahmed	196-203
29	Detection of Circulating Microparticles in Patients with Proliferative Diabetic Retinopathy Samy A Khodeir, Y M Abd El Raouf, Gihan Farouk and Mohammed EL-Bradey	204-209
30	Effect of the Strengthened Ribs in Hybrid Toughened Kenaf/ Glass Epoxy Composite Bumper Beam M.M. Davoodi, S.M. Sapuan, Aidy Ali, D. Ahmad	210-213
31	Impact of Orlistat on Body Weight and Lipid Profile of Adult Population Randa M Shams, Medhat A Saleh, Mohamed E Abdelrahim, Asmaa S M Mohamed	214-219
32	Synthesis of Some Aryl Thienopyridine, Pyridothienopyrimidine, and Pyridothienotriazolopyrimidine Derivatives Ali Khader El-Louh, Shadia Mahmoud Abdallah and Emtithal Ahmed El-Sawi	220-230
33	Designing A Model For Quality of Employee-Organization Relationships (EORs) Based On Analysis Hierarchical Process (AHP) PH.D. Professor Ali Akbar Farhangi , Sara moazen , Maryam Aliei	231-241
34	Upper Cretaceous Planktonic Foraminiferal Biostratigraphy of East Dorfak Area (Guilan – North of Iran) Mohammad Modaresnia, Khosro Khosrotehrani, Iraj Momeni, Seyed Ahmad Babazadeh	242-253
35	Multifunctionality of the Iranian Agriculture Sector in a Partial Equilibrium Framework Zahra Kiani-Feyzabad, Seyed-Ali Hosseini-Yekani, Seyed-Mojtaba Mojaverian	254-264

36	Association between CC16 Polymorphism and Bronchial Asthma Nisreen M.El Abiad, Hisham Waheed, William M. Morcos,SamarM. Salem, and Hala Ataa, Olfat G. Shaker	265-270
37	Laparoscopic / Thoracoscopic Ivor Lewis Esophageal Resection for Cancer (Report of Two Cases and Review of the Literature) Saleh M. Aldaqal	271-276
38	Determinants of Patient Satisfaction in the Surgical ward at a University Hospital in Saudi Arabia Saleh M. Aldaqal; Hattan Alghamdi; Hassan AlTurki; Basem S. El-deekandAhmed A. Kensarah	277-280
39	Transformational Leadership Role of Principals in Implementing Informational and Communication Technologies in Schools Mojgan Afshari, Simin Ghavifekr , Saedah Siraj andRahmad Sukor Ab. Samad	281-284
40	Effect of the Strengthened Ribs in Hybrid Toughened Kenaf/ Glass Epoxy Composite Bumper Beam M.M. Davoodi, S.M. Sapuan, Aidy Ali, D. Ahmad	285-289
41	Investigation of the Structural and Optical Properties of Bismuth Telluride (Bi₂Te₃) Thin Films F. S. Bahabri	290-294
42	Molecular characterization of <i>Cotugnia polycantha</i> (Cestoda, Cyclophyllidea, Davaineidae) infecting doves (<i>Streptopelia senegalensis</i>) and pigeons (<i>Columba livia Domestica</i>) from Egypt Sabry E. Ahmed	295-301
43	Risk Factors for the Development of Ventilator – Associated Pneumonia in Critically-Ill Neonates Mona Afify, Salha AI-Zahrani and Maha A Nouh	302-307

Genetic Variation among Nine Egyptian Gecko Species (Reptilia: Gekkonidae) Based on RAPD-PCR

Ramadan A. M. Ali

Zoology Dept., College for Girls for Science, Arts and Education, Ain-Shams Univ., Heliopolis, Cairo, Egypt
ramadanali27@gmail.com

Abstract: The RAPD-PCR in the present study was used to determine the genetic variation among nine Egyptian gekkonid species; *Tropicolotes tripolitanus*, *Tropicolotes nattererii*, *Hemidactylus turcicus*, *Cyrtopodion scaber*, *Stenodactylus petrii*, *Ptyodactylus guttatus*, *Ptyodactylus hasselquistii*, *Tarentola mauritanica* and *Tarentola annularis*. The animals were captured from several localities from Egypt (Giza, Sinai and Matruh governorates). A total of 94 bands were amplified by the four primers OPAO4, OPBO3, OPB18 and OPCO1 with an average of 23.5 bands per primer at molecular weights ranged from 1267 to 112 bp. The polymorphic loci between species were 91 with percentage 96.8 %. The similarity coefficients value between the nine gekkonid species are ranged from 0.313(31.3%) to 0.576 (57.6%) with an average of 0.42 (42%). The genetic distance between the nine species was ranged from 0.424 (42.4%) to 0.687 (68.7%) with an average of 0.58 (58 %). The dendrogram showed that, the nine gekkonid species separated from each other into two clusters. The first cluster includes *Tropicolotes tripolitanus*; *Tropicolotes nattererii*; *Hemidactylus turcicus*; *Cyrtopodion scaber*; *Stenodactylus petrii*. The second cluster includes the rest of gekkonid species. The clade *Tarentola annularis* is sister taxon to *T. mauritanica* and the clade *Ptyodactylus guttatus* is sister taxon to *P. hasselquistii*. It is also noted that, the genus *Tropicolotes* is closer to the genus *Cyrtopodion* than the other genera and the genus *Tarentola* is closer to the genus *Ptyodactylus* than the other genera. It is concluded that, the less similarity coefficient and the high genetic distance value between the 9 gekkonid species indicates that, the nine gekkonid species are not identical and separated from each other. [Ramadan A. M. Ali **Genetic Variation among Nine Egyptian Gecko Species (Reptilia: Gekkonidae) Based On RAPD-PCR**. Life Science Journal 2012;9(1):154-162]. (ISSN: 1545-1003). <http://www.lifesciencesite.com>

Key Words: *Gekkonidae*, RAPD-PCR, Phylogenetic Relationship, Dendrogram**1. Introduction**

The order Squamata includes 4900 lizard species, 3070 snake species and 200 amphisbaenians species (Vidal and Hedges, 2009). Lizards are cosmopolitan and geographically distributed over a wide range of habitats and have a striking range of morphological characteristics, ecological habitats and body sizes. In Egypt, most of the gekkonid species are living in and around human habitation however, some species are free living in Egyptian deserts (Goodman and Hobbs, 1994).

Many studies carried out to classify and determine the phylogenetic relationships among members of the family Gekkonidae on the bases of morphological and environmental characteristics (Anderson, 1898; Marx, 1968; Baha El Din, 1994 and 1997; Goodman and Hobbs, 1994; Saleh, 1997), chromosomal karyotyping (Chen, *et al.*, 1986; Castiglia, 2004; Kawai *et al.*, 2009), biochemical investigations (Macey *et al.*, 2000; Qin *et al.*, 2006), molecular DNA variation (Carranza *et al.*, 2000, 2002 and 2006; Han *et al.*, 2004; Rato *et al.*, 2010; Fujita and Papenfus, 2011), RAPD-PCR (Qin *et al.*, 2005) and mitochondrial DNA sequences (Jesus *et al.*, 2001 and 2005; Vences *et al.*, 2004; Rocha *et al.*, 2005; Carranza and Arnold, 2006; Bansal and Karanth, 2010; Busais and Joger, 2011).

The genus *Hemidactylus* is one of the most

diverse and widely distributed genus of the family *Gekkonidae* in the world (Baha El Din, 2003 and 2005; Baldo *et al.*, 2008).

The genus *Tarentola* comprises 21 species (Baha El Din, 1997; Sprackland and Swinney, 1998; Carranza *et al.*, 2002; Diaz and Hedges, 2008), most of which show low interspecific morphological variations. The species have been distributed in Libya, Sinai, Ethiopia and Somali land, Countries and Islands bordering the Mediterranean (Marx, 1968; Baldo *et al.*, 2008). Molecular genetic of *Tarentola* have been demonstrated by several studies (Carranza, *et al.*, 2000 and 2002; Harris *et al.*, 2009; Rato, *et al.*, 2010).

The *Ptyodactylus* species distribute in and around human habitations, and therefore are known to be commensal with humans (Goodman and Hobbs, 1994). They are found from wet tropical forest to arid deserts and tropical Asia and Africa and Algerian Sahara, Egypt (Anderson, 1898; Marx, 1968; Goodman and Hobbs, 1994; Ibrahim, 2001).

The genus *Stenodactylus* contains 13 recognized species. The species *Stenodactylus stenodactylus* and *S. petrii* allocate from Egypt, Sudan to Mauritania (Marx, 1968; Goodman and hobbs, 1994; Baha El Din, 2006); Iran, Iraq, Syria, Jordan and Arabian Peninsula (Anderson, 1999).

The *Tropicolotes* species allocate in and around

human habitations and are distributed from wet tropical forest to arid deserts and tropical Asia and Africa, Egypt to Tunisia and Sudan (Anderson, 1898; Marx, 1968; Goodman and Hobbs, 1994).

The genus *Cyrtodactylus* (*Cyrtopodion*) is a topic of taxonomic controversy (Macey *et al.*, 2000). Masroor (2008 and 2009) and Nazarov and Rajabizadeh (2007) considered *Cyrtopodion* as a distinct genus with two subgenera *Cyrtopodion* and *Mediodactylus*, while Shi and Zhao (2011) considered that the *Cyrtopodion* and *Mediodactylus* are Subgenera of the genus *Cyrtodactylus*. Macey *et al.* (2000) used the allozymic data to determine the phylogenetic relationships among the Asian genus *Cyrtodactylus* and found that, the subgenera of *Cyrtopodion* and *Mediodactylus* are separate monophyletic groups of the genus *Cyrtodactylus*. The mitochondrial and nuclear DNA sequences have used to resolve the phylogeny of *Cyrtodactylus* gecko species (Kasapidis *et al.*, 2005; Carranza and Arnold 2006; Bansal and Karanth, 2010).

Hence, it is necessary to study the RAPD- PCR analysis of the members of this family that may help in understanding the phylogeny of this primitive lacertilian family. Therefore, the present study aimed to discuss the phylogenetic relationships among nine Egyptian gekkonid lizard species belong to six genera based on RAPD-PCR technique.

2. Material and Methods

Animal dealer collected samples of nine Egyptian Gekkonid species from different localities (Giza, Sinai and Matruh governorates, Egypt). The nine species are belonging to six genera. Morphological identification and classification of the animals as well as scientific and common names of these species identified according to previous works (Anderson, 1898; Marx, 1968; Baha El Din, 1994).

The studied species: -

1-*Tropicolotes tripolitanus*

Common names: Tripoli gecko, Tripoli pigmy gecko, Bors Taht El Hagar

2- *Tropicolotes nattereri*

Common names: Natterer's gecko, Bors Taht El Hagar

3- *Hemidactylus turcicus*

Common names: Turkish gecko, warty gecko, Mediterranean gecko

4- *Cyrtopodion scaber*

Common name: Rough-skinned gecko, Rough-scaled gecko, Keeled rock gecko

5- *Ptyodactylus guttatus*

Common names: Fan-footed gecko, Bors Abu Kaff Sinai

6-*Ptyodactylus hasselquistii*

Common names: Fan-footed gecko, Bors Abu Kaff

Cairo

7- *Stenodactylus petrii*

Common name: Petrie's gecko , Bors Abu Ain Wasa'h.

8- *Tarentola mauritanica*

Common name: Moorish gecko, Moorish wall gecko

9- *Tarentola annularis*

Common name: Egyptian gecko, white-spotted Gecko, Bors Abu Arba'a Noqat

Genomic DNA extraction

Samples of muscle tissue from the nine gekkonid species taken and stored at -20 °C. DNA extracted according to the method of Yue and Orban (2005) with slight modifications. DNA quality and concentration determined by spectrophotometric analysis and run in 0.7 % agarose gel. Each sample of DNA examined by optical density values at 260 and 280 nm and only good quality DNA samples used in RAPD-PCR reaction.

RAPD-PCR reaction

Eight primers from Kits OP-A, OP-B and OP-C (Operon Technologies, Alameda, CA, USA) used for RAPD-PCR analysis (OPA-04, OPA-10, OPB-03, OPB-05, OPB-18, OPC-01, OPC-06 and OPC-10). Only four primers (OPA-04, OPB-03, OPB-18 and OPC-01) were reacted well and used to amplify DNA from all species (table 1). RAPD-PCR reactions carried out as described by Williams *et al.* (1990). PCR cycles performed with 60 s, 94°C initial denaturation and 35 cycles of 20 s, 94°C; 20 s, 35°C; and 30 s, 72°C. Final extension performed at 72°C for 5 min. PCR amplifications were carried out in 96 well Thermal Cycler (Eppendorf Master Cycler) and all amplifications were carried out at two times. A PCR mixture without template DNA placed in each analysis as a control. The PCR products separated on 1.5 % agarose gels (Sigma) containing ethidium bromide in 0.5 X TBE buffer at 100 V constant voltages. For evaluating the base pair length of bands, DNA ladder (Fermentas) was loaded with each gel.

Data and statistical analysis:-

The RAPD banding patterns scored for the presence (1) and absence (0) of bands for each sample. The scores obtained using all primers in the RAPD analysis combined to create a single data matrix. The statistical analysis of the data performed using the free software, Popgene version 1.31, computer program (Yeh *et al.*, 1999) including the calculation of allele frequencies according to Nei (1987). This program estimated the number and percentage of polymorphic loci and the genetic diversity according to Nei (1973). For constructing

the dendrogram, the data resulted from RAPD markers banding patterns was introduced to NTSYS-pc package program by Unweighted Pair Group Method using Arithmetic Averages (UPGMA) method (Rohlf, 2000).

3. Results

Figures 1, 2, 3 and 4 showed the PCR bands produced by four random primers (OPA-04, OPB-03, OPB-18 and OPC-01) for the investigation of the genetic variation between the nine studied gekkonid species. The four primers yielded a sufficient and variable number of bands for comparison between the gekkonid species. The primer OPB-03 produces the highest number of bands (32 bands) in comparison to the other primers.

As shown in tables 2 and 3 the primers demonstrated 94 RAPD-PCR bands among the nine gekkonid species. The RAPD profile generated from these primers and the RAPD scoring bands have utilized to estimate the band frequency .

Primer OPA-04 generated 19 polymorphic bands with molecular weight ranged from 1267 to 227 bp. Band frequency ranged from 0.1 to 0.89 with mean value 0.491 (49.1%). The bands at 460bp, 407bp and 227bp were present only in *Tropicolotes tripolitanus*, *Stenodactylus petrii* and *Hemidactylus turcicus* respectively. Primer OPB-03 produced 32 bands. Band frequency ranged from 0.1 to 1.0 with mean value 0.597(59.7%). Unique bands at 1256 bp and 112 bp are specific for *Tropicolotes tripolitanus* *Ptyodactylus hasselquistii* respectively. The nine species have a common shared band at molecular weights 329 bp and 400 bp. Primer OPB-18 created 23 bands with a common band at molecular weight 452bp. The band frequency ranged from 0.1-1.0 with mean value 0.521(52.1%). Primer OPC-01 amplified 20 bands with band frequency ranged from 0.1- 0.9 with mean value 0.421(42.1%). Bands at 1048bp and at 955bp are unique bands in *Ptyodactylus hasselquistii* while the band at 304bp for *Ptyodactylus guttatus*.

Table 3 showed 94 scorable amplified bands with an average 23.5 bands/primer at molecular weights ranged from 1267 to 112bp between the 9 Gekkonid species and 91 of them were polymorphic (96.8%) with an average 22.75 bands/ primer. The polymorphic bands were 19 (100 %), 30 (93.75%), 22(95.65%) and 20 (100%) for primers OPA-04, OPB-03, OPB-18 and OPC-01, respectively. Table 4 showed the similarity coefficient value between the 9 gekkonid species, which ranged from 0.313 (31.1%) to 0.576 (57.6%) with an average of 0.42 (42%). The genetic distance between the 9 species was ranged from 0.424 (42.4%) to 0.687 (68.7%) with an average of 0.58 (58 %).

As shown in figure 5 the UPGMA dendrogram constructed to show phylogenetic relationships and pointed out that, the nine gekkonid species separated from each other into two clusters. The first cluster includes two clades. The clade *Tarentola annularis* is sister taxon to *T. mauritanica* and the clade *Ptyodactylus guttatus* is sister taxon to *P. hasselquistii*. The second cluster contains the rest of the gekkonid species; *Tropicolotes tripolitanus*, *T. nattereri*, *Hemidactylus turcicus*, *Cyrtopodion scaber* and *Stenodactylus petrii*. In this cluster, the gekkonid species *Tropicolotes tripolitanus* is sister taxon to *T. nattereri* and the remaining species are represent a further subclades from these taxa and separate from each other.

4. Discussion

In this study, the inter-specific genomic polymorphisms in nine gekkonid species, *Tropicolotes tripolitanus*; *Tropicolotes nattereri*; *Hemidactylus turcicus*; *Cyrtopodion scaber*; *Ptyodactylus guttatus*; *Ptyodactylus hasselquistii*; *Stenodactylus petrii*; *Tarentola mauritanica*; *Tarentola annularis* were analyzed by using RAPD-PCR technique. The molecular technique RAPD-PCR analysis is currently used to differentiate between the genomes of the closely related species in order to determine the genetic distance and genetic diversity (Williams *et al.*, 1990; Camargo *et al.*, 2010). The primer OPB-03 has a high G+C content (70 %) and produces the highest number of amplified fragments (32 bands) of genomic DNA in the studied gekkonid species (Dinesh *et al.*, 1995).

The results of this study showed high inter and intra- specific genetic variation among gecko species. This genetic variations among gecko species proved by protein polymorphism, mitochondrial DNA and nuclear DNA sequences (Jesus *et al.*, 2002; Harris *et al.*, 2004; Kasapidis *et al.*, 2005; Arnold *et al.*, 2008; Perera and Harris, 2010). Qin *et al.* (2005) found high genetic diversity in the same species, *Gekko gecko* from six different localities of china with genetic distance (0.011-0.963) and similarity coefficient (38.17% – 98.88%) in relation to animal groups.

The results showed that the number of amplified bands for the 9 gekkonid species were 94 bands, 91 (96.8%) of them were polymorphic (Table 3). The genetic similarity between the 9 gekkonid species are ranged from 0.313 (31.3%) to 0.576 (57.6%) with average 0.42 (42%) and the genetic distance are ranged from 0.424 (42.4%) to 0.687 (68.7%) with average 0.58 (58 %). The low genetic similarity and the high genetic distance between the nine gekkonid species indicate that the nine species are separated from each other. According to Baker *et al.* (2006),

these species are considered distinct and separate from each other if they have a genetic distance greater than 5%.

The UPGMA dendrogram (Fig. 5) and table 4 showed that, the species *Tarentola annularis* and *T. mauritanica* are sister to each other but they have high genetic distance (0.431) and low genetic similarity (0.569). Therefore, these two species separated from each other. This observation is similar to that presented by **Carranza et al. (2002)**. They found that, *T. annularis* (subgenus, *Sahelogecko*) and *T. mauritanica* (subgenus, *Tarentolas*) are separated from each other by using molecular study. In addition, they found that, the *Tarentola mauritanica* is paraphyletic with *T. angustimentalis* in the Canary Islands by using mitochondrial DNA and nuclear sequences. Although, *Tarentola mauritanica* species is characterized by a conservative morphology and shows intraspecific high genetic diversity (**Carranza et al., 2000; Jesus et al., 2002; Harris et al., 2004 and 2009; Rato et al., 2010**). Therefore, *Tarentola mauritanica* is clearly a species complex. Moreover, the North African (Tunisia, Libya and Egypt) *Tarentola mauritanica fascicularis* and *Tarentola mauritanica mauritanica* show high genetic distinct polymorphism (8%) by using gene sequences (**Harris et al., 2004 and 2009**). The species *T. mauritanica*, *T. deserti* and *T. angustimentalis* are paraphyletic groups of the genus *Tarentola* (**Harris et al., 2009**). **Gubitz, 2005** found that the *Tarentola boettgeri* was monophyletic to *T. delalandii* by using cytochrome b and nuclear sequences. **Carranza et al. (2000 and 2002)** recorded that, the *Tarentola americana* is the sister taxon to remaining *Tarentola* species. In the present work, the genus *Tarentola* is closer to the genera *Ptyodactylus* and *Tropiocolotes* than the other gekkonid species. According to UPGMA dendrogram, the genus *Tarentola* is sister to the genus *Ptyodactylus*. **Gamble et al. (2008 and 2011)** previously postulated this observation. They found a strong sister relationship between *Ptyodactylus* and *Tarentola* genera by using molecular analyses. In addition, they postulated that, the genera *Ptyodactylus* and *Tarentola* are belong to Phylodactylidae family but the other Gekkotan genera are belong to the Gekkonidae family. Moreover, they observed that, the family Phylodactylidae is sister to the family Gekkonidae. Members of the genera *Tarentola* and *Geckonia* are more closely related to each other than to genera *Stenodactylus* and *ptyodactylus* and the species *Geckonia chazaliae* is evidently a member of the *Tarentola* clade by using mitochondrial and nuclear DNA (**Carranza et al., 2002**).

In the present work, the genus *Tropiocolotes* was closer to the genus *Cyrtopodion* than the genus *Stenodactylus* and *Hemidactylus*. **Fujita and Papenfuss (2011)** found that, the *Tropiocolotes Tropiocolotes* from Niger and *T. somalicus* from Djibouti were sister clade to a clade of *Stenodactylus* samples and some other species of the genus *Stenodactylus* is not monophyletic to *Tropiocolotes*. In addition, they found high genetic variation between the species of the genus *Stenodactylus* that found the genetic distance ranged from 14.6% to 43.2% by using mitochondrial DNA but the genetic distance was ranged from 0.60% to 6.80% by using nuclear data.

Hemidactylus species is one of the most diverse and widely distributed genera of reptiles in the world. Sometimes, very similar anatomical features *Hemidactylus* species show great genetic variation (1-2% variation) in mitochondrial DNA but most populations of *Hemidactylus mabouia* and *H. turcicus* are very uniform (**Carranza and Arnold, 2006**). Molecular study revealed that the *Hemidactylus robustus* and *H. turcicus* from Egypt have 14% genetic diversity (**Baha El Din, 2005**). Also, the morphological conservativeness of *Hemidactylus brooki*, *H. mabouia* and *H. frenatus* have been separated by using molecular data (**Jesus et al., 2005**). Recently, molecular work showed that *Hemidactylus anamallensis* was basal to all the *Hemidactylus* suggesting that *Hemidactylus anamallensis* was genetically very distinct from other *Hemidactylus* (**Bansal and Karanth, 2010**). In the present study, the genus *Hemidactylus* is closer to the genus *Tropiocolotes* than the genera *Cyrtopodion* and *Stenodactylus*. In the present work, the genetic variation between *Hemidactylus turcicus* and *Cyrtopodion scaber* is 0.532 (53.2%) and these two genera are not sister to each other but they have existed in the same cluster. This result is participated with the previous study for *Cyrtopodion kotschyi* and *Hemidactylus turcicus* (**Bauer et al., 2008**) and disagreement for **Kasapidis et al., 2005** and **Carranza and Arnold, 2006**. Also, the present work is in agreement with the results obtained by **Han et al. (2001)** who noticed that, the *Cyrtopodion elongates*, *C. russawi*, *Hemidactylus bowringii*, and *H. frenatus* were monophyletic lineage by using sequence of 12srRNA gene fragment. According to **Bauer et al. (2008)** although all gekkonidae are well studied ecologically and taxonomically, the phylogenetic relationship within and between the Gekkota have not been well established yet.

The conclusion derived from this work, within the Gekkonidae species from the Egyptian fauna shows that, the intergeneric relationships are poorly resolved

and the results suggest additional work is needed to clarify the taxonomy and monophyly of gecko genera.

Table 1: Sequence of primers employed in molecular phylogenetic relationship among the nine Gekkonid species.

Primer	Sequence	G C %
OPA-04	5'-AATCGGGCTG-3'	60
OPB-03	5'-CATCCCCCTG-3'	70
OPB-18	5'-CCACAGCAGT-3'	60
OPC-01	5'-TTCGAGCCAG-3'	60

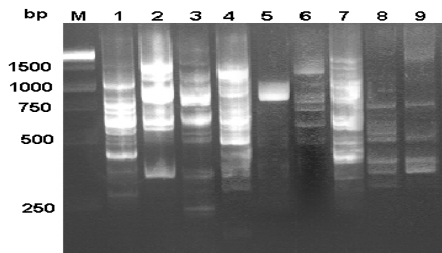


Figure 1. RAPD amplifications showing diagnostic markers for gekkonid species, with primer OP-A04. M, DNA size standard (1kb ladder). 1,*Tropiocolotes tripolitanus* ; 2,*Tropiocolotes nattereri* ; 3,*Hemidactylus turcicus* ; 4,*Cyrtopodion scaber* ; 5,*Ptyodactylus guttatus*; 6,*Ptyodactylus hasselquistii* ;7, *Stenodactylus petrii* ; 8,*Tarentola mauritanica* ; 9,*Tarentola annularis*.

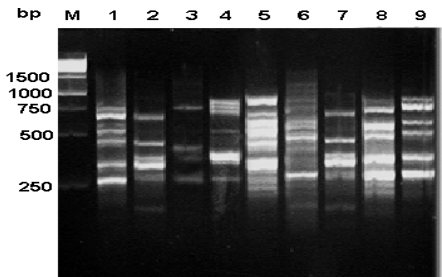


Figure 2. Gel electrophoresis represents RAPD - PCR products for DNA from gekkonid species (Lanes 1 to 9) with OP-C01 primer. 1,*Tropiocolotes tripolitanus* ; 2,*Tropiocolotes nattereri* ; 3,*Hemidactylus turcicus* ; 4,*Cyrtopodion scaber* ; 5,*Ptyodactylus guttatus*; 6,*Ptyodactylus hasselquistii* ;7, *Stenodactylus petrii* ; 8,*Tarentola mauritanica* ; 9,*Tarentola annularis*. M, DNA marker.

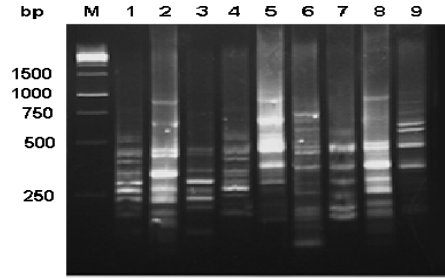


Figure 3. Gel electrophoresis represents RAPD - PCR products for DNA from gekkonid species (Lanes 1 to 9) with OP-B18 primer. M, DNA size standard (1kb ladder). 1,*Tropiocolotes tripolitanus* ; 2,*Tropiocolotes nattereri* ; 3,*Hemidactylus turcicus* ; 4,*Cyrtopodion scaber* ; 5,*Ptyodactylus guttatus*; 6,*Ptyodactylus hasselquistii* ;7, *Stenodactylus petrii* ; 8,*Tarentola mauritanica* ; 9,*Tarentola annularis*.

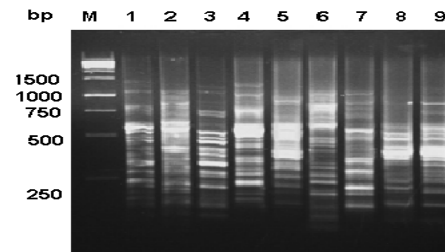


Figure 4. RAPD profile showing DNA fingerprint patterns generated from DNA from 1 of 9 for gekkonid species with primer OP-B03. M, DNA size standard (1kb ladder). 1,*Tropiocolotes tripolitanus* ; 2,*Tropiocolotes nattereri* ; 3,*Hemidactylus turcicus* ; 4,*Cyrtopodion scaber* ; 5,*Ptyodactylus guttatus*; 6,*Ptyodactylus hasselquistii* ;7, *Stenodactylus petrii* ; 8,*Tarentola mauritanica* ; 9,*Tarentola annularis*

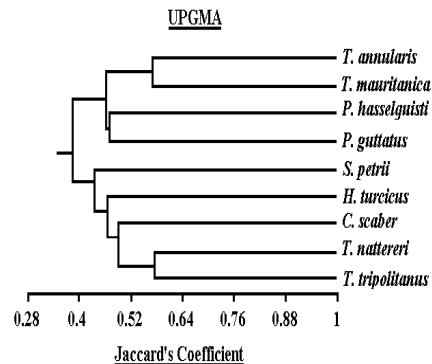


Figure 5. UPGMA based Dendrogram showing phylogenetic relationships among the eight Gekkonid species (1-9) based on RAPD-PCR by OP-A04, OP-B03, OP-B18 and OP-C01 primers.

Table 2. RAPD-PCR bands produced by A4, B3, B18 and C1 primers in 9 Gecko species.

Primer	Band number	Molecular weight (bp)	<i>Tropiocolotes tripolitanus</i>	<i>Tropiocolotes nattereri</i>	<i>Hemidactylus turcicus</i>	<i>Cyrtopodion scaber</i>	<i>Pyrodactylus guttatus</i>	<i>Pyrodactylus hasselquistii</i>	<i>Stenodactylus petrii</i>	<i>Tarentola mauritanica</i>	<i>Tarentola annularis</i>	Band frequency
OPA-04	1	1267	1	1	1	0	0	0	1	0	1	0.56
	2	1116	0	1	0	0	0	1	1	0	0	0.33
	3	1035	0	1	1	1	0	0	1	0	0	0.44
	4	959	1	0	0	0	0	1	1	0	1	0.44
	5	912	0	1	1	0	1	0	1	0	0	0.44
	6	825	1	1	1	1	1	1	1	0	0	0.78
	7	784	1	0	1	0	0	0	0	0	0	0.22
	8	709	1	1	0	1	0	1	0	1	1	0.67
	9	625	1	1	1	1	0	1	1	1	1	0.89
	10	565	1	1	1	1	0	1	1	1	1	0.89
	11	523	1	1	1	1	0	1	1	1	1	0.89
	12	473	0	0	0	0	0	0	1	1	1	0.33
	13	460	1	0	0	0	0	0	0	0	0	0.11
	14	428	1	0	0	1	0	0	1	0	0	0.33
	15	407	0	0	0	0	0	0	1	0	0	0.11
	16	368	1	0	0	1	0	0	0	1	1	0.44
	17	332	1	1	1	1	0	0	1	1	1	0.78
	18	278	1	0	1	1	0	0	1	1	0	0.56
	19	227	0	0	1	0	0	0	0	0	0	0.11
Total bands			13	10	11	10	2	7	14	8	9	
OPB-03	1	1256	1	0	0	0	0	0	0	0	0	0.11
	2	1139	1	0	1	1	0	1	0	0	0	0.44
	3	1067	0	0	0	0	0	0	0	0	1	0.44
	4	1032	1	1	0	0	0	1	0	0	0	0.33
	5	967	0	0	1	1	0	1	1	0	0	0.44
	6	906	0	1	0	1	1	1	0	0	0	0.44
	7	849	1	1	1	1	1	1	1	0	1	0.89
	8	769	0	0	1	1	1	1	1	0	0	0.56
	9	721	1	1	1	1	0	1	1	0	1	0.67
	10	675	0	0	0	0	1	1	1	0	0	0.33
	11	612	1	1	1	1	0	1	1	0	1	0.78
	12	573	1	1	0	1	1	1	0	1	1	0.56
	13	555	1	1	0	1	1	1	1	0	1	0.78
	14	503	1	1	1	1	1	0	1	1	1	0.78
	15	471	0	1	1	1	1	1	1	1	1	0.89
	16	456	1	1	1	0	0	1	0	0	0	0.44
	17	427	0	0	0	1	0	1	0	0	0	0.22
	18	400	1	1	1	1	1	1	1	1	1	1
	19	375	1	1	1	0	1	1	1	1	1	0.89
	20	329	1	1	1	1	1	1	1	1	1	1
	21	308	1	1	1	1	1	1	0	1	1	0.89
	22	289	0	0	0	1	0	0	0	0	0	0.22
	23	271	1	1	1	0	0	0	1	1	1	0.67
	24	262	0	0	1	1	1	1	0	1	1	0.67
	25	245	1	1	0	0	0	0	1	0	0	0.33
	26	230	1	1	1	0	1	1	0	1	1	0.78
	27	208	1	1	0	0	1	0	1	1	1	0.67
	28	189	0	1	1	1	1	1	1	1	1	0.89
	29	171	1	1	1	1	0	0	0	0	0	0.44
	30	155	1	1	1	0	1	1	1	1	1	0.89
	31	128	1	0	1	0	0	1	0	1	1	0.56
	32	112	0	0	0	0	0	1	0	0	0	0.11
Total bands			21	21	20	20	16	23	15	14	19	
OPB-18	1	866	0	1	0	0	1	1	0	1	1	0.56
	2	793	0	0	0	0	1	1	0	0	1	0.33
	3	704	0	0	1	0	1	1	1	1	1	0.67
	4	626	0	1	0	0	1	1	0	1	1	0.56
	5	556	0	0	0	0	0	1	0	0	1	0.22
	6	524	1	1	0	1	0	0	0	0	1	0.44
	7	494	0	0	0	0	1	1	0	0	1	0.33
	8	452	1	1	1	1	1	1	1	1	1	1
	9	426	1	1	1	1	1	1	1	1	0	0.89
	10	390	1	1	0	1	1	0	0	1	1	0.67
	11	347	1	0	1	0	1	1	1	1	1	0.78
	12	337	1	1	0	1	0	0	0	0	1	0.44
	13	317	1	1	0	1	1	0	0	0	0	0.44
	14	291	1	0	1	1	1	0	1	1	1	0.78
	15	274	0	0	0	0	1	1	0	1	0	0.33
	16	258	1	1	1	1	0	0	0	1	0	0.56
	17	243	0	0	0	1	1	1	0	1	0	0.44
	18	229	1	1	1	0	0	0	0	0	0	0.33
	19	204	1	0	1	1	1	0	1	1	0	0.67
	20	187	1	1	0	1	0	1	1	1	1	0.78
	21	171	0	1	0	0	1	1	0	0	0	0.33
	22	147	0	0	1	0	0	1	0	1	0	0.33
	23	123	0	0	0	0	0	1	0	0	0	0.11
Total bands			12	12	9	11	15	15	7	14	13	
OPC-01	1	1048	0	0	0	0	0	1	0	0	0	0.11
	2	955	0	0	0	0	0	1	0	0	0	0.11
	3	818	0	0	0	1	1	1	0	1	1	0.56
	4	745	1	0	1	0	0	1	0	0	1	0.44
	5	701	1	1	0	1	1	1	1	1	0	0.78
	6	582	1	0	0	0	1	1	1	1	1	0.56
	7	547	1	1	1	1	1	1	1	1	0	0.89
	8	498	1	0	0	0	1	1	0	0	1	0.44
	9	483	0	0	0	0	0	1	0	1	0	0.22
	10	454	1	1	0	0	1	0	1	0	0	0.44
	11	427	0	0	1	1	1	1	0	0	0	0.44
	12	389	0	0	0	1	0	0	1	0	0	0.22
	13	366	0	1	0	1	0	0	0	0	1	0.33
	14	333	1	1	0	0	1	1	1	1	1	0.78
	15	304	0	0	0	0	0	1	0	0	0	0.11
	16	285	0	1	0	0	0	1	1	0	1	0.44
	17	268	1	0	0	1	1	0	0	1	1	0.56
	18	237	0	0	0	0	1	0	0	1	0	0.22
	19	216	0	0	0	0	1	1	0	1	1	0.44
	20	179	0	1	0	0	0	1	1	0	0	0.33
Total bands			8	7	3	7	12	14	7	9	9	

Table (3): Total and averages of bands number, polymorphic bands, % of polymorphic bands, mean band frequency, unique bands and their size range (bp) for different primers in the nine gekkonid species .

Primer	Total No. of bands	No. of polymorphic bands	% of polymorphic bands	Band frequency	Mean sharing band frequency	Unique band	Size range (bp)
OPA-04	19	19	100%	0.1-0.89	0.491(49.1%)	3	1267-227
OPB-03	32	30	93.75%	0.1-1	0.597(59.7%)	2	1256-112
OPB-18	23	22	95.65%	0.1-1	0.521(52.1%)	1	866-123
OPC-01	20	20	100%	0.1-0.89	0.421(42.1%)	3	1048-179
Total (average)	94 (23.5)	91 (22.75)	96.8%	0.1-1	0.501(50.1%)	9(2.25)	1267-112

Table (4) : The similarity matrix among the ten Gekkonid species according to Jaccard's Coefficient

G. D. G. S.	1	2	3	4	5	6	7	8	9
1	---	0.424	0.508	0.50	0.662	0.654	0.574	0.544	0.529
2	0.576	---	0.569	0.515	0.623	0.603	0.524	0.60	0.567
3	0.492	0.431	---	0.532	0.687	0.60	0.542	0.581	0.631
4	0.50	0.485	0.468	---	0.632	0.627	0.621	0.569	0.657
5	0.338	0.377	0.313	0.368	---	0.529	0.646	0.57	0.518
6	0.346	0.397	0.40	0.373	0.471	---	0.62	0.592	0.534
7	0.426	0.476	0.458	0.379	0.354	0.38	---	0.625	0.631
8	0.456	0.40	0.419	0.431	0.43	0.408	0.375	---	0.431
9	0.471	0.433	0.369	0.343	0.482	0.466	0.369	0.569	---

G. D., Genetic distance; G. S., Genetic similarity

1, *Tropicolotes tripolitanus*; 2, *Tropicolotes nattereri*; 3, *Hemidactylus turcicus*; 4, *Cyrtopodion scaber*; 5, *Ptyodactylus guttatus*; 6, *Ptyodactylus hasselquistii*; 7, *Stenodactylus petrii*; 8, *Tarentola mauritanica*; 9, *Tarentola annularis*.

Corresponding Author:

Ramadan A. M. Ali
Department of Zoology, Univ. College for Women,
Ain Shams University, Egypt
ramadanali27@gmail.com

References

- Anderson J. (1898).** Zoology of Egypt. Volume 1, Reptilia and Batrachia. London: B. Quaritch. 371 pp.
- Anderson S.C. (1999).** The Lizards of Iran. Publications of Society for the Study of Amphibians and Reptiles, St Louis, Missouri.
- Arnold N., Vasconcelos R., Harris J., Mateo A. and Carranza S. (2008).** Systematics, biogeography and evolution of the endemic *Hemidactylus* geckos (Reptilia, Squamata, Gekkonidae) of the Cape Verde Islands: based on morphology and mitochondrial and nuclear DNA sequences. *Zoologica Scripta*, 37: 619–636.
- Baha El Din M. (1994).** A contribution to the herpetology of Sinai. *Br. Herpetol. Soc. Bull.*, 48: 18-27.
- Baha El Din M. (1997).** A new species of *Tarentola* (Squamata: Gekkonidae) from the western Desert of Egypt. *Afr. J. Herpetol.*, 46: 30-35.
- Baha El Din M. (2003).** A new species of *Hemidactylus* (Squamata: Gekkonidae) from Egypt. *Afr. J. Herp.*, 52: 39–47.
- Baha El Din M. (2005).** An overview of Egyptian species of *Hemidactylus* (Gekkonidae) with the description of a new species from the high mountains of South Sinai. *J. Zool. Middle East*, 34:11-26.
- Baha El Din M. (2006).** A Guide to Reptiles and Amphibians of Egypt. Cairo: American University in Cairo Press. 359 pp.
- Baker J., Pereira L., Haddrath P. and Edge K. (2006).** Multiple gene evidence for expansion of extant penguins out of Antarctica due to global cooling. *Proc. R. Soc. B.*, 273:11–17.
- Baldo D., Borteiro C., Brusquetti F., García E. and Prigioni C. (2008).** Notes on geographic distribution, Reptilia, Gekkonidae, *Hemidactylus mabouia*, *Tarentola mauritanica*: Distribution extension and anthropogenic dispersal. *Check List*, 4: 434–438.
- Bansal R. and Karanth P. (2010).** Molecular phylogeny of *Hemidactylus* geckos (Squamata: Gekkonidae) of the Indian subcontinent reveals an unique Indian radiation and an Indian origin of Asian house geckos. *Mol. Phylogenet. Evol.*, 57: 459–465.

- Bauer M., Todd R., Jackman R., Greenbaum E. and Gamble T. (2008).** Phylogenetic relationships of the Italian gekkotan fauna. *Herpetologia Sardiniae*, (Oristano, 1-5.X).
- Busais S. and Joger U. (2011).** Molecular phylogeny of the gecko genus *Hemidactylus* Oken, 1817 on the mainland of Yemen (Reptilia: Gekkonidae). *J. Zool. Middle-east*, 53: 25–34.
- Camargo A., Sinervo B. and Sites W. (2010).** Lizards as model organisms for linking phylogeographic and speciation studies. *Mol. Ecol.*, 19: 3250–3270.
- Carranza S. and Arnold N. (2006).** Systematics, biogeography, and evolution of *Hemidactylus* geckos (Reptilia: Gekkonidae) elucidated using mitochondrial DNA sequences. *Mol. Phylogenet. Evol.*, 38: 531-545.
- Carranza S., Arnold N., Mateo A. and Geniez P. (2002).** Relationships and evolution of the North African geckos, *Gekkonina* and *Tarentola* (Reptilia: Gekkonidae), based on mitochondrial and nuclear DNA sequences. *Mol. Phylogenet. Evol.*, 23: 244-256.
- Carranza S., Arnold N., Mateo A. and López-Jurado F. (2000).** Long-distance colonization and radiation in gekkonid lizards, *Tarentola* (Reptilia: Gekkonidae), revealed by mitochondrial DNA sequences. *Proc. R. Soc. London B*, 267: 637-649.
- Castiglia R. (2004).** First chromosomal analysis for the genus *Lygodactylus* (Gray, 1864): The karyotype of *L. picturatus* (Squamata, Gekkonidae, Gekkoninae). *Afr. J. Herpetol.*, 53: 95-97
- Červenka J. and Kratochvíl L. (2010).** Generic reassignment and validity of recently described species *Cyrtopodion dehakroense*. *Herpetol. Notes*, 3: 135-137.
- Chen C., Peng B. and Yu W. (1986).** Studies on the karyotypes of three species of the genus *Gekko*. *Acta Herpetologica Sinica*, 5:24–29
- Diaz M. and Hedges B. (2008).** A new gecko of the genus *Tarentola* (Squamata: Gekkonidae) from eastern Cuba. *Zootaxa*, 1743: 43-52.
- Dinesh R., Chan K., Lim M. and Phange E. (1995).** RAPD markers in fishes: An evaluation of resolution and reproducibility. *Asia-Pac. J. Mol. Biol. Biotechnol.*, 3: 112-118.
- Fujita K. and Papenfuss J. (2011).** Molecular systematics of *Stenodactylus* (Gekkonidae), an Afro-Arabian gecko species complex. *Mol. Phylogenet. Evol.*, 58: 71-75.
- Gamble T., Bauer A., Greenbaum E. and Jackman T. (2008).** Evidence for Gondwanan vicariance in an ancient clade of gecko lizards. *J. Biogeogr.*, 35: 88–104.
- Gamble T., Bauer M., Colli R., Greenbaum E., Jackman R., Vitt J. and Simons M. (2011).** Coming to America: multiple origins of New World geckos. *J. Evol. Biol.*, 24: 231–244 .
- Goodman S. and Hobbs J. (1994).** The distribution and ethnozoology of reptiles of the northern portion of the Egyptian eastern desert. *J. Ethnobiol.*, 14: 75–100.
- Gübitz T., Thorpe R. and Malhotra A. (2005).** The dynamics of genetic and morphological variation on volcanic islands. *Proc. R. Soc. (B)*, 272:751-757
- Han D., Zhou K. and Bauer M. (2004).** Phylogenetic relationships among gekkotan lizards inferred from C-mos nuclear DNA sequences and a new classification of the Gekkota. *Biol. J. Linn. Soc.*, 83: 353–368.
- Han D., Zhou K. and Wang Y. (2001).** Phylogeny of ten species of Chinese gekkonid lizards (Gekkonidae: Lacertilia) inferred from 12S rRNA DNA sequences. *Acta Zoologica Sinica*, 47: 139–144.
- Harris J., Batista V., Carretero A. and Ferrand N. (2004).** Genetic variation in *Tarentola mauritanica* (Reptilia: Gekkonidae) across the Strait of Gibraltar derived from mitochondrial and nuclear DNA sequences. *Amphibia-Reptilia*, 25: 451-459.
- Harris J., Carretero A., Corti C. and Lo Cascio P. (2009).** Genetic affinities of *Tarentola mauritanica* (Reptilia: Gekkonidae) from Lampedusa and Conigli islet (SW Italy) North-Western. *J. Zool.*, 5: 197-205.
- Ibrahim A. (2001).** Geographic distribution. *Ptyodactylus hasselquistii hasselquistii* (fan-toed gecko). *Herpetol. Rev.*, 32: 120 201.
- Jesus J., Brehm A. and Harris J. (2002).** Relationships of *Tarentola* (Reptilia: Gekkonidae) from the Cape Verde islands estimated from DNA sequence data. *Amphibia-Reptilia*, 22: 235-242.
- Jesus J., Brehm A. and Harris J. (2005).** Phylogenetic relationships of *Hemidactylus* geckos from the Gulf of Guinea islands: patterns of natural colonizations and anthropogenic introductions estimated from mitochondrial and nuclear DNA sequences. *Mol. Phylogenet. Evol.*, 34: 480-485.
- Jesus J., Brehm A., Pinheiro M. and Harris J. (2001).** Relationships of *Hemidactylus* (Reptilia: Gekkonidae) from the Cape Verde Islands: what mitochondrial DNA data indicate. *J. Herp.*, 35: 672–675.
- Kasapidis K., Magoulas A., Mylonas M. and Zouros E. (2005).** The phylogeography of the gecko *Cyrtopodion kotschy* (Reptilia: Gekkonidae) in the Aegean archipelago. *Mol. Phyl. Evol.*, 35: 612–623.
- Kawai A., Ishijima J., Nishida C., Kosaka A., Ota H., Kohno S. and Matsuda Y. (2009).** The ZW sex chromosomes of *Gekko hokouensis*

- (Gekkonidae, Squamata) represent highly conserved homology with those of avian species. *Chromosoma*, 118: 43–51.
- Macey R., Ananjeva B., Wang Y. and Papenfuss J. (2000).** Phylogenetic relationships among Asian gekkonid lizards formerly of the genus *Cyrtodactylus* based on cladistic analyses of allozymic data: monophyly of *Cyrtopodion* and *Mediodactylus*. *J. Herpetol.*, 34: 258–265.
- Marx H. (1968).** Checklist of the Reptiles and Amphibians of Egypt. Cairo: U.S. Naval Medical Research Unit Number Three.
- Masroor R. (2008).** A new species of *Cyrtopodion* (Sauria: Gekkonidae) from the northern areas of Pakistan. *Zootaxa*, 1857: 33–43.
- Masroor R. (2009).** A new arboreal species of *Cyrtopodion* (Squamata:Gekkonidae) from Deh Akro-II Wetlands Complex, Sindh, Pakistan. *Zootaxa*, 2243: 57–67.
- Nazarov A. and Rajabizadeh M. (2007).** A new species of angular-toed gecko of the genus *Cyrtopodion* (Squamata: Sauria: Gekkonidae) from south-east Iran (Sistan-Baluchistan province). *Russ. J. Herpetol.*, 14: 137–144.
- Nei M. (1973).** Analysis of gene diversity in subdivided populations. *Proc. Natl. Acad. Sci. USA*, 70: 3321–3323
- Nei M. (1987).** Molecular evolutionary genetics. Columbia University Press, New York.
- Pereira A. and Harris J. (2010).** Genetic variability within the Oudri's fan-footed gecko *Ptyodactylus oudrii* in North Africa assessed using mitochondrial and nuclear DNA sequences. *Mol. Phyl. Evol.*, 54: 634–639.
- Qin X., Liang Y. and Huang X. (2006).** Isozymes analysis on different tissues from three different populations of *Gekko gekko*[J]. *Guangxi Science*, 13 : 310-316.
- Qin X., Liang Y., Huang X. and Pang G. (2005).** RAPD analysis on genetic divergence and phylogenesis of *Gekko gekko* from different areas. *Chinese J. Zool.*, 40 : 14.
- Rato C., Carranza S., Pereira A., Carretero M. and Harris J. (2010).** Conflicting patterns of nucleotide diversity between mtDNA and nDNA in the Moorish gecko, *Tarentola mauritanica*. *Mol. Phylogenet. Evol.*, 56: 962–971.
- Rocha S., Carretero M. and Harris J. (2005).** Diversity and phylogenetic relationships of *Hemidactylus* geckos from the Comoro Islands. *Mol. Phylogenet. Evol.*, 35: 292–299.
- Rohlf F. J. (2000).** NTSYS-pc numerical taxonomy and multivariate analysis system. Version 2.1.
- Saleh M. A. (1997).** Amphibians and reptiles of Egypt. [Cairo]: Egyptian Environmental Affairs Agency. 233 pp. (Publication of National Biodiversity Unit (Egypt) 6.)
- Shi L. and Zhao E. (2011).** A New Gecko in the Genus *Cyrtopodion* Fitzinger, 1843 (Reptilia: Squamata: Gekkonidae) From Western China *Herpetol.*, 67: 186-193.
- Sprackland G. and Swinney N. (1998).** A new species of giant gecko of the genus *Tarentola* (Reptilia: Squamata:Gekkonidae) from Jamaica. *J. Zool.*, 245: 73–78.
- Vences M., Wanke S., Vieites R., Branch R., Glaw F. and Meyer A. (2004).** Natural colonization or introduction? Phylogeographical relationships and morphological differentiation of house geckos (*Hemidactylus*) from Madagascar. *Biol. J. Linnean Soc.*, 83: 115-130.
- Vidal N. and Hedges B. (2009).** The molecular evolutionary tree of lizards, snakes, and amphisbaenians. *C. R. Biol.*, 332: 129–139.
- Williams J., Kubelik R., Livak J., Rafalski A. and Tingey V. (1990).** DNA polymorphisms amplified by arbitrary primers are useful as genetic markers. *Nucleic Acids Res.*, 18: 6531–6535.
- Yeh C., Boyle T., Rongyai Y., Ye Z. and Xian M. (1999).** POPGENE, Version 1.31. A Microsoft Window based free ware for population genetic analysis. University of Alberta, Edmonton. Canada.
- Yue H. and Orban L. (2005).** A simple and affordable method for high-throughput DNA extraction from animal tissues for polymerase chain reaction. *Electrophoresis*, 26: 3081–3083.

12/22/2011

Role of Diffusion Tensor Imaging in Characterization and Preoperative Planning of Brain Neoplasms

Mohsen Gomaa and Yosra abdel zaher

Department of Radiodiagnosis, Ain Shams University
mostafa_redio@yahoo.com

Abstract: Background and purpose: DTI is an MR imaging measure of brain tissue integrity. It gives precise information about the involvement and integrity of the white matter tracts in the immediate region surrounding tumors. The purpose of our study is to evaluate the role of DTI in characterization and preoperative assessment of brain neoplasm. Materials and methods: 32 patients with intracranial neoplasm were included in this study which was conducted during a 2 years period. Conventional MRI before and after IV Gadolinium administration was done followed by DTI and diffusion tensor tractography, with FA and ADC values measurements of different white matter tracts in direct relation to the tumor. The values obtained were compared to the normal unaffected tract in the contralateral side. Results: White matter involvement by a tumor was classified according to the criteria of displacement, infiltration, disruption or edema. Patients were classified into two main groups according to the tumor type: Benign and Malignant groups. Prevalence of tract displacement was higher among benign group in comparison to malignant group with significant difference in between by using chi-square test (P value<0.05). While prevalence of disruption was higher among malignant group, in comparison to benign group with significant difference in between by using chi-square test. (P value<0.05). Conclusion: The information provided by DT imaging further defined precise relationships between the sub cortical white matter structures and the cerebral neoplasm. This potentially has a role in tumor characterization, and more importantly in surgical planning.

[Mohsen Gomaa and Yosra abdel zaher **Role of Diffusion Tensor Imaging in Characterization and Preoperative Planning of Brain Neoplasms**. Life Science Journal, 2012; 9(1):163-176] (ISSN: 1097-8135).
<http://www.lifesciencesite.com>

Key words: diffusion tensor imaging. Brain tumor. Preoperative planning. Glioma.

Abbreviations:

ADC: apparent diffusion coefficient **FA:** fractional anisotropy **DTI:** diffusion tensor imaging.

1. Introduction:

Before proper planning of brain surgery, it is very important to avoid several key functional regions of the brain; these include motor, sensory, auditory, language, and vision fields. We have a fair amount of knowledge about functional maps of the cortex, but we do not have equivalent maps of the white matter. The location and functions of the cortex can be deduced from the folding patterns of the cortex but the white matter appears as just a homogenous structure during surgery. Even if we avoid injury to an important cortical area, the patient could lose function if the white matter tract responsible for the function is cut. Therefore, the identification of motor, language, auditory, and visual pathways is very important for brain surgery (*Mori, 2007*).

Magnetic resonance (MR) imaging and MR Spectroscopy plays an important role in the detection and evaluation of brain tumors. In the past few years, however, a number of advanced MR imaging techniques have been developed that provide new methods for the assessment of brain tumors. One of these techniques is diffusion tensor imaging. (*Provenzale et al., 2006*).

DTI is a quantitative MR imaging technique that measures the 3D diffusion of water molecules within tissue through the application of multiple diffusion gradients (*Basser & Pierpaoli, 1996*). The power of diffusion techniques comes from measurement of molecular probing of tissue structures by water molecules at a microscopic scale well beyond the typical MR imaging resolution. By measuring the interaction of water molecules with cell membranes, myelin sheaths, and macromolecules, tissue integrity can be inferred (*Pierpaoli & Basser, 1996*). Tissue has physical structures that limit diffusion in different directions, so diffusion is typically described as a 3D ellipsoid through a 3×3 matrix. In nervous tissue, the largest (or primary) ellipsoid eigenvector represents diffusion along the length of a fiber tract and so is referred to as the $\lambda_{//}$. The other shorter 2 ellipsoid eigenvectors, when averaged together, are called λ_{\perp} . Clinical and pathologic studies have found that $\lambda_{//}$ tends to reflect axonal integrity, whereas λ_{\perp} corresponds more closely to myelin integrity (*DeBoy et al., 2007*). Animal and human studies suggest that $\lambda_{//}$ and λ_{\perp} are approximate measures of axonal and myelin integrity, particularly in acute injury (*Fox et al., 2010*).

Diffusion ellipsoids in highly organized fiber tracts (e.g., pyramidal tracts and the corpus callosum) are very elongated. The absence of fiber tracts in gray matter makes diffusion ellipsoids less elongated, though gray matter still demonstrates some anisotropy. FA is a common metric to describe the degree of diffusion directionality or elongation. A high FA within a single voxel would signify that diffusion occurs predominantly along a single axis. A low FA would signify that diffusion occurs along all 3 cardinal axes. An overall measure of diffusion magnitude is described by MD, which ignores anisotropy and simply describes the overall magnitude of diffusion (*Fox et al., 2010*).

Although routine structural MR images can accurately demonstrate brain tumors, they do not give precise information about the involvement and integrity of the white matter tracts in the immediate region surrounding tumors. Diffusion-tensor imaging may help in detection of white matter abnormalities in patients with malignant tumors in areas that appear normal on T2-weighted MR images, which raises the possibility that disruption of white matter tracts by tumor infiltration may be detectable by using diffusion-tensor imaging (*Provenzale et al., 2006*).

There are 2 main reasons why preoperative identification of white matter tracts is important. First, accurate localization of important white matter tracts can affect the decision of whether or not to operate. Secondly, preoperative localization of important white matter tracts is essential in surgical planning. (*Karimi et al., 2006*)

In this study, The hypothesis that diffusion tensor MR imaging can play a role in precise localization and assessment of the pertinent white matter tracts was assessed.

2. Material and Methods:

Study population:

32 patients (24 males and 8 females; age range 1-74 years; mean age 32.8±18 years) with intracranial neoplasms were included in this study. The tumors studied consisted of glioma (23 cases), metastasis (3 cases), lymphoma (one case), brain stem gliomas (3 cases) and meningiomas (2 cases).

MR Imaging Protocol:

A short acquisition time and instant processing are essential for the clinical feasibility of a certain procedure. We applied single-shot spin-echo echo-planar imaging (EPI) and parallel imaging techniques to achieve motion-free and higher signal-to-noise ratio (SNR) DTI. The total imaging time for DTI and FT was 7–9 minutes according to the section

numbers, which was added to the routine MR imaging examinations.

Acquisition of MR Images:

A 1.5-T MR unit (Gyrosan Intera; Philips Medical Systems, Best, the Netherlands) was used. The following sequences were acquired: T2-weighted sequences, fluid attenuated inversion recovery (FLAIR), T1-weighted sequences before and after intravenous administration of paramagnetic contrast material. DT imaging data were acquired by using a single-shot echo-planar imaging sequence with the sensitivity-encoding, or SENSE, parallel-imaging scheme (reduction factor, 2). The imaging matrix was 128 x 128, with a field of view of 220 x 220 mm. Transverse sections of 2.75mm thickness were acquired parallel to the anterior commissure–posterior commissure line. A total of 50 sections covered the entire hemisphere and brainstem without gaps. Diffusion weighting was encoded along 12 independent orientations, and the b value was 1000 mm²/sec. Other imaging parameters were as follows: echo time = 70 msec, repetition time = 6,599–8,280 msec, number of acquisitions = two. Coregistered magnetization-prepared rapid gradient-echo (MPRAGE) images of the same resolution were recorded for anatomic guidance.

H1 MR Spectroscopy was added in 25 cases, to characterize the nature of the tumor replacing biopsy.

The study was combined with fMRI in 15 cases to assess the relation of the tumor to the eloquent cortical areas, and use these areas as seed points in fiber tracking to precisely delineate the course of the pyramidal tract and separating the hands from the feet fibers.

Data processing:

We transferred the diffusion-tensor imaging data to an offline workstation (extended work space "EWS") (Release 2.5.3.0; Dell, Round Rock, Tex); PrIDE software (Philips Medical Systems) which is based on the Fiber Assignment by Continuous Tracking (FACT) method. Anisotropy was calculated by using orientation-independent fractional anisotropy (FA), and diffusion-tensor MR imaging–based color maps were created from the FA values and the three vector elements. The vector maps were assigned to red (x element, left-right), green (y, anterior-posterior), and blue (z, superior-inferior) with a proportional intensity scale according to the FA. Three-dimensional FT was then achieved by connecting voxel to voxel with the FACT algorithm. The threshold values for the termination of the fiber tracking were less than 0.3 for FA and greater than 45° for the trajectory angles between the ellipsoids.

Three-dimensional Tract Reconstruction:

To reconstruct tracts of interest, we used a multiple-region-of-interest (ROI) approach, which exploits existing anatomic knowledge of tract trajectories. Tracking was performed from all pixels inside the brain ("brute force" approach), and results

that penetrated the manually defined ROIs were assigned to the specific tracts associated with the ROIs. When multiple ROIs were used for a tract of interest, we used three types of operations, AND, OR, and NOT (Fig 1), the choice of which depended on the characteristic trajectory of each tract.

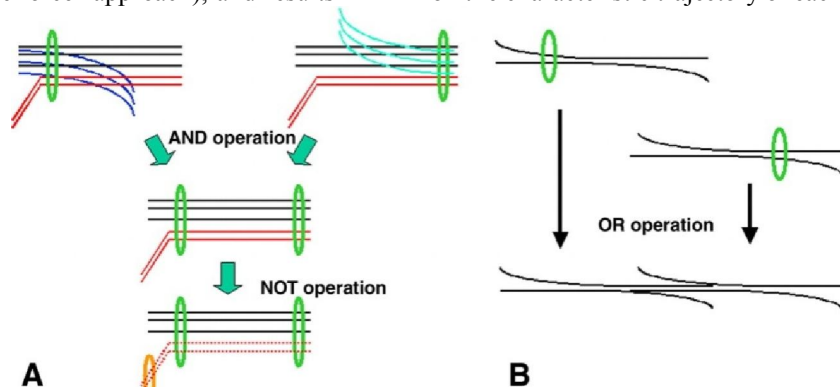


Figure 1. Diagram shows the three operations used in this study. *A*, AND and NOT operations. Two ROIs (green) are placed on anatomic landmarks. When the AND operation is used, tracts that penetrate both ROIs are selected. In this example, black and red tracts are selected, while blue tracts are removed. NOT operation is used to remove specific tracts that penetrate one or multiple ROIs (orange). In this example, red tracts are removed. *B*, OR operation. Multiple tracking results when multiple ROIs are combined. AND operation poses a strong constraint in tracking results by selecting only tracts with known trajectories. This is a conservative approach for which results are potentially more accurate, with the disadvantage that it does not allow visualization of branching patterns between ROIs. The OR approach may be more susceptible to noise and partial volume effects (*Quoted from Wakana et al., 2004*).

Tract evaluation with the aid of DT imaging:

Color-coded DTI maps were analyzed, followed by tractography of individual tracts. In most of patients the tumor was isolated to one hemisphere, and comparison was made between affected tracts by the tumor and the homologous tracts in the contralateral control hemisphere. White matter tracts were then characterized as: displaced (deviated), edematous, infiltrated and disrupted (destruction).

Displaced: if the tract showed normal or only slightly decreased FA, with abnormal location and/or direction, resulting from bulk mass displacement.

Edematous: if the tract maintained normal or slightly reduced anisotropy with normal orientation but demonstrated high signal intensity on T2WI.

Infiltrated: if the tract showed reduced anisotropy but remained identifiable on color maps.

Disrupted: if the tract showed isotropic (or near-isotropic) diffusion, such that it could not be identified on directional color maps.

Anatomic Landmarks and ROI Locations for Major White Matter Fibers:

For tracking of the white matter fibers, the region of interest (ROI) method was applied. We placed the single or multiple ROIs on the color maps. The plane of the ROI was varied according to the running direction of the white matter fibers (eg, corticospinal tract on the axial views, corpus callosum on the sagittal views).

For *corticospinal tract* tractography (*Fig. 2*), three ROIs were placed on transverse colour coded DT images according to established anatomic landmarks: The first ROI was placed in the pons anteriorly (where the CST is coded in blue), the second ROI was placed in the posterior limb of internal capsule, and the third ROI was placed at the motor cortex (precentral gyrus) which was identified on the basis of morphologic features of the sulci at the vertex. Fibers connecting the right and left corticospinal tracts via transverse pontine connection and fibers projecting into cerebellar peduncles were then removed by using the "NOT" operation because of apparent lack of compliance with classic definitions of the corticospinal tract.

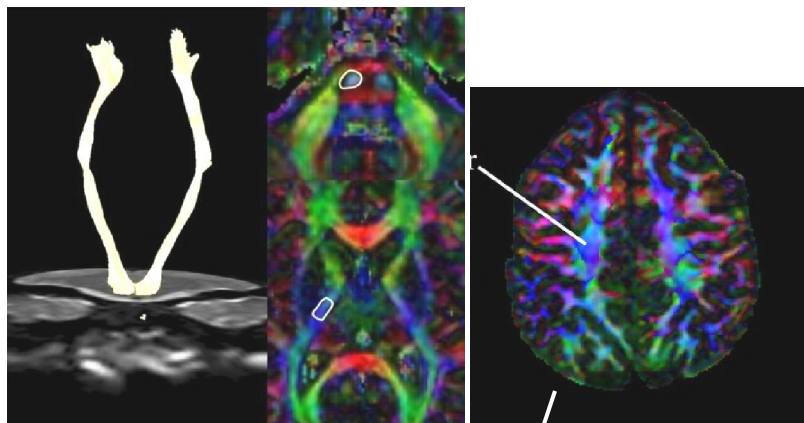


Fig 2: ROIS placement in CST fiber tracking

For the sensory tract, a pair of ROIs was placed at the dorsal part of the midbrain, pons, or both and the sensory cortex.

The superior longitudinal fasciculus was reconstructed at tractography by placing two ROIs in the cerebral deep white matter on a coronal directional color-coded map. The superior longitudinal fasciculus was identified on the coronal color-coded map as a region where the fiber orientation was anterior to posterior (green), lateral to the corona radiata (Mori et al., 2002). An anterior ROI was placed in the plane passing through the reconstructed corticospinal tract, and a posterior ROI was placed in the plane passing through the rostral surface of the splenium of the corpus callosum, with both ROIs covering the green area representing the superior longitudinal fasciculus (Fig. 3). Some "noise" fibers that were apparently tracing the error course were then removed (Wakana et al., 2004).

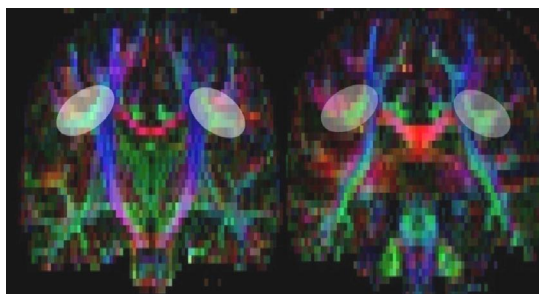


Fig 3: Coronal color-coded maps with ROIs (white ellipses). Anterior (left) and posterior (right) ROIs contain superior longitudinal fasciculus (green area lateral to corona radiata). (Quoted from Okada et al., 2006)

Also, superior longitudinal fasciculus, one ROI was defined on a coronal section of the DT imaging-based color-coded maps at the posterior tip of the putamen. Fiber tracts of other longitudinal fibers like the *cingulum* (c) and *inferior longitudinal fasciculus* (ilf) are also generated from coronal images (Fig. 4).

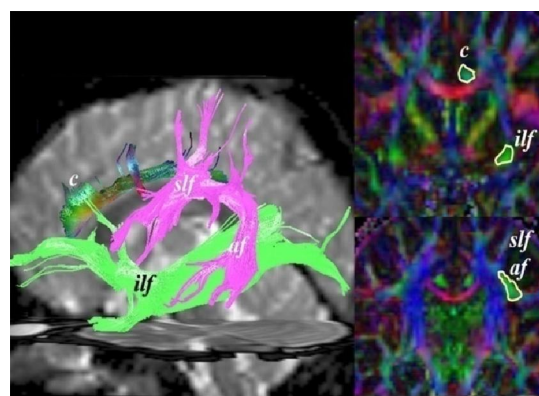


Fig 4: ROIs placement for tracking of association fibers. Cingulum (c), Superior longitudinal fasciculus (slf) Arcuate fasciculus (af), Inferior longitudinal fasciculus (ilf)

One ROI at the parieto-occipital sulcus, which was identified at the middle of the coronal section along the superior-inferior axis, was used for both the *inferior longitudinal fasciculus* and the *inferior fronto-occipital fasciculus*. For the inferior longitudinal fasciculus, an additional ROI was defined on a coronal section at the midtemporal lobe at the section level of the posterior tip of the putamen. For the inferior fronto-occipital fasciculus, an additional ROI was defined on a coronal section at the frontal lobe at the section level where the frontal and temporal lobes were separated. The ROIs for the inferior longitudinal fasciculus and the inferior fronto-occipital fasciculus were combined by using the operator AND.

Corpus callosum tractography was performed by imaging the combination of four different callosal fiber bundles. The primary ROI was placed in the corpus callosum in the midsagittal plane (Fig. 5). To visualize different parts of the callosal fibers, secondary ROIs were placed in four regions: two ROIs on the coronal color-coded map and two ROIs on the transverse color-coded map (Fig. 6). Anterior callosal fibers, referred to as minor forceps, were

reconstructed by placing the ROI covering the deep white matter in the coronal plane anterior to the genu of the corpus callosum. For reconstruction of the posterior callosal fibers, referred to as major forceps, the ROI was placed posterior to the splenium of the corpus callosum. Callosal body fibers were reconstructed by placing the ROI at the centrum semiovale in the transverse plane superior to the body of the corpus callosum. For reconstruction of the temporal interhemispheric connection fibers, referred to as tapetum, ROIs were placed bilaterally in the temporal deep white matter, lateral to the trigon of the lateral ventricles. These four fibers (ie, minor forceps, major forceps, callosal body fibers, and tapetum) were combined to delineate the entire corpus callosum (Okada et al., 2006).

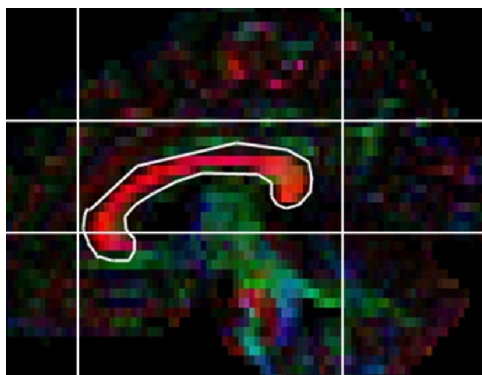


Fig 5: Primary ROI placed in corpus callosum on sagittal color-coded map. Vertical (coronal planes) and horizontal (transverse planes) white lines indicate section locations of secondary ROIs: anterior coronal section for minor forceps, posterior coronal for major forceps, superior transverse for body of corpus callosum, and inferior transverse for tapetum. (Quoted from Okada et al., 2006)

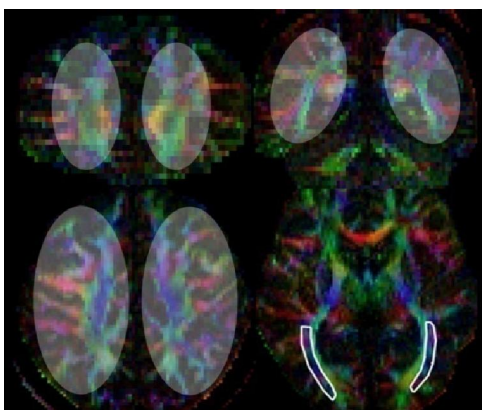


Fig 6: Transverse color-coded maps show secondary ROIs for corpus callosum: anterior ROIs for minor forceps (top left), posterior ROIs for major forceps (top right), superior ROIs for body of corpus callosum (bottom left), and inferior ROIs (white outlines) for tapetum (bottom right). (Quoted from Okada et al., 2006)

Limbic fibers through the fornix were reconstructed by placing one primary ROI and two secondary ROIs. The primary ROI was placed in the body of the fornix, and the secondary ROIs were placed in the crura of the right and left fornices anterolateral to the splenium of the corpus callosum (Fig. 7). (Okada et al., 2006)

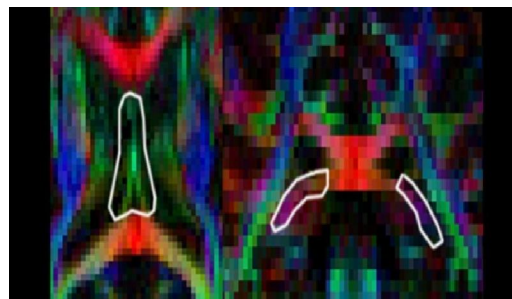


Fig 7: Transverse (left) and coronal (right) color-coded maps show ROIs (white outlines) for fornix. Primary (superior) ROI was placed at body of fornix (left); secondary (posterior) ROIs, at crura of fornices bilaterally (right). (Quoted from Okada et al., 2006)

Fiber tracking of the middle cerebellar peduncles was generated from single ROIs on the coronal view. These fiber tracts form a midline crossing by means of the transverse pontine fibers, and some extend to cortical connections superiorly (Fig. 8).

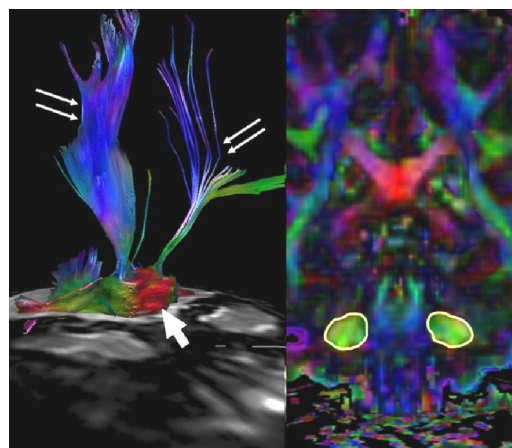


Fig 8: fiber tracking image of the middle cerebellar peduncles (left). Transverse pontine fibers (thick arrow), Cortical connections (thin arrows). ROIs placement on coronal colour map (right)

Fiber tracking of the *superior and inferior cerebellar peduncles* were generated from single ROIs on axial color maps (Fig. 9).

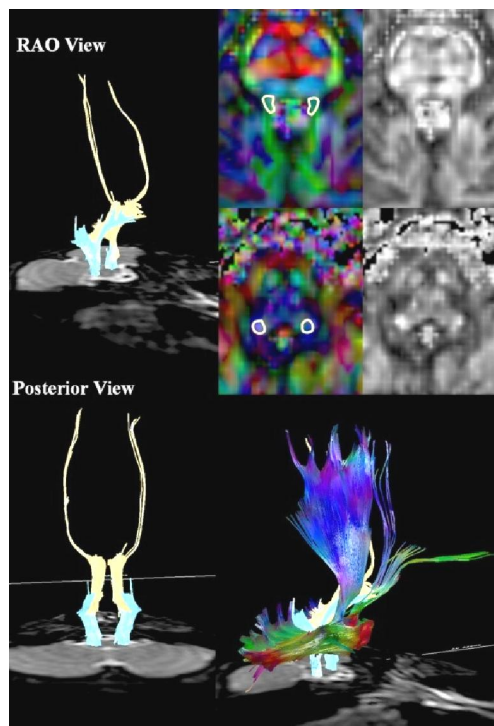


Fig. 9: Fiber tracking images of the superior (yellow) and inferior (blue) cerebellar peduncles (left and bottom right). ROIs on axial color maps (top right). RAO = right anterior oblique.

To reconstruct *optic radiation* tractography, the first "OR" ROI was placed on either side of the occipital lobe, including the calcarine cortex on coronal color-coded maps. The second "AND" ROI was at the ipsilateral temporal stem on sagittal color-coded mapping, including the Meyer loop. Most fibers in the temporal stem were green in the color-coded map, but the Meyer loop was red according to fiber direction and was distinguishable from other bundles. Various kinds of anteroposterior long association fibers or temporal projection fibers with diverting connectivity were included after these 2 ROI operations, such as the inferior occipitofrontal fasciculus and inferior longitudinal fasciculus. Based on the correlation between temporal fiber dissection and MR imaging, 2 more "NOT" ROI operations were applied to the ipsilateral temporal stem on coronal color-coded maps. One was lateral and the other medial to the Meyer loop. As a result, optic radiation tractography along the sagittal stratum was delineated (Fig. 10).

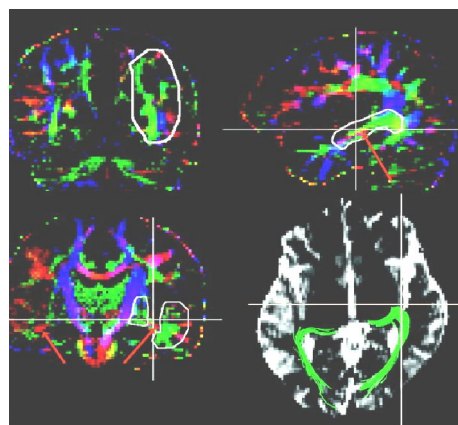


Fig 10: ROI segmentation for optic radiation tractography. The 4 kinds of ROIs (white polygon) are placed on coronal or sagittal color-coded maps. Cross lines indicate the orthogonal planes. The first "OR" ROI is placed at either side of the occipital lobe, including the calcarine cortex on the coronal plane through the anterior edge of the occipital-parietal sulcus (top left). The second "AND" ROI is placed at the ipsilateral temporal stem, including the Meyer loop on the sagittal plane (top right). Temporal stem is identified as green, and the Meyer loop is identified as a small red area inside the temporal stem (red arrow). The third and fourth "NOT" ROIs are placed on the same coronal plane through the dorsal end of the Sylvian fissure (bottom left). Bilateral Meyer loops are indicated as red arrows. Examples of bilateral optic radiation overlaid on transverse $b = 0$ images (TR/TE, 7000 ms/79 ms) are shown (bottom).

Presurgical tractographies of the *Meyer loop* (green in Fig. 11) were obtained with the seed area in the white matter that was located anterior to the lateral geniculate body and with the target area located in the ipsilateral sagittal stratum on the coronal planes at the level of the trigone.

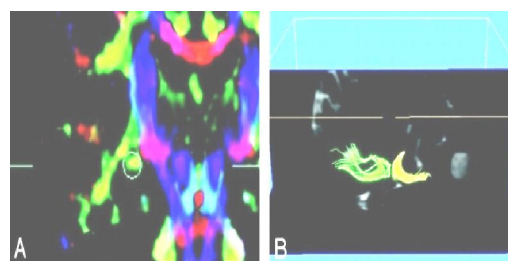


Fig 11: A, Coronal color coded map, the circle shows the seed area for the presurgical tractography. B, Tractography of the optic radiation (green) and uncinete fascicles is shown. Note that the 2 tracts are close together at the temporal stem. Thus, tractography of uncinete fascicles drawn in advance can be used as an assistant or a guide to draw the Meyer loop.

To help recognize the most anterior point of the Meyer loop in the presurgical images, we obtained tractographies of the *uncinate fasciculus* (yellow in

Fig. 11), which is located just anterior to the most anterior point of the Meyer loop. The seed area in the white matter of the frontal lobe was located on the coronal planes at the tip of the frontal horn of the lateral ventricle, and the target area in white matter was located on the coronal planes at the tip of the inferior horn of the lateral ventricle in the ipsilateral temporal tip.

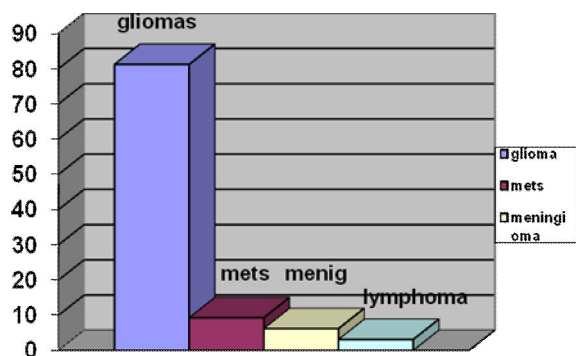
For reconstruction of the thalamic fibers, the entire thalamus was defined as the first ROI. The second ROI for the anterior and posterior thalamic radiations was placed on coronal sections to define the frontal lobe at the section level where the frontal and temporal lobes were separated and to define the occipital lobe at the section level of the posterior tip of the putamen, respectively. For superior thalamic radiation, the second ROI was defined on a transverse section above the corpus callosum, and it occupied the entire hemisphere. Again, the first and the second ROIs were combined by using the operator AND.

3. Results:

The population enrolled in this study comprises of 32 patients, 22(68.8%) were males and 10(31.3%) were females. Their age ranged from 1 to 74 years old with a mean age of 32.8 ± 18 .

The majority of the studied cases were above 40 years, and mostly males (68.8%), while females represents 31.3%.

The tumors studied consisted of 3 low grade gliomas, 10 grade II-III glioma, 2 grade III glioma, 5 glioblastoma multiforme, 3 gliomatosis cerebri, 3 metastasis, 1 lymphoma, 3 brain stem gliomas, 2 meningiomas (Graph 1)



Graph 1: Distribution of the studied cases as regard diagnosis

The diagnosis was based on biopsy and histopathology in 7 cases (21.8%), on H1 MR spectroscopy in 25 cases (78.2%).

Patients were classified into two main groups according to the tumor type:

1. Benign (including low grade gliomas, gliomatosis cerebri and meningiomas).
2. Malignant (high grade gliomas, metastasis and lymphoma).

Table (1) Comparison between both groups as regard general data

Variables	Benign N=11	Malignant N=21	X ²	P
Age				
≤10yrs	2(18.2%)	2(9.5%)		
11-20	1(9.1%)	4(19%)		
21-30	3(27.3%)	2(9.5%)	2.8	>0.05
31-40	2(18.2%)	4(19%)		NS
≥40	3(27.3%)	9(42.9%)		
Gender				
Male	5(45.5%)	17(81%)	4.2	<0.05
Female	6(54.5%)	4(19%)		S

This table shows that most of malignant group were males, while majority of benign group were females with significant difference in between by using chi-square test. No significant difference as regard age.

White matter pathway involvement was clearly identified in all patients by using color-coded DT imaging maps and 3D MR Tractography. Normal white matter pathways demonstrated on DT imaging appeared in the unaffected contra lateral hemisphere in 21 cases. Cases with bilateral tract involvement were compared with age matched normal controls.

The white matter tracts were color coded in a universal fashion based on their spatial orientation. Projection fibers were presented by blue color scheme, the commissural fibers were demonstrated by red color, and the association fibers were coded in green.

The white matter findings were characterized for each patient. White matter involvement by a tumor was classified according to the criteria of displacement, infiltration, disruption or edema. Displaced tracts maintained normal anisotropy but were situated in abnormal location or with abnormal orientation on color coded maps; edematous tracts maintained normal anisotropy and orientation but demonstrated high signal intensity on T2WI on conventional MRI. Infiltrated tracts showed reduced anisotropy but remained identifiable on orientation maps; and disrupted tracts showed markedly reduced anisotropy such that could not be identified on orientation maps. The involvement of the anatomically assigned pathways in the two main groups is summarized in the following tables:

Table (2) Comparison between both groups as regard MRI findings (edema)

Edema	Benign N=11	Malignant N=21	X ²	P
No	9 (81.8%)	16 (76.2%)	0.13	>0.05 NS
Yes	2 (18.2%)	5 (23.8%)		

This table shows that prevalence of edema was higher among malignant group in comparison to benign group but with no significant difference in between by using chi-square test.

Table (3) Comparison between both groups as regard MRI findings (displacement)

Displacement	Benign N=11	Malignant N=21	X ²	P
No	1 (9.1%)	9 (42.9%)	3.8	<0.05 S
Yes	10(90.9%)	12 (57.1%)		

This table shows that prevalence of displacement was higher among benign group in comparison to malignant group with significant difference in between by using chi-square test.

Table(4) Comparison between both groups as regard MRI findings (infiltration)

Infiltration	Benign N=11	Malignant N=21	X ²	P
No	6 (54.5%)	9 (42.9%)	0.4	>0.05 NS
Yes	5 (45.5%)	12 (57.1%)		

This table shows that prevalence of infiltration was higher among malignant group in comparison to benign group but with no significant difference in between by using chi-square test.

Table (5) Comparison between both groups as regard MRI findings (disruption)

Disruption	Benign N=11	Malignant N=21	X ²	P
No	10(90.9%)	9 (42.9%)	4.5	<0.05 S
Yes	1 (9.1%)	12 (57.1%)		

This table shows that prevalence of disruption was higher among malignant group in comparison to benign group with significant difference in between by using chi-square test.

Analysis of data was done by IBM computer using SPSS (statistical program for social science version 12) as follows :

Description of quantitative variables as mean, SD and range

Description of qualitative variables as number and percentage

Chi-square test was used to compare qualitative variables between groups.

P value >0.05 insignificant P<0.05 significant

P<0.01 highly significant

4. Discussion

Neurosurgery for a brain tumor is a trade-off between maximum surgical resection on one hand and maximum sparing of functions on the other hand. Extensive tumor resection can reduce the risk of relapse (particularly gliomas with low grade malignancy) and allow subsequent radiotherapy or chemotherapy to be more effective. On the other hand, sparing "functionally relevant" zones and therefore preservation of motor, visual or language functions significantly improves the quality of life of these patients (*Romano et al., 2007*). For realizing these goals, many imaging modalities were used to assess brain tumors, which include conventional MRI, Positron Emission Tomography and functional MRI (*Fujiwara et al., 2004*). Knowledge of the structural integrity and location of certain white matter tracts with respect to an intracranial lesion is crucial for neurosurgical planning, both for defining the surgical access point and identifying the extent of tumor resection (*Romano et al., 2007*).

DTI is a significant advancement in the field of diagnostic imaging. It is, in fact, the only method capable of displaying cerebral white matter tracts in vivo, and it has been shown that this knowledge can assist the neurosurgeon in preoperative planning (*Yu et al., 2005*).

Diffusion- tensor imaging provides information on the directionality of water molecules at the cellular level, thus indicating the orientation of fiber tracts. From DW image data sets, the diffusivity of water within tissue can be determined. In tissue with an ordered microstructure, like cerebral white matter, orientation can be quantified by measuring its anisotropic diffusion. Diffusion- tensor calculations permit the characterization of diffusion in heterogeneously oriented tissue. The spatial orientation of myelinated fiber tracts can then be represented as distinct white matter maps in easily read, color-coded directional maps (*Witwer et al., 2002*). Recently, various investigators have used directional diffusion information to create maps of white matter connectivity (*Stieltjes et al., 2001*). These techniques may be valuable for tract identification when the white matter tracts are displaced by tumor (*Witwer et al., 2002*).

The most significant use of DTI, in particular, is to preoperatively confirm the integrity and location of displaced white matter tracts (*Romano et al., 2007*).

White matter tracts may be pathologically altered by tumor in several ways; specifically, they may be displaced, infiltrated by tumor and/or edema, or destroyed. Four imaging patterns were identified that presumably reflected these alterations on FA-weighted directional color maps. Unfortunately,

however, these alterations are not mutually exclusive in a given tumor or even in a given white matter tract. (Field *et al.*, 2004).

Our study, being the first to be conducted in our department of radiology, in Ain Shams University, aimed at exploring the value of the state of the art Diffusion Tensor MR Imaging in the preoperative assessment of brain tumors. The study was conducted on 32 patients with different types of brain tumors, to demonstrate how DT mapping further elucidate the complex relationship between a lesion and its surrounding white matter. Their age ranged from 1 to 74 years old with a mean age of 32.8 ± 18 years.

The majority of the studied cases were above 40 years, and mostly males (68.8%). The most frequent neurological clinical presentation was hemiparesis.

The tumors studied consisted of 3 low grade gliomas, 10 grade II-III glioma, 2 grade III glioma, 5 glioblastoma multiforme, 3 gliomatosis cerebri, 3 metastasis, 1 lymphoma, 3 brain stem gliomas, and 2 meningiomas.

Conventional contrast enhanced MRI followed by MR Diffusion Tensor Imaging were acquired in all of the studied population. H1 MR Spectroscopy was added in 22 cases, and combined fMRI- DTI was performed in 15 cases.

White matter tracts involvement by a tumor was categorized into four patterns on DT mapping and Tractography, these are: *edema*, *displacement*, *infiltration* and *disruption*. Quantitative analysis was also obtained by measuring the FA and ADC values of each affected tract, with comparison with the contra lateral homologous tracts in the unaffected hemisphere in unilateral tumors, or age and sex matched controls in bi-hemispheric or brain stem lesions.

This classification of tract involvement was similar to the studies done by Witwer *et al.*, 2002 and Field *et al.*, 2004. However, this was slightly different from the classification done by Yu *et al.*, 2005, who divide the relationship between tumor and tracts into three types only; type I: simple displacement, type II: displacement with disruption, type III: simple disruption.

In the present study we classified the patients into two groups: *Benign group*: including low grade and benign tumors, and, *malignant group*: including high grade glial tumors, metastasis and lymphoma.

There was a statistical difference between these groups, with prevalence of displacement among benign group and disruption among the malignant group with P value < 0.05. This in contrary to the effect of edema and infiltration where there was no significant difference between the two groups, with P value > 0.05. This partially agreed with the study done by Field *et al.*, 2004. They identified

displacement and edema patterns in both benign and malignant tumors. Infiltration was limited to infiltrating gliomas, but there were only two of these. Destruction was limited to malignant tumors, in both high and low grade malignancies. This signifies that DTI has a potential role in characterization of brain tumors and differentiation between benign and malignant neoplastic lesions.

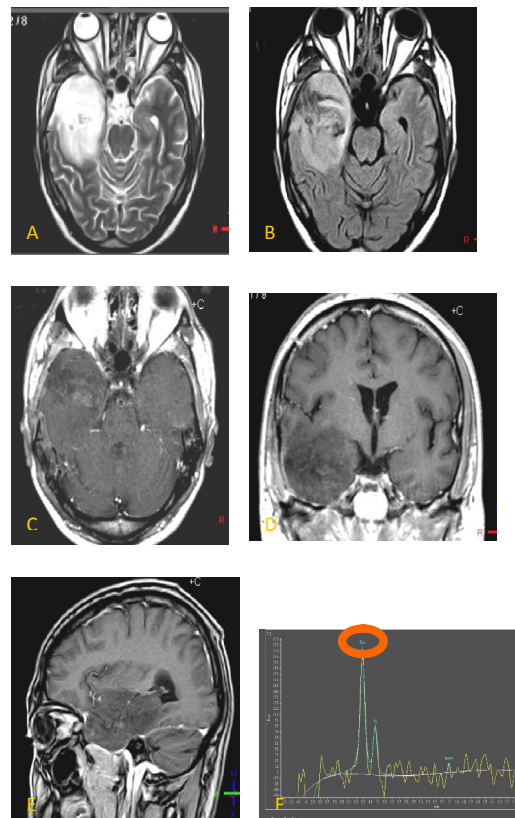


Fig. 12: 36 years old male patient known to have right temporal glioma and coming for follow up after therapy.

A) Axial T2WI MR image: Right temporo-parietal infiltrative expansive hyper intense SOL .

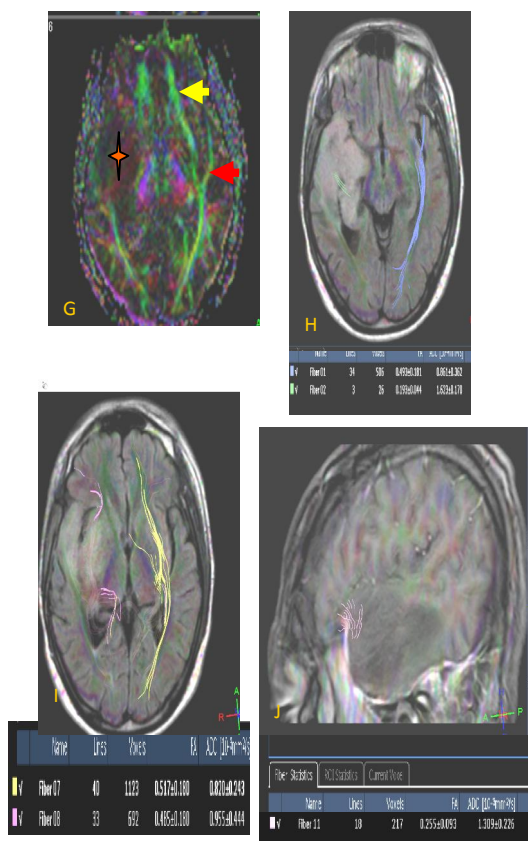
B) Axial FLAIR MR image "at the same level of A": the lesion exhibits heterogeneous, predominantly high, signal with minimal surrounding edema .

C) Axial post contrast T1WI +MTC: there is a small enhancing portion at infero-medial aspect of the lesion and inner non enhancing necrotic areas.

D) , E) Coronal (D) and sagittal (E) contrast enhanced T1WI : the lesion is faintly enhancing.

F) H1-MR Spectroscopy (single voxel, intermediate echo spectrum; TE=144): the lesion shows evident elevation of choline , denoting accentuated cell membrane turnover, especially at the enhancing portion.

MR Perfusion (not shown) revealed remarkable elevation of perfusion with rCBV ratio reaching 4 as compared to contra lateral normal side.



g) Axial color coded DTI map: the intact green fibers of the inferior longitudinal fasciculus (ILF) (red arrow) and the inferior occipito frontal fasciculus (IOF) (yellow arrow) within the unaffected temporal lobe of the left hemisphere are well identified. Corresponding fibers in the contra lateral temporal lobe are completely obliterated within the lesion (red asterix).

H) Tractography of both ILF: axial color coded DTI map overlaid on axial FLAIR MR image demonstrating intact fibers in the left side with normal course, while on the right side the fibers are disrupted with marked reduction of the FA values of the remaining identifiable fibers compared to the normal side with reciprocal increase in the ADC value.

I) Tractography of both IOF: axial color coded DTI map overlaid on axial FLAIR MR image demonstrating intact fibers in the left side, while on the right side the fibers are barely identified with marked reduction of the FA values of the remaining identifiable fibers compared to the normal side with reciprocal increase in the ADC value.

j) Tractography of the right uncinus fasciculus: sagittal color coded DTI map overlaid on sagittal post contrast T1WI MR image: the fibers appears disrupted with marked loss of anisotropy and increase in diffusivity.

The DTI and Tractography findings are in keeping with the diagnosis of high grade neoplasm as evident by disruption of the related fiber tracts.

We recommend to do gross total resection without undue concern for preserving these tracts or risking new functional deficits postoperatively.

Several studies have addressed the problem of discrimination between bland edema (tumor free) from infiltrating tumor (tumorous edema) through the analysis of ADC and FA values with mixed results. *Tropine et al., 2004*, demonstrated that DTI may not

reliably distinguish tumor infiltration from vasogenic edema in supratentorial gliomas glioblastomas. *Price et al., 2003* examined peritumoral DTI white matter "signatures" at 3 T field strength and concluded that more work is needed to establish the relationship between DTI parameters and tumor characteristics. *Sinha et al., 2002*, found significant difference of ADC values among apparently normal white matter, edematous brain and enhancing tumor margins, with the diffusion anisotropy data added no benefit in tissue differentiation. *Lu et al., 2003*, demonstrated that there are clear differences in the diffusion characteristics of the vasogenic edema surrounding brain tumors, when compared with those of normal-appearing white matter. In addition, peritumoral MD specifically may be useful in the preoperative discrimination of high-grade gliomas and metastatic tumors; however, the changes in FA showed no such statistical significance. The comparable decrease in FA for both disease processes is attributable to a large water influx surrounding metastatic tumors and contributions of both increased water content and tumor infiltration surrounding gliomas.

The present study must be encountered among those that were unable to discriminate tumor from edema on the basis of ADC and FA values alone. However, we have taken an additional step by analyzing the directional color map and performing tractography for the affected fibers, and our preliminary results are encouraging. We found that vasogenic edema in the absence of bulk mass displacement tends to exhibit reduced FA without associated directional changes, as reflected by normal hues on directional color maps. This is in contrast to infiltrating tumors, where the FA reduction was accompanied by a more severe form of disorganization reflected in abnormal hues on directional color maps. There did not appear to be sufficient bulk mass displacement to account for these changes. These findings strongly agreed with *Field et al., 2004*.

One situation in which DTI has high diagnostic capability is in cases of gliomatosis cerebri, which has a specific histopathological behavior. The neoplastic cells form parallel rows among nerve fibers preserving them, yet with destruction of the myelin sheath (*Cruz and Sorensen, 2006*). This results in preservation of the location and orientation of the fiber tracts on color coded DTI mapping with mild reduction of FA values of the involved tracts.

Three cases of gliomatosis cerebri were included in this current study, one of them was proved by histopathology, and two cases were diagnosed based on MR spectroscopy and MR perfusion data (*Fig. 13*). The DTI functional anisotropy maps and Tractography demonstrated that

the related fiber tracts were preserved, yet with mild reduction of in their FA values, reflecting normal underlying cytoarchitectural pattern of the nerve fibers.

As regard the brain stem tumors *Heltona et al., 2006*, had the first study to evaluate the quantitative the quantitative DTI measures of FA and ADC in pediatric patients with diffuse and focal **pontine tumors** and in those with "normal" brain stem, as determined by conventional MR imaging. Their results indicated that DTI analysis can delineate tract invasion and displacement. These tools may help to better discriminate between diffuse and focal brain stem **tumors** in the future and may be useful for guiding surgical biopsies. DTI analysis also shows promise of providing quantitative measures of risk stratification, prognosis, and treatment response.

This study included 3 cases with infiltrative pontine gliomas, two of them was in the pediatric age group. DTI has well demonstrated the affection of brain stem fiber tracts including; the corticospinal tract, medial lemniscus and transverse pontine fibers with various degrees of involvement as deduced from the quantitative ADC and FA measures as well as fiber tracking. The conventional MRI features was typical for infiltrative gliomas in the pediatric cases, however, it was slightly deceiving in the adult case. The lesion exhibited focal enhancement pattern while DTI demonstrated infiltration of the tracts beyond the enhancing tumor margin evident on DT color map and Tractography. This was confirmed by MR spectroscopy, showing evident elevation of Choline metabolic peak beyond the enhancing margin denoting neoplastic infiltration.

Diffuse pontine tumors comprise a group of malignant tumors with a much poorer prognosis than that of focal brain stem tumors. Pontine tumors account for about 15% of pediatric brain tumors and comprise approximately 20%–30% of posterior fossa tumors. Histopathologically, these diffuse pontine tumors are usually differentiated WHO grade II fibrillary astrocytomas or WHO grade III anaplastic astrocytomas at diagnosis and are known to infiltrate between normal axonal fibers (*Lesniak et al., 2003*). Although the appearance of focal brain stem tumors and that of diffuse brain stem tumors typically differ by conventional MR imaging, distinguishing focal from diffuse involvement is sometimes imprecise. The discovery of a method that distinguishes these 2 types of tumors is valuable because the treatment and prognosis for the brain stem tumors are substantially different. On T2-weighted MR images, focal tumors are typically well marginated, often enhance, may be exophytic, and occupy <50% of the axial diameter of the brain stem, whereas diffuse tumors are poorly marginated, rarely enhance, occupy more than 50%

of the axial diameter of the brain stem, lack an exophytic component, and commonly engulf the basilar artery (*Barkovich, 2000*).

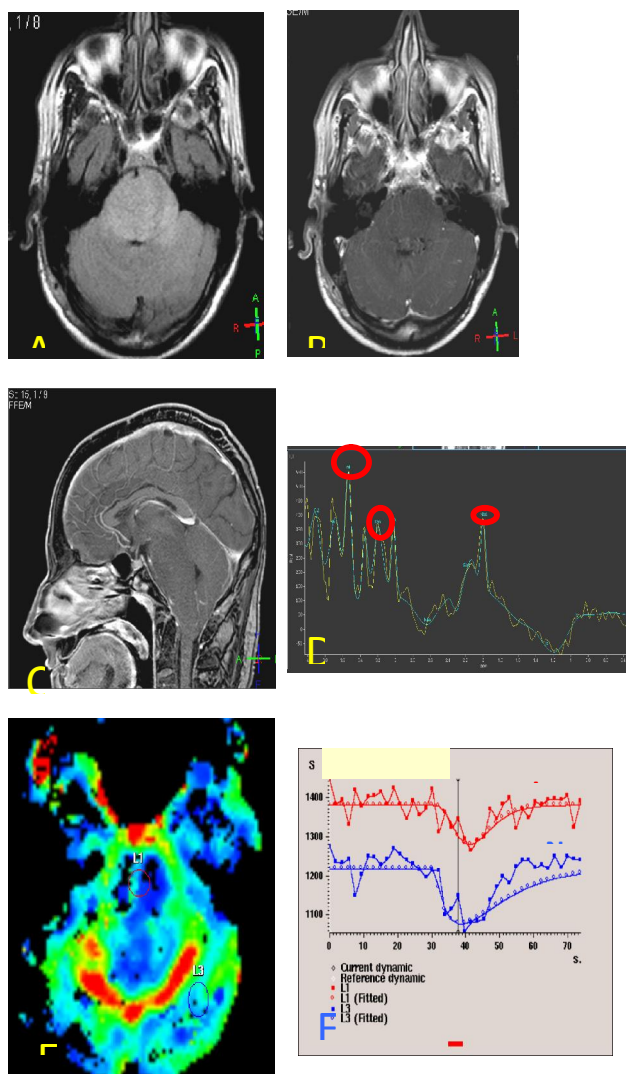
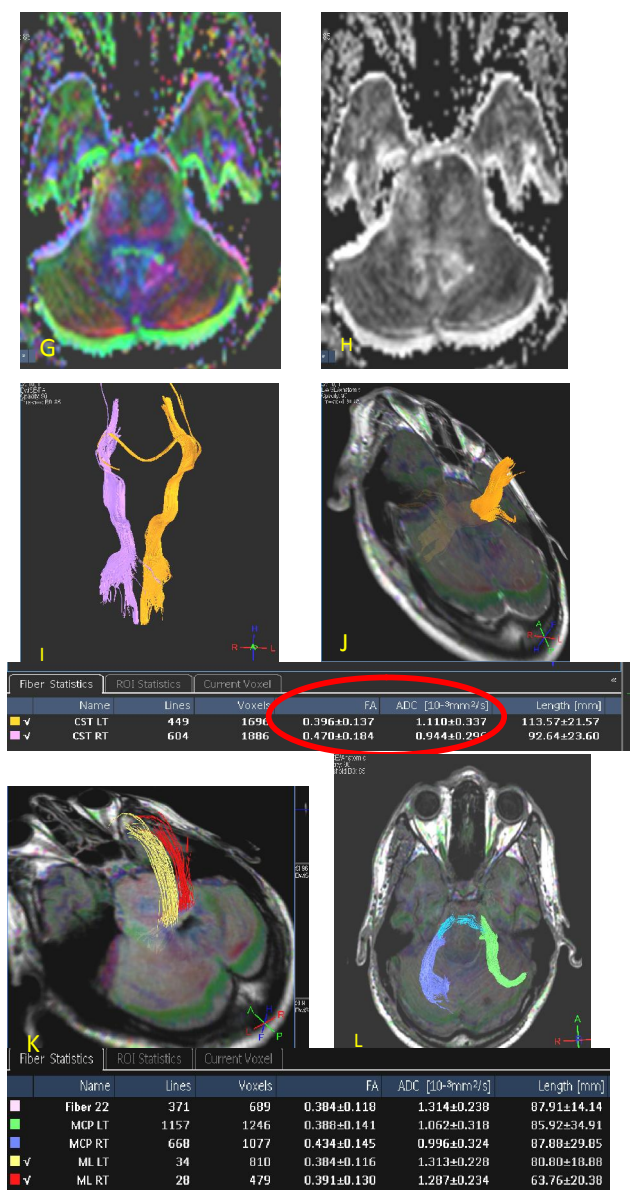


Fig. 13: 47 years old male patient complaining of symptoms of raised intracranial tension. He underwent ventriculo-peritoneal shunt to relieve his symptoms.

- A. Axial FLAIR MRI** shows diffuse signal abnormality and enlargement of the Pons with involvement of the cerebellum through the middle cerebellar peduncles. The fourth ventricle is encroached upon and attenuated.
- B. Axial post contrast T1WI+MTC:** The lesion does not show any enhancement.
- C. Sagittal post contrast T1WI :** The lesion extends to involve the medulla and midbrain with relative preservation of underlying brain architecture.
- D. H1 MR Spectroscopy,** single voxel, intermediate echo spectra (TE=144) shows marked elevation of myoinositol (mI), mildly increased choline (Cho) and decreased NAA.
- E. MR Perfusion color coded map:** the lesion is hypovascular.
- F. MR Perfusion dynamic curves** show low rCBV of the lesion (value of 1) compared to normal cerebellar hemisphere (value of 2.8) which correlates with lack of vascular hyperplasia.



G. Axial color map at the level of the brain stem: The corticospinal tracts coded in blue are expanded yet retaining their anatomical site and orientation with normal color hue (red arrow). The transverse pontine fibers (green arrow) and medial lemniscus (black arrow) are also involved but to a lesser extent. The ML fibers are backwardly displaced by virtue of the expanded CST.

H. Axial FA map at the same level: the brain stem tracts show mildly reduced anisotropy.

I. Tractography of the both CST: The fibers are retaining their normal location with maintained FA values.

J. Tractography of the left CST overlaid on anatomical T1WI+color coded map: the tracts are passing unaffected through the tumor denoting normal underlying cytoarchitectural pattern. , L)

K. Tractography of both ML (K) and MCP (L) overlaid on axial 3D T1WI+color coded DT map. The tracts same findings as in Fig. J.

Conventional MR imaging has demonstrated prognostic value in the treatment of brain stem tumors, but white matter appears homogeneous on MR images; therefore, this method cannot precisely define essential aspects of tract location, displacement, or invasion. In contrast, diffusion tensor imaging (DTI) detects anisotropic diffusion, thereby allowing the visualization of major fiber tracts in the brain stem. Thus, DTI may provide information about tumor involvement in white matter tracts (*Helton et al., 2006*).

As a part of self criticism, our study was lacking the postoperative follow up the patients to validate the impact of DTI on surgical planning ,as all the cases were performed in an out patient radiology center and not in hospital institution.

The preoperative depiction of a tumor relationships to white matter tracts using DTI and directional color mapping proved to be extremely useful to the neurosurgeons in a study done by *Field et al., 2004*. knowing that a white matter tract was intact but displaced by a tumor to a new location allowed the surgeon to adapt his approach to preserve this tract during resection. Similarly, knowing that a specific white matter tracts were destroyed by a tumor allowed the surgeon to attempt gross total resection without undue concern for preserving these tracts of risking new functional deficits postoperatively. Neurosurgeons at the authors' institution now obtain preoperative DTI routinely for any tumors thought to potentially involve critical white matter fiber tracts.

Yu et al., 2005, proposed to try one 's best to preserve displaced white matter tract while maximizing tumor resection, to enlarge the extent of tumor resection while preservation of the displaced part of the tract in cases where destruction and displacement of the tract co-exist, and maximize tumor resection while preservation of the residual part of the tract in cases with simple disruption.

Functional MRI was combined with DTI as a preoperative assessment for surgical planning of brain tumors in 15 cases in this study. We used the cortical activation areas as seed points to improve fiber tracking results. Also, we obtained essential information on the location of eloquent cortical areas in relation to a tumor to determine the risk of injury during surgery. The integration of both high-resolution anatomic (T1-weighted) data with fMRI data in the fiber-tracking procedure made an evaluation of the spatial relationship between tracked fibers and tumor borders possible. Separation of the different components of the corticospinal tract especially the hands and feet fibers was also possible.

Smits et al., 2007 had incorporated FMRI and DTI in the preoperative assessment in a series of

patients with brain tumors. They showed that tracking of the CST directly from the fMRI activation area can be used to visualize and distinguish the different components of the CST, especially the hand and foot fibers. In a healthy volunteer, the presented method showed that the tracked hand, foot, and lip fibers follow a distinct course, the foot fibers coursing posteromedially to the hand fibers within the posterior limb of the internal capsule (PLIC). This distribution within the corticospinal tract confirmed previous findings by *Holodny et al., (2005)* who also studied the CST by using DT tractography and found the same location and internal organization of the separate CST components within the PLIC. Both studies indicate that the hand and foot fibers are organized along the short (left-right) axis of the PLIC, rather than along the long (anteroposterior) axis of the PLIC, as has been previously assumed. (*Gray, 1989*)

Smits et al., showed that tracking the CST based only on anatomic landmarks may not be sufficient to visualize reliably the CST and that fMRI-based seed region-of-interest placement may be necessary to visualize the CST in its entirety. Furthermore, DT tractography of the CST was seen to be hampered in cases of anatomic distortion due to a mass effect of the lesion or in cases of altered diffusivity due to tumor infiltration or perifocal edema in the region of the CST. Tracking improved when the fMRI-based seed region-of-interest approach was used, thus providing more reliable preoperative information.

Several limitations need to be considered :

Firstly, there is no "gold standard" for in vivo Tractography. In fact, DTI is the only method that permits the calculation and visualization of fiber tracts trajectories in vivo.

Secondly, DTT is a user defined process. In particular, the tracking results were found to vary according to FA threshold, angular threshold, step length and numbers of sampling in a voxel length. Choosing different parameters can produce different fibers. And tracked volumes are also dependent on the size and locations of the seed ROIs.

Despite these intrinsic limitations, our study clearly showed that this technique can be very useful for correct preoperative planning and should be considered an important step forward in modern neuroradiological diagnostics for surgical planning in patients suffering from intracranial tumors.

In conclusion, the effect of cerebral neoplasm on white matter pathways is much more better evaluated with the aid of DTI than on conventional MRI. There can be one or more of four distinct patterns of white matter tracts alteration by a tumor. In this small cohort of patients the information provided by DT imaging further defined precise

relationships between the sub cortical white matter structures and the cerebral neoplasm. This potentially has a role in tumor characterization, and more importantly in surgical planning. MR Tractography offers the neurosurgeon an anatomical panoramic view and the opportunity for improved planning of surgical resection of intracranial lesions and in predicting the extent of safe resection.

Despite its limitations and potential pitfalls, DTI has proven to be the only clinically feasible method of demonstrating the white matter tracts *in vivo*.

Combination of fMRI and DTI fiber tracking appears to be a more promising tool in the preoperative planning of brain tumors. fMRI-based DT tractography is superior to DT tractography on the basis of anatomic landmarks alone, because only with fMRI-based DT tractography is a distinction between the several components of the CST possible. Furthermore, it allows decreasing the FA threshold if necessary and provides an improved visualization of the CST, in particular when fiber tracking is hampered by the presence of tumor or perifocal edema.

These new techniques should be considered an important step forward in modern neuro-radiological diagnostics for surgical planning of cerebral neoplasm.

Corresponding author

Mohsen Gomaa and Yosra abdel zaher
Department of Radiodiagnosis, Ain Shams University
mostafa_redio@yahoo.com

References:

1. Barkovich AJ. Pediatric neuroimaging. In: Barkovich AJ. Intracranial, Orbital, and Neck Tumors of Childhood. 3rd ed. Philadelphia, Pa: Lippincott Williams & Wilkins;2000 :462–70
2. Basser PJ, Pierpaoli C Microstructural and physiological features of tissues elucidated by quantitative-diffusion-tensor MRI. J Magn Reson 1996;111:209–19
3. Cruz CH and Sorenson AG. Diffusion Tensor Magnetic Resonance Imaging of Brain Tumors. Magn Reson Imaging N Am 2006;14:183-202
4. DeBoy CA, Zhang J, Dike S, et al High-resolution diffusion tensor imaging of axonal damage in focal inflammatory and demyelinating lesions in rat spinal cord. Brain 2007;130:2199–210
5. Fox R.J., Cronin T, Lin J., Wang X., Sakai K, Ontaneda D, Mahmoud SY, Lowe MJ, and Phillips MD. Measuring Myelin Repair and Axonal Loss with Diffusion Tensor Imaging AJNR Am J Neuroradiol 2011 32: 85-91.

6. Field AS, Alexander AL, Hasan KM, Wu YC, Witwe B and Badie B. Diffusion tensor eigenvector directional color imaging patterns in the evaluation of cerebral white matter tracts altered by tumor. *Journal of Magnetic Resonance Imaging* 2004;20:555-562.
7. Fujiwara N, Sakatani K and Katayama Y. Evoked-cerebral blood oxygenation changes in false negative activations in BOLD contrast functional MRI of patients with brain tumors. *Neuroimage* 2004;21:1464-71.
8. Gray H. Neurology. In: Williams P, Warwick R, Dyson M, et al., eds. *Gray's Anatomy*. Edinburgh, UK: Livingstone; 1989:1073
9. Heltona KJ, Phillipsa NS, Khana RB, Boopc FA, Sanfordc RA, Zoua P, Lib CS, Langstona JW and Ogga RJ. Diffusion Tensor Imaging of Tract Involvement in Children with Pontine Tumors *American Journal of Neuroradiology* 2006;27:786-793.
10. Holodny AI, Gor DM, Watts R, et al. Diffusion-tensor MR tractography of somatotopic organization of corticospinal tracts in the internal capsule: initial anatomic results in contradistinction to prior reports. *Radiology* 2005;234:649–53
11. Karimi S, Nicole M, Kyang K, et al. Advanced MR techniques in brain tumor imaging. *Appl.Rad.* 35(5):9-18,2006.
12. Lesniak MS, Klem JM, Weingart J, et al. Surgical outcome following resection of contrast-enhanced pediatric brainstem gliomas. *Pediatr Neurosurg* 2003;39:314–22
13. Lu S, Ahn D, Johnson G, Cha S. Peritumoral diffusion tensor imaging of high-grade gliomas and metastatic brain tumors. *AJNR Am J Neuroradiol* 2003;24:937–41.
14. M. Clinton Miller, Ph.D, Rebecca G. Knapp: *Clinical epidemiology and biostatistics*, published by Williams & Wilkins, Maryland: 3rd edition 1992.
15. Mori S, Frederiksen K, Van Zijl PCM, Stieltjes B, Kraut MA, Slaiyappan M, et al. Brain white matter anatomy of tumor patients evaluated with diffusion tensor imaging. *Ann Neurol* 2002;51: 377–80.
16. Pierpaoli C, Basser PJ. Toward a quantitative assessment of diffusion anisotropy. *Magn Reson Med* 1996;36:893–906
17. Okada T, Miki Y, Fushimi Y, et al. Diffusion-tensor fiber tractography: intraindividual comparison of 3.0-T and 1.5-T MR imaging. *Radiology* 2006;238:668–678.
18. Price SJ, Burnet NG, Donovan T, Green HAL, Pena A, Antoun NM, et al. Diffusion tensor imaging of brain tumors at 3T: a potential tool for assessing white matter tract invasion. *Clin Radiol* 2003;58:455–62.
19. Provenzale JM, Mukundan S and Barboriak DP. Diffusion weighted and perfusion MR imaging for brain tumor characterization and assessment of treatment response. *Radiology* 239:632-649.2006.
20. Romano A, Ferrante M, Cipriani V, Fasoli F, Andrea GD, Fantozzi LM, Bozzao A. Role of magnetic resonance tractography in the preoperative planning and intraoperative assessment of patients with intra-axial brain tumours. *Radiol med* 2007;112:906-920.
21. Sinha S, Bastin ME, Whittle IR, et al. Diffusion tensor MR imaging of high-grade cerebral gliomas. *AJNR Am J Neuroradiol* 2002;23:520–27
22. Smits M, Vernooij MW, Wielopolski PA, Vincent AJPE, Houston GC and van der Lugta A. Incorporating Functional MR Imaging into Diffusion Tensor Tractography in the Preoperative Assessment of the Corticospinal Tract in Patients with Brain Tumors. *American Journal of Neuroradiology* 2007; 28:1354-1361.
23. Tropine A, Vucurevic G, Delani P, et al. Contribution of diffusion tensor imaging to delineation of gliomas and glioblastomas. *J Magn Reson Imaging* 2004;20:905–12
24. Wakana S, Jiang H, Nagae-Poetscher LM, van Zijl PC, Mori S. Fiber tract-based atlas of human white matter anatomy. *Radiology* 2004; 230:77–87.
25. Witwer BP, Moftakhar R, Hasan KM, Deshmukh P, Haughton V, Field A, et al. Diffusion-tensor imaging of white matter tracts in patients with cerebral neoplasm. *J Neurosurg* 2002; 97:568–75.
26. Yu CS, Li KC, Xuan Y, Ji XM and Qin W. Diffusion tensor Tractography in patients with cerebral tumors: A helpful technique for neurosurgical planning and postoperative assessment. *European Journal of Radiology* 2005; 56: 197-204.

Detection of Genotoxicity of Phenolic Antioxidants, Butylated hydroxyanisole and *tert*-butylhydroquinone in Multiple Mouse Organs by the Alkaline Comet Assay

Ramadan, A.M. Ali^{1,2,*}, Takayoshi Suzuki²

¹Zoology Dept., College for Girls for Science, Arts and Education, Ain-Shams Univ., Heliopolis, Cairo, Egypt

²Division of Genetics and Mutagenesis, National Institute of Health Sciences, 1-18-1, Kamiyoga, Setagaya-ku, Tokyo 158, Japan

ramadanali27@gmail.com

Abstract: In this study we tested the genotoxicity of three widely used phenolic antioxidants, butylated hydroxyanisole (BHA) and *tert*-butylhydroquinone (t-BHQ) in multiple mouse organs using the alkaline comet assay. Tissue samples from four organs (stomach, liver, kidney and bone marrow) were collected from mice at 3 and 24 hrs post treatment with BHA (800 mg/kg) or t-BHQ (400 mg/kg) and examined for genotoxicity. The two compounds induced significant increase in DNA migration in a time dependant manner in specific organs. Extensive DNA damage was observed in stomach cells at 24 hrs post treatment in treatment groups. In addition to stomach, t-BHQ treatment induced significant increase in DNA migration in liver and kidney cells also. Although increased DNA damage was found in kidney cells of treatment groups at 3 hrs time point, at later time point it was persistent only in mice treated with tBHQ and in other treatment group (BHA) it appeared to be recovered with time. Evidently, bone marrow cells did not show genotoxicity in response to treatment with t-BHQ and BHA.

[Ramadan, A.M. Ali and Takayoshi Suzuki **Detection of Genotoxicity of Phenolic Antioxidants, Butylated hydroxyanisole and *tert*-butylhydroquinone in Multiple Mouse Organs by the Alkaline Comet Assay**] Life Science Journal 2012;9(1):177-183]. (ISSN: 1097-8135). <http://www.lifesciencesite.com>. 25

Key words: BHA; t-BHQ; comet assay; mice; bone marrow; liver; kidney; stomach; ENU.

1. Introduction

Butylated hydroxyanisole (BHA, 3-*tert*-butyl 4-hydroxyanisole) and its *O*-demethylated metabolite *tert*-butylhydroquinone (t-BHQ) are synthetic phenolic food antioxidants widely used to protect oils, fats and shortenings from oxidative deterioration and rancidity (Aluyor Ori-Jesu, 2008; Finley *et al.*, 2011). Both compounds are generally non-mutagenic and nearly all short-term genotoxicity tests including the classic *Salmonella typhimurium* (with or without S9 fraction), unscheduled DNA synthesis assay using rat hepatocytes, and except both positive and negative results with and without activation respectively in Chinese hamster cells for chromosomal aberration and sister chromatid exchange are negative (Rogers *et al.*, 1985; Williams *et al.*, 1990). However, chronic dietary administration of BHA resulted in papilloma and carcinoma formation in the forestomachs of rats, mice and hamsters (IARC, 1986; Clayson *et al.*, 1990; Chandra *et al.*, 2010). In fact, both BHA and t-BHQ have shown to contain both carcinogenic and anticarcinogenic properties (Whysner *et al.*, 1994; Hirose *et al.*, 1997; Kahl, 1997; Gharaviet *et al.*, 2007). While, anticarcinogenic activity of BHA has been ascribed to its ability to induce Phase II metabolic enzymes and its free radical trapping activity (Williams and Iatropoulos, 1997; Li *et al.*, 2005; Kadoma *et al.*, 2008; Cemeli and Anderson, 2011), its carcinogenicity has been often linked to its

quinone-forming metabolites, a property that BHA shares with benzene. Quinones are highly reactive molecules, which can bind to biological macromolecules (O'Brien, 1991; Tuet *et al.*, 2011) and induce chromosomal loss or chromosomal breakage (Dobo *et al.*, 1994; Jacobus *et al.*, 2008).

The scope of this research is to determine the *in vivo* genotoxic effects of t-BHQ and BHA in different organs of mouse. In this study we conducted the single cell gel electrophoresis assay (Comet assay) on four organs (stomach, liver, kidney and bone marrow) of mice treated with t-BHQ (400 mg/kg) or BHA (800 mg/kg). To identify possible time dependent effect, tissue samples were collected on two occasions, 3 and 24 hrs post treatment and subjected to the alkaline version of the comet assay. The comet assay is a sensitive cytogenetic assay with advantages of detecting broad spectrum of DNA damages which may lead into DNA strand breaks, the need of small number of cells per sample, and the short time needed to complete a study (Tice *et al.*, 2000). In addition, the comet assay can be applied to any tissue in the given *in vivo* model, and has potential advantages over other *in vivo* genotoxicity tests methods, which are reliably applicable to one or few tissues. This is very important for investigation of suspected tissue specific-genotoxic activity, which include 'site of contact' genotoxicity.

Material and Methods

Chemicals

All chemicals used in this study were purchased from Wako Pure Chemical Industries, Ltd. (Osaka, Japan).

Animals and treatment.

Male ddY mice were obtained from Japan SLC (Shizuoka, Japan) at 7 weeks of age and used after one week of acclimatization. They were maintained at 20–24°C and 55–65% humidity with a 12-hr light-dark cycle and fed commercial pellets (Oriental Yeast Industries Co., Tokyo, Japan) and tap water *ad libitum*. Aqueous solutions of t-BHQ (400 mg/kg) and BHA (800 mg/kg) were administered intragastrically to groups of three mice at a dose level of 10 ml/kg. A positive control (ENU, 20 mg/kg) group of two mice were treated at the same time in the same manner. The animals were sacrificed by cervical dislocation at 3 hr and 24 hrs after treatment and four organs - bone marrow, liver, kidney and stomach - were dissected out. Tissue samples were collected from four untreated mice at the latter sampling point (24 hrs) and treated as the negative control.

The tissue samples except bone marrow were washed in saline, minced, suspended at a concentration of 1 g/ml in ice cold homogenizing buffer (HBSS with 20 mM EDTA, 10% DMSO, pH 7.5) and homogenized gently using a Dounce's homogenizer. The marrow was collected from the femur bones and suspended in 1 ml of chilled homogenizing buffer. The cell suspensions were diluted in chilled homogenizing buffer appropriately and subjected to the alkaline comet assay immediately.

Comet assay

The alkaline comet assay was performed basically as described by Miyamae *et al.* (1998) with few modifications. The cell suspensions prepared as above were mixed 1:1 (v/v) with 1% low melting point (37°C) agarose (LMA) prepared in PBS, pH 7.4 and 75 µl of the mixture was quickly layered on a 1% normal melting point agarose (NMA) (prepared in distilled water) precoated and overnight dried slides and covered with a coverslip. Then the slides were placed on a chilled plate to allow complete polymerization of agarose. Finally 75 µl of 0.5% NMA in PBS was quickly layered in the same manner after removing the coverslip and allowed to solidify on chilled plate. The slides were immersed in freshly made chilled lysis solution (2.5M NaCl, 100mM Na₂EDTA, 10mM Trizma base, 10% DMSO and 1% Triton X-100; pH 10.0) in dark at 4°C for 60 min. The slides were then placed in a horizontal electrophoresis tank containing electrophoresis buffer (300mM NaOH and 1mM Na₂EDTA; pH 13.0) for

10 min, allowing salt equilibration and further DNA unwinding before electrophoresis at 25 V (0.8V/cm), 300 mA for 20 min. The slides were washed three times (5 min each) with chilled neutralizing buffer, 0.4M Tris-HCl (pH 7.5). After the third wash, the slides were stained with 50 µl EtBr (20 µl/ml) and covered with a coverslip. To prevent drying, the slides were stored in a humidified container until microscopic examination.

The slides were examined at 200x magnification using Olympus fluorescent microscope. All slides were coded and examined blindly. A total of 1000 randomly selected cells from two replicate slides (500 cells per slide) were examined per sample. The comets were classified into five categories (Type 1 – Type 5) depending on the fraction of DNA migrated out into the tail, and thus increasing degrees of damage (Miyamae *et al.*, 1998). The comets were assigned a value of 0, 1, 2, 3 or 4 (from undamaged, 0, to maximally damaged, 4). Thus, the total score for 1000 comets ranged from 0 (all undamaged) to 4000 (all damaged) in arbitrary units (Visvardis *et al.*, 1997; Piperakis *et al.*, 1998). In this method a large number of cells can be examined in a short time.

Statistical analysis

Results of the different treatment groups were compared to data obtained from four untreated mice using Students' one-tailed *t*-test. Significance was indicated by *P* values <0.05.

3. Results

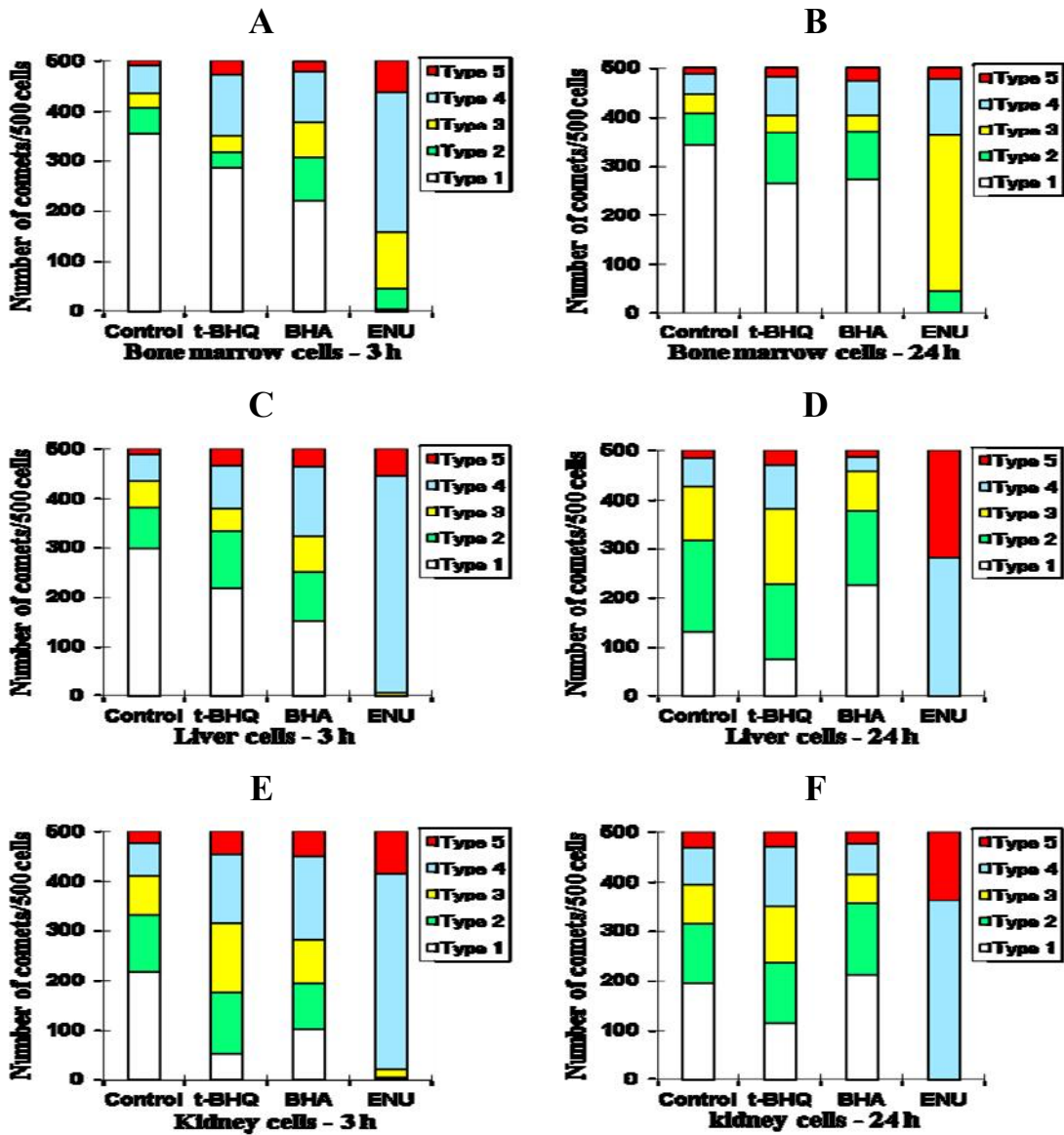
Table 1 presents the comet data measured by visual scoring from four organs (bone marrow, liver, kidney and stomach) from mice intragastrically treated with t-BHQ (400mg/kg b.w.) or BHA (800 mg/kg b.w.) for 3 and 24 hr. In this experiment comet data obtained from four untreated mice were treated as the negative control and used for comparison. Among t-BHQ treated animals, 24 hr after exposure mean DNA migration score was significantly (*P*<0.05) high in 3 organs (stomach, liver and kidney), although at earlier time point relative to control value it was different significantly only in kidney. In bone marrow the induced DNA strand breaks were not significant at both time points.

Exposure to BHA resulted in significant increase in DNA migration in a time dependent manner in specific organs. Although significant (*P*<0.05) increase in DNA damage was observed among stomach tissues at both sampling points, in kidney it occurred only at 3 hr time point and then decreased with time. Following BHA treatment liver and bone marrow cells did not yield any significant increase in mean DNA migration. ENU (20 mg/kg) treatment

produced highly significant ($P < 0.001$) DNA damage in all four tested organs at both time points.

Figure 1 shows the distribution pattern of nuclear DNA expressed as the percent cells in the five comet classes from Type 1 (undamaged) to Type 5 (maximally damaged) in various organs of mice belonged to different treatment groups. Except in ENU (positive control) treated group, in other samples some cells/nuclei remained undamaged (category Type 1). At both sampling time points in all treatment groups greater numbers of comets showed high levels of DNA damage (category Type

4) in stomach cells. The frequency distribution of DNA damage among individual hepatocytes showed that the number of damaged cells and the extent of damage were greatest among mice treated with tBHQ (Figs. 1-C and 1-D). Similarly in renal cells the extent of DNA damage decreased with time in BHA treated animals (Figs. 1-E and 1-F). Higher levels of damage were observed in renal cells from t-BHQ treated mice. Among bone marrow cells in treatment groups (t-BHQ and BHA) over 50% of the cells showed no damage (Figs. 1-A and 1-B).



G

H

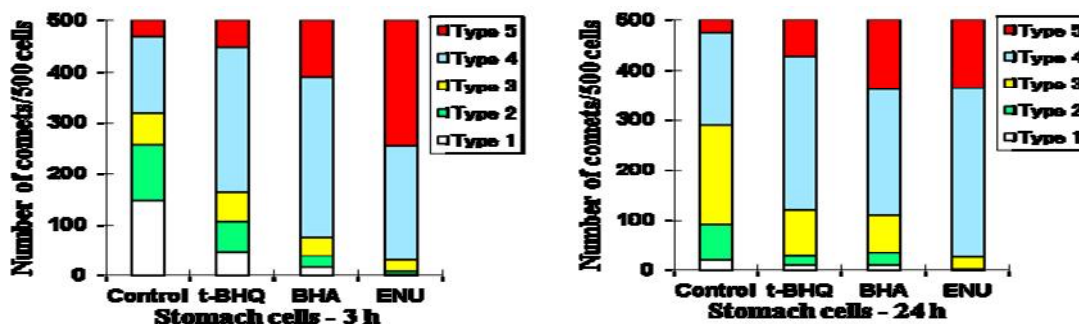


Fig. 1. Incidences of comet cells in mice treated with t-BHQ (400 mg/kg b.w.), BHA (800 mg/kg b.w.) and the positive control ENU (20 mg/kg b.w.) for 3 and 24 h. The comet cells derived from bone marrow (Figs. 1A and 1B), liver (Figs. 1C and 1D), kidney (Figs. 1E and 1F) and stomach (Figs. 1G

Table 1. Incidences of comet cells without type 1 in bone marrow, liver, kidney and stomach of mice treated with t-BHQ and BHA for 3 and 24 h.

Treatment	Pooled calculations of incidences of comets without type 0 (Average/500 cells \pm S.D.)							
	Bone marrow		Liver		Kidney		Stomach	
	3 h	24 h	3 h	24 h	3 h	24 h	2h	24 h
Control (Dis. H ₂ O)	146.3 \pm 125.3	156.5 \pm 16.3	202.0 \pm 116.0	369.5 \pm 99.3	283.3 \pm 110.3	305.3 \pm 94.6	350.0 \pm 109.4	479.5 \pm 14.5
t-BHQ (400 mg/kg)	213.7 \pm 136	234.3 \pm 37.7	274.5 \pm 61.3	425.2 \pm 59.6*	447.5 \pm 66.1	385.2 \pm 66.1*	453.5 \pm 29.1	490.3 \pm 8.1*
BHA (800 mg/kg)	279.3 \pm 171.5	226.0 \pm 45.1	345.0 \pm 40.5	237.2 \pm 72.2	397.2 \pm 79.1*	287.3 \pm 97.7	483.3 \pm 13.6*	490.1 \pm 11.6*
ENU (20 mg/kg)	495.0 \pm 6.0**	498.5 \pm 3.0**	500.0 \pm 0.0**	500.0 \pm 0.0**	500.0 \pm 0.0**	500.0 \pm 0.0**	498.25 \pm 2.1**	500.0 \pm 0.0**

n.b.

ns = non significant; * = (P<0.05); ** = (P<0.01); *** = (P<0.001)

4. Discussion

Considering the strong correlation between organ specific genotoxicity and organ specific carcinogenicity, the assessment of genotoxicity in multiple organs *in vivo* may indicate would be target organ(s) in humans and provide useful information for the evaluation of chemical safety. While other *in vivo* genotoxicity tests are limited to one or few tissues, the comet assay can be applied to any tissue provided that a single cell/nucleus suspension can be obtained. Therefore, in the present research, to test the tissue specific genotoxic effect of t-BHQ and, BHA mice were administered intragastrically with the test compounds and various organs were examined for genotoxicity using the comet assay. Results of this research suggest that the test compounds induced significant DNA strand breaks in stomach cells. The effect was more pronounced among BHA treated animals at both sampling occasions. With t-BHQ, a significantly higher degree of DNA damage was observed at 24 hr time point, although at earlier time point (3 hrs) the induced DNA damage in these treatment groups were not significantly different from control data. These observations again acknowledge the earlier findings

that stomach in particular forestomach in rodent is the target organ for BHA induced genotoxicity. It is also important to remember that there are several bioassay reports describing neoplasm-promoting effects of BHA and t-BHQ in the fore stomach when given after initiating carcinogens such as N-methyl-N-nitrosoguanidine (MNNG) (Takahashi *et al.*, 1986; Whysner *et al.*, 1994; Miyauchi *et al.*, 2002; Kuroiwa *et al.*, 2007; Liu and Russell, 2008), N-methyl-N-nitrosourea (NMU) (Imaida *et al.*, 1984; Tsuda *et al.*, 1984; García-González *et al.*, 2000), N,N-dibutyl nitrosamine (DBN) (Fukushima *et al.*, 1987). In this respect, there are studies, which demonstrated that BHA inhibits cell-to-cell communication (Williams *et al.*, 1990), which is often considered a marker for tumor promoters (Budunova and Williams, 1994; Yamasaki, 1996; Leithe *et al.*, 2006; Vinken *et al.*, 2009). In the bone marrow cells, although at earlier time point a non-significant increase in DNA migration was observed in BHA and t-BHQ treated animals, it was not persistent at latter time point and appeared to be recovered with time. *In vivo* BHA is metabolized to t-BHQ in the liver (Peters *et al.*, 1996; Moridani *et al.*, 2002). t-BHQ and HQ are further oxidized to

their respective quinone species, 1,4-benzoquinone and tertiary-butylquinone, which in turn may enter into a redox cycling between quinone and hydroquinone via semiquinone radicals and can generate reactive oxygen species (Peters *et al.*, 1996; Li *et al.*, 2002). These ROS may then react with cellular protein and DNA and thus cause large-scale chromosomal alterations (Cerutti, 1985). The test compounds used in this study have been reported to be nephrotoxic and can induce tumor in rodent kidney (Kari *et al.*, 1992; Shibata *et al.*, 1991; Tsuda *et al.*, 1984). Nonetheless, the evidence for genotoxicity as increased level of DNA migration in the liver and kidney was observed only in mice treated with t-BHQ. The nephrotoxicity of these compounds are often linked to their quinonethioether metabolites (Monks *et al.*, 1992) and their ability to react with DNA either directly (Jacobus *et al.*, 2008) or indirectly via reactive oxygen generation (Canales *et al.*, 1993; Li *et al.*, 2002; Li *et al.*, 2007). Hence, differences in metabolism of these compounds and ability of their metabolites to generate ROS could be a possible reason for the observed differences in toxicity (Kadoma *et al.*, 2008).

DNA strand breaks are associated both to the removal of DNA adducts by endonuclease and to the direct action of the chemicals and/or the free radicals produced during their metabolism, which then creates both single- and double-strand breaks in DNA (Bohr, 1991). Investigations of BHA and its metabolites have not demonstrated DNA adduct formation, as measured by the sensitive [³²P]postlabelling assay (Saito *et al.*, 1989). Previous research has showed that enzymatic oxidation of t-BTQ in rodent forestomach may occur via prostaglandin H synthase PHS (Schilderman *et al.*, 1993) or possibly a gastric peroxidase (Banerjee, 1988). It is widely believed that t-BHQ, a *O*-demethylated metabolite of BHA probably produces many of the toxic effects ascribed to BHA. It is also postulated that BHA and tBHQ act through ROS induced oxidative damage including DNA damage (Inverson, 1995). Supporting this suggestion studies have demonstrated the formation of 8-hydroxydeoxyguanosine, a marker for reactive oxygen formation and for DNA strand breaks (Okubo *et al.*, 1997; Schilderman *et al.*, 1995), in calf thymus DNA (Nagai *et al.*, 1996) and in isolated DNA and cultured rat hepatocytes (Li *et al.*, 2002) treated with tBHQ. Peters *et al.* (1996) have demonstrated that tBHQ and its glutathione conjugates are capable of catalyzing 8-hydroxydeoxyguanosin formation and thus induce oxidative DNA damage. Further, Dobo and Eastmond (1994) have demonstrated the role of reactive oxygen species in the chromosomal breakage induced by tBHQ in a prostaglandin H synthase containing Chinese hamster

V79 cell line. Considering these findings, although tBHQ and BHA are generally considered nongenotoxic, the DNA damage observed in this experiment may be related to their indirect action on DNA via ROS mechanism. Since toxicity of these compounds are often ascribed to their metabolic products such as quinonethioethers and hence differences in the metabolism of these compounds may play an important role in determining the target organ of toxicity.

Corresponding author

Ramadan A. M. Ali
Department of Zoology, Univ. College for Women,
Ain Shams University, Egypt
ramadanali27@gmail.com

References

- Aluyor E. and Ori-Jesu M. (2008). The use of antioxidants in vegetable oils – A review. *Afri. J. Biotechnol.*, 7 (25): 4836-4842.
- Banerjee K. (1988). Membrane peroxidase. *Mol. Cell Biochem.*, 83: 105-128.
- Bohr A. (1991). Gene specific DNA repair. *Carcinogenesis*, 12: 1983-1992.
- Budunova I.V. and Williams G.M. (1994). Cell culture assays for chemicals with tumor-promoting or tumor-inhibiting activity based on the modulation of intercellular communication. *Cell Biol. Toxicol.*, 10: 71-116.
- Canales P.L., Kleiner H.E., Monks T.J. and Lau S.S. (1993). Formation of 8-hydroxydeoxyguanosine by quinone-thioethers. *Toxicologists*, 13: 202 (Abstract).
- Cemeli E. and Anderson D. (2011). Mechanistic investigation of ROS-induced DNA damage by oestrogenic compounds in lymphocytes and sperm using the comet assay. *Int. J. Mol. Sci.*, 12: 2783-2796.
- Cerutti P.A. (1985). Prooxidant state and tumor promotion. *Science*, 227: 375-381.
- Chandra S., Nolan M. and Malarkey D. (2010). Chemical carcinogenesis of the gastrointestinal tract in rodents: An overview with emphasis on NTP carcinogenesis. *Bioassays Toxicol. Pathol.*, 38: 188-197.
- Clayson D.B., Iverson F., Nera E.A. and Lok E. (1990). The significance of induced forestomach tumors. *Ann. Rev. Pharmacol. Toxicol.*, 30: 441-463.
- Dobo K.L. and Eastmond D.A. (1994). Role of oxygen radicals in the chromosomal loss and breakage induced by the quinone-forming compounds, hydroquinone and *tert*-butylhydroquinone. *Environ. Mol. Mutagen.*, 24: 293-300.

- Finley J. Kong A., Hintze K., Jeffery E., Ji L. and Lei X. (2011). Antioxidants in foods: state of the science important to the food industry. *J. Agric. Food Chem.*, 59 (13): 6837–6846
- Fukushima S., Ogiso T., Kurata Y., Hirose M. and Ito N. (1987). Dose-dependent effects of butylatedhydroxytoluene and ethoxyquin for promotion of bladder carcinogenesis in N-butyl-N-(4-hydroxybutyl) nitrosamine-initiated, unilaterally ureter ligated rats. *Cancer Letters*, 34: 83-90.
- Gharavi N., Haggarty S. and El-Kadi A. (2007). Chemoprotective and carcinogenic effects of tert-butylhydroquinone and its metabolites. *Current Drug Metabolism*, 8: 1-7.
- Hirose M., Takesada Y., Tanaka H., Tamano S., Kato T. and Shirai T. (1997). Carcinogenicity of antioxidants BHA, caffeic acid, sesamol, 4-methoxyphenol and catechol at low doses, either alone or in combination and modulation of their effects in rat medium-term multiorgan carcinogenesis model. *Carcinogenesis*, 19: 207-212.
- IARC (1986). IARC monographs on the evaluation of the carcinogenic risks of chemicals to humans. vol. 40, some naturally occurring and synthetic food components, furocoumarins and ultraviolet radiation butylatedhydroxyanisole (bha), International Agency for Research on Cancer, Lyon. pp. 123-159.
- Iverson F. (1995) Phenolic antioxidants: health protection branch studies on butylatedhydroxyanisole. *Cancer Letters*, 93: 49-54.
- Jacobus J., Flor S., Klingelutz A., Robertson L., and Ludewig G. (2008). 2-(4'-chlorophenyl)-1,4-benzoquinone increases the frequency of micronuclei and shortens telomeres. *Environ Toxicol Pharmacol.*, 25(2): 267–272.
- Kadoma Y., Ito S., Yokoe I. and Fujisawa S. (2008). Comparative study of the alkyl and peroxy radical-scavenging activity of 2-*t*-butyl-4-methoxyphenol (bha) and its dimer, and their theoretical parameters. *In vivo*, 22: 289-296.
- Kahl R. (1997) Synthetic antioxidants: biochemical actions and interferences with radiation and toxic compounds, chemical mutagens and chemical carcinogens. *Toxicology*, 33: 185-228.
- Kari F.W., Bucher J., Eustis S.L., Haseman J.K. and Huff J.E. (1992). Toxicity and carcinogenicity of hydroquinone in F344/N rats and B6C3F₁ mice. *Food Chem. Toxicol.*, 30: 737-747.
- Kuroiwa, Y., Ishii, Y., Umemura, T., Kanki, K., Mitsumori, K., Nishikawa, A., Nakazawa, H. and Hirose, M. (2007). Combined treatment with green tea catechins and sodium nitrite selectively promotes rat forestomach carcinogenesis after initiation with *N*-methyl-*N'*-nitro-*N*-nitrosoguanidine. *Cancer Science*, 98: 949–957.
- Leithe E., Sirnes S., Omori Y. and Rivedal E. (2006). Downregulation of gap junctions in cancer cells. *Critical Reviews TM in Oncogenesis*, 12(3-4): 225–256
- Li Y., Zhong F., Wu S. and Shi N. (2007). NF-E2 related factor 2 activation and heme oxygenase-1 induction by tert-butylhydroquinone protect against deltamethrin-mediated oxidative stress in PC12 cells. *Chem. Res. Toxicol.*, 20(9): 1242-51.
- Li Y., Seacat A., Kuppasamy P., Zweier J.L., Yager J.D. and Trush, M.A. (2002). Copper redox-dependent activation of 2-*tert*-butyl(1,4)hydroquinone: formation of reactive oxygen species and induction of oxidative DNA damage in isolated DNA and cultured rat hepatocytes. *Mutat. Res.*, 518: 123-133.
- Li J., Johnson D., Calkins M., Wright L., Svendsen C. and Johnson J. (2005). Stabilization of Nrf2 by *t*BHQ confers protection against oxidative stress-induced cell death in human neural stem cells. *Toxicol. Sci.*, 83: 313-328.
- Liu C. and Russell R. M. (2008). Nutrition and gastric cancer risk: an update. *Nutr. Rev.*, 66: 237–249.
- Miyamae Y., Yamamoto M., Sasaki Y.F., Kobayashi H., Igarashi-Soga M., Shimoi K. and Hayashi M. (1998). Evaluation of a tissue homogenization technique that isolates nuclei for the in vivo single cell gel electrophoresis (comet) assay: a collaborative study by five laboratories. *Mutat. Res.*, 418: 131-140.
- Monks T.J., Hanzlik R.P., Cohen G.M., Ross D. and Graham D.G. (1992). Quinone chemistry and toxicity. *Toxicol. App. Pharmacol.*, 112: 2-16.
- Moridani M., Cheon S., Khan S. and O'Brien J. (2002). Metabolic activation of 4-hydroxyanisole by isolated rat hepatocytes. *Drug Metab. Dispos.*, 30(10): 1063-9.
- Nagai F., Okubo T., Ushiyama K., Satoh K. and Kano I. (1996). Formation of 8-hydroxydeoxyguanosine in calf thymus DNA treated with *tert*-butylhydroquinone, a major metabolite of butylatedhydroxyanisole. *Toxicol. Lett.*, 89: 163-167.
- O'Brien P.J. (1991). Molecular mechanisms of quinone cytotoxicity. *Chem. Biol. Inter.*, 80: 1-41.
- Okubo T., Nagai F., Ushiyama K. and Kano I. (1997). Contribution of oxygen radicals to DNA cleavage by quinone compounds derived from phenolic antioxidants, *tert*-butylhydroquinone and 2,5-di-*tert*-butylhydroquinone. *Toxicol. Lett.*, 90: 11-18.
- Peters M., Lau S., Dulik D., Murphy D., Ommen B., Bladeren P. and Monks T. (1996). Metabolism of *tert*-Butylhydroquinone to *S*-Substituted Conjugates

- in the Male Fischer 344 Rat. *Chem. Res. Toxicol.*, 9: 133-139.
- Piperakis S.M., Visvardis E-E., Sagnou M. and Tassiou A.M. (1998). Effects of smoking and ageing on oxidative DNA damage of human lymphocytes. *Carcinogenesis*, 19: 695-698.
- Rogers C.G., Nayak B.N. and Heroux-Metcalf C. (1985). Lack of induction of sister chromatid exchanges and of mutation to 6-thioguanine resistance in V79 cells by butylatedhydroxyanisole with and without activation by rat or hamster hepatocytes. *Cancer Lett.*, 27: 61-69.
- Saito K., Nakagawa S., Yoshitake A., Miyamoto J., Hirose M. and Ito N. (1989). DNA-adduct formation in the forestomach of rats treated with 3-tert-butyl-4-hydroxyanisole and its metabolites as assessed by an enzymatic ³²P-postlabeling method. *Cancer Lett.*, 48: 189-195.
- Schilderman P.A.E.L., Rhijnsburger E., Zwingmann I. and Kleinjans J.C.S. (1995). Induction of oxidative DNA damage and enhancement of cell proliferation in human lymphocytes *in vitro* by butylatedhydroxyanisole. *Carcinogenesis* 16: 507-512.
- Schilderman P.A.E.L., van Maanen J.M.S., Smeets E.J., ten Hoor F. and Kleinjans J.C.S. (1993). Oxygen radical formation during prostaglandin H synthase-mediated biotransformation of butylatedhydroxyanisole. *Carcinogenesis*, 14: 347-353.
- Shibata M.A., Asakawa E., Hagiwara A., Kurata Y. and Fukushima S. (1991). DNA synthesis and scanning electron microscopic lesions in renal pelvic epithelium of rats treated with bladder cancer promoters. *Toxicol. Lett.*, 55: 263-272.
- Takahashi M., Furukawa F., Toyoda K., Sato H., Hasegawa R. and Hayashi Y. (1986). Effects of four antioxidants on N-methyl-N'-nitro-N-nitrosoguanidine initiated gastric tumor development in rats. *Cancer Lett.*, 30: 161-168.
- Tice R.R., Agurell E., Anderson D., Burlinson B., Hartmann A., Kobayashi H., Miyamae Y., Rojas E., Ryu J.C. and Sasaki Y.F. (2000). The single cell gel/comet assay: guidelines for *in vitro* and *in vivo* genetic toxicology testing. *Environ. Mol. Mutagen.*, 35: 206-221.
- Tsuda H., Fukushima S., Imaida K., Sakata T. and Ito N. (1984). Modification of carcinogenesis by antioxidants and other compounds. *Acta Pharmacol. Toxicol.*, 2(Suppl.), 125-143.
- Tu T., Giblin D. and Gross M. (2011). Structural Determinant of Chemical Reactivity and Potential Health Effects of Quinones from Natural Products. *Chem. Res. Toxicol.*, 24 (9): 1527-1539
- Vinken M., Doktorova T., Decroock E., Leybaert L., Vanhaecke T. and Rogiers V. (2009). Gap junctional intercellular communication as a target for liver toxicity and carcinogenicity. *Crit. Rev. Biochem. Mol. Biol.*, 44(4):201-222.
- Visvardis E-E., Tassiou A.M. and Piperakis S.M. (1997). Study of DNA damage induction and repair capacity of fresh and cryopreserved lymphocytes exposed to H₂O₂ and γ -radiation with the alkaline comet assay. *Mutat. Res.*, 383: 71-80.
- Whysner J., Wang C., Zang E., Latropoulos M.J. and Williams G.M. (1994). Dose-response promotion by butylatedhydroxyanisole in chemically initiated tumors of the rodent forestomach. *Food Chem. Toxicol.*, 32: 215-222.
- Williams G. M. and Iatropoulos (1997). Anticarcinogenic effects of synthetic phenolic antioxidants. In *Oxidants, Antioxidants, and Free Radicals*, ed. S.I. Baskin and H. Salem, pp. 341-350. Taylor & Francis, New York.
- Williams G.M., McQueen C.A. and Tong C. (1990). Toxicity studies of butylatedhydroxyanisole and butylatedhydroxytoluene. I. Genetic and cellular effects. *Food Chem. Toxicol.*, 28: 793-798.
- Yamasaki H. (1996). Role of disrupted gap junctional intercellular communication in detection and characterization of carcinogens. *Mutat. Res.*, 365: 91-105.

12/20/2012

Natural Cases of Rickets in Baraki Goat Kids

Mona.S. Zaki¹, Awadalla. I.M², Mohamed. M.I², Iman. M. Zytaun³, Sami Shalaby⁴, Nagwa Atta⁵, and Suzan.O. Mostafa⁶.

¹ Hydrobiology of Department, National Research Center, Egypt.

² Animal Nutrition Department. National Research Center, Egypt.

³ Department of Microbiology and Internal medicine. Central lab Zagazig University, Egypt.

⁴ Department of Reproduction, National Research Center, Egypt.

⁵ Department of Microbiology and Immunology, National Research Center, Egypt.

⁶ Department of Biochemistry, National Research Center, Egypt.

Dr_mona_zaki@yaoo.co.uk

Abstract: Rickets was evaluated in 6 kids out 100 from different farms in Monofia Governorate of both sex, under 8 months of age. Clinical signs included anorexia stunted growth arched back, joint enlargement and abnormal, curvature of fore limb bones of the kids. Fed consisted of yellow corn 60% and dried trifolium Alexandrun 22% they housed in door, the main biochemical serum analysis recorded were hyperphosphatemia hypoc-alcemia and decrease the activities of Alkaline phosphatase significant increase of cortisol hormone. Urea, creatinine, glucose. P.C.V, and hemoglobin in blood. The results indicated that rations containing high level of com caused decreased digestion coefficient of all nutrients for both growing goat kids (healthy and Rickets). Also Rickets disease decreased digestibility, and nitrogen balance for kids fed two experimental rations. This study recommended that using balanced diets affect decreased significantly in digestion coefficient, feed intake and nitrogen balance.

[Mona.S. Zaki, Awadalla. I.M, Mohamed. M.I, Iman. M. Zytaun, Sami Shalaby, Nagwa Atta, and Suzan.O. Mostafa.. **Natural Cases of Rickets in Baraki Goat Kids.** Life Science Journal. 2012;9(1):184-188] (ISSN:1097-8135). <http://www.lifesciencesite.com>. 26

Keyword: Natural Cases, Rickets, Baraki, Goat Kids.

1. Introduction

Rickets is among the most devastating crippling disease-that affect lambs & kids young animal fed diet deficient in Vit.D and rich in phosphorous and housed in doors without exposure to ultraviolet irradiation develop Rickets, calcium deficiency, also will result in Rickets because of the failure to maintain an adequate ion product of serum calcium and phosphorous at (the zone of mineralization is bones enlarged of joints in a typical signs of rickets it involves lung bones and is usually accompanied by lateral or medial deviation. **Julb et al (1993)** Eruption of teeth is delayed and irregular severe deformity of chest h-one -and chronic ruminal tympany **R-adostits et al (2000)**.

The most consistent clinicopatho-logical finding in Rickets is change in serum sodium serum calcium phosphorous with hematological alteration hyperphosphatemia and drop of serum Alkaline phosphatase (**Elsayed & Siam 1992**).

* Aim of the present work: this work was conducted to study some Nutritional & clinicopathological findings in naturally affected kids in monofia governorate. to avoid the occurrence of this disease and correction of diet offered to kids.

2. Material and Methods

Out of 100 kids under 8 M. age were included in this work, 6 kids showing clinical signs of Rickets, this study was conducted in Manrofia governorate. and 6 apparently healthy control kids of same age.

All animals were examined clinically and blood samples were collected from jugular vein with & without EOT A. Blood samples were collected for determination of Hemoglobin, P.C.V volume were made, according -to **Hunger "ford (1989)** serum total protein, sodium, potassium, chloride, Urea. Creatinine, glucose, the activities of alkaline phosphatase and lactate dehydrogenase. **L.D.H**, calcium, phosphorous were measured colorimetrically by using commercial available test kits supplied by Bio Merieux lab. Reagent and instruments France. Cortisol hormone was measured according to **Kuehen and Burvenich (1986)**. Statistical analysis: statistical analysis of the obtained data were statistically analysed by T. test according to **Petrie & Waston (1999)**.

Twelve growing goat kids (6 normal and 6 Rickets Kids), 8-9 months old with an average body weight of 18.23 ± 1.87 kg were randomly assigned to

examine the effect of Rickets and high level of corn in the experimental rations on digestion coefficient and Nitrogen utilization by normal and Rickets Kids. Animals of each (normal and Rickets disease kids) were divided randomly into two equal groups. Animals of the first group were fed complete feed mixture ration (R₁, control), the second group was fed a complete feed mixture containing high level yellow corn (R₂). Tables (1) and (2) showed "The composition of experimental rations and its chemical composition. The animals are belonging to farm in monofia governorate to the sheep and goats research unit. El-Bostan -Nubaria, Animal Production. Dep. National" Research Center. Cairo, Egypt. Animals were individually placed into 12 metabolic cages and adapted for 21 days as a preliminary period followed by 7 days as a collection period. Faeces and urine were collected and sampled properly. Rations and water were available ad libitum. Samples from the residuals, faeces and urine were analysed for proximate analysis by **A.O.A.C (1980)**.

The data of nutritional parameters were analysed according to **SAS (1993)** procedures. The significance among means was tested by pie rang test (1959).

3. Results and Discussion

There was a significant decrease in total protein and alkaline phosphatase in groups (2) sodium, potassium, chlorine, and calcium and significant increase in serum Urea, creatinine, glucose, phosphorous and cortisol level. In diseased animal there was also significant increase in P.C.V & Hemoglobin as show in Table (3). A common cause of rickets is grain over load in support of t-his carbohydrate over load has been a reliable way to reproduce Rickets and housing indoors. In this study several reports of naturally occurring rickets **Crowley (1961)**, **Elsayed and Siam (1992)** in this work clinical Rickets was evidenced by anorexia, arched backs, stiffness in gait joint enlargement, similar signs were recorded by **Charyrabarti (2000)** **Radostities et al (2000)** **Smeth (1996)** and **Sonnenrirth & Jaratte (1580)** enlarge of joints are the most characterisitic features in our diseased kids. **Sonnenrirth & Jaratte (1980)** reported that phosphorous deficiency has commonly been in animal as major factor in the cause of Rickets sometimes alone or in association with Vit D deficiency our study disagree with this opinion. In this investigation there was no evidence of Hypophosphatemia, serum Kypocalcemia. and decrease in serum Alkaline phosphatase. This opinion agrees with. **Agag et al (2002)** in serum phosphate & serum calcium but disagree in serum alkaline phosphatase. The most prodominents

Biochemical finding in this study. The significant hyperphosphatemia was the results of elevated dieatry phosphorous this observation was previously recorded by **Mahin in et al (1984)** and **Haward (1982)** in lambs fed diets rich in cereal, and wheat bran respectively. **Hurgerfood (1989)** and **Agag et al (2002)** they described that concentrate which are particulary rich in posphorous and poor in calcium will cause bone abnormality and joint tranlules. The observed hypoproteemia in our work, could be attributed to prolonged anorexia, our study agree with **Agag et al (2002)**, this indicated by increase P.C.V & Hemoglobin concentration this finding attributed to loss of plasma water through large intestine of kids because of anorexia and adipsia. (**Beech 1994**). Hyperglycemia in diseased kids was probably due to hydrocortisone which has been indentified as the major free plasma **keneta (1989)**. **Field et al (1975)** glucocorticoid Rickets mentioned that increased hydrocortisone was probably responsible to some degree of leukocyte changes and the **hyperglycemia Somth (1996)** **Nislet et al (1966)**.

The elevated value of serum urea, creatmine and change in soduim and potassium value in disease kids may attribute to dehydration, glumerulonephrities, and medullary mecosis **Mahim et al (1984)** **Koneka (1989)**. L.D.H-, the significant increase in L.DH value may be due to hepatocellular changes from endot-oxin delivered in portal circulation of secondry bacterial invasion due to immunoligical suppression this result confirmed the result of **jull (1993)** who mentioned that there were muscular-and hepatic disorders associated with inmmunological suppression in animals suffered from Rickets. Concerning electrolyte changes were similar, to those reported by **Agag (2002)** A marked hypochloremia was recorded in diseased animal the obtained results may attributed to severe dehydration caused by excessive loss of fluid electrolytes this observation supported the results that, recorded by. **Oviisten (1964)** **Koneko (1989)**. We can concluded from this-study that Rickets in kids is a complex disorder and despite our best effect to p-revent treatment of diseased kids by offered a.balanced ration rich in mineral and put them in sun shine for at least 5-6 H every day **it is often featal to kids** and treatment should be given as soon as possible after clinical sign develop or preferably before, the best policy is to use high quality of roughge and to supplement with minimum grain.

Apparent digestibility and nutritive values:

Results in Table (4) indicated that rations containing high level of corn with normal kids did not affect the apparent nutrients digestibilites. While the apparent digestibility (%) of DM, OM,

CP, CF and NFE of experimental rations fed to the Rickets Kids were significantly ($P < 0.05$) decreased for both rations and increasing- level of corn (R_2) decreased the apparent digestibility than Rickets kids fed (R_1 , control) however, either extract digestibility was not significantly affected neither by Rickets disease or by high level of corn in the experimental rations. The significant reduction of nutrient digestibilities (**DM, OM, CP, CF and NFE**) as a result of high level of corn and Rickets disease by (CF in $R_1 = 15.61$) and (CF in $R_2 = 11.22$) was related to the increasing percentage of CF content of R_1 (Blaxter, 1967). Contrariwise, the DCP % increased ($P < 0.01$) for experimental ration (R_1 , control) containing high level of CP percentage (13.63% US 12.25%).

Highest nutritive value as **TDN** was observed for the control ration with normal kids followed by ration 2 with normal kids also. The results revealed also that TDN more affected by kids health, the lowest TDN was recorded by Rickets kids with R_1 followed by Rickets kids with R_2 . These results proved that Rickets disease of kids was reduced the total digestible nutrients intakes which consequently causing a reduction in TDN values recorded by Rickets kids. The due to the lower feed intake by Rickets kids and lower CP and CF content in R_2 than in R_1 .

Nitrogen utilization:

Results in Table (5) indicated that nitrogen intake expressed as (g/h/d) were significantly ($P < 0.05$) affected among rations. Whereas, high level of corn in R_2 decrease significantly ($P < 0.01$) the nitrogen intake from control ration (R_1). This difference could mainly due to the high level of corn and its lower contents of CP (El-Shaer and Kandil, 1990). For the above reason nitrogen losses in both faeces and urine were followed the same trend of nitrogen intake. Rickets kids fed experimental rations. Showed significant ($P < 0.01$) differences in nitrogen retention compared to the healthy kids fed the same rations. Nitrogen balance as percent of nitrogen intake (NB/NI) value for healthy kids fed control ration (R_1) was significantly ($P < 0.01$) higher than the other goat kids groups fed the control ration (Rickets kids) or highly corn in the other ration (R_2). (Normal and Rickets Kids) due to the rickets disease and the higher nitrogen intakes from rations.

In conclusion, under conditions of this study, data indicated that ration containing normal level of corn and balanced diet was the best ration for healthy kids to obtain satisfy digestion coefficient and nitrogen balance and reduced feeding cost. -Rickets disease decreased digestion coefficient for all nutrients and nitrogen balance. In the two experimental rations.

Table (1): Ingredients of experimental ratios used.

Item	Exp. Complete feed mixtures	
	R_1 (control)	R_2
Yellow corn	22	60
Wheat bran	25	5
Undecorticoated colton seed cake	20	10
Barssem hay	30	22
Lime stone	1.9	1.9
Common salt	1.0	1.0
Minerals mixtures	0.1	0.1
Vit& minerals mixtures	498	600
Total	100	100
Price of 1 ton. L.E	584	670

Product of RoviGypt Contain: 70g manganese, 20g copper, 50g zinc. 0.25 selenium, 4.0g iodine, 1.0g cobalt, 1.2×10^6 IU vit. A, 2×10^6 IU vit D3 . 15×10^4 IU vit E in 3.0 kg calcim carbonate.

Table (2): Chemical composition of experimental ration used.

Item	DM	% as DM basis					
		OM	CP	CF	EE	NFE	ASH
R_1 (control)	93.6	92.77	13.63	15.61	2.90	60.63	7.23
R_2	92.8	94.03	12.25	11.22	2.27	68.29	5.97

Table (3) Some biochemical & hematological parameters in diseased and control kids. Animal groups

parameters	Control kids	Diseased kids
Alkaline. phosphatase U/L. 216.2 10.24	216.210.24	189.2 9.47*
Total protein g/dl.	8.23 0.14	6.14 0.17*
Urea mg / dl	7.79 0.84	8.94 0.14*
C reatinine mg/dl	0.83 0.03	1.2 0.17*
Glucose mg/dl	6.70 1.79	7.84 0.80*
Sodium m. Eq/L	157.08 0.89	138 0.98*
Potassium m. Eq/L	2.70 0.54	1.98 0.64*
Chloride mmol / l	76 0.78	60 0.13*
Cortisol Hormone ug/dl	0.98 0.03	1.94 0.45*
p.c.v.%	32.9 0.78	40.2 1.70*
Hemoglobin g/dl	10.23 0.33	13.27 0.84*
L.D.H u/I	228.5 63.4	398 48.33*
Calcium ma / dl	1 1.33 9.78	9.24 0.54*
Phosphours. mg/dl.	8.94 0.27	12.42 0.13*

* P< 0.01

Table (4): Apparent nutrients digestibility and nutritive value of the experimental ration fed to growing goat kids.

Item	R ₁		R ₂		Significance
	Normal kids	Rickets kids	Normal kids	Rickets kids	
DM	72.27 2.31a	68.33 1.23	70.26 1.22	66.82 1.42	*
OM	71.90 1.76	66.17 2.14	71.22 2.36	63.19 1.97	*
CP	70.81 1.11	67.12 1.26	70.96 1.86	64.89 1.62	*
CF	71.66 1.92	66.71 1.55	71.12 1.01	62.37 2.67	*
EE	72.18 2.27	70.12 2.18	70.86 2.36	68.12 1.06	NS
NFE	70.73 1.27	65.56 0.99	71.36 1.26	61.16 1.49	*
TON	68.44 1.41	63.89 1.17	68.93 1.27	60.19 0.09	**
DCP	9.66 0.56	9.15 0.27	8.69 0.15	7.95 0.17	**

A.b.c values in the same row with different superscripts are significantly different *(P<0.05) **P<0.01

1) Apparent digestibility, %

2) Nutritive values. %

Table (5): Nitrogen utilization (g/h/d) of growing goat kids fed experimental rations.

Item	R ₁		R ₂		Significance
	Normal kids	Rickets kids	Normal kids	Rickets kids	
BW, Kg	17.9 1.26	18.0 1.47	18.6 1.13	18.4 0.97	*
DML, g	530 0.13	480 0.37	505 0.80	440 0.43	*
DML/BW, %	3 0.86	2.7 0.74	2.7 1.10	2.4 0.85	*
Faecal, N.	3.36 0.11	3.44 0.26	2.87 0.46	3.03 0.47	*
Urinary, N	4.67 0.66	5.17 1.16	4.81 0.70	4.13 1.11	NS
N-balance	3.52 0.23	1.86 0.30	2.22 0.66	1.46 0.14	*
NB of NI, %	30.48 1.26	17.77 1.23	22.42 1.11	16.94 0.80	**
Nitrogn I, g	11.55 0.17	10.47 0.37	9.90 0.44	8.62 0.31	*

A,b,c values in the same row with different superscript, are significantly different (p<0.05).

* p<0.05** p<0.01 NS=non-significant

Acknowledgement:

This work supported from internal project belonging National Research Center. Project No 10/8 the 1st research Dr. Mona. S. Zaki Associated Prof. of Clinical pathology and Awadalla I.M First researcher of project 107 64 and Mohamed I.M First Researcher of project 10/62.

References

1. **A.O.A.C. (1980)**. Association of official agriculture chemists. Official methods of analysis". 13th ed, Washington , DC., U.S.A.
2. **Agag B.I, Naima A Afify and El Seidy I.A. (2002)** Egypt comp. Clinical pathology vol 15 No. 141-148.

3. **Blaxter, K. L. (1967)**. The energy metabolism of ruminants. 2nd Ed. Hutchinson and Co. Ltd. London.
4. **Charkrabarti A (2000)**: Text Book of clinical veterinary Medicine "Deprint of the 2nd Ed. P.p. 392-393 Taj "Press A - 3514 Maja puriphase-1 Newdelhi.
5. **Crowly J.P (1961)** Veterinary Record 73; 295 by Bannivell et al (1988).
6. **Duncan, D.B (1955)**. Multiple Range and Multiple F-test. Biometrics, 11.1.
7. **El-Sayd R.F and Siam A.A (1992)** Clinical and Biochemical aspects associated with Rickets in young goats. Assuit vet. Med J 27 (54): 162-167.
8. **El-Shaer, H.M and Kandil H.M. (1990)**. Compartive study on the nutritional value of wild and cultivated Atriplex halimus by sheep and goat in Sinai: Com. Sei. And Dev. Res., 29 81 .
9. **Field A.C., Suttle N.F and Nibest D.J (1975)** Effects of diets low in calcium and phosphorous on the development. of growing lamb J dge 85: 435.
10. **Howard J. LC (1982)** the southwestern veterinarian 34: 88 cited by hahin et al(1984).
11. **Hungerford T.G (1989)** diseases of livestock. 8th Ed pp 1045-1046 Me grow Hill Book company Sydney.
12. **Juble, K.V, Kennedy P.C, and pulmer N. (1993)**: pathology of Domestic Animals 4th ed vol. 1 Pp. 67-77 Academic press. Inc U.S.A.
13. **Kaneko J.(1989)** clinical Biochemistry of Domestic animals 4th ed pp. 699-730 academic press In. San Diega.
14. **Kuehm and Burvenichic (1986)** Cortisol and thyroid hormones after endotoxin administration in lactating goats Arch Int. Physiol. Biocher 94, 37, 386.
15. **Mahind. L.ghaldi M. and Marrou A (1984)** Osteody strophying growing lambs feat a diet rich in wheat Bran vet Rec. 115:355-357.
16. **Nisbet D. Buttler E. J and Robertson J. M (1966)**. Osteodystraphic diseases of sheep, osteomolacia and asteprasis in lactating ewes in west Scotland hill farms. J. comp. Path 80: 535-542.
17. **Petrie A. and Waston P. (1999)** statistics for veterinary and animals science T Ed pp. 90-99 the Black well science. Td united Kingdom.
18. **Radostits O.M, Blood D.C, and Goy C.C (2000)** Vet. Mediune 8th ed p.p 1435-1438 Bailliere trindall london.
19. **SAS (1993)**. **SAS user's guide**: Statistics, SAS Inst. Inc. Gary. NC. Rel. eigh.
20. **Smith B.D (1996)**: darge Animal Internal medicine 2nd Ed P 1263-1264 Masly Yeurbook In new york U.S. A
21. **Smith. M.C and sherman D.M (1994)** goot Medicine pp. 99-100 leu and Feliger Philadelphia.
22. **Somenwith A.C and jarette L. (1980)**: Gradwal's clinical laboratory methods. and Diagnosis Vol 1,8th Ed. Pp. 258-259. the C.V Moshy cost louis Toronta. London.

12/20/2011

Filename: 026_7566life0901_184_188.doc
Directory: G:\net_fulltext2012010911222\journal\life\life0901
Template: C:\Users\Administrator\AppData\Roaming\Microsoft\Templates\Normal.dotm
Title: NATRAL CASES OF RICKETS IN BARAKI GOAT KIDS
Subject:
Author: PC
Keywords:
Comments:
Creation Date: 1/22/2012 6:17:00 PM
Change Number: 20
Last Saved On: 1/25/2012 11:22:00 PM
Last Saved By: Administrator
Total Editing Time: 27 Minutes
Last Printed On: 1/25/2012 11:22:00 PM
As of Last Complete Printing
Number of Pages: 5
Number of Words: 2,749 (approx.)
Number of Characters: 15,671 (approx.)

Clinical and laboratory approach for the identification of the risk for tumour lysis syndrome in children with acute lymphoblastic leukemia.

Hesham A. Abdel-Baset¹, Eman Nasr Eldin¹, Azza A. Eltayeb², Almontaser M. Hussein².

¹Clinical Pathology Department, ² Pediatric Department, Faculty of Medicine, Assiut University- Egypt.
emannasr2000@yahoo.com

Abstract: Tumour lysis syndrome (TLS) is a life-threatening oncological emergency characterized by metabolic abnormalities including hyperuricaemia, hyperphosphataemia, hyperkalaemia and hypocalcaemia. These metabolic complications predispose the cancer patient to clinical toxicities including renal insufficiency, cardiac arrhythmias, seizures, neurological complications and potentially sudden death. TLS is a well-recognized complication of acute lymphoblastic leukemia (ALL). The ability to predict children at differing risk of TLS would be an early step toward risk-based approaches. However with the increased availability of newer therapeutic targeted agents, there are no published guidelines on the risk classification of TLS for individual patients at risk of developing this syndrome. Risk factors included biological evidence of laboratory TLS, proliferation, bulk and stage of malignant tumour and renal impairment at the time of TLS diagnosis. The objectives of the current study were to describe a sensitive prediction rule to identify patients at risk of TLS in childhood ALL. Sixty children aged ≤ 18 years who were diagnosed as ALL were studied. TLS was defined by the presence of ≥ 2 laboratory abnormalities occurring in the time of interest (before and 5 days after initiation of chemotherapy). From the total 60 patients include, 45% met criteria for TLS. TLS predictive factors were male sex (odds ratio [OR], 3.0; $P = 0.08$), age ≥ 10 years (OR, 1.3; $P < 0.2$), splenomegaly (OR, 4.2; $P = 0.008$), generalized lymphadenopathy (OR, 1.0; $P = 0.2$), white blood count (WBC) $\geq 20 \times 10^9/L$ ($P = < .0001$), T-cell phenotype (OR, 8.0; $P = 0.002$), and lactate dehydrogenase ≥ 1000 U/L (OR, 5.0; $P .002$). **In conclusion**, children with ALL who are at low risk for TLS can be identified early at the time of hospital presentation and may benefit from a risk-stratified approach directed at reduced intensity of laboratory monitoring and limited TLS prophylactic measures.

[Hesham A. Abdel-Baset, Eman Nasr Eldin, Azza A. Eltayeb, Almontaser M. Hussein. **Clinical and laboratory approach for the identification of the risk for tumour lysis syndrome in children with acute lymphoblastic leukemia.** Life Science Journal, 2012; 9(1):189-195] (ISSN: 1097-8135). <http://www.lifesciencesite.com>. 27

Key words: Tumour lysis syndrome; hyperuricaemia; hyperphosphataemia; hyperkalaemia; hypocalcaemia.

1. Introduction

Tumor lysis syndrome (TLS) is a group of metabolic abnormalities consists of hyperuricemia, hyperkalemia, hyperphosphatemia, and hypocalcemia that result from the rapid release of intracellular metabolites such as nucleic acids, proteins, phosphorus and potassium from lysed malignant cells (Cairo *et al.*, 2010). This process can potentially cause hyperuricaemia, hyperkalaemia, hyperphosphataemia, with or without hypocalcaemia and uraemia, arrhythmias, seizures and even death. TLS symptoms can occur before (spontaneously) or within 12–72 hrs after initiation of cytoreductive chemotherapy for malignancies (Kedar *et al.*, 1995; Akoz *et al.*, 2007).

TLS is most frequently associated with non-Hodgkin lymphoma (NHL), particularly Burritt's lymphoma/leukaemia, as well as other haematological malignancies, such as acute myeloid leukaemia (AML) and acute lymphoblastic leukaemia (ALL) (Hochberg & Cairo, 2008; Konuma *et al.*, 2008), and require prompt recognition followed by

aggressive management (Chen & Chuang, 2009; Choi *et al.*, 2009).

TLS may also occur in other tumour types, especially tumours sensitive to cytotoxic treatment, which have a high proliferative rate or have a large tumor size or burden (Vaisban *et al.*, 2001; Coiffier *et al.*, 2008). Other studies have been reported the unexpected cases of TLS where a high TLS risk was not evident and for which appropriate risk assessment and management could make the difference between life and death (Francescone *et al.*, 2009; Lin *et al.*, 2009).

It is essential to identify patients at risk of TLS because this life-threatening condition may occur rapidly and is preventable. However, standardized procedures for assessing risk have been lacking until now (Levine, 2002; Cairo *et al.*, 2010). Complications resulting from TLS, can compromise the efficacy or further administration of chemotherapy (Yim *et al.*, 2003; Hsu *et al.*, 2004) and have an impact on morbidity and mortality. They are also associated with longer and more costly

hospital stays (Annemans *et al.*, 2003; Candrilli *et al.*, 2008).

Previous studies focused primarily on identifying patients at increased risk of TLS for the purpose of selecting those who may benefit from increased laboratory monitoring or urate oxidase therapy (Goldman *et al.*, 2001; Coiffier *et al.*, 2003, Goldman, 2003) TLS risk derives from the collective contribution of several individual risk factors and underlines the critical need for a risk model that integrates them in order to identify high TLS risk, even in unusual settings. Risk factors include: age, type of malignancy, presentation with a high initial white blood cell (WBC) count; evidence of large tumor burden (bulky disease, hepatosplenomegaly); high blood lactate dehydrogenase (LDH) (Csako *et al.*, 1982; Hande & Garrow, 1993) or increased uric acid levels; pre-existing dehydration, oliguria, or renal failure (Michallet *et al.*, 2005); and malignancies with high chemosensitivity (Sparano *et al.*, 1990; Rajagopal *et al.*, 1992).

However, the majority of children with newly diagnosed ALL who are treated with standard TLS prophylactic measures do not experience clinically significant laboratory abnormalities either before or shortly after chemotherapy (Kedar *et al.*, 1995). Yet patients without high-risk features may be subjected to prophylactic measures and monitoring similar to those used in patients with high-risk features. Standard preventative approaches to minimize this complication include hyperhydration, urine alkalization, xanthine oxidase inhibitors (allopurinol), and recombinant urate oxidase (Cairo & Bishop, 2004; Davidson *et al.*, 2004).

Some risk stratification systems have been developed by regional entities, and each system addresses different diseases, using different criteria and different thresholds for risk (Tosi *et al.*, 2008). One of these guidelines is the TLS risk guidelines (Bertrand *et al.*, 2008) developed by the French Society for the Prevention of Cancer in Children and Adolescents (SCFE) which addressed only T-cell lymphoma, B-cell lymphoma, ALL and AML and did not assess TLS risk in adult patients. Similarly, the TLS risk stratification system developed by the Berlin–Frankfurt–Münster (BFM) Group is restricted to children (Seidemann *et al.*, 1998; Wossmann *et al.*, 2003) and focuses only on B-NHL and T-lymphoblastic lymphoma (T-LBL), while other guidelines proposed by an international panel of experts (Coiffier *et al.*, 2008) do not address all malignancies or uniformly assess risk based on renal involvement. None of these guidelines can be uniformly applied to all patients at risk of developing TLS; so the need for a straightforward and unifying risk stratification model is particularly important for

TLS because it is encountered almost exclusively by physicians with a haematology/oncology, nephrology and/or emergency room background (Montesinos *et al.*, 2008).

With the long-term aim of a risk-stratified approach to the prevention of TLS, the objectives of the current study were to describe the predictors of TLS in childhood ALL and to develop a sensitive rule to identify patients who are at risk for TLS.

2. Material and Methods:

Sixty children aged ≤ 18 years that were diagnosed as ALL at pediatric oncology unit and received the same line of chemotherapeutic treatment protocol were included. All the patients were diagnosed by complete blood picture, bone marrow aspirate and/or biopsy, cytochemical staining and immunophenotyping by flowcytometry (using BD FACSCalibur-flow cytometer) according to clinical and morphological characteristics including: Lymphoid Panel : T- lymphoid panel (Sm/cCD3, CD2, CD4, CD8, CD5, CD7, CD1a), B- lymphoid panel (CD19, CD22, CD20, CD10, CytIg μ , sIg μ , sIg κ , sIg λ), Others (CD23, FMC7), Myloid Panel (Anti-cMPO, CD13, CD33, CD14, CD41, anti-glycophorin A), Non lineage specific markers (HLA-DR, CD34, CD45, TdT). The patients then followed within the time frame of interest (from the date of presentation to the fifth day after initiation of chemotherapy).

Potential Predictors Evaluated

The potential predictors of TLS included laboratory features, such as white blood cells (WBC) and lactate dehydrogenase (LDH) [Initial LDH was defined as the first level obtained at admission], and clinical indicators of disease bulk, such as the presence of lymphadenopathy, hepatomegaly, and splenomegaly as assessed by the physical examination on admission. Other potential predictors examined were central nervous system (CNS) status at diagnosis and renal involvement by leukemia as inferred by renal enlargement on abdominal imaging studies, when available.

Outcomes Assessed

The primary outcome was the development of laboratory TLS, which was defined as the occurrence of any 2 or more of the following 5 laboratory abnormalities during the time frame of interest: hyperkalemia, hyperphosphatemia, hypocalcemia, hyperuricemia, and azotemia (creatinine ≥ 1.5 times the age-defined upper limit of normal). Laboratory data were collected during the time frame of interest, starting from the date of presentation, through to the day of chemotherapy

initiation (Day 0), and for each of the following 5 days (Day +5).

Statistical analysis:

Statistical analysis including mean values and their standard deviations, were calculated for each variable under study using the Statistical Package for Social Sciences for windows (SPSS) version 11.0. Statistical comparison between groups was performed through Student's *t*-test.

Predictors of TLS were determined using univariate logistic regression analyses. Results are summarized as the Odds ratio, 95% confidence interval, and P-value. P values of < 0.05 were considered significant, and highly significant at *P* < 0.01.

3. Results

Sixty patients were included, their demographics, and clinical features are shown in Table 1. No CNS or renal involvement encountered by laboratory and radiological examination at presentation in our study group.

Table 2 shows the laboratory abnormalities in the studied population from the date of presentation to 5 days after initiation of chemotherapy. TLS, [which was defined as the presence of at least 2 laboratory abnormalities during the time frame of interest] occurred in 27 of 60 children (45%). The single laboratory abnormality encountered most often was hypocalcemia (39 of 60 patients; 65%), whereas the least frequent abnormality was azotemia (9 of 60 patients; 15%). The most common laboratory abnormality pair for TLS was hypocalcemia and hyperuricemia (21 of 60 patients; 35%), followed by concurrent abnormalities of calcium and phosphate and hyperphosphatemia and hyperuricemia (30% for both), where combined hyperkalemia and azotemia was observed in only (5%) (Table 2). The peak laboratory values of potassium, phosphate, uric acid, and creatinine as well as the nadir of calcium and the day on which these peaks/nadirs occurred are shown in (Table 3). Comparison between those laboratory values in patients with and without TLS are shown in (Table 3).

Predictor factors that were associated with TLS include male sex, age ≥ 10 yrs, splenomegaly,

hepatomegaly, lymphadenopathy, initial WBC $\geq 20 \times 10^9/L$, initial LDH ≥ 1000 IU/L and T-cell immunophenotyping, univariate logistic regression analyses of these factors are shown in table 4. All cases 27/27 (100%) developed TLS presented with high initial WBC $\geq 20 \times 10^9/L$. T-cell immunophenotyping was the strongest predictor of TLS (odds ratio [OR], 8.0; 95% confidence interval; [95% CI], 1.9-32.7; *P* = .0002) and followed by initial LDH ≥ 1000 IU/L (OR, 5.0; 95% CI, 1.2-20.9; *P* = .0002).

Table 1. Study Population

Characteristic	No. of patients (%), N = 60
Sex	
Male	48(80)
Female	12(20)
Acute lymphoblastic leukemia immunophenotype	
B-cell :	45 (75)
<i>Early pre- B</i>	6(13)
<i>Pre-B</i>	20(44)
<i>Common- B</i>	16 (36)
<i>Mature -B</i>	3(7)
T-cell:	15 (25)
<i>Early -T</i>	6(40)
<i>Intermediate-T</i>	3(20)
<i>Mature - T</i>	6(40)
Lymphadenopathy	33(55)
Hepatomegaly	30(50)
Splenomegaly	36(60)

Table 2. Laboratory Abnormalities in Childhood Acute Lymphoblastic Leukemia From the Date of Presentation to Day +5:

Laboratory parameter	No. of patients (%), N = 60
Hypocalcemia	39(65)
Hyperuricemia	24 (40)
Hyperphosphatemia	21 (35)
Hyperkalemia	15(25)
Azotemia	9(15)
Hypocalcemia and hyperuricemia	21 (35)
Hypocalcemia and hyperphosphatemia	18 (30)
Hyperphosphatemia and hyperuricemia	18 (30)
Hyperkalemia and hyperuricemia	15 (25)
Hyperkalemia and hypocalcemia	12 (20)
Hyperkalemia and hyperphosphatemia	12 (20)
Hypocalcemia and azotemia	9 (15)
Hyperphosphatemia and azotemia	9 (15)
Hyperuricemia and azotemia	9 (15)
Hyperkalemia and azotemia	3(5)

Table 3. Laboratory Abnormality in patients with and without TLS and Time Relative to Chemotherapy Initiation.

Laboratory parameter	TLS present, N = 27		TLS absent, N = 33		P
	Mean	± SD	Mean	± SD	
Potassium peak, mmol/L	4.9	±0.5	4.2	±0.4	.02*
Phosphate peak, mg/dl	6.4	±1.3	4.3	±0.5	.001**
Calcium nadir, mg/dl	7.3	±0.8	8.7	±0.5	.005**
Uric acid peak, mg/dl	9.1	±2.5	5.4	±0.9	.004**
Creatinine peak, mg/dl	1.5	±0.4	1.0	±0.2	.03*
Mean day to potassium peak [±]	3.3	±0.7	2.5	±1.2	.04*
Mean day to phosphate peak [±]	3.0	±1.0	2.1	±1.4	.2
Mean day to calcium nadir [±]	2.3	±0.9	1.5	±0.5	.02*
Mean day to uric acid peak [±]	3.2	±0.7	2.0	±1.3	.05
Mean day to creatinine peak [±]	3.1	±1.2	2.3	±1.1	.2

*TLS = tumor lysis syndrome; SD= standard Deviation; * = significant; ** highly significant.

Table 4. Predictors of Tumor Lysis Syndrome by Univariate Analysis

Variable	No. of patients (%)		OR	95% CI	P
	TLS present (N = 27)	TLS absent (N = 33)			
Male sex	24(89)	24(73)	3	0.7-12.5	0.08
Female sex	3(11)	9(27)	0.3	0.1-1.4	0.08
Age ≥10 y	9(33)	9(27)	1.3	0.4-4.0	0.2
Splenomegaly	21(78)	15(45)	4.2	1.4-13.1	0.008**
Hepatomegaly	18(67)	12(36)	3.5	1.2-10.2	0.01*
Lymphadenopathy	15(56)	18(54)	1	0.4-2.9	0.2
Initial WBC ≥20×10 ⁹ /L	27(100)	9(27)		1.2***	<.0001**
Initial LDH ≥1000 IU/L	9(33)	3(9)	5	1.2-20.9	0.02*
T-cell immunophenotype	12(44)	3(9)	8	1.9-32.7	0.002**
B-cell immunophenotype	15(56)	30(91)	0.1	0.03-0.5	0.002**

*TLS = tumor lysis syndrome; OR= odds ratio; 95% CI=95% confidence interval; WBC= white blood count; LDH= lactate dehydrogenase.

***Variance of Haldane. P value from univariate logistic regression analyses. * = significant; ** highly significant.

Six cases out of 60 (10%) were considered low risk TLS group (which was defined by the absence of all 4 predictors of TLS). Of those who fulfilled low-risk TLS criteria, none of them develop TLS.

4. Discussion

Tumor lysis syndrome (TLS) is potentially life-threatening metabolic disorders which are associated with lymphoproliferative malignancies that occurs when tumor cells undergo rapid decomposition spontaneously or in response to cytoreductive therapy (Cairo *et al.*, 2010). Delayed recognition of the metabolic imbalances caused by the massive release of tumor cell contents may result in clinical complications such as acute kidney injury, seizures, and cardiac arrhythmias. The key principle

in TLS management relies on the identification of patients at risk for developing TLS during chemotherapy or because of disease progression (Coiffier *et al.*, 2008). TLS-related risk factors pertain to tumor type (particularly hematologic malignancies), specific tumor characteristics (e.g. bulky tumor, high cellular proliferation rate, sensitivity to cytoreductive therapy), and other host-related factors (Truong *et al.*, 2007). A comprehensive grading system proposed by Cairo and Bishop, 2004 classifies TLS syndromes into laboratory or clinical TLS, thus facilitating TLS prevention and management. The mainstays of TLS management include monitoring of electrolyte abnormalities, vigorous hydration, prophylactic antihyperuricemic therapy with allopurinol, and rasburicase treatment of patients at high TLS risk or

with established hyperuricemia (Bosly *et al.*, 2003). Urine alkalization in an attempt to increase uric acid solubility and use of diuretics remain controversial (Mughal *et al.*, 2010). Titration of sodium bicarbonate infusions to maintain a urine pH between 6.5 and 7.5 is a burden to nursing staff, whereas calcium-phosphate precipitation and subsequent nephrocalcinosis is more likely in alkali settings (Davidson *et al.*, 2004). Furthermore, over-alkalinization may lead to precipitation of uric acid precursors, such as hypoxanthine or xanthine (Jones *et al.*, 1995). Although urine alkalization still is considered the standard of care in many institutions and treatment protocols (Albano *et al.*, 2004) the ability to stop this maneuver in a low-risk group of children would be beneficial. In addition, although it is demonstrably effective at lowering uric acid levels and eliminating the need for alkalization, urate oxidase is very expensive (Calvo-Villas *et al.*, 2008); and the definition of a low-risk group would be valuable to help avoid that unnecessary expense and the rare but real risk of hemolysis in glucose-6-phosphate dehydrogenase-deficient patients (Kopečna *et al.*, 2002).

There is no clear prediction for the development of TLS that could enable early detection of manifestation of this severe condition yet. Recent studies define a subgroup of patients at higher risk of renal failure during induction chemotherapy to standardize this clinical gestalt and further reduce TLS preventative measures (such as alkalization) and limit laboratory monitoring in the low-risk population (Cairo *et al.*, 2010).

By using a very inclusive definition of TLS, Truong and coworkers, 2007 observed that the prevalence of TLS in children with ALL before and within 1 week of chemotherapy initiation was 23%. They the absence of 4 independent risk factors at presentation (age ≥ 10 years, splenomegaly, mediastinal mass, and initial WBC $\geq 20 \times 10^9/L$) to develop a prediction rule for identifying those at low risk of TLS. In the absence of all 4 factors, there was a 97% probability that TLS would not occur; and, those cases that did occur were relatively mild, were identified early, and did not require significant interventions.

We found that the strongest predictors for TLS was the presentation with high initial WBC $\geq 20 \times 10^9/L$, followed by T-cell immunophenotyping (OR, 8.0; 95% CI, 1.9-32.7; $P = .0002$) and then initial LDH ≥ 1000 IU/L, and splenomegaly (OR, 5.0; 95% CI, 1.2-20.9; $P = .0002$; OR, 4.0; 95% CI, 1.4-13.1; $P = .008$ respectively). In our study six cases out of 60 (10%) were considered low risk TLS group none of them develop TLS. The mean peak values of potassium, phosphate, uric acid, and creatinine as

well as the nadir of calcium were different between patients with and without TLS in this study and this difference was statistically highly significant as regard phosphate, uric acid, and calcium ($P < 0.01$), and statistically significant for potassium and creatinine level ($P < 0.05$).

These prediction rules should be applied at the time of initial hospital presentation, thus enabling the early identification of a group of children at low risk for developing TLS who may be candidates for less intensive TLS monitoring and prophylactic interventions. Reducing the frequency of unnecessary laboratory monitoring would minimize trauma to young patients.

We conclude that children with ALL who are at low risk for TLS can be identified early at the time of hospital presentation and may benefit from a risk-stratified approach directed at reduced intensity of laboratory monitoring and limited TLS prophylactic measures.

References:

1. Akoz, A.G., Yildirim, N., Engin, H., Dagdas, S., Ozet, G., Tekin, I.O. & Ceran, F. (2007): An unusual case of spontaneous acute tumor lysis syndrome associated with acute lymphoblastic leukemia: a case report and review of the literature. *Acta Oncologica*, 46:1190–1192.
2. Albano EA, Sandler E. (2004): Oncological emergencies. In: AltmanAJ, ed. *Supportive Care of Children with Cancer: Current Therapy and Guidelines from the Children's Oncology Group*, 3rd ed. Baltimore, Md: Johns Hopkins University Press; 221–242.
3. Annemans, L., Moeremans, K., Lamotte, M., Garcia Conde, J., Van Den Berg, H., Myint, H., Pieters, R. & Uyttebroeck, A. (2003): Incidence, medical resource utilisation and costs of hyperuricemia and tumour lysis syndrome in patients with acute leukaemia and non-Hodgkin's lymphoma in four European countries. *Leukaemia & Lymphoma*, 44:77–83.
4. Bertrand, Y., Mechinaud, F., Brethon, B., Mialou, V., Auvrignon, A., Nelken, B., Notz-Carrere, A., Plantaz, D., Patte, C., Urbietta, M., Baruchel, A. & Leverger, G. (2008): (SFCE) recommendations for the management of tumor lysis syndrome (TLS) with rasburicase: an observational survey. *Journal of Pediatric Hematology/oncology*, 30:267–271.
5. Bosly, A., Sonet, A., Pinkerton, C.R., McCowage, G., Bron, D., Sanz, M.A. & Van den Berg, H. (2003): Rasburicase (recombinant urate oxidase) for the management of hyperuricemia in patients with cancer: report of

- an international compassionate use study. *Cancer*, 98:1048–1054.
6. Cairo, M.S. & Bishop, M. (2004): Tumour lysis syndrome: new therapeutic strategies and classification. *British Journal of Haematology*, 127:3–11.
 7. Cairo MS, Coiffier B, Reiter A, Younes A. (2010): Recommendations for the evaluation of risk and prophylaxis of tumour lysis syndrome (TLS) in adults and children with malignant diseases: an expert TLS panel consensus. *British Journal of Haematology*. 149(4): 578–586.
 8. Calvo-Villas, J.M., Urcuyo, B.M., Umpierrez, A.M. & Sicilia, F. (2008): Acute tumor lysis syndrome during oral fludarabine treatment for chronic lymphocytic leukemia. Role of treatment with rasburicase. *Onkologie*, 31: 197–199.
 9. Candrilli, S., Bell, T., Irish, W., Morris, E., Goldman, S. & Cairo, M.S. (2008): A comparison of inpatient length of stay and costs among patients with hematologic malignancies (excluding Hodgkin disease) associated with and without acute renal failure. *Clinical Lymphoma & Myeloma*, 8: 44–51.
 10. Chen, R.L. & Chuang, S.S. (2009): Transient spontaneous remission after tumor lysis syndrome triggered by a severe pulmonary infection in an adolescent boy with acute lymphoblastic leukemia. *Journal of Pediatric Hematology/oncology*, 31: 76–79.
 11. Choi, K.A., Lee, J.E., Kim, Y.G., Kim, D.J., Kim, K., Ko, Y.H., Oh, H.Y., Kim, W.S. & Huh, W. (2009): Efficacy of continuous venovenous hemofiltration with chemotherapy in patients with Burkitt lymphoma and leukemia at high risk of tumor lysis syndrome. *Annals of Hematology*, 88: 639–645.
 12. Coiffier, B., Altman, A., Pui, C.H., Younes, A. & Cairo, M.S. (2008): Guidelines for the management of pediatric and adult tumor lysis syndrome: an evidence-based review. *Journal of Clinical Oncology*, 26:2767–2778.
 13. Coiffier B, Mounier N, Bologna S, et al. (2003): Efficacy and safety of rasburicase (recombinant urate oxidase) for the prevention and treatment of hyperuricemia during induction chemotherapy of aggressive non-Hodgkin's lymphoma: results of the GRAAL1 (Groupe d'Etude des Lymphomes de l'Adulte Trial on Rasburicase Activity in Adult Lymphoma) study. *J Clin Oncol.*; 21: 4402–4406.
 14. Csako G, Magrath IT, Elin RJ. (1982): Serum total and isoenzyme lactate dehydrogenase activity in American Burkitt's lymphoma patients. *Am J Clin Pathol.* ; 78: 712–717.
 15. Davidson MB, Thakkar S, Hix JK, Bhandarkar ND, Wong A, Schreiber MJ. (2004): Pathophysiology, clinical consequences, and treatment of tumor lysis syndrome. *Am J Med.*; 116: 546–554.
 16. Goldman SC. (2003): Rasburicase: potential role in managing tumor lysis in patients with hematological malignancies. *Expert Rev Anticancer Ther.* ; 3: 429–433.
 17. Goldman SC, Holcenberg JS, Finklestein JZ, et al. (2001): A randomized comparison between rasburicase and allopurinol in children with lymphoma or leukemia at high risk for tumor lysis. *Blood.*; 97: 2998–3003.
 18. Francescone, S.A., Murphy, B., Fallon, J.T., Hammond, K. & Pinney, S. (2009): Tumor lysis syndrome occurring after the administration of rituximab for posttransplant lymphoproliferative disorder. *Transplantation Proceedings*, 41: 1946–1948.
 19. Hande, K.R. & Garrow, G.C. (1993): Acute tumor lysis syndrome in patients with high-grade non-Hodgkin's lymphoma. *American Journal of Medicine*, 94:133–139.
 20. Harbour, R. & Miller, J. (2001): A new system for grading recommendations in evidence based guidelines. *BMJ*, 323: 334–336.
 21. Hochberg, J. & Cairo, M.S. (2008): Tumor lysis syndrome: current perspective. *Haematologica*, 93: 9–13.
 22. Hsu, H.H., Chan, Y.L. & Huang, C.C. (2004): Acute spontaneous tumor lysis presenting with hyperuricemic acute renal failure: clinical features and therapeutic approach. *Journal of Nephrology*, 17:50–56.
 23. Jones DP, Mahmoud H, Chesney RW. (1995): Tumor lysis syndrome: pathogenesis and management. *Pediatr Nephrol.*; 9: 206–212.
 24. Kedar A, Grow W, Neiberger RE. (1995): Clinical versus laboratory tumor lysis syndrome in children with acute leukemia. *Pediatr Hematol Oncol.* ; 12: 129–134.
 25. Konuma, T., Ooi, J., Takahashi, S., Tomonari, A., Tsukada, N., Kato, S., Sato, A., Monma, F., Uchimaru, K. & Tojo, A. (2008): Fatal acute tumor lysis syndrome following intrathecal chemotherapy for acute lymphoblastic leukemia with meningeal involvement. *Internal Medicine*, 47:1987–1988.
 26. Kopečna L, Doležel Z, Osvaldová Z, Starha J, Hrstková H. (2002): The analysis of the risks for the development of tumour lysis syndrome in children. *Bratisl Lek Listy*; 103: 206–209.
 27. Levine, A.M. (2002): Challenges in the management of Burkitt's lymphoma. *Clinical Lymphoma*, 3(Suppl. 1): S19–S25.

28. Lin, T.S. (2008): Novel agents in chronic lymphocytic leukemia: efficacy and tolerability of new therapies. *Clinical Lymphoma & Myeloma*, 8(Suppl. 4): S137–S143.
29. Lin, C.J., Chen, H.H., Hsieh, R.K., Chen, Y.C. & Wu, C.J. (2009): Acute tumor lysis syndrome in a hemodialysis patient with diffuse large B cell lymphoma. *Medical Oncology*, 26:93–95.
30. Michallet, A.S., Tartas, S. & Coiffier, B. (2005): Optimizing management of tumor lysis syndrome in adults with hematologic malignancies. *Supportive Cancer Therapy*, 2:159–166.
31. Montesinos, P., Lorenzo, I., Martin, G., Sanz, J., Perez-Sirvent, M.L., Martinez, D., Orti, G., Algarra, L., Martinez, J., Moscardo, F., De La Rubia, J., Jarque, I., Sanz, G. & Sanz, M.A. (2008): Tumor lysis syndrome in patients with acute myeloid leukemia: identification of risk factors and development of a predictive model. *Haematologica*, 93: 67–74.
32. Mughal TI, Ejaz AA, Foringer JR, Coiffier B. (2010) : An integrated clinical approach for the identification, prevention, and treatment of tumor lysis syndrome. *Cancer Treat Rev*. Apr; 36(2):164-76.
33. Rajagopal S, Lipton JH, Messner HA. (1992): Corticosteroid induced tumor lysis syndrome in acute lymphoblastic leukemia. *Am J Hematol.* ; 41: 66–67.
34. Seidemann, K., Meyer, U., Jansen, P., Yakisan, E., Rieske, K., Fuhrer, M., Kremens, B., Schrappe, M. & Reiter, A. (1998): Impaired renal function and tumor lysis syndrome in pediatric patients with non-Hodgkin's lymphoma and B-ALL. Observations from the BFM-trials. *Klinische Padiatrie*, 210: 279–284.
35. Sparano J, Ramirez M, Wiernik PH. (1990): Increasing recognition of corticosteroid-induced tumor lysis syndrome in non-Hodgkin's lymphoma. *Cancer*; 65: 1072–1073.
36. Tosi, P., Barosi, G., Lazzaro, C., Liso, V., Marchetti, M., Morra, E., Pession, A., Rosti, G., Santoro, A., Zinzani, P.L. & Tura, S. (2008): Consensus conference on the management of tumor lysis syndrome. *Haematologica*, 93:1877–1885.
37. Truong, T.H., Beyene, J., Hitzler, J., Abla, O., Maloney, A.M., Weitzman, S. & Sung, L. (2007): Features at presentation predict children with acute lymphoblastic leukemia at low risk for tumor lysis syndrome. *Cancer*, 110: 1832–1839.
38. Vaisban, E., Zaina, A., Braester, A., Manaster, J. & Horn, Y. (2001): Acute tumor lysis syndrome induced by high-dose corticosteroids in a patient with chronic lymphatic leukemia. *Annals of Hematology*, 80:314–315.
39. Wossmann, W., Schrappe, M., Meyer, U., Zimmermann, M. & Reiter, A. (2003): Incidence of tumor lysis syndrome in children with advanced stage Burkitt's lymphoma/leukemia before and after introduction of prophylactic use of urate oxidase. *Annals of Hematology*, 82:160–165.
40. Yim, B.T., Sims-McCallum, R.P. & Chong, P.H. (2003): Rasburicase for the treatment and prevention of hyperuricemia. *Annals of Pharmacotherapy*, 37: 1047–1054.

12/21/2011

Application of chitosan for wound repair in dogs.

Inas, N.El-Husseiny¹ and Kawkab, A. Ahmed²

Departments of ¹Surgery, Anesthesiology and Radiology and ²Department of Pathology, Faculty of Veterinary Medicine, Cairo University.

drinasnabil@gmail.com

Abstract: This experimental work was applied to study the effect of topical application of chitosan powder on the stimulation of healing of full thickness skin wounds. Experimental surgical wounds were done in 12 apparently healthy male Mongrel dogs of nearly the same age and weight. Experimental animals were classified into 4 groups each consisted of 3 dogs according to time of euthanasia. Full thickness equal longitudinal skin incision wounds were created on each dog's both side at the dorsal aspect of the animal. A comparative study was applied between wounds treated with chitosan powder and control wounds washed only by saline solution. Wound healing was clinically evaluated during the period of the experiment. Euthanasia was done at different period intervals, one week, two weeks, three weeks and four weeks after incisions. Specimen were taken for histopathological investigations. Results proved rapid regeneration and reepithelization of the wounds treated with chitosan powder compared with those of the control group. Clinically, complete healing was seen after 3 weeks in the chitosan treated wounds which delayed to 4 weeks in the control ones. Histopathological investigations proved presence of more pronounced granulation tissues in the chitosan treated wounds than in the control ones. Healing started at 3 weeks post- incision in the treated group and complete repair was achieved at four weeks. Complete regeneration of epidermal cells with keratin layer occurred which was similar to the normal skin associated with dermal connective tissue proliferation. The fibroblast cells laid down a network of collagen fibers which appeared as wavy collagen bundles surrounding the neovasculature of the wounds, whereas, in control group, hyalinosis of subcutaneous granulation tissue and haphazardly arranged collagen fibers were observed. In conclusion, chitosan proved to be a suitable biomedical agent used for the acceleration of wound repair due to its biocompatibility, easy application and high effectiveness.

[Inas, N.El-Husseiny and Kawkab, A. Ahmed. **Application of chitosan for wound repair in dogs.** Life Science Journal, 2012; 9(1): 196-203] (ISSN: 1097-8135). <http://www.lifesciencesite.com>. 28

Keywords: chitosan, chitin, shell products, biomaterials.

1. Introduction

The skin is considered the largest organ of the body and it has many different functions. Cells on the surface of the skin are constantly being replaced by regeneration from below with the top layers sloughing off. The repair of an epithelial wound is merely a normal physiological process (Willi and Sharma, 2004). Wound healing depends on elimination of any source of infection and regeneration of the lost layers (Ishihara, Ono, Sato, Nakanishi, Saito, Yura, Matsui, Hattori, Fujita, Kikuchi and Kurita, 2001).

The majority of wounds heal without any complications, other types are chronic and resist the normal repair. Chronic non-healing wounds involving progressively more tissue loss giving rise to the biggest challenge to wound-care product researchers (Ueno, Yamada, Tanaka, Kaba, Matsuura^c, Okumura, Kadosawand Fujinaga , 1999)

One of those new products widely used in the medical field is chitosan , a water soluble and a bioadhesive product extracted primarily from shellfish sources. More than 40 years have elapsed since this biopolymer had aroused the interest of the scientific

community around the world for its potential biomedical applications (Takashi and Toru, 2001 and Stoker, Reber, Waltzman, 2008). Its role in wound healing has been studied by many researchers (Ueno, Yamada, Tanaka, Kaba, Matsuura, Okumura, Kadosawa & Fujinaga, 1999).

Chitosan is also one of the bioactive dressing which delivers substances active in wound healing (Jayasree , Rathinam and Sharma, 1995). In dogs satisfactory results were obtained regarding healing with fast hemostasis, rapid regeneration of the full thickness wounds that involved the muscle layers (Ueno Yamada, Tanaka Kaba, Mitsunobu Matsuura , Okumura, Kadosawa & Fujinaga, 1999).

Biochemical and histological changes of chitosan in wound healing has been reviewed by (Azad, Sermsintham, Chandkrachang, and Stevens, 2004) as chitosan provides a non-protein matrix for three dimensions tissue growth and activates macrophages for tumoricidal activity. It stimulates cell proliferation and histoarchitectural tissue organization. It will gradually depolymerize to release N-acetyl-b-D-glucosamine, which initiates fibroblast proliferation

and helps in ordered collagen deposition, stimulating increased level of natural hyaluronic acid synthesis at the wound site. **Okamoto, Shibasaki, Minami, Matsuhashi, Tanioka, Shigemasa (1995)** and **Jarmila & Vavrikov (2001)** mentioned that, chitosan helps in faster wound healing and scar prevention, chitosan derivatives have also an antimicrobial, antitumour and antioxidant activities. The introduction of azido functions in chitosan has provided photo-sensitive hydrogels that crosslink in a matter of seconds, thus paving the way to cytocompatible hydrogels for surgical use in wounds as coatings, scaffolds, drug carriers and implants capable to deliver cells and growth factors (**Minami, Okamoto, Matsuhashi, 1992**).

The aim of the present work was to study the effect of topical application of chitosan on full thickness open skin wound regeneration and to evaluate its efficacy as an accelerator in wound repair.

2. Material and Methods

This experimental work was carried out on 12 experimental apparently healthy male Mongrel dogs of nearly the same age and weight. The animals were divided into 4 groups each group consisted of 3 animals. Aseptic preparation for the intended surgical fields was done and two full-thickness equal 10 cm longitudinal skin incisions were created on each dog's both side at the dorsal aspect of the animal. In each dog, one wound (left side) was treated with chitosan powder and the other wound (right side) was washed by saline solution and considered as a control. The 4 groups were divided according to time of euthanasia as follows: group I intended for euthanasia 1 week postwounding, group II 2 weeks, group III 3 weeks and group IV at 4 weeks post- incision. .

Chitosan powder was repeatedly applied on the wounded areas (one application per day) and the control wounds were washed only by saline solution (fig.1). Clinical observations were done at 3 days and 1,2,3,4 weeks post-incision. Examined clinical parameters included measuring the wound length, examination of the wound for the presence or absence of infection and progress of healing process.

All animals were euthanatized at each intended previously mentioned period and full thickness specimen were taken from each wound site including the neighboring tissue for histopathological examination to evaluate the process of wound

healing. Collected samples were preserved in formalin solution 10 % concentration, sectioned and processed, then stained with Hematoxylin & Eosin as well as Trichrome stain (**Bancroft, Stevens, and Turner, 1996**) and subjected for histopathological examination.



Fig (1): An experimentally incised wound in a dog, showing topical application of chitosan powder.

3. Results

Clinical observation of the treated and control wounds indicated that hemostasis was clear directly after the topical application of chitosan. After 3 days, treated wounds showed fresh well defined straight lips diminished from 10 cm length to 8 cm and the muscle layers showed coaptation and healing in the treated wounds faster than in the control ones. One week postwounding the chitosan-dressed wounds had been healed more promptly as compared with the control wounds manifested by regular wound lips and the wound's depth diminished with minimal gap than in the control group (fig. 2). Two weeks post- incision, the chitosan treated wounds showed clean sharp apposed wound lips with complete muscle and subcutaneous tissue healing compared with the control wounds which showed larger apertures and delay in muscle healing (figs.3,4). Three weeks post- incision, nearly complete regeneration of all treated wounds occurred which delayed in the control wounds. The incisions of the chitosan treated wounds occluded with growth of hair tufts covering the healed lips. The control wounds showed partial occlusion with little apertures indicating delayed healing (fig. 5). Four weeks post-incision, the control group showed complete healing and the skin was covered with hair.



Fig (2): One week postwounding. A- represents the chitosan treated wounds B- represents the control wounds



Fig (3): Two weeks postwounding , notice, A- treated wounds diminished in size and healed faster and in a regular manner than the control ones, B.



Fig. (4): Two weeks postwounding, notice the muscle layer healed in the chitosan group (A) faster than in the control group (B).



Fig (5): A- Three weeks postwounding representing treated wounds completely healed and covered by hair, B- Control wounds. Notice , healing and closure of the wounds was delayed with the presence of small aperture.

Histopathological results:

Results correlated well to gross findings. One week post-incision, the chitosan treated wounds showed a hyperactive fibroblastic proliferation (fig.6 a), whereas, in control group, the pronounced picture was massive infiltration with neutrophils associated with haemorrhage (fig.6 b).

At 2 weeks post- wounding, angiogenesis was early in the treated group with formation of new blood vessels, fibroblasts proliferation associated with infiltration with polymorphnuclear cells and macrophages (fig. 6 c). Examined control sections revealed epidermal and dermal necrosis associated with infiltration with neutrophils and macrophages with fibroblasts proliferation (fig. 6 d).

3 weeks post-wounding granulation tissue was more pronounced by the chitosan treatment than in the control group, proliferation of epidermal cells with different mitotic figures (fig. 6 e) as well as highly vascularized and organized subcutaneous granulation tissue was noticed (fig. 6 f).

In the chitosan treated group, 4 weeks post-wounding, complete regeneration of epidermal cells with keratin layer similar to the normal skin associated with dermal connective tissue proliferation (fig. 7 a). The fibroblast cells laid down a network of collagen fibers appearing as wavy collagen bundles surrounding the neovasculature of the wound (figs. 7 b & c), whereas, in control group, examined sections revealed massive infiltration with polymorphnuclear cells, hyalinosis of subcutaneous granulation tissue (fig. 7 d) and haphazardly arranged collagen fibers (fig. 7 e).

4. Discussion

Restoration of tissue continuity after injury is a natural phenomenon, The process of wound healing begins immediately following surface lesions or just

after exposure to radiation, chemical agents or extreme temperatures (Cohen, 1989). Some biomaterials were found to accelerate wound regeneration and increase the quality of the wound healing (Gomma, 2010). One of the new biomaterials is chitosan which exhibits a variety of physicochemical and biological properties resulting in numerous applications in fields such as water treatment, agriculture, fabric and textiles, cosmetics, nutritional enhancement, and food processing (Willi, Paul and Sharma, 2004). In addition to its lack of toxicity and allergenicity, and its biocompatibility, biodegradability and bioactivity make it a very attractive substance for diverse applications as a biomaterial in pharmaceutical and medical fields (Balassa & Prudden, 1984 and Sevda & McClure, 2004).

The present study investigated its use for wound repair and in promoting skin wound epithelisation where it has been tried as a wound-healing accelerator in veterinary medicine (Gomma, 2010).In the present study, after the application of chitosan topically, local hemostasis was directly observed in all treated animals which is considered beneficial in accidental bleeding wounds and could act as a hemostatic dressing as well as for wound healing.This result agreed with (Pusateri, McCarthy, Gregory, Harris, Cardenas, McManus and Goodwin, 2004) who mentioned that hemostasis is immediately obtained after application of most of the commercial chitin-based dressings to traumatic and surgical wounds. Our clinical observations indicated that chitosan showed effective results in treatment of open wounds as the surgical wounds treated with chitosan powder had accelerated and early stages of healing compared with the control wounds applied in the same animal under the same conditions, this was attributed to its action as chitosan

is considered a film forming and protective polysaccharide.

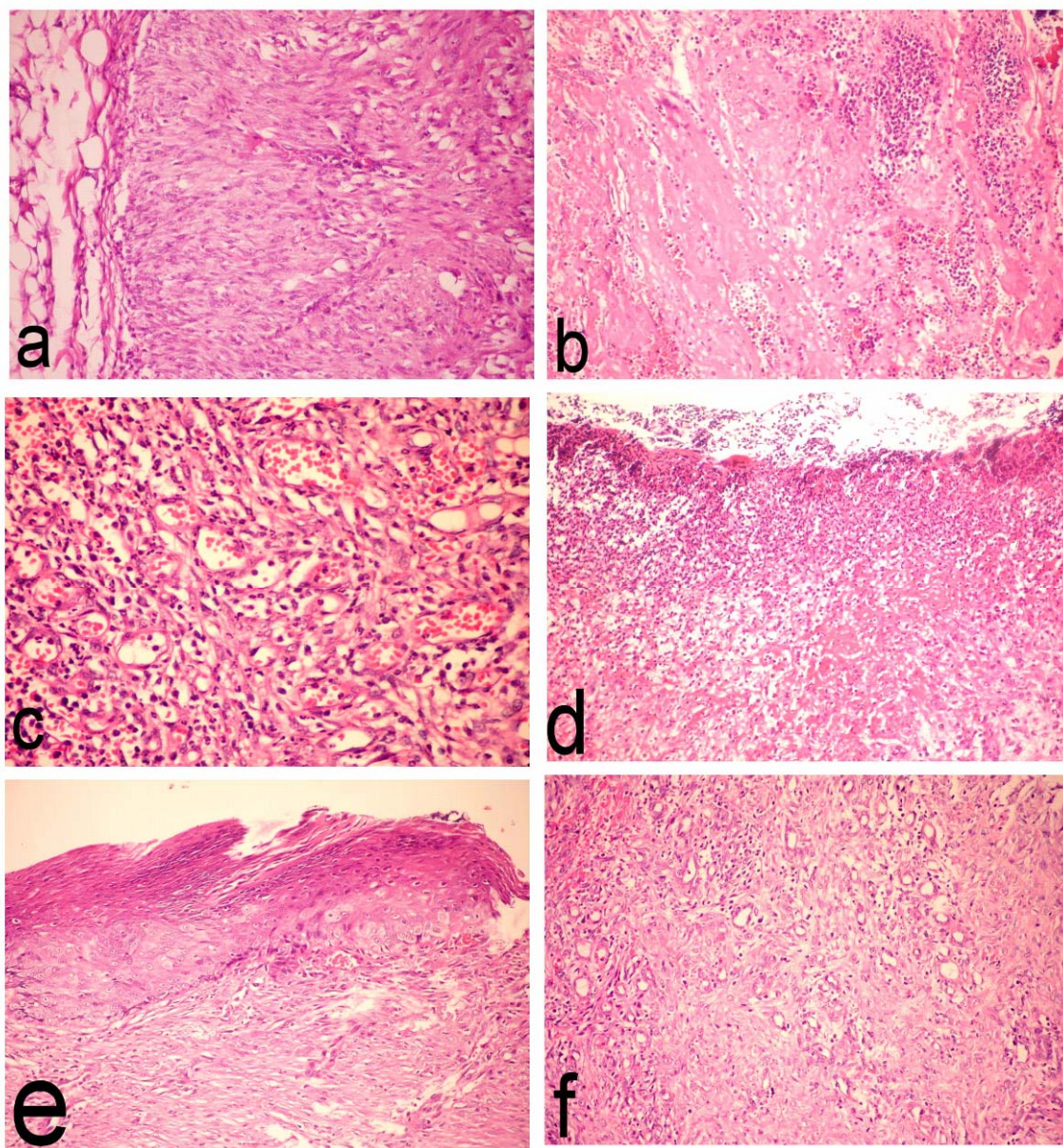


Fig. (6): Photomicrograph of skin wounds in the experimental cases:

- a.** Wounds treated with chitosan 1 week post-wounding showing hyperactive fibroblasts proliferation (H & E stain X 400).
- b.** Control wounds 1 week post-wounding showing massive infiltration with neutrophiles associated with haemorrhage (H & E stain X 200).
- c.** Wounds treated with chitosan 2 weeks post-wounding showing angiogenesis with formation of new blood vessels, fibroblasts proliferation associated with infiltration with polymorphnuclear cells and macrophages (H & E stain X 400).
- d.** Control wounds 2 weeks post-incision showing epidermal and dermal necrosis associated with infiltration with neutrophiles and macrophages with fibroblasts proliferation (H & E stain X 200).
- e.** Wounds treated with chitosan 3 weeks post-incision showing proliferation of epidermal cells with different mitotic figures and dermal granulation tissue formation (H & E stain X 200).
- f.** Chitosan treated wounds 3 weeks post-wounding showing highly vascularized and organized subcutaneous granulation tissue (H & E stain X 200).

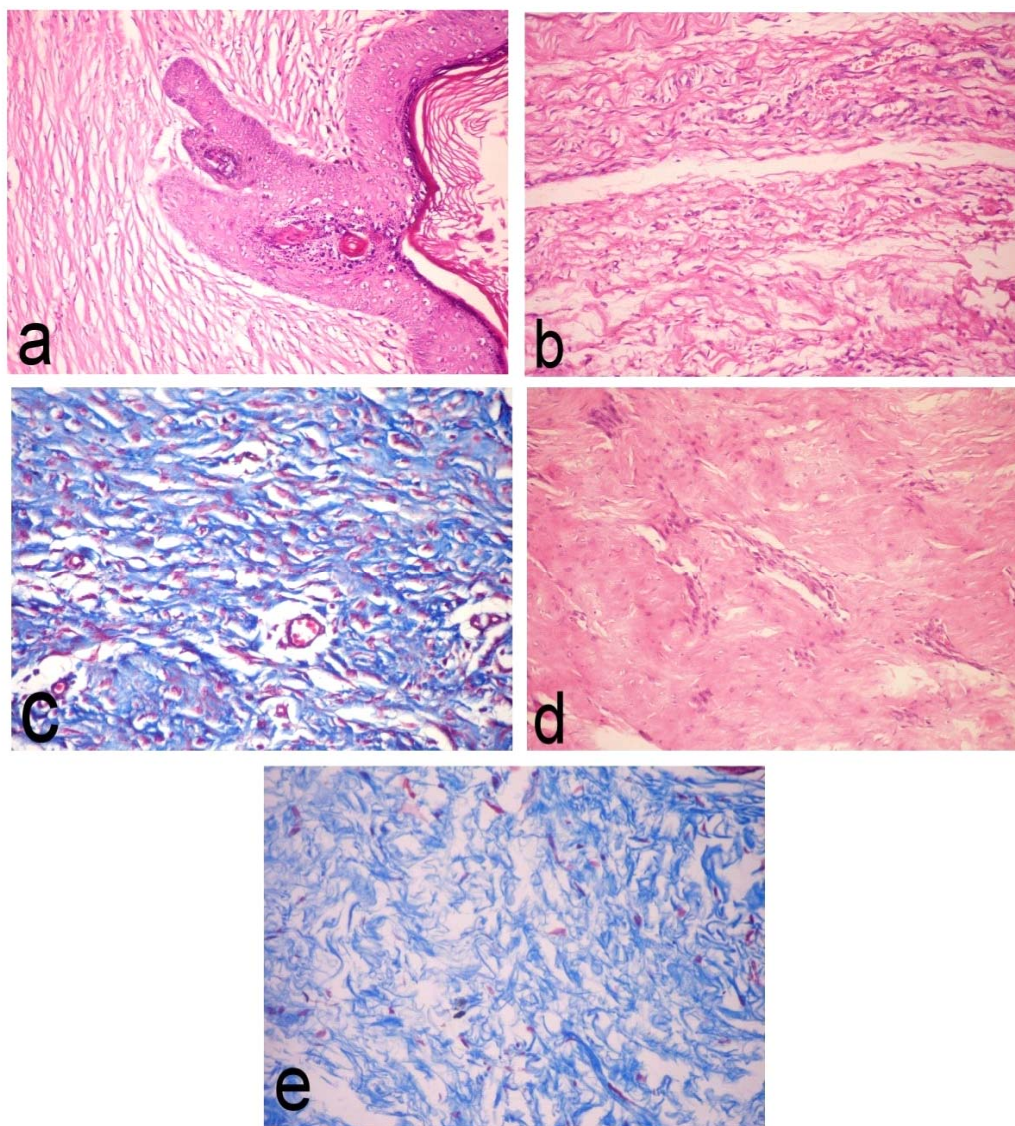


Fig. (7): Photomicrograph of skin wounds in the experimental cases:

- a. Wounds treated with chitosan 4 weeks post-wounding showing complete regeneration of epidermal cells with keratin layer similar to the normal skin associated with dermal connective tissue proliferation (H & E stain X 200).
- b. Wounds treated with chitosan 4 weeks post-wounding showing wavy collagen bundles surrounding the neovasculation of the wound (H & E stain X 200).
- c. Wounds treated with chitosan 4 weeks post-wounding showing wavy collagen bundles surrounding the neovasculation of the wound (Trichrome stain X 200).
- d. Control wound 3 weeks post-wounding showing hyalinosis of subcutaneous granulation tissue (H & E stain X 200).
- e. Control wound 3 weeks post-wounding showing haphazardly arranged collagen fibers (Trichrome stain X 200).

It also promotes the healing of ulcers and burns as was mentioned by (Muzzarelli, 2009). In previous studies, it was mentioned that, the aqueous solution of water soluble chitosan embedded in the wounds was

found to be more efficient as a wound-healing accelerator (Minami, Okamoto, Tanioka, 1992).

Our histopathological results correlated well with the clinical observations as wounds treated with chitosan at 1 week post-wounding showed hyperactive

fibroblasts proliferation which appeared earlier compared with the control wounds that showed massive infiltration with neutrophils associated with haemorrhage.

Two weeks postwounding, advanced granulation tissue formation was more pronounced by the chitosan treatment associated with formation of new blood vessels than in the control group. At that time, there was an increase in the fibroblasts proliferation with infiltration of polymorphonuclear cells which was attributed to the effect of chitosan that enhances the functions of inflammatory cells and phagocytosis to promote healing as was mentioned by (Takashi and Toru, 2001). Promoted angiogenesis was explained by (Muzzarelli, 2009 and Gomma, 2010) as production of the vascular endothelial growth factor is strongly up-regulated in wound healing when macrophages are activated by chitosan. Also blood platelets were activated by chitosan with redundant effects and superior performance which was necessary to support physiologically ordered tissue formation. On the other hand, at that time, control wounds showed epidermal and dermal necrosis associated with infiltration with neutrophils and macrophages with fibroblasts proliferation.

Wounds treated with chitosan 3 weeks post-incision showed early proliferation of epidermal cells and reepithelization with different mitotic figures and dermal granulation tissue formation. On the other hand, in the control wounds, results showed hyalinosis of subcutaneous granulation tissue. Highly vascularized and well organized subcutaneous granulation tissue was seen in the treated wounds, however, the control wounds showed haphazardly arranged collagen fibers.

Four weeks post-incision treated wounds showed complete regeneration of epidermal cells with keratin layer similar to the normal skin associated with dermal connective tissue proliferation. Wavy well oriented mature collagen bundles were seen. On the other hand, control group showed haphazard orientation of the collagen fibers. Those results coincided with Yong-Woo, Yong-Nam, Sang-Hun, Gyeol, Sohk-won, (1999).

Those previous results indicated acceleration of the wound healing compared with the normal physiological repair. Same findings were mentioned by (Muzzarelli, 2009) as chitosan enhances the functions of inflammatory cells and production of leukotriene B₄, macrophages interleukin (IL)-1, transforming growth factor β 1 and platelet derived growth factor and fibroblasts. Moreover (Ishihara et al; 2001) added that, the chitosan mesh membrane showed a positive effect on the re-epithelialization and the regeneration of the granular layer.

In this experimental work, all the chitosan treated wounds were not dressed by any local antiseptic and animals did not receive systemic antibiotics but showed clean and uncomplicated healing this may be attributed to the biological properties of chitosan as it possess bacteriostatic and fungistatic properties particularly useful for wound treatment as was mentioned by (Jarmila and Vavřiková, 2011).

It is important to mention that, in this experiment all the wounds were surgical incisions where there was very little tissue loss, aseptic operations and were easy to heal, meanwhile, accidental or chronic wounds disrupt normal process of healing and is often not sufficient itself to effect repair.

As was mentioned by (Okamoto *et al.*, 1995), complications of chitosan application included the potential for allergy in individuals allergic to shellfish. Clinical trials reported few adverse events, generally limited to flatulence and constipation. Second complication was lethal pneumonia in dogs when given a high dose of chitosan. On the other hand, our results in the application of chitosan powder in dogs did not face any complications, this may be due to the low doses topically applied on treated wounds. Previous researches considered the use of chitosan solution is more suitable for wound-healing than powder due to its easy application and high effectiveness.

In conclusion this study proved that the biomedical product chitosan is effective for tissue regeneration and showed better and faster tissue epithelization. As far as we can see, chitosan seemed to have no known side-effects and safe. Moreover from the different studies reported in the available literatures and our results, chitosan seems to be an excellent candidate dressing material for wound repair.

Reference

1. Azad Sermsintham, Chandkrachang and Frans Stevens (2004): Chitosan membrane as a wound-healing dressing: Characterization and clinical application. *Journal of Biomedical Materials Research Part B: Applied Biomaterials*, 69B(2): 216–222.
2. Balassa L.L., Prudden J.F. (1984): Applications of chitin and chitosan in wound healing acceleration, in *Chitin, Chitosan and Related Enzymes*, Academic Press, San Diego, 296-305.
3. Bancroft, J.D.; Stevens, A. and Turner, D.R. (1996): *Theory and Practice of Histological Techniques*. 4th Ed. New York, Churchill, Livingstone.
4. Cohen IK. A. (1989): *Brief History of Wound Healing*. 1st ed. Yardley, PA: Oxford Clinical Communications Inc;

5. Eokamoto Y, Shibazaki K, Minami S, Matsuhashi A, Tanioka S, Shigemasa Y. *J Vet Med Sci.* (1995): Evaluation of chitin and chitosan on open wound healing in dogs; *57(5)*:851-4.
6. Gomma, A.A. (2010): The role of some biomaterials in wound healing. Thesis for M.V.Sc., Dept of Surg. Anaesthes. and Radiol.. Faculty of Vet. Med. Monofia University
7. Ishihara, M.; Ono, K.; Sato, M.; Nakanishi, K.; Saito, Y.; Yura, H.; Matsui, T.; Hattori, H.; Fujita, M.; Kikuchi, M.; Kurita, A. (2001): Acceleration of wound contraction and healing with a photocross linkable chitosan hydrogel. *Wound Repair Regen.*, *9(6)*: 513-521.
8. Jarmila, V and Vavříková, E. (2011): Chitosan derivatives with antimicrobial, antitumour and antioxidant activities - a review. *Curr Pharm Des.*; *17(32)*:3596-607.
9. Jayasree R.S., Rathinam K., Sharma C.P., J. (1995) *Biomater. Appl.*, *10*, 144-153.
10. Minami S., Okamoto Y., Matsuhashi A., (1992): Application of chitin and chitosan in large animal practice, In Brine C.J., Sandford P.A., Zikakis J.P., 1st Ed., *Advances in chitin and chitosan*, Elsevier, 61-69,
11. Muzzarelli R.A. (1989): Amphoteric derivatives of chitosan and their biological significance, in *Chitin and Chitosan*, Elsevier Applied Science, London, 87-99,.
12. Muzzarelli, R. A. (2004): Potential applications of chitosan in veterinary medicine: Original Research Article *Advanced Drug Delivery Reviews*, *56*, (10): 1467-1480
13. Muzzarelli, R.A. (2009): Chitins and chitosans for the repair of wounded skin, nerve, cartilage and bone Review Article *Carbohydrate Polymers*, *76*, (2):,167.
14. Okamoto, Y.; Shibazaki, K.; Minami, A.; Tanioka, S. and Shigemasa, Y. (1995): Evaluation of chitin and chitosan on open wound healing in dogs. *J. Vet. Med. Sci.*, *57(5)*: 851-854.
15. Pusateri, A. E., S. J. McCarthy, K. W. Gregory, R. A. Harris, L. Cardenas, A. T. McManus & C. W. Goodwin Jr. (2003): "Effect of a chitosan-based hemostatic dressing on blood loss and survival in a model of severe venous hemorrhage and hepatic injury in swine". *Journal of Traumat.*, *4(1)*: 177-182.
16. Sevda Şenel, Susan J McClure (2004): Potential applications of chitosan in veterinary medicine *Advanced Drug Delivery Reviews*, Volume 56, 10 1467-1480.
17. Stoker, DG; Reber, KR and Waltzman, LS, (2008) : Analgesic efficacy and safety of morphine-chitosan nasal solution in patients with moderate to severe pain following orthopedic surgery. *Pain Med.*; *9(1)*:3
18. Takashi Mori and Toru Fujinaga (2001): Topical formulations and wound healing applications of chitosan. *Advanced Drug Delivery Reviews* *52*, *12*, 105-115
19. Ueno Yamada, Tanaka Kaba, Mitsunobu Matsuura, Okumura, Kadosawa, Fujinaga. (1999): Accelerating effects of chitosan for healing at early phase of experimental open wound in dogs: *Biomaterials* Volume 20, (15) 1407-1414.
20. Willi, Paul and Chandra, P. Sharma (2004): Chitosan and Alginate Wound Dressings: A Short Review. *Trends Biomater. Artif. Organs*, *18(1)* 18-23.
21. Yong-Woo Choa, Yong-Nam Chob, Sang-Hun Chungb, Gyeol Yoob, Sohk-Won Koa (1999): Water-soluble chitin as a wound healing accelerator: *Biomaterials* *20*, (22): 2139-2145.

12/22/2011

Detection of Circulating Microparticles in Patients with Proliferative Diabetic Retinopathy

Samy A Khodeir¹, Y M Abd El Raouf¹, Gihan Farouk² and Mohammed EL-Bradey³

Departments of ¹Internal Medicine ²Clinical Pathology and ³Ophthalmology, Faculty of Medicine, Tanta University
masyasser@yahoo.com

Abstract: Background: The development of vasculopathies in diabetes involves multifactorial processes including pathological activation of vascular cells. Release of microparticles by activated cells has been reported in diseases associated with thrombotic risk, but few data are available in diabetes. Diabetic retinopathy is associated with increased local activation or apoptosis of retinal, neural, and vascular endothelial cells in the eye which indicate that microparticles (MPs) of different cellular origin might be locally generated in the eye of diabetic patients. Aim: The aim of this study is to investigate the presence of endothelial, platelet, and retinal-derived microparticles both in the vitreous and in the plasma of diabetic patients compared with that of non diabetic ones. Subjects and methods: In a case-control study, this study included 45 patients: 25 diabetic patients with non proliferative diabetic retinopathy (NPDR), and 20 diabetic patients with proliferative diabetic retinopathy (PDR) compared with control group consists of non diabetic 10 subjects. Blood samples were analyzed by flow cytometry. Microparticles present in plasma and vitreous were analyzed according to their parameters of size and fluorescence. Results: As regard plasma samples, there was significant increase in CD144 and CD41 in groups II, III as compared with control group ($p = 0.001$). Peanut agglutinin PNA was not detected in plasma sample among all studied groups. Whereas, as regard to the vitreous sample, there was significant increase in CD144, CD41 and PNA in groups II,III as compared with control group ($p = 0.048, 0.009, 0.048$), ($P = 0.001$) respectively. Conclusion: microparticles appear as a new prognostic potential of type 2 diabetes in the early detection of vascular complications. Moreover significant increase of different types of microparticles in vitreous fluid of membrane in patients with PDR, may contribute to disease progression.

[Samy A Khodeir, Y M Abd El Raouf, Gihan Farouk and Mohammed EL-Bradey **Detection of Circulating Microparticles in Patients with Proliferative Diabetic Retinopathy**. Life Science Journal, 2012; 9(1): 204-209] (ISSN: 1097-8135). <http://www.lifesciencesite.com>. 29

Key words: Microparticles, diabetic retinopathy, endothelial cell dysfunction.

1. Introduction

Long term micro- and macrovascular complications represent the main cause of morbidity and mortality in both type 1 and type 2 diabetes. Microangiopathy is a common feature of both types of diabetes, whereas macroangiopathy occurs more frequently in type 2 diabetes on account of the clustering of other traditional risk factors of atherosclerosis, i.e., hypertension, dyslipidemia, or obesity. The pathogenesis of diabetic vascular complications is complex and multifactorial. Early alterations of endothelial function may be involved in the development of both micro- or macroangiopathy in diabetic patients⁽¹⁾.

Diabetic patients also show hypercoagulability and platelet hyperaggregability with increased levels of platelet activation-markers such as P-selectin, soluble CD40 ligand and microparticles (MPs)⁽²⁾.

It is well accepted that in response to activation or apoptosis, all eukariotic cells shed microparticles (MPs). These elements are produced from the plasma membrane after the flip-flop of the membrane phospholipids leading to a loss of

membrane asymmetry. The blebs formed at the cell surface are then shed in the circulation under the form of vesicles ranging in size from 0.1 to 1 μ m. Increased levels of microparticles, mainly derived from platelets and to a lesser extent from leukocytes and endothelial cells⁽³⁾.

Microparticles have been identified not only in human plasma but also in other tissues with high cellular activation, inflammation, or apoptosis, such as human atherosclerotic plaques or synovial fluid in rheumatoid arthritis^(4,5).

Endothelial microparticles (EMPs) are an emerging marker of endothelial cell (EC) dysfunction, and their circulating numbers are elevated in a number of pathologic states including cardiovascular disease⁽⁶⁾. Since vascular-endothelial cadherin is exclusively expressed by endothelial cells, CD144-positive microparticles may be regarded as endothelium-derived microparticles (EMPs), directly reflecting endothelial damage. However, it is unknown whether circulating EMPs are cause or consequence of CVD, and whether their occurrence associates with CVD per se or, rather,

with diabetes-related metabolic abnormalities⁽²⁾.

Platelet-derived MPs contain surface receptors for both factor VIII⁽⁷⁾, and FVa, which combines with FXa to form the prothrombinase complex⁽⁸⁾. High- and low-affinity binding sites for activated FIX are also present on platelet-derived MPs⁽⁹⁾. These findings suggest that platelet-derived MPs can exert procoagulant distant effects from the site of platelet activation, and for a period longer than that of activated platelets. In addition, **Sinauridze et al.**, reported that platelet-derived MPs have 50- to 100-fold higher specific procoagulant activity than activated platelets⁽¹⁰⁾.

Despite current treatments and existing knowledge, diabetic retinopathy remains to be a major cause of blindness in patients. New evidence indicates that diabetic retinopathy may be an inflammatory disease. The retinal vasculature of diabetic humans contains increased numbers of leukocytes, a finding that coincides with the increased expression of ICAM-1 in retinal vasculature. The increased density of leukocytes in the retinal vasculature results in injury to the endothelium via a FasL-mediated mechanism; a process that leads to breakdown of the blood-retinal barrier. Blood-retinal barrier breakdown develops early in the course of diabetic retinopathy in humans and, as a long term lesion is the major pathology leading to macular edema and the risk of subsequent visual loss⁽¹¹⁾.

Diabetic retinopathy is associated with increased local activation or apoptosis of retinal, neural, and vascular endothelial cells in the eye. These findings indicate that microparticles of different cellular origin might be locally generated in the eye of diabetic patients.⁽¹²⁾

The aim of this study is to investigate the presence of endothelial, platelet, and retinal-derived microparticles both in the vitreous and in the plasma of diabetic patients compared with that of non diabetic ones.

2. Patients and Methods

This study was performed on 45 patients (age range 36–69 years, mean 57) who underwent vitrectomy at Tanta University Hospital. All patients signed a written informed consent. Prior to surgery, diabetic retinopathy was evaluated according to the simplified international diabetic retinopathy classification⁽¹³⁾, made on the basis of clinical data, intraoperative assessment by the surgeon, and review of fundus and fluorescein angiography.

The patients of the study were divided into three groups:

Group I: control group consists of non diabetic 10 subjects.

Group II: 25 diabetic patients with non proliferative diabetic retinopathy (NPDR).

Group III: 20 diabetic patients with proliferative diabetic retinopathy (PDR).

Venous blood samples (10 ml) were collected on EDTA tubes before vitrectomy and platelet-free plasma (PFP) from 55 subjects was immediately prepared by successive centrifugations according to the methodology of **Amabile et al.**,⁽¹⁴⁾

Undiluted vitreous fluid samples (300–400 μ l) were collected from patients' eyes at the start of a standard three-port pars plana vitrectomy for the treatment of retinal diseases. A core vitrectomy was performed using the vitreous cutter (Accurus 800, Fortworth, Texas). Vitreous samples were collected at the beginning of vitrectomy before opening the balanced salt solution infusion line to maintain intraocular pressure. The tube vacuum connection was then disconnected and the vitreous was aspirated using sterile syringe. The vitreous sample is then homogenized by gently pipetting the suspension up and down several times. Samples were collected from the eyes of the patients with diabetic retinopathy. The control group consisted of vitreous samples from 10 eyes of 10 non diabetic patients with an idiopathic macular hole, an idiopathic epiretinal membrane, a rhegmatogenous retinal detachment, or age-related macular degeneration. Vitreous microparticles were isolated from fresh vitreous drawn at beginning of the surgery. Vitreous was separated from cells and platelets after two centrifugations (500g for 15 min and 13,500g for 5 min).

Reagents

Fluorescein isothiocyanate (FITC)-conjugated monoclonal antibody (mAb) against vascular endothelial (VE)-Cadherin (CD144) and phycoerythrin (PE)-conjugated mAb against platelet glycoprotein GPIIb/IIIa (PE-CD41, clone P2) were used to identify endothelial microparticle (EMP) and platelet microparticle (PMP), respectively. Lectins from arachis hypogaea peanut agglutinin (PNA) conjugated with FITC were from Sigma Aldrich, France PE- and FITC-conjugated isotype controls (PEIgG2, FITC-IgG1) were used to define the background noise of the labeling. Microparticle absolute values were determined using Flowcount beads (Beckman Coulter, Margency, France).

Microparticle quantitation

Numeration of platelet- and endothelial-derived microparticles was performed, as previously described⁽¹⁵⁾, using anti-CD41 and anti-CD144 labeling, respectively. After thawing, 30 μ l of plasma was incubated with either FITC-CD41 or

with PE-CD144 PE and their corresponding isotype control. FITC-conjugated lectins were diluted in PBS to reach the final concentration of 100 g/ml. Human vitreous (60 l) was incubated with lectin from PNA FITC (20 g. Its respective control was preincubated with D-galactose (80 mmol/l for 30 min) (Sigma-Aldrich). Then, 30 l of Flowcount beads was added to each sample for calculation of microparticle absolute value. Microparticles were gated as events with a 0.1-to 1.0- μ m diameter identified in forward-scatter and sidescatter intensity dot-plot representation using standards synthetic beads of 1 μ m in diameter (Polyscience).

Flow cytometric analysis.

After labeling, samples were analyzed by FACS caliber flow cytometry. Microparticles present in plasma and vitreous were analyzed according to their parameters of size and fluorescence.

Statistical analysis:

Statistical presentation and analysis of the present study was conducted, using the mean, standard deviation, t. test and Linear Correlation Coefficient by SPSS V.16.⁽¹⁶⁾.

3. Results

This study was performed on 45 patients with type 2 diabetes mellitus, 25 patients with NPDR as group II and 20 patients with PDR as group III and

compared with 10 non diabetic subjects (group I).

As regard plasma samples, there was significant increase in CD144 and CD41 in group II as compared with control group and in group III as compared with group II ($p=0.001$). PNA was not detected in plasma sample among all studied groups as shown in table 1

Whereas, as regard to the vitreous sample, there was significant increase in CD144, CD41 and PNA in group II as compared with control group ($p=0.048, 0.009, 0.048$) respectively. There was also significant increase in CD144, CD41 and PNA in group III as compared with control group ($p=0.001$) and in group III as compared with group II (0.001). Table 2

Table 3 demonstrate that in group II, there was significant positive correlations between CD144 and CD 41 in plasma sample ($p=0.004$) and in vitreous sample, there was significant positive correlation between CD144 and CD 41, CD41 and PNA and between CD 144 and PNA ($p=0.014, 0.035$ and 0.059) respectively.

Table 4 demonstrate that in group III, there was significant positive correlations between CD144 and CD 41 in plasma sample ($p=0.032$) and in vitreous sample, there was significant positive correlation between CD144 and CD 41, CD41 and PNA and between CD 144 and PNA ($p=0.029, 0.028$ and 0.037) respectively.

Table (1): Plasma levels of endothelial, platelet and photoreceptor derived micoparticles in all studied groups:

	Group I (n=10)	Group II (n=25)	Group III (n=20)	P1	P2	P3
CD 144	125.9 \pm 12	355.6 \pm 64.8	912 \pm 89.4	0.001*	0.001*	0.001*
CD 41	530.8 \pm 35.7	1440 \pm 79.17	2170.4 \pm 109	0.001*	0.001*	0.001*
CD PNA	0	0	0	-	-	-

* Highly Significant ($p < 0.001$)

P1 comparison between GI&GII, P2: GI&GIII, P3: GII&GIII

Table (2): Vitreous levels of endothelial, platelet and photoreceptor derived micoparticles in all studied groups:

	Group I (n=10)	Group II (n=25)	Group III (n=20)	P1	P2	P3
CD 144	35.44 \pm 9.3	42.7 \pm 12.10	213.2 \pm 77.1	0.048**	0.001*	0.001*
CD 41	23.25 \pm 10	46 \pm 21.32	158.44 \pm 56.1	0.009**	0.001*	0.001*
CD PNA	13.32 \pm 4.4	15.77 \pm 3	178.30 \pm 34.4	0.048**	0.001*	0.001*

* Highly significant ($p < 0.001$)

**Significant ($p < 0.05$)

P1 comparison between GI&GII, P2: GI&GIII, P3: GII&GIII,

Table (3): Correlation between all studied parameters in group II:

	Plasma sample		Vitreous sample	
	CD41	CD144	CD144	CD41
CD144	r.0.569 p0.004*			r.0.358 P0.014*
CD PNA			r.0.214 p0.059	r.0.299 P0.035*

** Highly significant (p< 0.001)

*Significant (p< 0.05)

Table (4): Correlation between all studied parameters in group III:

	Plasma sample		Vitreous sample	
	CD41	CD144	CD144	CD41
CD144	r.0.310 p0.032*			r.0.417 P0.029*
PNA			r.352 P0.037*	r.0.410 P0.028*

** Highly Significant (p< 0.001)

*Significant (p< 0.05)

4. Discussion

DM is associated with increased levels of circulating EMPs. This agrees with previous studies where levels of endothelial microparticles (EMPs) were associated with microalbuminuria and microvascular complications in patients with diabetes, suggesting that EMPs could be a marker of diabetes associated endothelial dysfunction^(17,18).

This study revealed significant increase in EMPs (CD144) and platelet derived MPs (CD 41) in the studied diabetic patients as compared with control group and significant increase in diabetic patients with PDR as compared with diabetic patients without PDR in venous sample. Also, PNA was not detected in plasma sample among all studied groups.

These results were in agreement with **Tramontano *et al.***, who found that the absolute median number of EMP was significantly increased in DM population⁽¹⁹⁾. However, diabetic patients differ by the procoagulant activity and the cellular origin of microparticles. Indeed, EMP and PMP, levels and procoagulant activity were elevated in type 1 diabetes. Interestingly, this procoagulant activity was correlated with levels of HbA1c⁽¹⁸⁾.

The immunophenotype of MPs depends on whether they are released by cell activation or by apoptotic stimulus⁽²⁰⁾. Cellular apoptosis is associated with an increase in cytosolic calcium, with changes in the transmembrane steady state leading to the cleavage of cytoskeleton filaments. These phenomena result in the blebbing and shedding of membrane-derived MPs into the extracellular fluid⁽²¹⁾.

MPs released from apoptotic cells may be different in lipid and protein composition from membrane vesicles shed following cell activation and could possibly have different patho-physiological effects. Blebbing of cellular membrane occurs rapidly after cells enter the apoptotic process⁽²⁰⁾.

The reason that cells shed MPs from their main

body may be an attempt to reverse the apoptotic process by getting rid of unwanted signaling molecules like the proapoptotic caspase 3⁽²²⁾. The release of MPs would also allow cells to escape phagocytosis by removing quickly from the cell surface “eat-me-signals,” such as phosphatidylserine⁽²³⁾. Alternatively, membrane shedding could constitute a signaling entity to phagocytes and neighbor cells, because their interaction modulates inflammation, immune responses, and repair mechanisms⁽²⁴⁾.

Actually, the release of membrane vesicles to signal to neighbor or remote target cells is not a specific property of eukaryotic cells^(25,26). These results might be interpreted as an indication of enhanced endothelial cell apoptosis, rather than activation in those having DM⁽¹⁹⁾.

Endothelial cell-derived MPs express many receptors and components of the parent endothelial cell including tissue factor (TF) and can support thrombin generation by the TF/FVIIa pathway^(27,28). That is to say, endothelial cell-derived MPs provide a source of TF, as well as a catalytic surface, for assembly of prothrombinase complex. Furthermore, endothelial cell-derived MPs are possible to be a marker of endothelial activation in patients with the metabolic syndrome^(29,30).

Microparticles can also directly affect vascular endothelial cells by increasing leukocyte adhesion, triggering cytokine production, and exposing tissue factor or P-selectin^(31,32). In addition, microparticles promote endothelial dysfunction by impairing the endothelial NO pathway and inducing proinflammatory responses⁽³³⁻³⁵⁾.

In this study, it was found that in vitreous sample, there was significant increase in CD144, CD41 and PNA in diabetic group without PDR (group II) as compared with control group and in diabetic group with PDR (group III) as compared with group II

These results were in agreement with a study by **Chaded *et al.***, who reported that there were vitreous levels of platelet CD41 and endothelial CD144 microparticles were all markedly increased in diabetic compared with control. Microparticles of endothelial origin, identified as expressing VE-cadherin (CD144), were the most abundant microparticle subpopulation in vitreous samples from diabetic patients. Vitreous levels of endothelial CD144, and platelet CD41 microparticles were increased in association with PDR compared with non-PDR (NPDR) ⁽³⁶⁾.

Significant numbers of endothelial microparticles found in the vitreous fluid could be generated from local microvascular endothelial cells in PDR or that clearance of endothelial microparticles was abnormal. On the contrary, the ratio for platelet CD41 microparticles was lower than unity, favoring the interpretation that platelet microparticles present in PDR vitreous fluid likely originate from the plasma ⁽³⁶⁾.

Sabatier *et al.*, reported that levels of platelet-derived MPs and monocyte derived MPs have been shown to correlate with diabetic complications or the extent of diabetic retinopathy, which is associated with microvascular damage ⁽²⁸⁾.

PDR is associated with ocular increases in oxidative stress, protein glycation, growth factors, inflammatory cytokines, and cell apoptosis, all of which stimulate the shedding of membrane microparticles from retinal or vascular cells ^(5,37). In addition, this demonstrates the presence of microparticles positively labeled with either PNA in vitreous samples but not in plasma, indicating their photoreceptor or microglial origin, respectively. These microparticles originate from cells localized in deeper retinal layers and may be released in vitreous fluid following the tear of the retinal internal limiting membrane ⁽³⁸⁾.

In conclusion, MPs appears as a new prognostic potential of type 2 diabetes in the early detection of vascular complications. Elevation of plasma MPs levels, particularly those of endothelial origin, reflects cellular injury and may be a useful as a surrogate marker of vascular dysfunction. Moreover the presence of different types of microparticles in vitreous fluid of membrane shed from retinal, endothelial, and circulating cells and their significant increase in patients with PDR, may contribute to disease progression.

Corresponding author

Y M Abd El Raouf

Department of Internal Medicine, Faculty of Medicine, Tanta University
masyasser@yahoo.com

References

- 1- Kirpichnikov D and Sowers JR(2002). Diabetes mellitus and diabetes-associated vascular disease. *Trends Endocrinol Metab.*; 12:225–230.
- 2- Maarten ET, Rienk N, Cees R, Bert E H, August S, Robert JH and Michaela D (2007). Elevated Endothelial microparticles following consecutive meals are associated with vascular endothelial dysfunction in type 2 diabetes. *Diabetes Care*; 30 (3): 728-730.
- 3- Zwaal RF, Comfurius P and Bevers EM(1992). Platelet procoagulant activity and microvesicle formation: its putative role in hemostasis and thrombosis. *Biochim Biophys Acta*; 1180:1–8.
- 4- Berckmans RJ, Nieuwland R, Tak PP, Boing AN, Romijn FP, Kraan MC, Breedveld FC, Hack CE and Sturk A(2002). Cell-derived microparticles in synovial fluid from inflamed arthritic joints support coagulation exclusively via a factor VII-dependent mechanism. *Arthritis Rheum.*;46: 2857–2866
- 5-Boulanger CM, Amabile N and Tedgui A(2006). Circulating microparticles: a potential prognostic marker for atherosclerotic vascular disease. *Hypertension*; 48: 180–186
- 6- Mallat Z., H. Benamer and B. and Hugel(2000). Elevated levels of shed membrane microparticles with procoagulant potential in the peripheral circulating blood of patients with acute coronary syndromes. *Circulation*; 101(8): 841–843.
- 7- Gilbert GE, Sims PJ, Wiedmer T, Furie B, Furie BC and Shattil SJ(1991). Platelet-derived microparticles express high affinity receptors for factor VIII. *J Biol Chem* ;266: 1726-8.
- 8- Comfurius P, Senden JMG, Tilly RHJ, Schroit AJ, Bevers EM and Zwaal RFA (1990). Loss of membrane phospholipid asymmetry in platelets and red cells may be associated with calcium-induced shedding of plasma membrane and inhibition of aminophospholipid translocase. *Biochim Biophys Acta*; 1026: 153-60.
- 9- Hoffnan M, Monroe DM and Roberts HR(1992). Coagulation factor IXa binding to activated platelets and platelet-derived microparticles: a flow cytometric study. *Thromb Haemost.*; 68: 74-8.
- 10-Sinauridze EI, Kireev DA and Popenko NY(2007). Platelet microparticle membranes have 50- to 100-fold higher specific procoagulant activity than activated platelets. *Thromb Haemost.*; 97: 425- 34.
- 11- Jousen, A. M. (2003). Suppression of Fas-FasL-induced endothelial cell apoptosis prevents diabetic blood-retinal barrier breakdown in a model of streptozotocin-induced diabetes. *FASEB J*; 17: 76–78.
- 12- Jousen AM, Poulaki V, Le ML, Koizumi K, Esser C, Janicki H, Schraermeyer U, Kociok N, Fauser S, Kirchhof B, Kern TS and Adamis AP (2004). A central role for inflammation in the pathogenesis of diabetic retinopathy. *Faseb J*; 18: 1450–1452.
- 13- Mizutani M, Kern TS and Lorenzi M (1996). Accelerated death of retinal microvascular cells in human and experimental diabetic retinopathy. *J Clin Invest.*; 97: 2883–2890.
- 14- Amabile N, Guerin AP, Leroyer A, Mallat Z, Nguyen C, Bodaert J, London GM, Tedgui A and Boulanger

- CM(2005). Circulating endothelial microparticles are associated with vascular dysfunction in patients with end-stage renal failure. *J Am Soc Nephrol.*; 16: 3381–3388.
- 15- Ogata N, Nomura S, Shouzu A, Imaizumi M, Arichi M, Matsumura M (2006). Elevation of monocyte-derived microparticles in patients with diabetic retinopathy. *Diabetes Res Clin Pract.*; 73: 241–248.
- 16- Knapp R.G (1992): Describing the performance of a diagnostic test. *Clinical Epidemiology and Biostatistics* P. 42.
- 17- Diamant M., Nieuwland R., Pablo R. F, Sturk, J. W. Smit A, and. Radder J. K (2002). Elevated numbers of tissue factor exposing microparticles correlate with components of the metabolic syndrome in uncomplicated type 2 diabetes mellitus. *Circulation*; 106(19): 2442–2447
- 18- Sabatier F., Darmon P and Hugel B(2002). Type 1 and type 2 diabetic patients display different patterns of cellular microparticles. *Diabetes*; 51(9): 2840–2845.
- 19- Tramontano A. F., Lyubarova R., Tsiakos J., Palaia T. DeLeon J. R and Ragolia L (2010). Circulating endothelial microparticles in diabetes mellitus. *Mediators Inflamm.*; 2010: 250476.
- 20- Jimenez JJ, Mauro LM, Soderland C, Hostman LL and AHN YS (2003). Endothelial cell release phenotypically and quantitatively distinct microparticles in activation and apoptosis. *Thromb Res.*; 109: 175-180
- 21- Blankenberg S., Barboux S. and Tired L(2003). Adhesion molecules and atherosclerosis. *Atherosclerosis* ; 170 (2) : 191– 203
- 22- Jimenez JJ, Mauro LM, Ahn YS, Newton KR, Mendez AJ, Arnold PI, Schultz DR (2002). Agonist-induced capping of adhesion proteins and microparticle shedding in cultures of human renal microvascular endothelial cells. *Endothelium*; 9: 179 –189.
- 23- Fadok VA, Bratton DL, Rose DM, Pearson A, Ezekewitz RA, Henson PM(2000). A receptor for phosphatidylserine-specific clearance of apoptotic cells. *Nature*; 405: 85–90.
- 24- Golpon HA, Fadok VA, Taraseviciene-Stewart L, Scerbavicius R, Sauer C, Welte T, Henson PM and Voelkel NF(2004). Life after corpse engulfment: phagocytosis of apoptotic cells leads to VEGF secretion and cell growth. *Faseb J*; 18: 1716 –1718.
- 25- Mashburn LM, Whiteley M (2005). Membrane vesicles traffic signals and facilitate group activities in a prokaryote. *Nature*; 437: 422– 425.
- 26- Chantal M. Boulanger, Nicolas Amabile, Alain Tedgui (2006). Circulating Microparticles. A potential prognostic marker for atherosclerotic vascular disease. *Hypertension*; 48: 180-186
- 27-Freyssinet JM(2003). Cellular microparticles: What are they bad or good for? *J Thromb Haemost.* ; 1: 1655-62.
- 28-Sabatier F, Roux V, Anfosso F, Camoin L and Sanpognat- George F (2002). Interaction of endothelial microparticles with monocytic cells in vitro induces tissue factor-dependent procoagulant activity. *Blood*; 99(11): 3962-70.
- 29- Arteaga RB, Chirinos JA and Soriano AO(2006). Endothelial microparticles and platelet and leukocyte activation in patients with the metabolic syndrome. *Am J Cardiol.*; 98: 70-4.
- 30- Shosaku Nomura (2009). Dynamic role of microparticles in type 2 diabetes mellitus. *Curr Diabetes Rev.*; 5(4): 245-51.
- 31- Van Wijk MJ, Van Bavel E, Sturk A and Nieuwland R(2003). Microparticles in cardiovascular diseases. *Cardiovasc Res.*; 59: 277– 87.
- 32- Wagner DD. (2005): New links between inflammation and thrombosis. *Arterioscler Thromb Vasc Biol.*, 25(7): 1321-4.
- 33- Boulanger CM, Scoazec A, Ebrahimian T, Henry P, Mathieu E and Tedgui A (2001). Circulating microparticles from patients with myocardial infarction cause endothelial dysfunction. *Circulation*; 104: 2649–52
- 34- Brodsky SV, Zhang F, Nasjletti A and Goligorsky MS(2004). Endothelium derived microparticles impair endothelial function in vitro. *Am J Physiol Heart Circ Physiol.*; 286(5): H1910– 5.
- 35- Boulanger CM and Tedgui A(2005). Dying for attention: Microparticles and angiogenesis. *Cardiovascular Research*; 67: 1 –3.
- 36- Chahed S, 'lie A S, Leroyer, Benzerroug M, Gaucher D and Georgescu A (2010). Increased vitreous shedding of microparticles in proliferative diabetic retinopathy stimulates endothelial proliferation . *Diabetes*; 59: 694–701.
- 37- Hugel B, Martinez MC, Kunzelmann C and Freyssinet JM (2005). Membrane microparticles: two sides of the coin. *Physiology (Bethesda)*; 20: 22–27.
- 38- Taraboletti G, D'Ascenzo S, Borsotti P, Giavazzi R, Pavan A and Dolo V(2002). Shedding of the matrix metalloproteinases MMP-2, MMP-9, and MT1-MMP as membrane vesicle-associated components by endothelial cells. *Am J Pathol* ;160:673–680.

12/21/2011

Effect of the Strengthened Ribs in Hybrid Toughened Kenaf/ Glass Epoxy Composite Bumper Beam

M.M. Davoodi¹, S.M. Sapuan¹, Aidy Ali¹, D. Ahmad²

¹Department of Mechanical and Manufacturing Engineering, Universiti Putra Malaysia, 43400 UPM Serdang, Selangor, Malaysia

²Department of Biological and Agricultural Engineering, Universiti Putra Malaysia, 43400 UPM Serdang, Selangor, Malaysia

makinejadm2@asme.org

Abstract: The growth of car production governs new environmental regulations “End-of Life Vehicles” (ELV) to enforce car manufacturer to substitute synthetic material to bio based materials. Low mechanical properties of natural fibre composite confine their application in automotive non-structural components. Hybridizations of kenaf with glass fibre along with epoxy PBT toughening did not completely fulfill the required impact property of the developed bio-composite bumper beam to substitute with typical material of the bumper beam glass mat thermoplastic (GMT). Therefore, in the first stage of the geometrical improvement “concept selection” concluded that the double hat profile (DHP) is the most suitable concept out of eight bumper beam concepts when six parameters with different weight are determined. In second trial, the usage of strengthen rib is employed to improve the impact property and performance of the bumper beam for utilization of hybrid kenaf/glass fibre as a car bumper beam.

[Majid Davoodi Makinejad, Mohammad Sapuan Salit, Aidy Ali, Desa Ahmad. **Effect of the Strengthen Ribs in Hybrid Toughened Kenaf/ Glass Epoxy Composite Bumper Beam**. Life Science Journal.2012;9(1):210-213]. (ISSN:1097-8135). <http://www.lifesciencesite.com>. 30

Keywords: Bumper beam; Finite element analysis; Hybrid material; Natural fibre composite

1. Introduction

Strengthen ribs are exploited to improve the structural strength of hybrid kenaf/glass epoxy composite bumper beam in second trial of geometrical improvement in order to improve the performance of utilizing the developed material in structural component's applications. Strengthen ribs increase distortion resistance and structural stiffness with fewer materials in slender wall (Al-Ashaab, Rodriguez, 2003). It can decrease the bumper beam deflection, elongation and increase impact energy (Brydson, 1999, Hosseinzadeh, Shokrieh, 2005, Marzbanrad, Alijanpour, 2009). The previous result showed that the toughened hybrid kenaf/glass fibre epoxy composite cannot fulfill the GMT impact strength. The geometry improvement commenced with bumper concept selection within six criteria with different weight and concluded with double hat profile (DHP) as a best one out of eight concepts.

There are different parameters that effect in the rib strength (pattern, thickness, top and bottom fillet, weld line area, position) (Harper, 2006, Smith and Suh, 1979, Zhang, Liu, 2009). Besides, load direction, load position, material and manufacturing process should be considered in rib design (Samaha, Molino, 1998). Hosseinzadeh, Shokrieh 3) compare the bumper beam made from SMC and GMT with and without ribs. It is resulted that the rib in the GMT bumper beam can decrease the deflection of the beam 13% and slightly increases the impact force;

however, the ease of manufacturing should be focused. Marzbanrad, Alijanpour 4) shown that the ribbed bumper increase the rigidity and enhance the impact force by 7% in steel bumper beam.

This study focused on the bumper beam structure under low speed impact test with vertical strengthening thin-walled ribs and analyzing the energy absorption improvement of the selected concept. It emphasize on the structural performance of the ribbed bumper beam with developed toughened hybrid kenaf/glass epoxy. The material model of the developed hybrid bio-composite was extracted from the previous study experimental test and checked with the same simulated impact condition. The parameters of the model such as type and size of the element and meshes were modified to match the results together. Then the exact low speed impact test condition (ECE R42) was simulated by finite-element software, ABAQUS Ver16R9. The impact loads defined while the impactor with 1000 kg hit to the bumper beam, which is fixed from both end sides while attached to a solid block, which represent the car weight in center of mass at $x=530$. The meshes, steps, interactions and jobs are defined. Strain energy and deflection of double hat profile (DHP) is analyzed when the vertical ribs are added. It is concluded that the ribbed bumper beam decrease the deflection by 11% and increase the strain energy by 11.3% compared with unribbed bumper beam. The result can increase the reliability of the

developed hybrid bio composite material for utilization in the car bumper beam.

2. Material and Methods

The ingredients of the hybrid bio-composite material consist of kenaf fiber, glass fibre, epoxy and PBT respectively were provided from Institute of Tropical Forestry and Forest Products (INTROP) (Malaysia), Fibreglass Enterprise (China), LECO Corporation (USA), CBT® 160 (PBT) from CYCLICS Corporation (USA). Three plies of glass fibers, and two plies of stretched twisted long kenaf with orientation (0, 90, 0, 90, 0) are prepared. The PBT 5% (w/w) is added under structure-less method to the epoxy and sprayed to the prepared plies and compressed by a preheated mold T=85° C under controlled conditions (P=80 bars and T=85° C). The property of the material which is conducted from the previous study was imported to the ABAQUS V16R9.

The low-speed impact (ECE R42) was simulated in ABAQUS Ver16R9. A pendulum with weight 1000 kg and speed 4 km/h at the contact point, hit to the bumper beam, while is fixed from both sides by two energy absorbers to the block which present the car weight (center of mass at X=530). Figure 1 shown pendulum and boundary conditions.

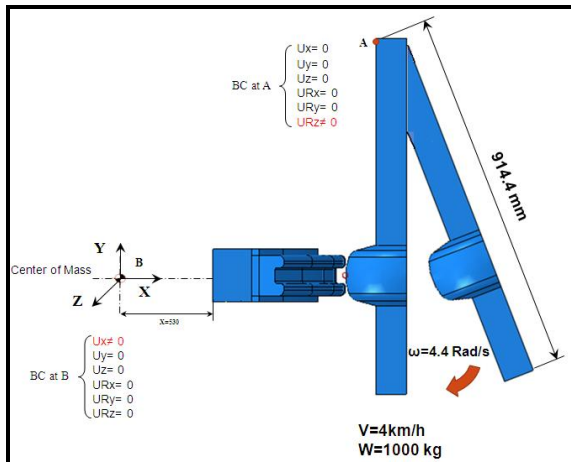


Figure 1. Low impact test simulation and boundary condition

The whole of the elements characteristics are introduced in Table 1.

Table1. Elements characteristics in FEA

No	Part Name	Element type	Element No.	Node	Element Name
1	Barrier	C3D4	2196	620	tetrahedral
2	Mass	C3D8R	16510	19712	hexahedral
3	Left Holder	S4R	513	509	quadrilateral
4	Right Holder	S4R	520	517	quadrilateral
5	Beam	S3	1228	1328	triangular
Total			20967	22686	

Every plies of the hybrid composite is defined separately in ABAQUS with thickness 0.8 mm and 0, 90 direction. The main properties extracted from experimental test and defined in ABAQUS. Since impact property is the main interested objective in this study, the same impact condition was simulated to match the compatibility between experimental by changing the parameters such as type and number of element and method of meshing. (Figure 2).

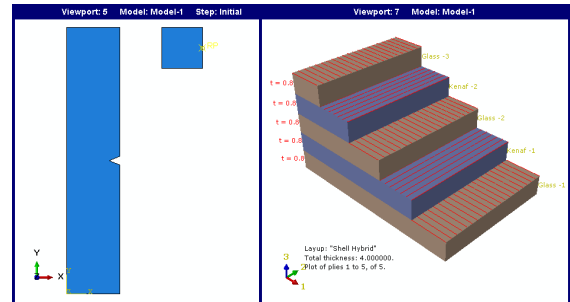


Figure 2. Hybrid kenaf/glass modeling for verification with impact test condition

The low-impact test condition is defined for elastic deformation of the bumper beam (AISI, 2006). Since the bumper beam is fixed from both end's sides, the applied impact load tends it to bend. In bending, the composite failure initiates with matrix cracking followed by debonding between layers, delamination and finally fibre fracture. In ABAQUS, the progressive damage and failure prediction of both fibre and matrix failure determine based on Hashin theory (Hashin, 1980). The Hashin introduced four criteria modes: fibre tension, fibre compression, matrix tension and matrix compression. In this study, matrix tension as an initiation step of failure is considered.

$$F_{mt} = \left[\frac{\sigma_{22}^o}{Y^T} \right]^2 + \left[\frac{\sigma_{12}^o}{S^L} \right]^2 = 1$$

$$\sigma_{22}^o \geq 0$$

σ^o = effective stress

σ = true stress

d_f, d_m, d_s = damage variables

The effective stress can determine from product of the following matrix to the true stress. However, in the software just should input the requested parameters for Hashin criteria consideration.

$$\sigma^{\circ} = \begin{bmatrix} 1 & 0 & 0 \\ 1-d_f & 0 & 0 \\ 0 & 1 & 0 \\ 0 & 0 & 1 \\ 0 & 0 & 1-d_s \end{bmatrix} \sigma$$

Eight vertical ribs (200 mm distance between adjacent ribs and end cap) with 4 mm thickness is inserted in longitudinal direction of the bumper beam. The ribs are placed along the X direction for ejection purposes except end caps (Figure 3).

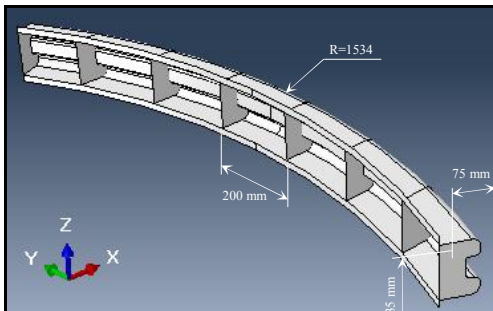


Figure 3. The strengthen ribs of bumper beam

3. Results

The vertical ribs with thickness 4 mm prevent the deflection of the lateral beam surfaces. Making ribs in the beam needs cavities in the die, which makes a difficulty in mold making and production. It causes the compressive pressure increase to flow the material to the thin cavity for forming the ribs. Deflection of the both bumper beams during the impact is shown in figure 4.

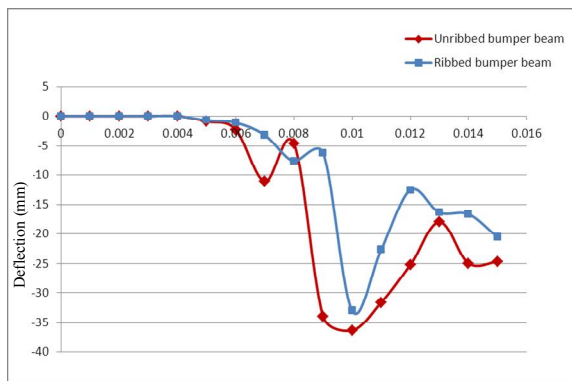


Figure 4. Deflection of Time (Sec) and unribbed bumper beam

From the graph, it is evident that the maximum deflection of the unribbed bumper is 3.30 mm more than the ribbed bumper. In other words, the vertical ribs decreased deflection of the bumper beam by 11%. Moreover, the unribbed bumper beam

deflection commenced earlier than ribbed one, since it has less solidified.

Figure 5 shows the strain energy of both ribbed and unribbed bumper beam. It is evident that the strain energy in the ribbed bumper beam commenced earlier than unribbed one because of more stability of the ribbed bumper beam in energy absorption, cause faster response to the external impact load. Moreover, it is presented that the maximum amount of strain energy in the ribbed bumper beam increased by 11.3% compare with unribbed bumper beam because of rigidity enhancement of the structure. The strain energy undulation of the ribbed bumper beam cause by the rib zone strain energy removal and unsteady load distribution from the rigid pendulum to the beam and side energy absorbers.

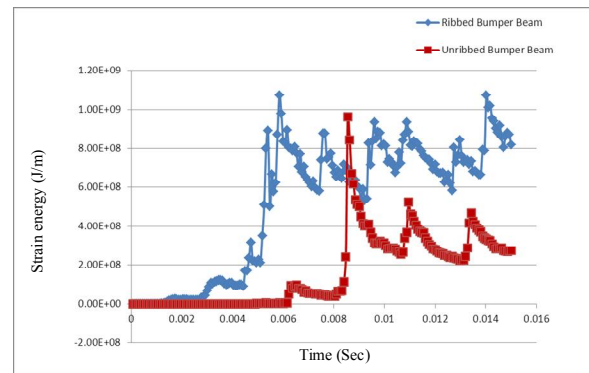


Figure 5. Strain energy of ribbed and unribbed bumper beam

4. Discussions

The accurate design of the strengthened ribs and its effective parameters such as features, spacing, thickness, height, can increase the energy absorption capacity (Murata, Shioya, 2004) as well as reduce the shrinkage and thermal expansion in the bumper beam. The unribbed bumper beam makes less-rigid sections and may absorb more impact energy by elastic deformation without damage (Rosato and Murphy, 2004).

The additional ribs slightly increase strain energy and decrease deflection in bumper beam, but cause weight rises and manufacturing difficulty (Hosseinzadeh, Shokrieh, 2005, Marzbanrad, Alijanpour, 2009). Besides, it requires more pressure to flow the material to the ribbed cavities and cause bumper beam denser and more solid. The author recommends the experimental approach in order to verify the developed toughened hybrid kenaf/glass epoxy composite for low weight passenger car application and control various parameters for a reasonable replacement solution of new developed material.

Acknowledgements:

The principal author wishes to thank the Universiti Putra Malaysia for supporting this research financially through the Research University Fellowship Scheme.

Corresponding Author:

M.M. Davoodi

Department of Mechanical and Manufacturing Engineering, Universiti Putra Malaysia, 43400 UPM Serdang, Selangor, Malaysia

E-mail: makinejadm2@asme.org

References

1. Al-Ashaab, A., et al., Internet-based collaborative design for an injection-moulding system. *Conc. Eng.*, 2003; 11(4): 289.
2. Brydson, J.A., *Plastics Materials*. New Delhi: Butterworth-Heinemann; 1999.
3. Hosseinzadeh, R., Shokrieh, M., and Lessard, L., Parametric study of automotive composite bumper beams subjected to low-velocity impacts. *Compos. Struct.*, 2005; 68(4): 419-427.
4. Marzbanrad, J., Alijanpour, M., and Kiasat, M., Design and analysis of an automotive bumper beam in low-speed frontal crashes. *Thin. Walled. Struct.*, 2009; 47(8-9): 902-911.
5. Harper, C.A., *Handbook of plastic processes*: Wiley-Interscience; 2006.
6. Smith, K.L. and Suh, N.P., An approach towards the reduction of sink marks in sheet molding compound. *Polym.Eng.Sci.*, 1979; 19(12): 829-834.
7. Zhang, Z., Liu, S., and Tang, Z., Design optimization of cross-sectional configuration of rib-reinforced thin-walled beam. *Thin. Walled. Struct.*, 2009; 47(8-9): 868-878.
8. Samaha, R.R., Molino, L.N., and Maltese, M.R. Comparative performance testing of passenger cars relative to FMVSS 214 and the EU 96/EC/27 side impact regulations: phase I. 1998.
9. Hashin, Z., Failure criteria for unidirectional fiber composites. *Journal of applied mechanics*, 1980; 47: 329.
10. Murata, S., Shioya, S., and Suffis, B., *Expanded Polypropylene (EPP): A Global Solution for Pedestrian Safety Bumper Systems*. 2004.
11. Rosato, D.V. and Murphy, J., *Reinforced plastics handbook*: Elsevier Advanced Technology; 2004.

12/23/2011

Impact of Orlistat on Body Weight and Lipid Profile of Adult Population

Randa M Shams¹, Medhat A Saleh¹, Mohamed E Abdelrahim², Asmaa S Mohamed²

¹. Public Health and Community Medicine Department - Faculty of Medicine, Assiut University.

². Clinical Pharmacy Department, Faculty of Pharmacy, Beni – Suef University.

medhatelaraby75@yahoo.com

Abstract: Orlistat is currently the best available form of prescribed obesity medication which acts on the gastrointestinal system and works by reducing fat absorption in the gut which is eliminated in bowel movements. **The aim of this study** was to determine the impact of Orlistat on weight reduction, body mass index (BMI) and lipid profile of the Egyptian peoples. **Methodology** We recruit 55 healthy obese persons (BMI more than 30) and the same number of normal weight act as a control; both groups completed a questionnaire for demographic data and risk factors of obesity and the obese group takes Orlistat for 2 months while the control group take placebo tablet containing vitamins and both groups adheres to 1200 Calories diet. Weight and lipid profile (Total cholesterol, Triglycerides, LDL and HDL) were measured before and after Orlistat administration in both groups. By the end of two months only 35 obese and 38 none obese complete the study and the remaining were dropped out from the study. **Results:** The results showed that there is a statistical significant difference in BMI before and after Orlistat ($P < 0.001$) as it decreased from 37.08 ± 4.67 before to 35.40 ± 4.60 after, the same occurred in weight reduction as it decreased from 95.3 ± 12.6 kg before orlistat to 91.1 ± 12.9 after, Waist circumference decreased from 113.0 ± 11.2 to 109.6 ± 11.7 and this difference was statistically significant also. there is a statistical significant difference in all parameters of lipid profile before and after Orlistat treatment as total cholesterol decreased from 199.9 ± 29.5 to 173.7 ± 27 and . Triglycerides from 199.4 ± 54.6 to 174.3 ± 50.7 , LDL cholesterol decreased from 120.7 ± 24.8 to 102.4 ± 25.1 , while HDL cholesterol increased from 38.3 ± 4.6 to 42.5 ± 5.5 and p value was <0.001 . **We conclude** that Orlistat is one of the best prescribed obesity medications available for obese patients. Although research indicates that it can promote weight loss, there remain problems with adherence and much variability in patient outcomes.

[Randa M Shams, Medhat A Saleh, Mohamed E Abdelrahim; Asmaa S M Mohamed.. Impact of Orlistat on Body Weight and Lipid Profile of Adult Population.]. Life Science Journal 2012; 9(1): 214-219] (ISSN: 1097-8135).

<http://www.lifesciencesite.com>. 31

Keywords: obesity, Orlistat, body weight, Lipid profile.

1. Introduction

Orlistat (marketed under the trade name Xenical[®] by Roche; or as alli [1] by GlaxoSmithKline also known as (tetrahydrolipstatin) is a drug designed to treat obesity[2]. Its primary function is preventing the absorption of fats from the human diet, thereby reducing caloric intake. It is intended for use in conjunction with a physician-supervised reduced-calorie diet. Orlistat is the saturated derivative of lipstatin a potent natural inhibitor of pancreatic lipases isolated from the bacterium *Streptomyces toxytricini* [3]. However, due to simplicity and stability, Orlistat rather than lipstatin was developed into an anti-obesity drug [4].

Orlistat works by inhibiting pancreatic lipase, an enzyme that breaks down triglycerides in the intestine. Without this enzyme, triglycerides from the diet are prevented from being hydrolyzed into absorbable free fatty acids and are excreted undigested. Only trace amounts of Orlistat are absorbed systemically; the primary effect is local lipase inhibition within the GI tract after an oral dose. The primary route of elimination is through the feces.

It also blocks the availability of fat-soluble vitamins (vitamins A, D, E, and K), so patients may need to take a vitamin supplement [5]. At the standard prescription dose of 120 mg three times daily before meals, Orlistat prevents approximately 30% of dietary fat from being absorbed and about 25% at the standard over-the-counter dose of 60 mg and Higher doses do not produce more potent effects[6].

Current recommendations suggest that it is used for patients who have a history of failed weight-loss attempts using behavioral methods and who can demonstrate at least 2.5kg weight loss by diet and exercise in the month prior to their first prescription. It is suggested that patients reduce their daily calorie intake by 500 to 1000 calories to promote weight loss, and the Dietary Guidelines for Americans recommend that dietary fat is limited to about 30% of daily calories. As a result of its impact upon fat absorption, Orlistat has unpleasant side effects including liquid stools, an urgency to go to the toilet, and anal leakage which are particularly apparent following a high-fat meal as the drug causes the fat consumed to be removed from the body. Between

1998 and 2005, Orlistat prescriptions rose 36-fold from 17,880 to 646,700 and the total cost increased by over 35-fold [7].

Research has explored the effectiveness of Orlistat in treatment of obesity improved weight loss, weight-loss maintenance, (BMI) and reduces cholesterol blood levels. Research indicates that Orlistat can improve weight loss if used alongside behavioral and lifestyle interventions. There remain, however, two main problems with Orlistat as a treatment for obesity. First, although evidence indicates that it can improve weight-loss outcomes, these improvements are not always substantial and there is much variability with many patients showing no improvements at all. Second, research also indicates high attrition rates with patients not adhering to their medication due to the unpleasant side effects and many stopping taking the drug entirely or using it selectively according to the content of their diet. In summary, although Orlistat is currently the most commonly prescribed medication for the obese, there remains much variability in its effectiveness with only a minority of patients showing weight loss (8).

Research has therefore explored the possible reasons for the effectiveness of Orlistat and whereas some studies have emphasized baseline characteristics, others have highlighted changes in beliefs and behavior brought about by the mechanisms of the drug itself. To date, however, such studies have focused either on drugs other than Orlistat or have used small qualitative designs. The present study, therefore, aimed to explore weight loss following a two months course of Orlistat (9). The amount of weight loss achieved with Orlistat varies. In one-year clinical trials, between 35.5% and 54.8% of subjects achieved a 5% or greater decrease in body mass, although not all of this mass was necessarily fat. Between 16.4% and 24.8% achieved at least a 10% decrease in body mass.[9] After Orlistat was stopped, a significant number of subjects regained weight—up to 35% of the weight they had lost [10]. Despite this relatively small body mass effect, there was a 37% reduction in the incidence of type 2 diabetes, a significant difference. This study (XENDOS) proved that the side effect profile of Orlistat remained the same up to 4 years. Respondents who lost 5% of their initial body weight in the first three months plus 2.5 gm in the first 4 weeks prior to the study, lost 16.4% of their weight at the end of one year [11].

2. Subjects and Methods

Design:

The study was composed of two parts: the first part was case control and the second part was controlled clinical trial one.

Study site:

The study was conducted in a private clinic concerned with obesity management in Mallawi city in El Minia Governorate, where all anthropometric measures and data collection was done.

Data collection techniques and tools

Data was collected by two well-designed structural questionnaires which filled by the investigator himself. Each subject was informed about the aim and the details of the study and give initial verbal consent to participate in the study. Questionnaire (1) asks about risk factors and comorbidities of obesity. It includes data such as Personal data including age, sex, residence and occupation, Family history of obesity. Socio-economic status of the participants using suitable socioeconomic score. While Questionnaire (2) includes the Anthropometric measurements including weight, height, BMI and waist circumference,

Lipid profile (total cholesterol, triglyceride, LDL and HDL) was determined in blood samples from participants post 12 hours fasting. Analysis of the samples was done by the following techniques:

1- Triglycerides: Caymans Triglycerides assay method [12, 13]

2- Cholesterol: Caymans Cholesterol assay method [14, 15]

3- High density lipoprotein (HDL) and Low density lipoproteins (LDL) measured by using phosphotungstic acid method [16-17].

Then the same anthropometric measures and blood analysis was done after 2 months of Orlistat.

Sample size

We start the study by 55 obese persons as cases and the same numbers as control and at the end of the 2 months of intervention only 35 obese subjects complete the study and 38 non obese subjects as control, we chose the obese subjects with BMI 30 kg/m² or more for both sexes. Waist circumference 94 cm or more for men and 80 cm or more for women, cases and control were 18 years old or older and with in 5 years age group regarding study and control were matched as regards sex.

Data analysis

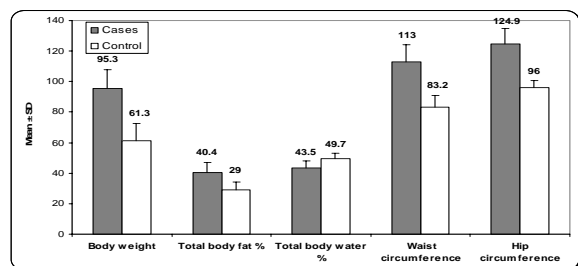
Data was entered and cleaned in Excel sheet, and then analyzed using SPSS software package version 16 that was used for data processing. Descriptive statistics was done in the form of mean and SD. paired t-test was used to compare numerical parametric data before and after Orlistat administration. Values were considered significant when P values were equal or less than 0.05.

3. Results

Figure 1 shows the anthropometric measures of cases and control and demonstrated that the mean body weight of cases was 96.3 kg while that of the control was 61.3 kg, it also shows marked differences of all body parameters between cases and control in the form of total body fat %, total body water, waist and hip circumferences.

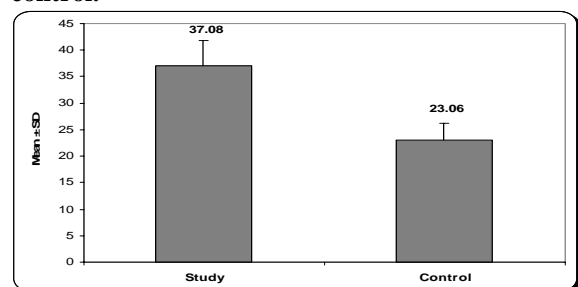
Figure 2 shows the difference of BMI between cases and control and shows that mean BMI of cases was 37.08 while that of control was 23.06 with statistical significant difference of BMI between cases and control.

Figure (1): Differences in anthropometric measures between cases and control



Independent sample t test was used.

Figure (2): BMI before treatment in cases and control.



Independent sample t test was used P = 0.001*

Table (1): lipid profile of cases and control in the studied sample

Variable	Cases (n= 55)	Control (n= 55)	P-value
Total cholesterol Mean ± SD	199.89 ± 29.54	176.63 ± 21.42	0.163
Range	150 – 277	146 – 232	
Triglycerides Mean ± SD	199.43 ± 54.55	106.23 ± 42.79	0.001*
Range	105 – 315	45 – 250	
LDL cholesterol Mean ± SD	120.66 ± 24.83	113.34 ± 17.97	0.001*
Range	77 – 180	79 – 160	
HDL cholesterol Mean ± SD	41.83 ± 6.09	42.86 ± 5.45	0.459
Range	32 – 65	33 – 54	

Independent sample t-test was used

Table (1) shows Lipid profile of cases and control and shows that there was a statistical

significant difference between the 2 groups in Triglycerides and LDL cholesterol while shows no statistical significant differences in Total cholesterol and HDL cholesterol .

Table (2): Anthropometric measures of obese persons before and after Orlistat

Type of anthropometric measures	Before (n= 55)	After (n= 35)	P-value
Body weight: Mean ± SD	95.3 ± 12.6	91.1 ± 12.9	<0.001*
Range	65.0 – 126.8	60.0 – 120.8	
Waist circumference: Mean ± SD	113.0 ± 11.2	109.6 ± 11.7	<0.001*
Range	86 – 133	82 – 129	
Hip circumference: Mean ± SD	124.9 ± 9.8	120.0 ± 10.1	<0.001*
Range	106 – 144	100 – 139	
Body fat %: Mean ± SD	40.4 ± 6.7	38.9 ± 6.9	0.034*
Range	24.9 – 50.8	21.0 – 47.0	
Body water %			0.827
Mean ± SD	43.5 ± 4.6	43.6 ± 4.3	
Range	36.0 – 53.2	37.0 – 54.0	

Paired t test was used

Table (2) shows the mean ± SD of anthropometric measures before and after Orlistat treatment and demonstrate a statistical significant difference in weight reduction (P = 0.001) as it decreased from 95.3 ± 12.6 kg before Orlistat to 91.1 ± 12.9 after, Waist circumference decreased from 113.0 ± 11.2 to 109.6 ± 11.7 and this difference was statistically significant also, the same finding was observed in hip circumference and in total body fat %, while there was no statistical significant difference in total body water percentage .

Table (3) shows lipid profile of the studied sample before and after Orlistat treatment and shows that there is a statistical significant difference in all parameters of lipid profile before and after Orlistat treatment as total cholesterol decreased from 199.9 ± 29.5 to 173.7 ± 27 and p value was <0.001. Triglycerides decreased from 199.4 ± 54.6 to 174.3 ± 50.7 and p value was <0.001, LDL cholesterol decreased from 120.7 ± 24.8 to 102.4 ± 25.1 and p value was <0.001, while HDL cholesterol increased from 38.3 ± 4.6 to 42.5 ± 5.5 and p value was <0.001.

Table (3): lipid profile of obese persons before and after Orlistat.

Variable	Before (n= 55)	After (n= 35)	P-value
Total cholesterol:			<0.001*
Mean ± SD	199.9 ± 29.5	173.7 ± 27	
Range	155 – 277	120 – 243	
Triglycerides:			<0.001*
Mean ± SD	199.4 ± 54.6	174.3 ± 50.7	
Range	105 – 315	95 – 295	
LDL cholesterol:			<0.001*
Mean ± SD	120.7 ± 24.8	102.4 ± 25.1	
Range	77 – 180	65 – 163	
HDL cholesterol:			<0.001*
Mean ± SD	38.3 ± 4.6	42.5 ± 5.5	
Range	29-49	33-54	

Paired t test was used

Table (4): BMI in obese persons before and after Orlistat.

	Before	After	P-value
Mean ± SD	37.08 ± 4.67	35.40 ± 4.60	0.001*
Range	27.41 – 49.47	25.30 – 46.22	

Paired t test was used

Table (4) shows the BMI of cases before and after Orlistat treatment and shows that there is a statistical significant difference in BMI before and after Orlistat ($P < 0.001$) as it decreased from 37.08 ± 4.67 before to 35.40 ± 4.60 after Orlistat.

4. Discussions

The present study aimed to explore the predictors of weight loss and lipid profile following 2 months of Orlistat therapy. The results showed that by the end of 2 months patients reported both weight loss and reduction in their BMI and lipid profile (except HDL) that falling within the expected range with previous outcome studies (18, 19). Furthermore, just about 10% reported flexibly in response to their dietary choices, habits and behaviors. Also the attrition rate was 20% which is consistent with attrition rates found in previous studies and the use of Orlistat as a lifestyle drug [19, 20].

Research has explored the effectiveness of Orlistat compared to other drug treatments, placebo, or behavior-focused interventions. For example Padwal *et al.* [19] reported that patients taking Orlistat lost 2.7kg more than patients taking placebo, and Avenell *et al.* [20] carried out systematic review

of trials involving a combination of diets, drug therapy, exercise, and behavior therapy and concluded that adding Orlistat to a dietary intervention improved weight loss by 3.26 kg up to 24 months. Research also indicated that Orlistat reduces cholesterol and blood pressure levels and improves glycemic control when compared to placebo [19]. Basal cholesterol absorption from the test meal (without Orlistat) was $59 \pm 6\%$. Cholesterol absorption from the test meal given concomitantly with Orlistat was $44 \pm 5\%$. Therefore; Orlistat decreased the absolute amount of cholesterol absorbed from the test meal by $23 \pm 5\%$ (from 43 to 32 mg; $p < 0.01$) [20].

In other study a total of 448 patients with elevated cholesterol according to cardiovascular risk factors entered a 2 week single-blind run-in period on a hypocaloric diet. Of 384 patients was subsequently assigned double-blind treatment with Orlistat (3 x 120 mg/day) or placebo for 6 months in conjunction with the hypo caloric diet. The result weight loss in the Orlistat group was 7.4 kg vs. 4.9 kg with placebo. Total and low-density lipoprotein cholesterol decreased by 25-30 mg/dl vs. 10-15 mg/dL with placebo. Reduction of cholesterol with Orlistat was significantly greater than anticipated from weight loss alone. In patients with cardiovascular risk factors entering the study with lower cholesterol values Orlistat was also superior to placebo. On the contrary, reduction of cholesterol concentrations never exceeded 20% [21].

Similarly, Phelan and Wadden [22] concluded from their review that adding Orlistat to lifestyle modification interventions improves both weight loss and weight-loss maintenance. Furthermore, in a recent updated meta-analysis, Rucker *et al.* (23) synthesized the results of randomized placebo controlled trials of approved anti-obesity drugs in adults aged 18 and over for one to four years. They concluded that with the active drug treatments patients were more likely to reach 5% and 10% weight-loss thresholds and that weight losses for three key drugs were as follows: Sibutramine: 4.2kg, rimonabant: 4.7kg, and Orlistat: 2.9kg. Research therefore indicates that Orlistat can improve weight loss if used alongside behavioral and lifestyle interventions.

There remain however, two main problems with Orlistat as a treatment for obesity. First, although evidence indicates that it can improve weight-loss outcomes, these improvements are not always substantial and there is much variability with many patients showing no improvements at all. Second, research also indicates high attrition rates with patients not adhering to their medication due to the unpleasant side effects and many stopping taking the

drug entirely or using it selectively according to the content of their diet. For example, Padwal *et al.* [19] concluded from their review of randomized control trials that the mean attrition rate for Orlistat was 33% and Vray *et al.* [24] suggested that in clinical practice attrition rates are even higher at 64%–77%. In our study the attrition rate for Orlistat was 20%. Research has therefore addressed how the effectiveness of Orlistat can be improved. However other researchers exploring alternative forms of medical management has explored a range of clinical, psychological, and behavioral variables as predictors of outcomes (e.g., [25–26]), research focusing on Orlistat has mainly emphasized laboratory and clinical variables [27].

In general, however such studies conclude that the best predictor of outcome following medical management is initial weight loss, but to date few studies have explored psychological and behavioral predictors of outcome following Orlistat. An alternative approach has addressed the mechanisms of how Orlistat works, by reducing fat absorption in the gut. However due to the unpleasant side effects, Finer has labeled it the anti-abuse effect” as it deters the intake of high-fat foods [28].

Further, Ogden and Sidhu [29] carried out a qualitative study with patients who had taken Orlistat to explore their beliefs about why it either did or did not facilitate weight loss. The results showed that inline with previous research some patients stopped taking their medication due to the unpleasant symptoms such as anal leakage or oily stools. Many obese people focus on medical causes of their problem such as hormones and genetics [30, 31] the results from this qualitative study of Orlistat users indicated that Orlistat make them taking a healthier diet. Leventhal *et al.* [32] described the notion of coherence between beliefs about causes and solutions to any particular medical problem. Inline with this, Ogden and Sidhu [29] argued that Orlistat functions by educating patients and creating coherence between behavioral causes and therefore behavioral solutions for obesity. To date, however, this process remains untested in a larger quantitative study.

In Somchai *et al.*, study they take study sample as Participants were females aged 18-45 years with BMI of more than 25 kg/m² and were medical examined to receive either Orlistat or Sibutramine. Participants could read and write Thailand (Thia) language and could completely join the project (i.e. visiting a physician every two weeks for 6 weeks). The instrument tool was a 6-page questionnaire. It was divided into 4 parts: part 1 is demographic data i.e. age, occupation, education, salary, marital status, weight, height, waist circumference and hip circumference; part 2 is question about exercise (e.g. type of exercise,

duration, frequency per week) and the calories burnt by exercise were calculated from the data; part 3 is question about eating behavior which could classify participants into 4 types: heavy eating, over eating, moderate eating, and on diet, and part 4 is question about satisfaction of drug used, side effect and drug adverse reaction. Then Data were collected for a period of six months from March 2004 to August 2004. Data were 100% collected (n = 160). From Table 1, average ages of participants were 36.20 ± 4.10 years old for Orlistat group and 37.11 ± 6.01 years old for Sibutramine group. Most of the participants were married and housewives. The largest subgroup at a particular level of educational attainment had completed high school after 6 weeks of drug treatment, the means of BMI of Orlistat and Sibutramine groups are significantly decreased (p = 0.03 and 0.02 respectively) during the treatment period[33].

Conclusion:

Orlistat is the best prescribed obesity medication available for obese patients which acts on the gastrointestinal system and works by reducing fat absorption in the gut. Although it can promote weight loss, decrease lipid profile and increase HDL, there remain problems with adherence and much variability in patient outcomes.

References

1. Bodkin J, Humphries E, McLeod M (2003): The total synthesis of (–)-tetrahydrolipstatin. *Australian Journal of Chemistry*, 56 (8): 795–803.
2. Barbier P, Schneider F (1987): Syntheses of tetrahydrolipstatin and absolute configuration of tetrahydrolipstatin and lipstatin. *Helvetica Chimica Acta*, 70 (1): 196–202.
3. Pommier A, Pons M, Kocienski P (1995): The first total synthesis of (–)-lipstatin. *Journal of Organic Chemistry* 60 (22): 7334–7339.
4. Physicians' Desk Reference (PDR) (2006). Thomson PDR. ISBN 1-56363-527-5.
5. Somchai Mekaroonreung*, Titinun Auamnoy and Pagorn Taweechotepatr (2006): Comparison of weight reduction and satisfaction of Orlistat and sibutramine. Faculty of Pharmaceutical Sciences, Chulalongkorn University, Bangkok 10330, Thailand.
6. National Institute for Clinical Excellence (2001): Guidance on the use of Orlistat for the treatment of obesity in adults. *Technology Appraisal Guidance No.22*,.
7. Royal College of Physicians of London (2003): “Anti-obesity drugs: Guidance on appropriate prescribing and management,” A report of the Nutrition Committee of the Royal College of Physicians of London.
8. Myalli.Com – Frequently Asked Questions. GlaxoSmithKline (2007). Retrieved on 2007-08-18.

9. Parker-Pope, Tara (2007): Weighing the Pros and Cons of New Fat-Blocking Drug Alli", the Wall Street Journal, June 19, pp. D1. Retrieved on 2007-08-18.
10. Xenical Pharmacology, Pharmacokinetics, Studies, Metabolism. RxList.com (2007). Retrieved on 2007-03-16.
11. Srishanmuganathan J., H. Patel, J. Car, and A. Majeed(2007):National trends in the use and costs of anti-obesity medications in England 1998–2005. *Journal of Public Health*, 29(2): 199-202.
12. Cole, T G.; Klotzsch, S. G.; McNAMARA, J. R. (1997): Measurement of Triglyceride Concentration in Handbook of Lipoprotein Testing. N. Rifai, *et al.*, ED.AACC Press. Washington DC, 115.
13. Fredrickson, D.S., Levy, R.I., and Lees, R.S (1967): Fat transport in Lipoproteins - an integrated approach to mechanisms and disorders. *New England Journal of Medicine*, 276(1):34-42.
14. Jauhiainen, M. and Dolphin, P.J (1986): Human plasma lecithin-cholesterol acyltransferase. An elucidation of the catalytic mechanism. *J. Biol. Chem.*, 261(15):7032-7043.
15. Matsuura, E. and Lopez, L.R (2004): Are oxidized LDL/ β 2-glycoprotein I complexes pathogenicantigens in autoimmune-mediated atherosclerosis? *Clinical & Developmental Immunology*, 11(2):103-111.
16. Burstein. M. Scholnick HR and Morfin R. (1970): The use of high – carbohydrate, high fiber diets. *J of Lipid Res* .11 583
17. Lopes –Virella, M.F. Grundy SM, Balady GJ and Criqui MH (1977): Cholesterol Determination *Clin Chem.*,23: 882- 884
18. Fruchart J. C. (1982): HDL cholesterol. *Des Laboratories*, 103, 882-3
19. Padwal, S. K. Li, and D. C. W. Lau (2003): Long-term pharmacotherapy for overweight and obesity: a systematic review and meta-analysis of randomized controlled trials. *International Journal of Obesity*, 27(12):1437–1446.
20. Bettina Mittendorfer, Richard E. Ostlund Jr, Bruce W. Patterson, and Samuel Klein (2001): Obesity Research Orlistat Inhibits Dietary Cholesterol Absorption. Department of Internal Medicine and Center for Human Nutrition, Washington University School of Medicine, St. Louis, Missouri.
21. Erdmann J, Lippl F, Klose G, Schusdziarra V. (1998): Cholesterol lowering effect of dietary weight loss and Orlistat treatment--efficacy and limitations. Department of Internal Medicine II, Technical University of Munich, Munich, Germany. .
22. Phelan and T. A. Wadden (2002): Combining behavioral and pharmacological treatments for obesity, *Obesity Research*, 10(6):560–574 .
23. Rucker, R. Padwal, S. K. Li, C. Curioni, and D. C. W. Lau (2007): Long term pharmacotherapy for obesity and overweight: updated meta-analysis. *British Medical Journal*, 335(7631): 1194–1199,.
24. Vray, J.-M. Joubert, E. Eschwège *et al.* (2005), "Results from the observational study EPIGRAM: management of excess weight in general practice and follow-up of patients treated with Orlistat. *Therapie*, 60(1):17–24.
25. V. Hainer, M. Kunesova, F. Bellisle *et al.* (2005): Psychobehavioral and nutritional predictors of weight loss in obese women treated with sibutramine. *International Journal of Obesity*, 29(2):208–216.
26. Hansen D. L., A. Astrup, S. Toubro *et al.* (2001): "Predictors of weight loss and maintenance during 2 years of treatment by sibutramine in obesity. Results from the European multi-centre STORM trial. *International Journal of Obesity*, 25(4):496–501,.
27. Dhurandhar N V., R. C. Blank, D. Schumacher, and R. L. Atkinson. (1999): Initial weight loss as a predictor of response to obesity drugs," *International Journal of Obesity*, 23(12): 1333–1336.
28. J. J. G. Martinez, F. A. Ruiz, and S. D. Candil (2006): Baseline serum folate level may be a predictive factor of weight loss in a morbid-obesity-management programme. *British Journal of Nutrition*, 96(5): 956–964,
29. Ogden J and S. Sidhu(2006): Adherence, behavior change, and visualization: a qualitative study of the experiences of taking an obesity medication. *Journal of Psychosomatic Research*, 61(4): 545–552..
30. Ogden J (2000): The correlates of long-term weight loss: a group comparison study of obesity. *International Journal of Obesity*, 24 (8): 1018–1025,
31. Ogden J, I. Bandara, H. Cohen *et al.* (2001): General practitioners' and patients' models of obesity: whose problem is it? *Patient Education and Counseling*, 44(3): 227–233,
32. Leventhal H., M. Diefenbach, and E. A. Leventhal (1992): "Illness cognition: using common sense to understand treatment adherence and affect cognition interactions. *Cognitive Therapy and Research*, 16(2):143–163.
33. Somchai Mekaroonreung (2006):Titinun Auamnoy and Pagorn Taweechoatpatr Faculty of Pharmaceutical Sciences, Chulalongkorn University, Bangkok 10330, Thailand (Comparison of weight reduction and satisfaction of Orlistat and sibutramine).

12/21/2011

Synthesis of Some Aryl Thienopyridine, Pyridothienopyrimidine, and Pyridothienotriazolopyrimidine Derivatives

Ali Khalil El-Louh¹, Shadia Mahmoud Abdallah^{2*} and Emtithal Ahmed El-Sawi²

¹Department of Chemistry, Faculty of Science, Al-Azhar University-Gaza, Gaza, Palestine

²Department of Chemistry, University College of Women for Arts, Science, and Education, Ain Shams University, Cairo-Egypt

shdiamabdallah@yahoo.com

Abstract: Synthesis of 2-thioxopyridine-3-carbonitriles **3a-d** and their reaction with chloroacetonitrile **4a** or chloroacetamide **4b** afforded pyridin-2-ylthioacetonitriles **5a-d** and pyridin-2-ylthioacetamides **6a-d**, respectively, which on cyclization gave the corresponding 3-aminothienopyridine derivatives **7a-d** and **8a-d**. Reaction of triethyl orthoformate in acetic anhydride gave with **7a-d** 3-ethoxymethylenethienopyridine derivatives **9a-d** which on their reaction with hydrazine hydrate yielded 3-amino-4-imino-3,4-dihydropyridothienopyrimidine derivatives **10a-d**. Reaction of triethyl orthoformate with **10a-d** produced pyridothienotriazolopyrimidine derivatives **11a-d**, where Dimroth rearrangement yielded 4-hydrazinopyridothienopyrimidine derivatives **12a-d**. On the other hand reaction of **8a-d** with triethyl orthoformate in acetic anhydride gave pyridothienopyrimidine-4-one derivatives **13a-d**, which on their chlorination produced 4-chloropyridothienopyrimidine derivatives **14a-d**, and treatment with hydrazine hydrate authenticated **12a-d**. Reaction of compounds **8a-d** with nitrous acid afforded 3,4-dihydropyridothienotriazin-4-ones **15a,b,d**. Compounds **12a-d** reacted with benzaldehyde, diethylmalonate, and acetylacetone, to give 4-benzylidenehydrazinopyridopyrimidines **16a-d**, ethyl 1,2,4-triazolopyridothienopyrimidin-3-ylacetates **17a-d**, and 4-(3,5-dimethylpyrazolo)pyridothienopyrimidines **18a-d**, respectively.

[Ali Khader El-Louh, Shadia Mahmoud Abdallah and Emtithal Ahmed El-Sawi **Synthesis of Some Aryl Thienopyridine, Pyridothienopyrimidine, and Pyridothienotriazolopyrimidine Derivatives**] Life Science Journal 2012;9(1):220-230. (ISSN: 1097-8135). <http://www.lifesciencesite.com>. 32

Keywords: Thioxopyridine; carbonitrile; thienopyridine; pyridothienopyrimidine; triazolopyridothienopyrimidine; pyridothienopyrazolopyrimidine

1. Introduction

Several thienopyridines have been synthesized and their pharmaceutical medicinal activities evaluated and used as diabetes mellitus,¹⁻³ analgesics and anti-inflammatory,^{4,6} sedatives,³ anticoagulants,⁶ anti-arterosclerotics,⁷ and gonadotropin releasing hormone antagonists.^{8,9} Moreover the pyridothienopyrimidines showed analgesic,^{10,11} antipyretic,¹² anti-inflammatory,¹³ antianaphylactic,^{14,15} and antimicrobial^{16,17} activities.

In our previous work to synthesize some thienopyridine and pyridothienopyrimidine derivatives,¹⁸⁻²³ the formation of o-aminonitrile²⁴⁻²⁹ in 3-aminothienopyridine-2-carbonitrile derivatives **7-8**, which is expected to have biological activities, attracted us to extend this work and synthesize more new thienopyridine, pyridothienopyrimidine and annulated thienopyridine derivatives.

2. Experimental

All melting points are uncorrected and measured on a Gallenkamp apparatus. IR spectra were recorded on a Pye Unicam SP 3-300 and a Shimadzu FT IR 8101 PC IR spectrophotometer (KBr pellets). ¹H and ¹³C-NMR spectra were recorded on a Varian Mercury VX-300 MHz NMR

spectrometer in DMSO-d₆ solution using TMS as an internal reference. Electron impact mass spectra were obtained with a 70 eV Shimadzu GCMS-QP 1000 EX spectrometer also elemental analyses were carried out in Micro Analytical Center, Cairo University, Giza, Egypt.

A mixture of (0.01 mol) cyanothioacetamide³⁰⁻³² **1** and, -unsaturated carbonyl compounds³³ (**2a-d**); (E)-3-(benzo[d][1,3]dioxol-5-yl)-1-(naphthalen-1-yl)prop-2-en-1-one **2a**, (E)-3-(benzo[d][1,3]dioxol-5-yl)-1-(naphthalen-2-yl)prop-2-en-1-one **2b**, (E)-3-(3,4-dimethoxyphenyl)-1-(naphthalen-1-yl)prop-2-en-1-one **2c**, or (E)-3-(3,4-dimethoxyphenyl)-1-(naphthalen-2-yl)prop-2-en-1-one **2d**, was refluxed in absolute ethanol (25 mL) containing (0.3 mL) piperidine for 5-6 hrs. The reaction mixture was concentrated and cooled to give products which on filtration and crystallization from the appropriate solvent gave 2-thioxo-1,2-dihydropyridine-3-carbonitrile derivatives **3a-d**, respectively.

To a stirred mixture of **3a-d** (0.01 mol) and sodium methoxide (0.01 mol) in methanol (30 mL), chloroacetonitrile **4a** or chloroacetamide **4b** (0.01 mol) was added portion wise. The stirring was continued for 2-3 hrs at room temperature. The product formed was filtered, washed with cold

ethanol and crystallized from the proper solvent to give 3-cyanopyridin-2-ylthioacetone nitriles **5a-d** or 3-cyanopyridine-2-ylthioacetamide derivatives **6a-d**, respectively.

Cyclization of **5a-d** and **6a-d** (0.01 mol) by their reflux with 10% KOH solution for 2 hrs followed by cooling and acidification with HCl gave the corresponding 3-aminothieno[2,3-b]pyridine **7a-d** and **8a-d**, respectively which were crystallized from the suitable solvent.

A solution of **7a-d** (0.01 mol) was refluxed with triethyl orthoformate (0.02 mol) in acetic anhydride (30 mL) for 4 hrs. The reaction mixture was cooled, the product obtained filtered, washed and crystallized from the proper solvent, to give 3-(ethoxymethyleneamino)thieno[2,3-b]pyridine derivatives **9a-d** respectively.

To a stirred cold solution of compounds **9a-d** (0.01 mol) in (20 mL) ethanol, (3 mL) of 99% hydrazine hydrate was added drop wise. The reaction mixture was continuously stirred at room temperature for 6 hrs and left overnight. The solids precipitated was filtered, washed with cold ethanol and purified by crystallization from the proper solvent to give the corresponding 3-amino-4-imino-3,4-dihydropyrido[3',2':4,5]thieno[3,2-d]pyrimidine **10a-d**, respectively.

A solution of **10a-d** (0.01 mol) in triethyl orthoformate (0.025 mol) was refluxed for 1-2 hrs and left overnight. The precipitated product was collected by filtration and crystallized from the proper solvent to give pyrido[3',2':4,5]thieno[3,2-d][1,2,4]triazolo[5,1-f]pyrimidine derivatives **11a-d**, respectively.

Treatment of **10a-d** (0.01 mol) by their reflux with 10% KOH solution for 2 hrs followed by cooling and acidification with HCl gave the corresponding 4-hydrazinopyrido[thienopyrimidine] **12a-d**, respectively due to Dimroth rearrangement. The products were crystallized from the suitable solvent.

Reaction of **8a-d** (0.01 mol) with triethyl orthoformate (0.02 mol) in acetic anhydride (30 mL) for 4 hrs, followed by cooling the reaction mixture filtration of the product, and crystallization from the proper solvent gave pyrido[thienopyrimidine]-4-one derivatives **13a-d**, respectively.

Chlorination of **13a-d** (0.01 mol) took place by its heating under reflux with POCl₃ (15 mL) for 4 hrs. The reaction mixture was cooled then poured with vigorous stirring on ice-cold water. The products formed were filtered, and crystallized from the proper solvent to give 4-chloropyrido[thienopyrimidine] derivatives **14a-d**, respectively.

Reflux of **14a-d** (0.01 mol) with 3 mL hydrazine hydrate in 30 mL ethanol for 2-3 hrs gave

after cooling the corresponding compounds **12a-d**, respectively.

Sodium nitrite solution (12 mL, 10%) was added to a solution of **8a,b,d** (0.01 mol) in conc. H₂SO₄ (5 mL) and glacial CH₃COOH (5 mL) at 0 °C over 5 min with stirring. The precipitated solids were filtered and crystallized from the proper solvent to give 3,4-dihydropyrido[3',2':4,5]thieno[3,2-d][1,2,3]triazin-4-one derivatives **15a,b,d**, respectively.

A mixture of **12a-d** (0.01 mol) and benzaldehyde (0.01 mol) in absolute ethanol (25 mL) was refluxed for 3 hrs. The solid that precipitated on cooling was collected and crystallized from the proper solvent to give 4-benzylidenehydrazinopyrido[3',2':4,5]thieno[3,2-d]pyrimidine derivatives **16a-d**, respectively.

Reaction of **12a-d** (0.01 mol) with diethyl malonate (15 mL) in presence of few drops of acetic acid under reflux for 2 hrs gave an oily product which was triturated with ethanol (20 mL) to form white solid. The products were crystallized from the proper solvents to give the corresponding ethyl 1,2,4-triazolo[4",3"-c]pyrido[3',2':4,5]thieno[3,2-d]pyrimidin-3-ylacetate **17a-d**, respectively.

A mixture of **12a-d** (0.01 mol) and acetyl acetone (5 mL) were heated under reflux for 4 hrs. The reaction products were solidified by their triturated with ethanol. The products were crystallized from the proper solvent to give 4-(3,5-dimethylpyrazolo)pyrido[3',2':4,5]thieno[3,2-d]pyrimidine derivatives, **18a-d**, respectively.

4-(Benzo-1,3-dioxol-5-yl)-6-(1-naphthyl)-2-thio-1,2-dihydropyridine-3-carbonitrile (3a): Crystallized from ethanol as orange solid (58%), mp 274 °C. IR: ν (cm⁻¹) = 3349 (NH) and 2217 (CN). ¹H-NMR: δ (ppm) = 6.11 (s, 2H, OCH₂O), 6.96 - 7.91 (m, 11H, Ar-H), 13.21 (br., 1H, NH). ¹³C-NMR: δ (ppm) = 176.1 (C=S), 161.6, 159.8, 157.5, 154.8, 154.3, 152.7, 151.5, 151.0, 149.7, 148.3, 147.3, 146.6, 145.3, 141.6, 137.1, 126.7, 120.3, 117.3, 114.2, 109.6, 108.5 (Ar-C, CN), 101.2 (OCH₂O). MS: m/z = 382. Analysis for C₂₃H₁₄N₂O₂S (382.44): Calcd. (Found) = C 72.23 (71.39), H 3.69 (3.82), N 7.32 (7.25), S 8.38 (8.12).

4-(Benzo-1,3-dioxol-5-yl)-6-(2-naphthyl)-2-thio-1,2-dihydropyridine-3-carbonitrile (3b): Crystallized from ethanol as yellow solid (74%), mp 256 °C. IR: ν (cm⁻¹) = 3351 (NH) and 2224 (CN). ¹H-NMR: δ (ppm) = 6.15 (s, 2H, OCH₂O), 6.86-7.98 (m, 11H, Ar-H), 13.11 (br., 1H, NH). MS: m/z = 382. Analysis for C₂₃H₁₄N₂O₂S (382.44): Calcd. (Found) = C 72.23 (72.41), H 3.69 (3.79), N 7.33 (7.42), S 8.38 (8.17).

4-(3,4-Dimethoxyphenyl)-6-(1-naphthyl)-2-thio-1,2-dihydropyridine-3-carbonitrile (3c): Crystallized from ethanol as orange solid (52%), mp 268 °C. IR: ν (cm^{-1}) = 3321 (NH) and 2218 (CN). H-NMR: δ (ppm) = 3.72, 3.84 (2 s, 6H, 2 \times OCH₃), 6.79-7.90 (m, 11H, Ar-H), 13.74 (br., 1H, NH). MS: m/z = 398. Analysis for C₂₄H₁₈N₂O₂S (398.49): Calcd. (Found) = C 72.23 (71.39), H 3.69 (3.82), N 7.33 (7.25), S 8.05 (8.25).

4-(3,4-Dimethoxyphenyl)-6-(2-naphthyl)-2-thio-1,2-dihydropyridine-3-carbonitrile (3d): Crystallized from ethanol as orange solid (54%), mp 286 °C. IR: ν (cm^{-1}) = 3372 (NH) and 2222 (CN). H-NMR: δ (ppm) = 3.72, 3.84 (2 s, 6H, 2 \times OCH₃), 6.72-7.93 (m, 11H, Ar-H), 13.61 (br., 1H, NH). MS: m/z = 398. Analysis for C₂₄H₁₈N₂O₂S (398.49): Calcd. (Found) = C 72.23 (71.38), H 3.69 (3.58), N 7.32 (7.25), S 8.05 (7.89).

[4-(Benzo-1,3-dioxol-5-yl)-3-cyano-6-(1-naphthyl)pyridin-2-yl]thioacetamide (5a): Crystallized from ethanol as yellow solid (86%), mp 166 °C. IR: ν (cm^{-1}) = 2222, 2216 (2 \times CN). H-NMR: δ (ppm) = 3.92 (s, 2H, SCH₂), 6.15 (s, 2H, OCH₂O), 6.92-8.01 (m, 11H, ArH's). C-NMR: δ (ppm) = 160.3, 158.6, 157.7, 156.2, 154.3, 153.1, 152.6, 152.0, 149.3, 148.5, 147.1, 146.2, 145.5, 142.3, 139.3, 127.6, 120.3, 119.1, 116.4, 115.2, 110.5, 108.6 (Ar-C, CN), 101.1 (OCH₂O), 33.95 (SCH₂). MS: m/z = 421. Analysis for C₂₅H₁₅N₃O₂S (421.47): Calcd. (Found) = C 71.24 (71.02), H 3.59 (3.42), N 9.97 (9.74), S 7.61 (7.34).

[4-(Benzo-1,3-dioxol-5-yl)-3-cyano-6-(2-naphthyl)pyridin-2-yl]thioacetamide (5b): Crystallized from ethanol as yellow solid (81%), mp 184 °C. IR: ν (cm^{-1}) = 2223, 2218 (2 \times CN). H-NMR: δ (ppm) = 3.90 (s, 2H, SCH₂), 6.12 (s, 2H, OCH₂O), 6.90-8.05 (m, 11H, Ar-H). MS: m/z = 421. Analysis for C₂₅H₁₅N₃O₂S (421.48): Calcd. (Found) = C 71.24 (71.41), H 3.59 (3.67), N 9.97 (9.79), S 7.61 (7.55).

[3-Cyano-4-(3,4-dimethoxyphenyl)-6-(1-naphthyl)pyridin-2-yl]thioacetamide (5c): Crystallized from dioxane as orange solid (81%), mp 172 °C. IR: ν (cm^{-1}) = 2221, 2214 (2 \times CN). H-NMR: δ (ppm) = 3.73, 3.87 (2 s, 6H, 2 \times OCH₃), 3.97 (s, 2H, SCH₂), 6.79-7.90 (m, 11H, Ar-H). MS: m/z = 437. Analysis for C₂₆H₁₉N₃O₂S (437.52): Calcd. (Found) = C 71.38 (71.35), H 4.38 (4.57), N 9.60 (9.54), S 7.33 (7.08).

[3-Cyano-4-(3,4-dimethoxyphenyl)-6-(2-naphthyl)pyridin-2-yl]thioacetamide (5d):

Crystallized from dioxane as orange solid (77%), mp 186 °C. IR: ν (cm^{-1}) = 2223, 2217 (2 \times CN). H-NMR: δ (ppm) = 3.71, 3.85 (2 s, 6H, 2 \times OCH₃), 3.98 (s, 2H, SCH₂), 6.99-7.98 (m, 11H, Ar-H). MS: m/z = 437. Analysis for C₂₆H₁₉N₃O₂S (437.52): Calcd. (Found) = C 71.38 (71.41), H 4.38 (4.22), N 9.60 (9.64), S 7.33 (7.12).

[4-(Benzo-1,3-dioxol-5-yl)-3-cyano-6-(1-naphthyl)pyridin-2-yl]thioacetamide (6a): Crystallized from ethanol as yellow solid (57%), mp 176 °C. IR: ν (cm^{-1}) = 3412, 3247, (NH₂), 2221 (CN), 1663 (amidic CO). H-NMR: δ (ppm) = 3.87 (s, 2H, SCH₂), 6.11 (s, 2H, OCH₂O), 6.34 (br., 2H, NH₂), 6.95-8.11 (m, 11H, Ar-H). MS: m/z = 439. Analysis for C₂₅H₁₇N₃O₃S (439.49): Calcd. (Found) = C 68.32 (68.12), H 3.90 (3.88), N 9.56 (9.66), S 7.30 (7.02).

2-[4-(Benzo-1,3-dioxol-5-yl)-3-cyano-6-(2-naphthyl)pyridin-2-yl]thioacetamide (6b): Crystallized from ethanol as yellow solid (69%), mp 182 °C. IR: ν (cm^{-1}) = 3421, 3265 (NH₂), 2219 (CN), 1668 (amidic CO). H-NMR: δ (ppm) = 3.93 (s, 2H, SCH₂), 6.13 (s, 2H, OCH₂O), 6.44 (br., 2H, NH₂), 6.86-8.00 (m, 11H, Ar-H). MS: m/z = 439. Analysis for C₂₅H₁₇N₃O₃S (439.49): Calcd. (Found) = C 68.32 (68.45), H 3.90 (3.83), N 9.56 (9.81), S 7.30 (7.10).

[3-Cyano-4-(3,4-dimethoxyphenyl)-6-(1-naphthyl)pyridin-2-yl]thioacetamide (6c): Crystallized from ethanol as yellow solid (81%), mp 172 °C. IR: ν (cm^{-1}) = 3411, 3298 (NH₂), 2216 (CN), 1665 (amidic CO). H-NMR: δ (ppm) = 3.71, 3.85 (2 s, 6H, 2 \times OCH₃), 3.94 (s, 2H, SCH₂), 6.37 (br., 2H, NH₂), 6.79-7.90 (m, 11H, Ar-H). MS: m/z = 455. Analysis for C₂₆H₂₁N₃O₃S (455.54): Calcd. (Found) = C 68.55 (68.66), H 4.65 (4.57), N 9.22 (9.01), S 7.04 (7.33).

[3-Cyano-4-(3,4-dimethoxyphenyl)-6-(2-naphthyl)pyridin-2-yl]thioacetamide (6d): Crystallized from ethanol as yellow solid (88%), mp 184 °C. IR: ν (cm^{-1}) = 3441, 3335 (NH₂), 2220 (CN), 1662 (amidic CO). H-NMR: δ (ppm) = 3.72, 3.86 (2 s, 6H, 2 \times OCH₃), 3.98 (s, 2H, SCH₂), 6.52 (br., 2H, NH₂), 6.79-7.90 (m, 11H, Ar-H). MS: m/z = 455. Analysis for C₂₆H₂₁N₃O₃S (455.53): Calcd. (Found) = C 68.55 (68.54), H 4.65 (4.54), N 9.22 (9.36), S 7.04 (7.32).

3-Amino-4-(benzo-1,3-dioxol-5-yl)-6-(1-naphthyl)thieno[2,3-*b*]pyridine-2-carbonitrile (7a): Crystallized from ethanol as orange solid (57%), mp 274 °C. IR: ν (cm^{-1}) = 3428, 3187 (NH₂), 2218 (CN). H-NMR: δ (ppm) = 6.67 (br., 2H, NH₂), 6.14 (s, 2H, OCH₂O), 6.86-7.97 (m, 11H, Ar-H). MS:

$m/z = 421$. Analysis for $C_{25}H_{15}N_3O_2S$ (421.48): Calcd. (Found) = C 71.24 (71.07), H 3.59 (3.81), N 9.97 (10.2), S 7.61 (7.35).

3-Amino-4-(benzo-1,3-dioxol-5-yl)-6-(2-naphthyl)thieno[2,3-*b*]pyridine-2-carbonitrile (7b): Crystallized from ethanol as yellow solid (91%), mp 246 °C. IR: ν (cm^{-1}) = 3421, 3175 (NH_2), 2220 (CN). H-NMR: δ (ppm) = 5.57 (br., 2H, NH_2), 6.12 (s, 2H, OCH_2O), 6.88-8.59 (m, 11H, Ar-H). MS: $m/z = 421$. Analysis for $C_{25}H_{15}N_3O_2S$ (421.48): Calcd. (Found) = C 71.24 (71.32), H 3.59 (3.93), N 9.97 (9.75), S 7.61 (7.88).

3-Amino-4-(3,4-dimethoxyphenyl)-6-(1-naphthyl)thieno[2,3-*b*]pyridine-2-carbonitrile (7c): Crystallized from ethanol-acetic acid mixture (4:1) as yellow solid (57%), mp 262 °C. IR: ν (cm^{-1}) = 3415, 3347 (NH_2), 2221 (CN). H-NMR: δ (ppm) = 3.71, 3.85 (2 s, 6H, $2 \times OCH_3$), 5.83 (br., 2H, NH_2), 6.99-8.01 (m, 11H, Ar-H). MS: $m/z = 437$. Analysis for $C_{26}H_{19}N_3O_3S$ (437.52): Calcd. (Found) = C 71.38 (71.22), H 4.38 (4.40), N 9.60 (9.74), S 7.33 (7.11).

3-Amino-4-(3,4-dimethoxyphenyl)-6-(2-naphthyl)thieno[2,3-*b*]pyridine-2-carbonitrile (7d): Crystallized from ethanol-acetic acid mixture (4:1) as yellow solid (90%), mp 274 °C. IR: ν (cm^{-1}) = 3421, 3344 (NH_2), 2220 (CN). H-NMR: δ (ppm) = 3.72, 3.87 (2 s, 6H, $2 \times OCH_3$), 5.92 (br., 2H, NH_2), 6.87-8.00 (m, 11H, Ar-H). MS: $m/z = 437$. Analysis for $C_{26}H_{19}N_3O_3S$ (437.52): Calcd. (Found) = C 71.38 (71.28), H 4.38 (4.27), N 9.60 (9.55), S 7.33 (7.04).

3-Amino-4-(benzo-1,3-dioxol-5-yl)-6-(1-naphthyl)thieno[2,3-*b*]pyridine-2-carboxamide (8a): Crystallized from dioxane as yellow solid (74%), mp 258 °C. IR: ν (cm^{-1}) = 3428, 3356, 3267, 3187 ($2 \times NH_2$), 1668 (amidic CO). H-NMR: δ (ppm) = 5.87 (br., 2H, NH_2), 6.14 (s, 2H, OCH_2O), 6.89-7.99 (m, 11H, Ar-H), 8.51 (br., 2H, NH_2). MS: $m/z = 439$. Analysis for $C_{25}H_{17}N_3O_3S$ (439.50): Calcd. (Found) = C 68.32 (68.51), H 3.90 (3.80), N 9.56 (9.67), S 7.30 (7.14).

3-Amino-4-(benzo-1,3-dioxol-5-yl)-6-(2-naphthyl)thieno[2,3-*b*]pyridine-2-carboxamide (8b): Crystallized from dioxane as yellow solid (76%), mp 232 °C. IR: ν (cm^{-1}) = 3415, 3347, 3252, 3133 ($2 \times NH_2$), 1661 (amidic CO). H-NMR: δ (ppm) = 5.63 (br., 2H, NH_2), 6.11 (s, 2H, OCH_2O), 6.92-8.02 (m, 11H, Ar-H), 8.82 (br., 2H, NH_2). MS: $m/z = 439$. Analysis for $C_{25}H_{17}N_3O_3S$ (439.49): Calcd. (Found) = C 68.32 (68.42), H 3.90 (3.96), N 9.56 (9.49), S 7.30 (7.11).

3-Amino-4-(3,4-dimethoxyphenyl)-6-(1-naphthyl)thieno[2,3-*b*]pyridine-2-carboxamide (8c): Crystallized from ethanol as yellow solid (79%), mp 244 °C. IR: ν (cm^{-1}) = 3412, 3345, 3298, 3189 ($2 \times NH_2$), 1664 (amidic CO). H-NMR: δ (ppm) = 3.72, 3.86 (2 s, 6H, $2 \times OCH_3$), 5.19, 6.37 (two br., 4H, two NH_2), 6.94-7.98 (m, 11H, Ar-H). MS: $m/z = 455$. Analysis for $C_{26}H_{21}N_3O_3S$ (455.54): Calcd. (Found) = C 68.55 (68.46), H 4.65 (4.62), N 9.22 (9.14), S 7.04 (7.26).

3-Amino-4-(3,4-dimethoxyphenyl)-6-(2-naphthyl)thieno[2,3-*b*]pyridine-2-carboxamide (8d): Crystallized from dioxane as yellow solid (82%), mp 264 °C. IR: ν (cm^{-1}) = 3423, 3364, 3254, 3171 ($2 \times NH_2$), 1663 (amidic CO). H-NMR: δ (ppm) = 3.72, 3.85 (2 s, 6H, $2 \times OCH_3$), 5.25, 6.44 (two br., 4H, two NH_2), 6.95-8.02 (m, 11H, Ar-H). MS: $m/z = 455$. Analysis for $C_{26}H_{21}N_3O_3S$ (455.54): Calcd. (Found) = C 68.55 (68.64), H 4.65 (4.43), N 9.22 (9.49), S 7.04 (7.24).

Ethyl [4-(1,3-benzodioxo-5-yl)-2-cyano-6-(1-naphthyl)thieno[2,3-*b*]pyridin-3-yl]imidoformate (9a): Crystallized from ethanol as white solid (56%), mp 186 °C. IR: ν (cm^{-1}) = 2221 (CN). H-NMR: δ (ppm) = 1.12 (t, $J = 7.2$ Hz, 3H, OCH_2CH_3), 3.94 (q, $J = 7.2$ Hz, 2H, OCH_2CH_3), 6.10 (s, 2H, OCH_2O), 6.85-8.01 (m, 11H, Ar-H), 8.21 (s, 1H, $CH=N$). MS: $m/z = 477$. Analysis for $C_{28}H_{19}N_3O_3S$ (477.55): Calcd. (Found) = C 70.42 (70.31), H 4.01 (4.11), N 8.80 (8.68), S 6.71 (6.62).

Ethyl [4-(1,3-benzodioxo-5-yl)-2-cyano-6-(2-naphthyl)thieno[2,3-*b*]pyridin-3-yl]imidoformate (9b): Crystallized from ethanol as white solid (63%), mp 170 °C. IR: ν (cm^{-1}): 2219 (CN). H-NMR: δ (ppm) = 1.04 (t, $J = 7.2$ Hz, 3H, OCH_2CH_3), 4.04 (q, $J = 7.2$ Hz, 2H, OCH_2CH_3), 6.13 (s, 2H, OCH_2O), 6.92-8.02 (m, 11H, Ar-H), 8.22 (s, 1H, $CH=N$). MS: $m/z = 477$. Analysis for $C_{28}H_{19}N_3O_3S$ (477.55): Calcd. (Found) = C 70.43 (70.35), H 4.01 (4.06), N 8.80 (8.99), S 6.71 (6.59).

Ethyl [4-(3,4-dimethoxyphenyl-5-yl)-2-cyano-6-(1-naphthyl)thieno[2,3-*b*]pyridin-3-yl]imidoformate (9c): Crystallized from ethanol as white solid (78%), mp 164 °C. IR: ν (cm^{-1}) = 2217 (CN). H-NMR: δ (ppm) = 1.01 (t, $J = 7.2$ Hz, 3H, OCH_2CH_3), 3.74, 3.88 (2 s, 6H, $2 \times OCH_3$), 4.00 (q, $J = 7.2$ Hz, 2H, OCH_2CH_3), 6.87-8.00 (m, 11H, Ar-H), 8.19 (s, 1H, $CH=N$). MS: $m/z = 493$. Analysis for $C_{29}H_{23}N_3O_3S$ (493.59): Calcd. (Found) = C 70.57 (70.37), H 4.70 (4.87), N 8.51 (8.44), S 6.50 (6.29).

Ethyl [4-(3,4-dimethoxyphenyl-5-yl)-2-cyano-6-(2-naphthyl)thieno[2,3-*b*]pyridin-3-

yl]imidofornate (9d): Crystallized from ethanol as white solid (78%), mp 164 °C. IR: ν (cm⁻¹) = 2219 (CN). H-NMR: δ (ppm) = 1.02 (t, J = 7.2 Hz, 3H, OCH₂CH₃), 3.73, 3.88 (2 s, 6H, 2 × OCH₃), 4.10 (q, J = 7.2 Hz, 2H, OCH₂CH₃), 6.90-8.03 (m, 11H, ArH's), 8.24 (s, 1H, CH=N). MS: m/z = 493. Analysis for C₂₉H₂₃N₃O₃S (493.59): Calcd. (Found) = C 70.57 (70.59), H 4.70 (4.94), N 8.51 (8.61), S 6.50 (6.53).

3-Amino-4-imino-9-(benzo-1,3-dioxol-5-yl)-7-(1-naphthyl)-3,4-dihydropyrido[3',2':4,5]thieno[3,2-*d*]pyrimidine (10a): Crystallized from dioxane as white solid (84%), mp 274 °C. IR: ν (cm⁻¹) = 3394, 3325, 3025 (NH₂, NH), 1614 (C=N). H-NMR: δ (ppm) = 5.72 (s, 2H, NH₂), 6.12 (s, 2H, OCH₂O), 6.89-8.02 (m, 11H, Ar-H), 8.29 (s, 1H, pyrimidine CH), 8.71 (br., 1H, NH). MS: m/z = 463. Analysis for C₂₆H₁₇N₅O₂S (463.51): Calcd. (Found) = C 67.37 (67.41), H 3.70 (3.60), N 15.11 (15.24), S 6.92 (6.86).

3-Amino-4-imino-9-(benzo-1,3-dioxol-5-yl)-7-(2-naphthyl)-3,4-dihydropyrido[3',2':4,5]thieno[3,2-*d*]pyrimidine (10b): Crystallized from dioxane as white solid (91%), mp 244 °C. IR: ν (cm⁻¹) = 3422, 3325, 3232 (NH₂, NH), 1617 (C=N). H-NMR: δ (ppm) = 5.63 (s, 2H, NH₂), 6.11 (s, 2H, OCH₂O), 6.95-8.11 (m, 11H, Ar-H), 8.32 (s, 1H, pyrimidine CH), 8.87 (br., 1H, NH). MS: m/z = 463. Analysis for C₂₆H₁₇N₅O₂S (463.52): Calcd. (Found) = C 67.37 (67.28), H 3.70 (3.81), N 15.11 (15.19), S 6.92 (6.87).

3-Amino-4-imino-9-(3,4-dimethoxyphenyl)-7-(1-naphthyl)-3,4-dihydropyrido[3',2':4,5]thieno[3,2-*d*]pyrimidine (10c): Crystallized from dioxane as pale yellow solid (74%), mp 296 °C. IR: ν (cm⁻¹) = 3412, 3354, 3064 (NH₂, NH), 1619 (C=N). H-NMR: δ (ppm) = 3.72, 3.84 (2 s, 6H, 2 × OCH₃), 6.95-8.10 (m, 11H, Ar-H), 8.37 (s, 1H, pyrimidine CH), 8.76 (br., 1H, NH). MS: m/z = 479. Analysis for C₂₇H₂₁N₅O₂S (479.56): Calcd. (Found) = C 67.62 (67.65), H 4.41 (4.32), N 14.60 (14.56), S 6.69 (6.59).

3-Amino-4-imino-9-(3,4-dimethoxyphenyl)-7-(2-naphthyl)-3,4-dihydropyrido[3',2':4,5]thieno[3,2-*d*]pyrimidine (10d): Crystallized from dioxane as pale yellow solid (76%), mp > 300 °C. IR: ν (cm⁻¹) = 3417, 3323, 3054 (NH₂, NH), 1616 (C=N). H-NMR: δ (ppm) = 3.73, 3.87 (2 s, 6H, 2 × OCH₃), 6.94-8.12 (m, 11H, Ar-H), 8.35 (s, 1H, pyrimidine CH), 8.89 (br., 1H, NH). MS: m/z = 479. Analysis for C₂₇H₂₁N₅O₂S (479.56):

Calcd. (Found) = C 67.62 (67.65), H 4.41 (4.32), N 14.60 (14.56), S 6.69 (6.59).

7-(Benzo-1,3-dioxol-5-yl)-9-(1-naphthyl)pyrido[3',2':4,5]thieno[3,2-*d*][1,2,4]-triazolo[5,1-*f*]pyrimidine (11a): Crystallized from dioxane as white solid (84%), mp 274 °C. IR: ν (cm⁻¹) = 3025 (aromatic CH), 2943, 2867 (aliphatic CH). H-NMR: δ (ppm) = 6.13 (s, 2H, OCH₂O), 6.93-7.89 (m, 11H, Ar-H), 8.27 (s, 1H, triazole CH), 8.32 (s, 1H, pyrimidine CH). MS: m/z = 473. Analysis for C₂₇H₁₅N₅O₂S (473.52): Calcd. (Found) = C 68.49 (68.65), H 3.19 (3.21), N 14.79 (14.84), S 6.77 (6.87).

7-(Benzo-1,3-dioxol-5-yl)-9-(2-naphthyl)pyrido[3',2';4,5]thieno[3,2-*d*][1,2,4]-triazolo[5,1-*f*]pyrimidine (11b): Crystallized from dioxane as white solid (91%), mp 244 °C. IR: ν (cm⁻¹) = 3036 (aromatic CH), 2923, 2821 (aliphatic CH). H-NMR: δ (ppm) = 6.10 (s, 2H, OCH₂O), 6.92-8.01 (m, 11H, Ar-H), 8.25 (s, 1H, triazole CH), 8.35 (s, 1H, pyrimidine CH). MS: m/z = 473. Analysis for C₂₇H₁₅N₅O₂S (473.52): Calcd. (Found) = C 68.49 (solid 68.36), H 3.19 (3.25), N 14.79 (14.84), S 6.77 (6.89).

7-(3,4-Dimethoxyphenyl)-9-(1-naphthyl)pyrido[3',2':4,5]thieno[3,2-*d*][1,2,4]-triazolo[5,1-*f*]pyrimidine (11c): Crystallized from dioxane as pale yellow solid (77%), mp 296 °C. IR: ν (cm⁻¹) = 3019 (aromatic CH), 2915, 2794 (aliphatic CH). H-NMR: δ (ppm) = 3.71, 3.83 (2 s, 6H, 2 × OCH₃), 6.96-8.02 (m, 11H, Ar-H), 8.29 (s, 1H, triazole CH), 8.38 (s, 1H, pyrimidine CH). MS: m/z = 489. Analysis for C₂₈H₁₉N₅O₂S (489.56): Calcd. (Found) = C 68.70 (68.78), H 3.91 (4.11), N 14.31 (14.57), S 6.55 (6.64).

7-(3,4-Dimethoxyphenyl)-9-(2-naphthyl)pyrido[3',2':4,5]thieno[3,2-*d*][1,2,4]-triazolo[5,1-*f*]pyrimidine (11d): Crystallized from dioxane as white solid (79%), mp > 300 °C. IR: ν (cm⁻¹) = 3032 (aromatic CH), 2924, 2787 (aliphatic CH). H-NMR: δ (ppm) = 3.72, 3.85 (2 s, 6H, 2 × OCH₃), 6.99-8.00 (m, 11H, Ar-H), 8.27 (s, 1H, triazole CH), 8.32 (s, 1H, pyrimidine CH). MS: m/z = 489. Analysis for C₂₈H₁₉N₅O₂S (489.56): Calcd. (Found) = C 68.70 (68.81), H 3.91 (3.98), N 14.31 (14.43), S 6.55 (6.34).

9-(Benzo-1,3-dioxol-5-yl)-4-hydrazino-7-(1-naphthyl)pyrido[3',2':4,5]thieno[3,2-*d*]pyrimidine (12a): Crystallized from dioxane as white solid (87%), mp 282 °C. IR: ν (cm⁻¹) = 3423, 3364, 3254 (NH, NH₂). H-NMR: δ (ppm) = 5.14 (br., 2H, NH₂), 6.12 (s, 2H, OCH₂O), 6.96-8.01 (m, 11H, Ar-H), 8.32

(s, 1H, pyrimidine CH), 9.10 (br., 1H, NH). MS: m/z = 463. Analysis for $C_{26}H_{17}N_5O_2S$ (463.52): Calcd. (Found) = C 67.37 (67.24), H 3.70 (3.66), N 15.11 (15.31), S 6.92 (6.68).

9-(Benzo-1,3-dioxol-5-yl)-4-hydrazino-7-(2-naphthyl)pyrido[3',2':4,5]thieno-[3,2-*d*]pyrimidine (12b): Crystallized from dioxane as white solid (92%), mp 296 °C. IR: ν (cm^{-1}) = 3423, 3364, 3254 (NH, NH₂). H-NMR: δ (ppm) = 5.14 (br., 2H, NH₂), 6.12 (s, 2H, OCH₂O), 6.96-8.01 (m, 11H, Ar-H), 8.32 (s, 1H, pyrimidine CH), 9.10 (br., 1H, NH). MS: m/z = 463. Analysis for $C_{26}H_{17}N_5O_2S$ (463.52): Calcd. (Found) = C 67.37 (67.28), H 3.70 (3.81), N 15.11 (15.29), S 6.92 (6.66).

9-(3,4-Dimethoxyphenyl)-4-hydrazino-7-(1-naphthyl)pyrido[3',2':4,5]thieno-[3,2-*d*]pyrimidine (12c): Crystallized from ethanol as white solid (92%), mp 296 °C. IR: ν (cm^{-1}) = 3417, 3334, 3224 (NH, NH₂). H-NMR: δ (ppm) = 3.74, 3.88 (2 s, 6H, 2 × OCH₃), 4.94 (br., 2H, NH₂), 6.98-8.04 (m, 11H, Ar-H), 8.32 (s, 1H, pyrimidine CH), 9.31 (br., 1H, NH). MS: m/z = 479. Analysis for $C_{27}H_{21}N_5O_2S$ (479.56): Calcd. (Found) = C 67.62 (67.87), H 4.41 (4.45), N 14.60 (14.53), S 6.69 (6.88).

9-(3,4-Dimethoxyphenyl)-4-hydrazino-7-(1-naphthyl)pyrido[3',2':4,5]thieno-[3,2-*d*]pyrimidine (12d): Crystallized from ethanol as white solid (92%), mp 296 °C. IR: ν (cm^{-1}) = 3417, 3334, 3224 (NH, NH₂). H-NMR: δ (ppm) = 3.74, 3.88 (2 s, 6H, 2 × OCH₃), 4.94 (br., 2H, NH₂), 6.98-8.04 (m, 11H, Ar-H), 8.32 (s, 1H, pyrimidine CH), 9.31 (br., 1H, NH). MS: m/z = 479. Analysis for $C_{27}H_{21}N_5O_2S$ (479.56): Calcd. (Found) = C 67.62 (67.87), H 4.41 (4.45), N 14.60 (14.53), S 6.69 (6.88).

9-(Benzo-1,3-dioxol-5-yl)-7-(1-naphthyl)-3,4-dihydropyrido[3',2':4,5]thieno-[3,2-*d*]pyrimidine-4-one (13a): Crystallized from acetic acid as white solid (59%), mp > 300 °C. IR: ν (cm^{-1}) = 3216 (NH), 1660 (amidic CO). H-NMR: δ (ppm) = 6.10 (s, 2H, OCH₂O), 6.90-7.99 (m, 11H, Ar-H), 8.32 (s, 1H, pyrimidine CH), 12.3 (br., 1H, NH). MS: m/z = 449. Analysis for $C_{26}H_{15}N_3O_3S$ (499.49): Calcd. (Found) = C 69.48 (69.43), H 3.36 (3.51), N 9.35 (9.44), S 7.13 (7.24).

9-(Benzo-1,3-dioxol-5-yl)-7-(2-naphthyl)-3,4-dihydropyrido[3',2':4,5]thieno-[3,2-*d*]pyrimidine-4-one (13b): Crystallized from acetic acid as white solid (69%), mp > 300 °C. IR: ν (cm^{-1}) = 3224 (NH), 1662 (amidic CO). H-NMR: δ (ppm) = 6.11 (s, 2H, OCH₂O), 6.95-7.98 (m, 11H, Ar-H), 8.34 (s, 1H, pyrimidine CH), 12.5 (br., 1H, NH). MS: m/z = 449.

Analysis for $C_{26}H_{15}N_3O_3S$ (499.49): Calcd. (Found) = C 69.48 (69.25), H 3.36 (3.21), N 9.35 (9.54), S 7.13 (7.00).

9-(3,4-Dimethoxyphenyl)-7-(1-naphthyl)-3,4-dihydropyrido[3',2':4,5]thieno[3,2-*d*]pyrimidine-4-one (13c): Crystallized from acetic acid as white solid (78%), mp 298 °C. IR: ν (cm^{-1}) = 3214 (NH), 1667 (amidic CO). H-NMR: δ (ppm) = 3.71, 3.83 (2 s, 6H, 2 × OCH₃), 6.91-8.01 (m, 11H, Ar-H), 8.31 (s, 1H, pyrimidine CH), 11.3 (br., 1H, NH). MS: m/z = 465. Analysis for $C_{27}H_{19}N_3O_3S$ (465.53): Calcd. (Found) = C 69.66 (69.59), H 4.11 (4.15), N 9.03 (8.89), S 6.89 (6.69).

9-(3,4-Dimethoxyphenyl)-7-(2-naphthyl)-3,4-dihydropyrido[3',2':4,5]thieno[3,2-*d*]pyrimidine-4-one (13d): Crystallized from acetic acid as white solid (78%), mp 298 °C. IR: ν (cm^{-1}) = 3214 (NH), 1667 (amidic CO). H-NMR: δ (ppm) = 3.71, 3.83 (2 s, 6H, 2 × OCH₃), 6.91-8.01 (m, 11H, Ar-H), 8.31 (s, 1H, pyrimidine CH), 11.3 (br., 1H, NH). MS: m/z = 465. Analysis for $C_{27}H_{19}N_3O_3S$ (465.53): Calcd. (Found) = C 69.66 (69.59), H 4.11 (4.15), N 9.03 (8.89), S 6.89 (6.69).

9-(Benzo-1,3-dioxol-5-yl)-4-chloro-7-(1-naphthyl)pyrido[3',2':4,5]thieno[3,2-*d*] pyrimidine (14a): Crystallized from dioxane as white solid (71%), mp 208 °C. IR: ν (cm^{-1}) = 3032 (aromatic CH), 2911, 2801 (aliphatic CH). H-NMR: δ (ppm) = 6.10 (s, 2H, OCH₂O), 6.79-7.95 (m, 11H, Ar-H), 8.30 (s, 1H, pyrimidine CH). MS: m/z = 467.5. Analysis for $C_{26}H_{14}N_3O_2S_2Cl$ (467.94): Calcd. (Found) = C 66.74 (66.79), H 3.02 (3.12), N 8.98 (8.84), S 6.85 (6.94).

9-(Benzo-1,3-dioxol-5-yl)-4-chloro-7-(2-naphthyl)pyrido[3',2':4,5]thieno[3,2-*d*] pyrimidine (14b): Crystallized from dioxane as white solid (83%), mp 192 °C. IR: ν (cm^{-1}) = 3047 (aromatic CH), 2924, 2824 (aliphatic CH). H-NMR: δ (ppm) = 6.11 (s, 2H, OCH₂O), 6.84-7.94 (m, 11H, Ar-H), 8.31 (s, 1H, pyrimidine CH). MS: m/z = 467.5. Analysis for $C_{26}H_{14}N_3O_2S_2Cl$ (467.94): Calcd. (Found) = C 66.74 (66.88), H 3.02 (3.21), N 8.98 (8.74), S 6.85 (6.79).

4-Chloro-9-(3,4-dimethoxyphenyl)-7-(1-naphthyl)pyrido[3',2':4,5]thieno[3,2-*d*]pyrimidine (14c): Crystallized from dioxane as white solid (77%), mp 188 °C. IR: ν (cm^{-1}) = 3027 (aromatic CH), 2922, 2815 (aliphatic CH). H-NMR: δ (ppm) = 3.73, 3.84 (2 s, 6H, 2 × OCH₃), 6.92-8.01 (m, 11H, Ar-H), 8.32 (s, 1H, pyrimidine CH). MS: m/z = 483.5. Analysis for $C_{28}H_{18}N_3O_3S_2Cl$ (483.98): Calcd.

(Found) = C 67.01 (67.21), H 3.75 (3.68), N 8.68 (8.79), S 6.63 (6.47).

4-Chloro-9-(3,4-dimethoxyphenyl)-7-(2-naphthyl)pyrido[3',2':4,5]thieno[3,2-d]pyrimidine (14d): Crystallized from dioxane as white solid (79%), mp 202°C. IR: ν (cm^{-1}) = 3025 (aromatic CH), 2917, 2811 (aliphatic CH). H-NMR: δ (ppm) = 3.72, 3.84 (2 s, 6H, 2 \times OCH₃), 6.97-8.00 (m, 11H, Ar-H), 8.30 (s, 1H, pyrimidine CH). MS: m/z = 483.5. Analysis for C₂₈H₁₈N₃O₂Cl (483.98): Calcd. (Found) = C 67.01 (67.13), H 3.75 (3.60), N 8.68 (8.57), S 6.63 (6.77).

9-(Benzo-1,3-dioxol-5-yl)-7-(1-naphthyl)-3,4-dihydropyrido[3',2':4,5]thieno-[3,2-d][1,2,3]triazin-4-one (15a): Crystallized from dioxane as white solid (67%), mp 272 °C. IR: ν (cm^{-1}) = 3247 (NH), 1659 (amidic CO). H-NMR: δ (ppm) = 6.13 (s, 2H, OCH₂O), 6.89 - 7.98 (m, 11H, Ar-H), 8.29 (s, 1H, pyrimidine CH), 9.31 (br., 1H, NH). MS: m/z = 450. Analysis for C₂₅H₁₄N₄O₃ (450.48): Calcd. (Found) = C 66.66 (66.77), H 3.13 (3.23), N 12.44 (12.45), S 7.12 (7.34).

9-(Benzo-1,3-dioxol-5-yl)-7-(2-naphthyl)-3,4-dihydropyrido[3',2':4,5]thieno-[3,2-d][1,2,3]triazin-4-one (15b): Crystallized from dioxane as white solid (86%), mp 254 °C. IR: ν (cm^{-1}) = 3237 (NH), 1662 (amidic CO). H-NMR: δ (ppm) = 6.12 (s, 2H, OCH₂O), 6.91 - 7.99 (m, 11H, Ar-H), 8.33 (s, 1H, pyrimidine CH), 9.24 (br., 1H, NH). MS: m/z = 450. Analysis for C₂₅H₁₄N₄O₃ (450.48): Calcd. (Found) = C 66.66 (66.56), H 3.13 (3.03), N 12.44 (12.34), S 7.12 (7.01).

9-(3,4-Dimethoxyphenyl)-7-(2-naphthyl)-3,4-dihydropyrido[3',2':4,5]thieno-[3,2-d][1,2,3]triazin-4-one (15d): Crystallized from dioxane as white solid (68%), mp 286°C. IR: ν (cm^{-1}) = 3274 (NH), 1664 (amidic CO). H-NMR δ (ppm): 3.71, 3.82 (2 s, 6H, 2 \times OCH₃), 6.98-8.00 (m, 11H, Ar-H), 8.32 (s, 1H, pyrimidine CH). MS: m/z = 466. Analysis for C₂₆H₁₈N₄O₃ (466.52): Calcd. (Found) = C 66.94 (66.88), H 3.89 (3.64), N 12.01 (12.34), S 6.87 (6.73).

9-(Benzo-1,3-dioxol-5-yl)-4-benzylidenehydrazino-7-(1-naphthyl)pyrido[3',2':4,5]thieno[3,2-d]pyrimidine (16a): Crystallized from dioxane as white solid (64%), mp 286 °C. IR: ν (cm^{-1}) = 3305 (NH), 1646 (C=N). H-NMR: δ (ppm) = 6.13 (s, 2H, OCH₂O), 6.87-8.04 (m, 16H, Ar-H), 8.19 (s, 1H, CH=N), 8.29 (s, 1H, pyrimidine CH). MS: m/z = 551. Analysis for C₃₃H₂₁N₅O₂S (551.63): Calcd. (Found) = C 71.85 (71.67), H 3.84 (3.67), N 12.70 (12.81), S 5.81 (5.88).

9-(Benzo-1,3-dioxol-5-yl)-4-benzylidenehydrazino-7-(2-naphthyl)pyrido[3',2':4,5]thieno[3,2-d]pyrimidine (16b): Crystallized from dioxane as white solid (73%), mp 262 °C. IR: ν (cm^{-1}) = 3248 (NH), 1646 (C=N). H-NMR: δ (ppm) = 6.12 (s, 2H, OCH₂O), 6.91 - 8.06 (m, 16H, Ar-H), 8.17 (s, 1H, CH=N), 8.31 (s, 1H, pyrimidine CH). MS: m/z = 551. Analysis for C₃₃H₂₁N₅O₂S (551.63): Calcd. (Found) = C 71.85 (71.91), H 3.84 (3.94), N 12.70 (12.64), S 5.81 (5.87).

4-Benzylidenehydrazino-9-(3,4-dimethoxyphenyl)-7-(1-naphthyl)pyrido[3',2':4,5]thieno[3,2-d]pyrimidine (16c): Crystallized from dioxane as white solid (77%), mp 274 °C. IR: ν (cm^{-1}) = 3274 (NH), 1652 (C=N). H-NMR: δ (ppm) = 3.72, 3.83 (2 s, 6H, 2 \times OCH₃), 6.95-8.00 (m, 16H, Ar-H), 8.18 (s, 1H, CH=N), 8.27 (s, 1H, pyrimidine CH). MS: m/z = 567. Analysis for C₃₄H₂₅N₅O₂S (567.67): Calcd. (Found) = C 71.94 (71.87), H 4.44 (4.45), N 12.34 (12.24), S 5.65 (5.39).

4-Benzylidenehydrazino-9-(3,4-dimethoxyphenyl)-7-(2-naphthyl)pyrido[3',2':4,5]thieno[3,2-d]pyrimidine (16d): Crystallized from dioxane as white solid (69%), mp 258 °C. IR: ν (cm^{-1}) = 3265 (NH), 1651 (C=N). H-NMR: δ (ppm) = 3.73, 3.85 (2 s, 6H, 2 \times OCH₃), 6.96-8.02 (m, 16H, Ar-H), 8.16 (s, 1H, CH=N), 8.30 (s, 1H, pyrimidine CH). MS: m/z = 567. Analysis for C₃₄H₂₅N₅O₂S (567.67): Calcd. (Found) = C 71.94 (71.98), H 4.44 (4.38), N 12.34 (12.51), S 5.65 (5.47).

Ethyl 7-(benzo-1,3-dioxol-5-yl)-9-(1-naphthyl)-1,2,4-triazolo[4'',3''-c]pyrido-[3',2':4,5]thieno[3,2-d]pyrimidin-3-ylacetate (17a): Crystallized from dioxane as white solid (56%), mp 192 °C. IR: ν (cm^{-1}) = 1728 (ester CO). H-NMR: δ (ppm) = 1.02 (t, 3H, ester CH₃), 3.98 (s, 2H, CH₂), 4.12 (q, 2H, ester CH₂), 6.11 (s, 2H, OCH₂O), 6.81-8.04 (m, 11H, Ar-H), 8.30 (s, 1H, pyrimidine CH). MS: m/z = 559. Analysis for C₃₁H₂₁N₅O₄S (559.61): Calcd. (Found) = C 66.54 (66.51), H 3.78 (3.68), N 12.51 (12.72), S 5.73 (5.47).

Ethyl 7-(benzo-1,3-dioxol-5-yl)-9-(2-naphthyl)-1,2,4-triazolo[4'',3''-c]pyrido-[3',2':4,5]thieno[3,2-d]pyrimidin-3-ylacetate (17b): Crystallized from dioxane as white solid (76%), mp 212 °C. IR: ν (cm^{-1}) = 1723 (ester CO). H-NMR: δ (ppm) = 1.04 (t, 3H, ester CH₃), 4.02 (s, 2H, CH₂), 4.11 (q, 2H, ester CH₂), 6.13 (s, 2H, OCH₂O), 6.89-8.02 (m, 11H, Ar-H), 8.31 (s, 1H, pyrimidine CH). MS: m/z = 559. Analysis for C₃₁H₂₁N₅O₄S (559.61): Calcd. (Found) = C 66.54 (66.62), H 3.78 (3.73), N 12.51 (12.77), S 5.73 (5.58).

Ethyl 7-(3,4-dimethoxyphenyl)-9-(1-naphthyl)-1,2,4-triazolo[4'',3''-c]pyrido-[3',2':4,5]thieno[3,2-d]pyrimidin-3-ylacetate (17c):

Crystallized from dioxane as white solid (66%), mp 178 °C. IR: ν (cm⁻¹) = 1723 (ester CO). H-NMR: δ (ppm) = 9.99 (t, 3H, ester CH₃), 3.73, 3.86 (2 s, 6H, 2 × OCH₃), 4.01 (s, 2H, CH₂), 4.09 (q, 2H, ester CH₂), 6.84-8.03 (m, 11H, Ar-H), 8.26 (s, 1H, pyrimidine CH). MS: m/z = 575. Analysis for C₃₂H₂₅N₅O₄S (575.65): Calcd. (Found) = C 66.77 (66.68), H 4.38 (4.46), N 12.17 (12.01), S 5.57 (5.42).

Ethyl 7-(3,4-dimethoxyphenyl)-9-(2-naphthyl)-1,2,4-triazolo[4'',3''-c]pyrido-[3',2':4,5]thieno[3,2-d]pyrimidin-3-ylacetate (17d):

Crystallized from dioxane as white solid (66%), mp 178 °C. IR: ν (cm⁻¹) = 1723 (ester CO). H-NMR: δ (ppm) = 10.1 (t, 3H, ester CH₃), 3.72, 3.85 (2 s, 6H, 2 × OCH₃), 4.02 (s, 2H, CH₂), 4.10 (q, 2H, ester CH₂), 6.79-8.01 (m, 11H, Ar-H), 8.31 (s, 1H, pyrimidine CH). MS: m/z = 575. Analysis for C₃₂H₂₅N₅O₄S (575.65): Calcd. (Found) = C 66.77 (66.84), H 4.38 (4.27), N 12.17 (12.33), S 5.57 (5.39).

9-(Benzo-1,3-dioxol-5-yl)-4-(3,5-dimethylpyrazolo)-7-(2-naphthyl)pyrido[3',2':4,5]thieno[3,2-d]pyrimidine (18a):

Crystallized from dioxane as white solid (72%), mp 242 °C. IR: ν (cm⁻¹) = 3047 (aromatic CH), 2914, 2794 (aliphatic CH), 1654 (C=N). H-NMR: δ (ppm) = 2.41, 2.83 (2 s, 6H, 2 × CH₃ at pyrazole ring), 6.11 (s, 2H, OCH₂O), 6.59 (s, 1H, pyrazole CH), 6.92-8.03 (m, 11H, Ar-H), 8.27 (s, 1H, pyrimidine CH). MS: m/z = 527. Analysis for C₃₁H₂₁N₅O₂S (527.61): Calcd. (Found) = C 70.57 (70.43), H 4.01 (4.02), N 13.27 (13.52), S 6.08 (6.24).

9-(Benzo-1,3-dioxol-5-yl)-4-(3,5-dimethylpyrazolo)-7-(2-naphthyl)pyrido[3',2':4,5]thieno[3,2-d]pyrimidine (18b):

Crystallized from dioxane as white solid (83%), mp 248 °C. IR: ν (cm⁻¹) = 3031 (aromatic CH), 2924, 2793 (aliphatic CH), 1652 (C=N). H-NMR: δ (ppm) = 2.44, 2.82 (2 s, 6H, 2 × CH₃ at pyrazole ring), 6.12 (s, 2H, OCH₂O), 6.61 (s, 1H, pyrazole CH), 6.90-8.01 (m, 11H, Ar-H), 8.28 (s, 1H, pyrimidine CH). MS: m/z = 527. Analysis for C₃₁H₂₁N₅O₂S (527.61): Calcd. (Found) = C 70.57 (70.61), H 4.01 (4.04), N 13.27 (13.33), S 6.08 (6.11).

9-(3,4-Dimethoxyphenyl)-4-(3,5-dimethylpyrazolo)-7-(1-naphthyl)pyrido[3',2':4,5]thieno[3,2-d]pyrimidine (18c):

Crystallized from dioxane as white solid (83%), mp 248 °C. IR: ν (cm⁻¹) = 3027 (aromatic CH), 2917, 2789 (aliphatic CH), 1654 (C=N). H-NMR: δ (ppm) = 2.43, 2.84 (2

s, 6H, two CH₃ at pyrazole ring), 3.77, 3.84 (2 s, 6H, 2 × OCH₃), 6.60 (s, 1H, pyrazole CH), 6.88-8.02 (m, 11H, Ar-H), 8.25 (s, 1H, pyrimidine CH). MS: m/z = 543. Analysis for C₃₂H₂₅N₅O₂S (543.65): Calcd. (Found) = C 70.70 (70.68), H 4.61 (4.57), N 12.88 (12.82), S 5.90 (5.84).

9-(3,4-Dimethoxyphenyl)-4-(3,5-dimethylpyrazolo)-7-(2-naphthyl)pyrido[3',2':4,5]thieno[3,2-d]pyrimidine (18d):

Crystallized from dioxane as white solid (77%), mp 262 °C. IR: ν (cm⁻¹) = 3028 (aromatic CH), 2922, 2787 (aliphatic CH), 1653 (C=N). H-NMR: δ (ppm) = 2.41, 2.78 (2 s, 6H, 2 × CH₃ at pyrazole ring), 3.76, 3.82 (2 s, 6H, 2 × OCH₃), 6.62 (s, 1H, pyrazole CH), 6.87-8.02 (m, 11H, Ar-H), 8.27 (s, 1H, pyrimidine CH). MS: m/z = 543. Analysis for C₃₂H₂₅N₅O₂S (543.65): Calcd. (Found) = C 70.70 (70.74), H 4.61 (4.66), N 12.88 (12.71), S 5.90 (5.88).

3. Results and discussion

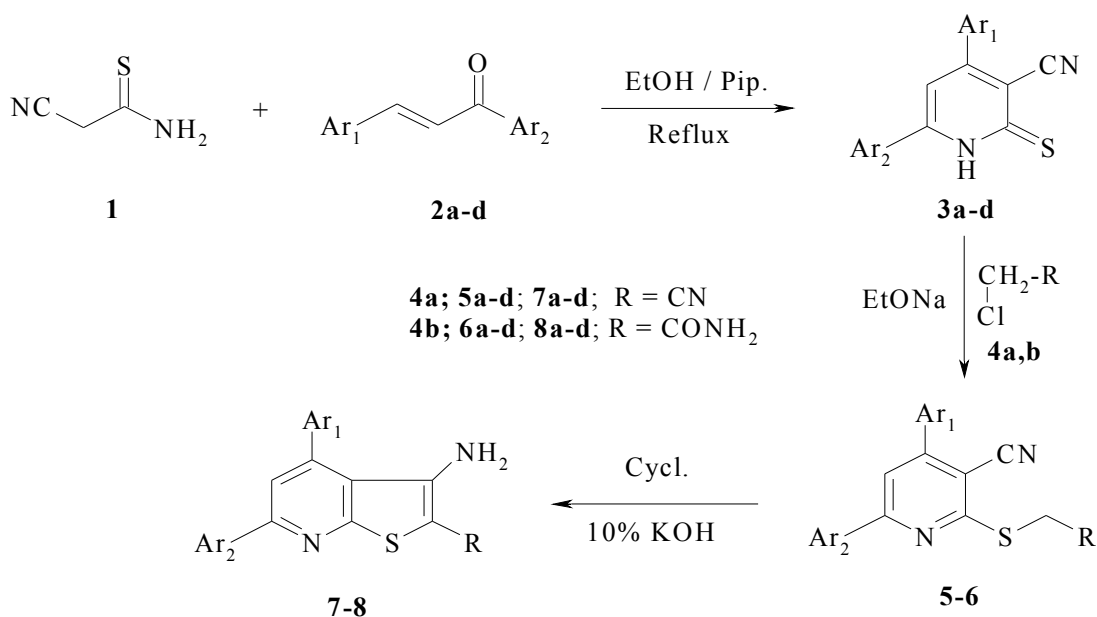
The results obtained showed that reaction of cyanothioacetamide **1** with α,β -unsaturated carbonyl compounds **2a-d** afforded 2-thioxo-1,2-dihydropyridine-3-carbonitrile **3a-d**. Structure of compounds **3a-d** has been elucidated from their spectral data, elemental analysis, and chemical reactions. Their IR spectra showed absorption bands at 3321-3372, and 2217-2224 cm⁻¹, characteristic for NH and CN groups, respectively. Moreover, upon their reaction with chloroacetonitrile **4a** or chloroacetamide **4b**, 3-cyanopyridin-2-ylthioacetamides **5a-d** and 3-cyanopyridine-2-ylthioacetamides **6a-d** were formed, respectively. Also, cyclization of compounds **5-6** with ethanolic 10% KOH ascertained their structure, where an addition of methylene protons to cyano group took place, to give 3-aminothieno[2,3-b]pyridine derivatives **7-8**, respectively (Scheme I).

Condensation of compounds **7a-d** with triethyl orthoformate in acetic anhydride gave 3-(ethoxymethyleneamino)thieno[2,3-b]pyridine derivatives **9a-d** which on their treatment with hydrazine hydrate produced 3-amino-4-imino-3,4-dihydropyrido[3',2':4,5]thieno[3,2-d]pyrimidine derivatives **10a-d**. The presence of amino and imino groups in **10a-d** was confirmed by their reaction with triethyl orthoformate to give pyrido[3',2':4,5]thieno[3,2-d][1,2,4]triazolo[5,1-f]pyrimidine derivatives **11a-d**. Also the structure of compounds **10a-d** was substantiated by their heating with aqueous KOH solution where Dimroth rearrangement took place to give 4-hydrazinopyrido[thienopyrimidines **12a-d**. However, the condensation of compounds **8a-d** with triethyl orthoformate in acetic anhydride gave

pyridothienopyrimidine-4-one derivatives **13a-d**. Chlorination of them with POCl_3 afforded 4-chloropyridothienopyrimidine derivatives **14a-d** which on their reaction with hydrazine hydrates authenticated derivatives **12a-d**. The structure of compounds **13** and **14** was confirmed by their IR spectra where they showed bands at 3214-3224 and 1660-1667 cm^{-1} characteristic for NH and CO amidic group, respectively. Structure of compounds **8a-d** has been confirmed by their nitrosation with nitrous acid where they gave only 3,4-dihydropyrido[3',2':4,5]thieno[3,2-d][1,2,3]triazin-4-one derivatives **15a,b,d**. All trials carried out to synthesize derivative **15c** were failed. Structures of

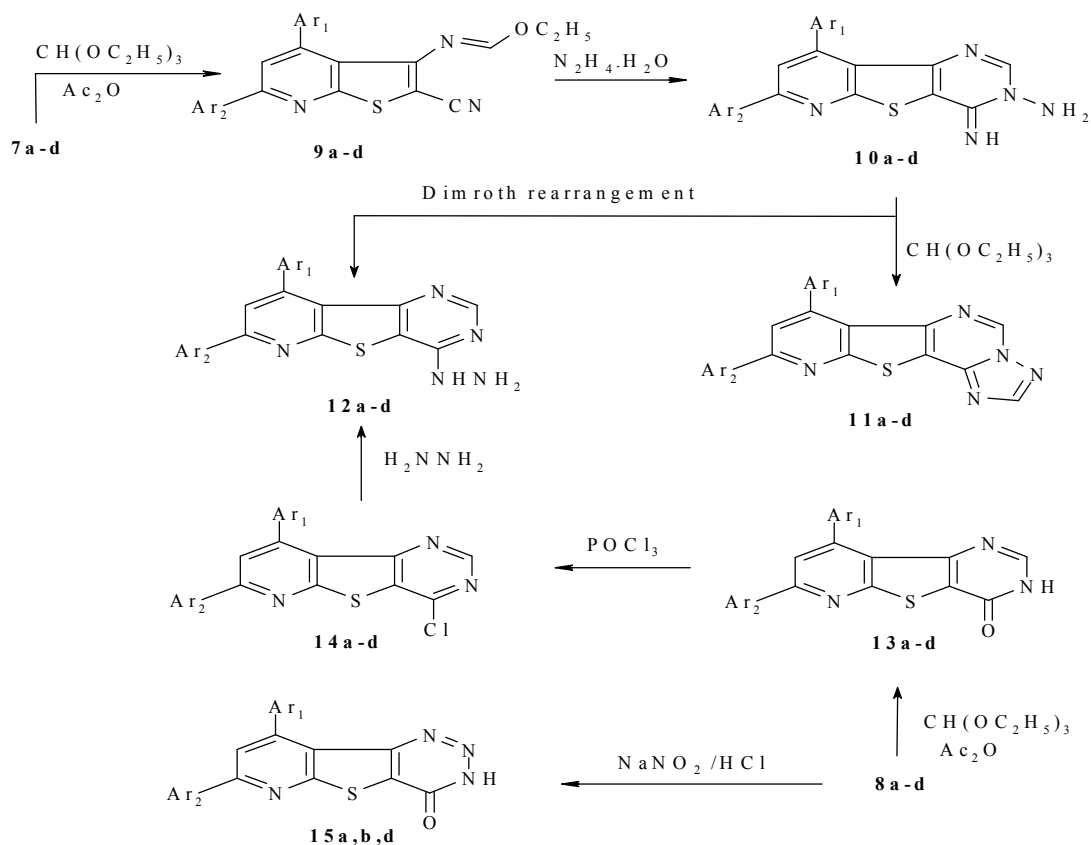
the products were ascertained by their IR spectra where they showed bands at 3237-3274 and 1659-1664 cm^{-1} characteristic for NH and CO amidic group, respectively (Scheme II).

The presence of hydrazino group in compounds **12a-d** was ascertained by its condensation with benzaldehyde, diethyl malonate, and acetylacetone to give 4-benzylidenehydrazinopyrido[3',2':4,5]thieno[3,2-d]pyrimidine **16a-d**, ethyl 1,2,4-triazolo[4",3"-c]pyrido[3',2':4,5]thieno[3,2-d]pyrimidin-3-ylacetate **17a-d** and 4-(3,5-dimethylpyrazolo)pyrido[3',2':4,5]thieno[3,2-d]pyrimidine **18a-d**, respectively (Scheme III).



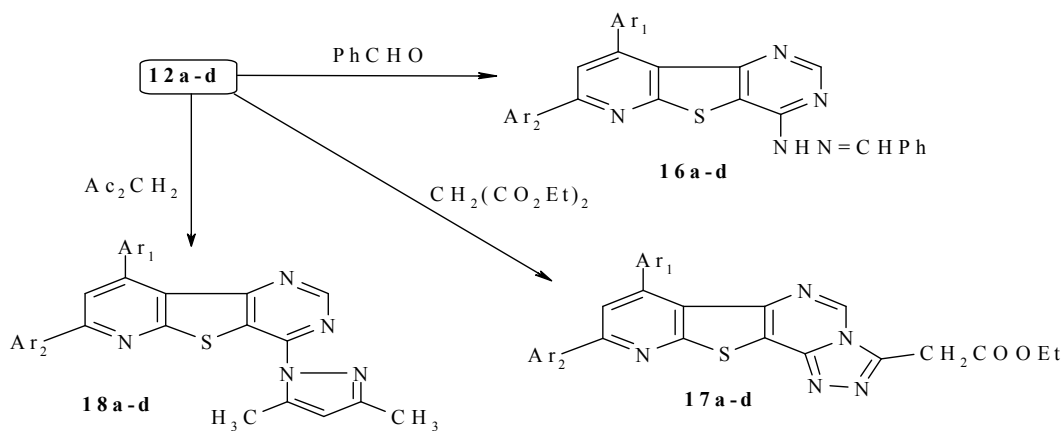
2-8	a	b	c	d
Ar_1	3,4-(CH_2O_2) C_6H_3	3,4-(CH_2O_2) C_6H_3	3,4(CH_3O) $_2\text{C}_6\text{H}_3$	3,4(CH_3O) $_2\text{C}_6\text{H}_3$
Ar_2	α -naphthyl	β -naphthyl	α -naphthyl	β -naphthyl

Scheme I



9-15	a	b	c	d
Ar ₁	3,4-(CH ₂ O ₂)C ₆ H ₃	3,4-(CH ₂ O ₂)C ₆ H ₃	3,4(CH ₃ O) ₂ C ₆ H ₃	3,4(CH ₃ O) ₂ C ₆ H ₃
Ar ₂	α-naphthyl	β-naphthyl	α-naphthyl	β-naphthyl

Scheme II



16-18	a	b	c	d
Ar ₁	3,4-(CH ₂ O ₂)C ₆ H ₃	3,4-(CH ₂ O ₂)C ₆ H ₃	3,4(CH ₃ O) ₂ C ₆ H ₃	3,4(CH ₃ O) ₂ C ₆ H ₃
Ar ₂	α-naphthyl	β-naphthyl	α-naphthyl	β-naphthyl

Scheme III

Conclusion

The achieved derivatives of thienopyridine, pyridothienopyrimidine, and pyridothienotriazolopyrimidines that are expected to have pharmaceutical, medicinal, and biological activities, have been synthesized and their structures confirmed by their spectral data, elemental analyses, and with some chemical reactions.

Acknowledgements

The authors would like to thank the Department of Chemistry, University College of Women for Arts, Science, and Education; Ain Shams University and department of chemistry, Faculty of Science, Al-Azhar University-Gaza, Gaza, Palestine for their support during carrying out this work.

Corresponding author

Shadia Mahmoud Abdallah²

Department of Chemistry, University College of Women for Arts, Science, and Education, Ain Shams University,
shdiamabdallah@yahoo.com,

References

- Mongevega, A.; Aldama, I.; Robbani, M. M.; Fernandez-Alvarez, E. J. *Heterocycl. Chem.* **1980**, 17, 77-86.
- Bellary, J. M.; Badiger, V. V. *Indian J. Chem.* **1981**, 20B, 654-662.
- Joshi, K. C., Chand, P.; *J. Heterocycl. Chem.* **1980**, 17, 1783-1784.
- Youssef, M. S. K.; Hassan, K. M.; Atta, F. M.; Abbady, M. S. J. *Heterocycl. Chem.* **1984**, 21, 1565-1568.
- Potts, K. T.; Husain, S. J. *Org. Chem.* **1971**, 36, 10-13.
- Bridson, P. K.; Davis, R. A.; Renner, L. S. J. *Heterocycl. Chem.* **1985**, 22, 753-755.
- Saito, Y.; Yasushi, M.; Sakoshita, M.; Toyda, K.; Shibazalti, T. *European Patent Appl.* **1993**, 535548; *Chem. Abstr.* **1993**, 119, 117112e.
- Furuya, S.; Takeru, N.; Matsumoto, H. *Jpn Kokai Tokkyo Koho JP 09169766*; *Chem. Abstr.* **1997**, 127, 176416v.
- Furuya, S.; Choh, N.; Suzuki, N.; Imada, T. *PCT Int. Appl. WO 000 00 493*. **2000**, *Chem. Abst.* **2000**, 132, 64179.
- Gad-Elkareem, M.; Abdel-Fattah A.; Elneairy, M. *Phosphorus, Sulfur Silicon Relat. Elem.* **2006**, 181, 891-911.
- Dave, C. G.; Shah, P. R.; Shah, A. B.; Dave, K. C.; Patel, V. J. *J. Indian Chem. Soc.* **1989**, 66, 48-56.
- Bousquent, E.; Romero, G.; Guerrero, F.; Caruso, A.; Amico-Roxas, M.; Farmaco, Ed. *Sci.* **1985**, 40, 869-874.
- Leistner, S.; Wagner, G.; Guetschow, M.; Glusa E. *Pharmazie* **1986**, 41, 54-55.
- Wagner, G.; Leistner, S.; Vieweg, H.; Krasselt, U.; Prantz, J. *Pharmazie* **1993**, 48, 342-346.
- Boehm, N.; Krasselt, U.; Leistner S.; Wagner, G. *Pharmazie* **1992**, 47, 897-901.
- Abdel-Rahman, E. A.; Bakhite, E. A.; Al-Taifi, E. A. *J. Chin. Chem. Soc.* **2002**, 49, 223-231.
- Hussein, A. M.; Abu-Shanab, F. A.; Ishak, E. A. *Phosphorus, Sulfur, Silicon Relat. Elem.* **2000**, 159, 55-68.
- Abunada, N. M.; El-Louh, A. K. K.; Al-Zaeem, I. S. *Phosphorus, Sulfur Silicon Relat. Elem.* **2009**, 184, 591-601.
- El-Louh, A. K. K.; Abunada, N. M.; El-Abbady, S. M.; El-Shoubaki, M. J. *Asian Journal of Chemistry* **2007**, 19, 1283-1292.
- El-Louh, A. K. K.; Abunada, N. M.; Khudeir, N. J. *J. Al-Azhar University-Gaza (Natural Science)* **2006**, 8, 13-21.
- Attaby, F.; Eldin, S. M.; Elneairy, M. A. A.; El-Louh, A. K. K.; *Phosphorous, Sulfur Silicon Relat. Elem.* **2004**, 179, 2205-2220.
- Elneairy, M. A. A.; Eldin, S. M.; Attaby, F. A.; El-Louh, A. *Phosphorous, Sulfur Silicon Relat. Elem.* **2000**, 167, 289-295.
- Attaby, F. A.; Ibrahim, L. I.; Eldin, S. M.; El-Louh, A. K. K. *Phosphorous, Sulfur Silicon Relat. Elem.* **1992**, 73, 127-135.
- Elkholy, Y. M.; Morsy, M. A. *Molecules* **2006**, 11, 890-903.
- El-Assiery, S. A.; Sayed, G. A.; Fouda, A. *Acta Pharm.* **2004**, 54, 143-150.
- El-Saghier, A. M. M. *Molecules* **2002**, 7, 756-766.
- El-Agrody, A. M.; Abd Latif, M. S.; El-Hady, N. A.; Fakery, A. H.; Bedair, A. H. *Molecules* **2001**, 6, 519-527.
- Al-Afaleq, E. I.; Abushait, S. A. *Molecules* **2001**, 6, 621-638.
- Raj, T. T.; Ambekar S. Y. *J. Indian Chem. Soc.* **1990**, 67, 260-271.
- Grinstein, V.; Serina, L.; Latvijas PSR Zinatru Akad. Vestis, *Khim Ser. (Russ)*; **1963**, 4, 469; *C.A.* **1964**, 60, 5391.
- Gattow, G.; Manz, w.; *Z. Anorg. Allg. Chem. (Ger.)*; **1988**, 149, 559; *C. A.* **1988**, 109, 210505.
- McCall, M. A.; *J. Org. Chem.* **1962**, 27, 2433; *C.A.*, 1963, 58, 8914.
- Ankhiwala, M. D.; *J. Indian Chem. Soc.* **1990**, 67(3), 258-260.

12/23/2011

Designing A Model For Quality of Employee-Organization Relationships (EORs) Based On Analysis Hierarchical Process (AHP)

PH.D. Professor Ali Akbar Farhangi *, Sara moazen **, Maryam Aliei ***

* Tehran university International campus Kish Island. Email: dr-aafarhangi@yahoo.com

** Tehran university International campus Kish Island. Email: S.moazen@yahoo.com

*** Department of Management, Shahrood industrial University, Shahrood, Iran. Email: info@aliei.com

Abstract: Interpersonal relationships created a scale that consists of three components: personal relationship, community relationship, and professional relationship. Research in interpersonal Relationships and the psychology of interpersonal relationships shows that the following four outcomes are good indicators of successful interpersonal relationships. In this survey we show a model for Quality of employee-organization relationships (EORs) and evaluation interpersonal Relationships by this model. An EOR is dynamic and can be measured using perceptions of either or both parties regarding four “indicators representing the quality relationships or relationship outcomes: satisfaction, trust, commitment, and control mutuality. by this model and use AHP model for analysis this paper we evaluation type of interpersonal relationships. finally we found that to each Specific dimension of quality can be follow a particular interpersonal relationships, but the best approach is professional relationship.

[Ali Akbar Farhangi, Sara moazen, Maryam Aliei. **Designing A Model For Quality of Employee-Organization Relationships (EORs) Based On Analysis Hierarchical Process (AHP)**. Life Science Journal 2012;9(1):231-241]. (ISSN: 1097-8135). <http://www.lifesciencesite.com>. 33

Keywords: Employee-Organization Relationships (EORs), Quality, Analysis Hierarchical Process (AHP)

Introduction

Interpersonal relationships created a scale that consists of three components: personal relationship, community relationship, and professional relationship. The scale's three components are measured by a bank of 15 items that revolve around the public relations issues of reciprocity, mutual legitimacy, and mutual understanding. (Bruning & Galloway, 2002) Banning (2007). When you are successful at failing in interpersonal relationships, you also know how to be successful at succeeding in relationships, once the concept is understood. An individual who fails at a relationship is a person who neglects the needs of the partner. So it would follow that the first step to a successful relationship is to determine what needs the other person has. It is also vital to understand your own needs so that you can help the other person in the relationship to fill your needs. we explain interpersonal relationships for help Banning (2007) :

1. personal relationship
2. community relationship
3. professional relationship

Personal relationship: Framework for Studying Personal Relationships

The study of the personal relationships that exist between individuals can be conceptualized as a component of the relationship that exists between an organization and particular public, such as customers, donors, or employees (Toth, 2000). This kind of

relationship is commonly referred to in the literature as an organization-public relationship (Broom et al., 2000). (Gallicano: 2008)

There are three components of Broom et al.'s (2000) conceptualization of organization-public relationships. First, organization-public relationships involve repeated experiences of interaction, linkage, and exchange of information, energy, and resources. Second, they have characteristics that participants do not necessarily perceive. Third, although organization-public relationships evolve, people can discuss them at a single moment and monitor them over time.

Grunig and Huang (2000) took existing public relations literature from the excellence study, Huang's (1997) dissertation, and other sources and positioned it within a relationship management framework. They filtered this literature into antecedents, cultivation strategies, and outcomes for organization-public relationships. Relationship antecedents consist of the reasons why organizations and publics form relationships with each other (e.g., Broom et al., 2000; Grunig & Huang, 2000; Thomlison, 2000). Grunig (2002) defined cultivation strategies as “the communication methods that public relations people use to develop new relationships with publics and to deal with the stresses and conflicts that occur in all relationships” (p. 5). The (inter)personal influence model and other strategies to cultivate personal relationships can be conceptualized as types of cultivation strategies. Broom et al. (2000) defined

relationship outcomes as the consequences that alter the environment and secure, maintain, or adjust goals both within and outside of organizations. The next section is a review of the public relations literature about personal relationship strategies and outcomes.

Management Strategies for Cultivating Personal Relationships

Two strategies were classified as management strategies because they do not involve direct engagement with the public examined in this study. These two strategies include investment in the local level for building relationships and targeting “aware” affiliates for personal help with relationship building in diverse communities.

1. Investment in local level or relationship building

The national and state offices drive resources to the affiliate level to cultivate relationships. For example, the national office created a template for an awareness walk that helps the local level develop social bonds among members, raise money for local services, and recruit members. In addition, the national office has regional representatives who resolve local challenges, including interpersonal disagreement. A national staff member hoped that the state and affiliate leaders would spread good messages about the national organization to the grassroots. She explained, “There’s just sort of a sense that builds – yeah, those are good guys: I interviewed who did not have leadership positions and who did not attend the national convention did not experience this level of trickle-down, as suggested by their reluctance to evaluate the national organization beyond reflecting on the national office’s membership magazine.

Targeting of aware affiliates

With more than a thousand affiliates, achieving the goal of requisite variety (in this case, having the diversity of the membership reflect the diversity of the community) is no easy feat. The organization shares diversity tips through conventional venues, such as meetings, publications, and conferences. For deciding where to place limited personal attention from the national level, Adriana follows a strategy that her professor taught her. She stated, “I had a professor of mine. He would have a drawing. He used to say, ‘We have two options. Trying to fight people you’ll never change and trying to focus on people you might change.’”

Personal Relationship Outcomes

The second research question is “What are the outcomes of personal relationships in this case study?” The relationship outcomes of cultivating

personal relationships in this study include affective commitment, political leverage, social capital, and member recruitment and retention.

1. Affective commitment

Personal relationships between staff and members, in addition to personal relationships among members, can result in developing an emotional bond with the organization. Ken said that when people contact him for help, he needs to give them emotional support, in addition to skills and knowledge for navigating the system. He explained, “One way to do that is to become their friend or someone who they call and trust.” Representing a member perspective, Gertrude said that she appreciates the organization because of “the camaraderie.” She explained, “We’ve been through hell together, and we have such strong bonds.” The deep disclosure that occurs is one reason why lasting bonds develop. From what I could assess from my participant population, many if not most staff members seem to share the illness that members or members’ loved ones have, or staff members have a family member who has the illness, or all of the above.

2. Political leverage

Personal relationships with people in the health system enable staff to obtain political leverage and deliver relatively quick results that members are unlikely to receive elsewhere. Roger stated I have personal relationships with the chairs of the Departments of [health name omitted] from all [of the medical universities in the area], as well as with the heads of maj or community agencies, the public providers, insurance companies. ... If there is a problem in accessing services for an individual in [my city], it is highly likely that I have a personal relationship with someone who can break down any existing barriers. If I don’t have this – I know who does! Such is the nature of how things are accomplished in a large urban area. It may take me a few e-mails or phone calls – but I will get some satisfaction for the individual in need. ... Because of my personal relationships with this cadre of individuals, I am in a unique position to persuade them to fulfill needs. Echoing this theme, Ken stated, “When something happens here, everybody knows me, and I know everybody in the system. So it’s pretty easy for me to make a phone call.”

3. Social capital

Another valuable outcome of personal relationships is social capital. Explaining the value of relationships, Amber stated It means that if we want something from one another, it’s much easier to get it in all directions, because the relationships are there, and you don’t have to negotiate every transaction. ... It greases the wheels somebody needs to ... get going on. It’s much easier to come out and go zero to 60

rather than taking the slow ramp up. ... It encourages growth in the organization. Amber explained that part of the failure of a policy change that the national office tried to implement for state organizations and affiliates was that the national executive director at the time (who was later asked to step down) "had no relationships in the field." In contrast, the current executive director of the national office started at the state level as an executive director for six years.

4. Member recruitment and retention

Personal relationships between staff and members, in addition to personal relationships among members, can also help with recruiting and retaining members. Amber stated, "If there's this sense of connectivity, then people want to draw other people in. If it feels like it's hard work and it's hostile, you don't bring other people into that fire. The organization is then ever shrinking."

Some former members who participated in this study ended their participation due to not getting along with other members. For example, Doris felt alienated when members crossed her privacy boundaries by asking what she felt to be invasive questions. She recounted that members said something like "'Ew, that drug,' and they make a face, and they moan." Good relationships can attract members and poor relationships can hurt an organization's retention.

Building community relationships

Leaders know that building and sustaining good community relationships is important to the well-being and culture of their organization. Building relationships prepares the ground for effective consultation and for creating partnerships.

1. Leading the school community

Effective principals are community leaders. They work in a wide range of school contexts, groups and organizations. They build partnerships based on addressing the needs of staff and improving their learning outcomes.

2. Building partnerships

Organizations need the support of their local community to achieve their goals. School leaders have to work out how to make their relationships with external organizations, people, and groups productive so that all parties benefit.

3. Consulting with communities

Effective community partnerships are built on open dialogue and communication. Leaders regularly consult with their local community to construct and share a common vision and goals.

4. Involving parents and families

Effective partnerships between schools and parents and communities can result in better outcomes

for students. The better the relationship and engagement, the more positive the impact on students' learning.

3. Professional Relationships

Establishing professional relationships can be the cornerstone of success in an organization. Part of why you should value internal relationships and work to make them productive is to foster credibility and enable you to get things done. If you are in a managerial position, the interactions with your staff need to be positive to drive success for everyone

Six Strategic for Professional Relationships

Jakol, D.S (2011)" explain Six Strategic for Professional Relationships

1. Define Responsibilities.

Volunteers must know what is expected for them to be successful. Carefully define, in writing, the responsibilities for each position. Be honest; don't minimize the commitment.

2. Select and Recruit.

You must have a complete team to play the game—no holes in the "line"; no holes in the "backfield." You use your relationships with volunteers to recruit key people who are, in turn, good recruiters and who attract to other people. It's like compound interest on your investments! Then you use your relationship with these new people to enlarge or complete your team.

3. Orient and Train.

Provide each person with prompt orientation on the individual assignment and with adequate training to be successful. The key is to give a person enough information to quickly begin their new task. Don't overload them with too many books, too many forms, or too much information. The new district chair doesn't need to know how to run the annual recognition banquet, yet—but rather what key vacancies need to be filled and what to emphasize at the next district meeting.

Much of the training of district and council volunteers is done through defined training courses. However, important informal training occurs through the relationship and contacts with the professional.

4. Coach Volunteers.

Your coaching will take many forms on many topics—all of it directed to a single objective: enabling each volunteer to be successful in their Scouting responsibilities. Sometimes it will involve removing roadblocks to success; sometimes it's more serious counseling; sometimes just serving as a sounding board or reassuring volunteers about the great things they're doing. Often professional coaching involves helping each volunteer to understand the way in which his/he ask connects to the tasks of others.

5. Recognize Achievement.

Prompt volunteer recognition has an important impact on the tenure and quality of volunteer service in the district or council. Recognition must be sincere, timely, and earned.

6. Evaluate Performance

Help volunteers regularly evaluate how they're doing. Use the Self-Evaluation for Unit Commissioners; Self-evaluation is probably the least threatening, especially if it is focused on the end result in the Scouting program. This minimizes the possibility of destructive judgment and criticism. Evaluation must also be a part of your discussions with a volunteer. Jakol, D.S (2011)

Build A Strong Professional Relationship With Your Employer

Relationships with employers can be tricky. You want to be friendly and establish a rapport with your employer, but you want to steer clear of a highly personal relationship. You want to feel comfortable enough with your employer to share your ideas-but you don't want to run the risk of offending him or her.

Your relationship with your employer is also highly important-not only for the short-term, but for the long-term as well. You want the kind of relationship that makes it a pleasure to come to work every day. Yet, you realize that no job lasts forever and that, at some point, you might want to move on. In such a case, you want to do everything you can to ensure that your current employer will serve as a favorable reference later on. But how can you go about building a strong professional relationship with your employer? Nokava(2010)

1. Act professional

It is important that you act professional at all times and in all situations. In this way, you will gain the respect of your employer. Be sure to be polite in all your dealings with fellow employees and clients. Dress well; speak well; and keep up to date on all the latest information in your particular field.

It is critical that you develop a bond of trust with your employer. If your employer sees you putting forth your best effort day in and day out.if he or she sees you going above and beyond the call of duty.if he or she recognizes that you are a highly capable individual and a valuable employee.chances are greater that your employer will have full faith in you and your abilities.

2. Be honest and open

You need to be honest and open with your employer-especially when problems arise. If you are candid-without being cruel-it is likely that your employer will respect you even more. However, if you gloss over problems or fail to discuss what's bothering you, a certain degree of distrust may develop between you and your employer.

Most employers respect honest feedback. They are striving to constantly improve their companies; therefore, they need to know about not only what's going right-but also what's going wrong. Chances are you will be rewarded for your willingness to tell the truth in all situations.

3. Respect deadlines

Believe it or not, a number of employees have a blasé attitude about deadlines. They figure that they will be granted more time to complete a project if they need it. However, if you abide by deadlines, your status is likely to rise in the eyes of your employer. In other words, it pays to do your work on time.

4. Compliment your employer when appropriate

Be sure to tell your employer when a policy is working particularly well or a recent hire appears to be outstanding. This will help to promote good feelings between you and your employer. Unfortunately, too many employees are quick to criticize and slow to praise. You are more likely to build a strong professional relationship with your employer if you don't fall

Organization–public relationship (OPR)

Since the 1980s Organization–public relationship (OPR) management has been widely used as a useful framework for public relations research, teaching, and practice (e.g., Hon & Grunig, 1999; Huang, 2001; Ledingham, 2003). Two extensively examined models of OPRs include (1) Broom, Casey, and Ritchey's (2000) model emphasizing perceptions, motives, needs, and behaviors as predictors of relationships and their consequences (p. 16), and (2) Grunig and Huang's (2000) model elaborating situational antecedents, relationship maintenance strategies, and relationship outcomes (p. 34). Nevertheless, the two models have not been extensively applied to employee publics (Freitag & Picherit-Duthler, 2004; McCown, 2007). One important research direction that has not been fully developed is new models of relationships integrating variables that can impact the development of relationships between organizations and their strategic employees (Kim, 2007)(jiang :2011).

Six Types of OPRs (hung 2009)

Mills and Clark (1982, 1986, 1994) developed two major types of relationships frequently used in the study of organization–public relationships in public relations: communal and exchange relationships (e.g., Hon & Grunig, 1999; Hung, 2002, 2005; Jo, 2006). In communal relationships, benefits are given in order to please the other. Even though this may sound like an exchange relationship, members who give benefits do not expect the other's return or obligation to pay back (Mills & Clark, 1994). An exchange relationship

suggests that members benefit one another in response to specific benefits received in the past or expected in the future. Hung (2002, 2005) adopted Mills, Clark, and their colleagues' work on communal and exchange relationships (Clark, 1984; Clark & Mills, 1979, 1993; Clark, Mills, & Corcoran, 1989; Clark, Powell, & Mills, 1986; Clark, Ouellette, Powell, & Milberg, 1987; Clark & Taraban, 1991; Clark & Waddell, 1985) and developed additional six types of OPRs:

1. **Exploitive relationships:** exploitive relationships arise when one takes advantage of the other when the other follows communal norms, or when one does not fulfill his/her obligation in an exchange relationship (Clark & Mills, 1993).

2. **Manipulative relationships:** a manipulative relationship happens when an organization, with the knowledge of what publics want, applies asymmetrical or pseudo-symmetrical approaches to communicate with publics to serve its own interests (Hung, 2005, p. 408).

3. **Symbiotic relationships:** it happens when organizations, realizing their interdependence in the environment, work together with certain publics with the common interest of surviving in the environment. However, they acknowledge this interdependence and understand the influence of their behavior on one another.

4. **Contractual relationships:** contractual relationships start when parties agree on what each should do in the relationships. It is like writing a contract at the beginning of a relationship. Contractual relationships cannot promise equal relationships (Hung, 2005, p. 398).

5. **Covenantal relationships:** a covenantal relationship means both sides commit to a common good by their open exchanges and the norm of reciprocity. Individuals in the relationship always provide the others an opportunity to "ask for insight, to provide criticism, and to place a claim upon some of the individual's time" (Benette, p. 9).

6. **Mutual communal relationships:** Hon and Grunig (1999) defined communal relationships as "both parties provide benefits to the other because they are concerned for the welfare of the other—even when they get nothing in return" (p. 21). Yet, what they identified is a more sophisticated level of relationships, as what Mills and Clark (1994) defined as "mutual communal relationships (i.e., relationships in which each person has a concern for the welfare of the other)" (p. 30). Mutual communal relationships are different from covenantal relationships, in which the latter emphasizes open exchanges between the two parties, while the former emphasizes the psychological intention to protect the welfare of each other (Hung, 2005)

Quality of employee–organization relationships (EORs)

employee–organization relationships (EORs) is regarded as one type of organization–public relationships (OPRs). In an EOR, the behaviors of one party result in consequences upon the other in different states of the relationship (e.g., Hon & Grunig, 1999; Huang, 2001). Distinct from its antecedents and consequences, an EOR is dynamic and can be measured using perceptions of either or both parties regarding four "indicators representing the quality of [Employee–Organization] relationships" or relationship outcomes: satisfaction, trust, commitment, and control mutuality (Grunig & Huang, 2000, p. 42) at specific points of time. (jiang:2011)

1. **Control mutuality**--The degree to which parties agree on who has the rightful power to influence one another. Although some imbalance is natural, stable relationships require that organizations and publics each have some control over the other.

2. **Trust**--One party's level of confidence in and willingness to open oneself to the other party. There are three dimensions to trust: integrity: the belief that an organization is fair and just... dependability: the belief that an organization will do what it says it will do... and, competence: the belief that an organization has the ability to do what it says it will do (Hon and Grunig). That an organization will do what it says it will do. The notion of a fiduciary relationship operates particularly when a not-for-profit organization is a party to the relationship (Ledingham and Bruning).

3. **Commitment**--The extent to which each party believes and feels that the relationship is worth spending energy to maintain and promote. Two dimensions of commitment are continuance commitment, which refers to a certain line of action, and affective commitment, which is an emotional orientation (Hon and Grunig). Perceived levels of commitment are an indication of OPR quality (Ledingham and Bruning).

4. **Satisfaction**--The extent to which each party feels favorably toward the other because positive expectations about the relationship are reinforced. A satisfying relationship is one in which the benefits outweigh the costs.

For Measuring Relationships we need:

For Control Mutuality

1. This organization and people like me are attentive to what each other say.
2. This organization believes the opinions of people like me are legitimate.
3. In dealing with people like me, this organization has a tendency to throw its weight around. (Reversed)

4. This organization really listens to what people like me have to say.

5. The management of this organization gives people like me enough say in the decision-making process.

For Trust

1. This organization treats people like me fairly and justly.

2. Whenever this organization makes an important decision, I know it will be concerned about people like me.

3. This organization can be relied on to keep its promises.

4. I believe that this organization takes the opinions of people like me into account when making decisions.

5. I feel very confident about this organization's skills.

6. This organization has the ability to accomplish what it says it will do.

For Commitment

1. I feel that this organization is trying to maintain a long-term commitment to people like me.

2. I can see that this organization wants to maintain a relationship with people like me.

3. There is a long-lasting bond between this organization and people like me.

4. Compared to other organizations, I value my relationship with this organization more.

5. I would rather work together with this organization than not.

For Satisfaction

1. I am happy with this organization.

2. Both the organization and people like me benefit from the relationship.

3. Most people like me are happy in their interactions with this organization.

4. Generally speaking, I am pleased with the relationship this organization

has established with people like me.

5. Most people enjoy dealing with this organization.

1. Work-life conflict

Many employees find that the requirements from their work and the obligations from their personal life are very often incompatible and thus cause some degree of work-life conflict (Reynolds, 2005). Work-life conflict can be classified as time-based and strain-based. Time-based work-life conflict refers to the situation that time committed to duties in work makes it physically difficult for an individual to perform activities required by his or her nonwork roles (Pleck, Staines, & Lang, 1980). For instance, a scheduled business meeting may interfere with a child's school event (Grant-Vallonea & Ensherb,

2001). As strain-based work-life conflict entails, employees, when being psychologically preoccupied with work, are unable to fully comply with those commitments in their non-work roles (Netemeyer, Boles, & McMurrin, 1996). An example is when a social worker fails to rescue an abused woman from her dangerous marriage, he or she might go back home stressed out and become preoccupied with the frustration (Lambert, Pasupuleti, Cluse-Tolar, Jennings, & Baker, 2006).

2. Transformational leadership

Compatible with the essence of two-way symmetrical communication, transformational leadership emphasizes participative management, individual empowerment, negotiation, sharing of information and power in the workplace (Aldoory, 1998), and therefore can help organizations cultivate relationships with their employees. Transformational leadership is made up of the following four components/dimensions: (1) idealized influence, charisma (II): A spiritual power or personal quality that gives an individual influence or authority over large numbers of people, (2) inspirational motivation (IM), (3) intellectual stimulation: The ability of a leader to keep those following him or her thinking about the task at hand, asking questions, and solving problems. (IS), and (4) individualized consideration: The ability of a leader to pay special attention to the needs and problems of each individual person. (IC) (Bass & Avolio, 2004; Chemers, 1997).

3. Procedural justice

Public relations scholars have suggested that procedural justice is based on the principle of two-way symmetry too and closely relevant to employee-organization relationships (Grunig & White, 1992). Procedural justice refers to the perceived fairness of the procedures through which outcomes are decided (Cohen-Charash & Spector, 2001; Colquitt, Conlon, Wesson, Porter, & Ng, 2001; Luo, 2007).

4. Family-supportive workplace initiatives

Scholars have classified three main categories of family-supportive workplace initiatives, including (1) policies (e.g., flex-time, telecommuting, job-sharing, and personal level), (2) services (e.g., organization-sponsored full-time childcare centers and referral information about childcare), and (3) benefits (e.g., childcare subsidies) (Lapierre & Allen, 2006; Wadsworth & Owens, 2007). Therefore, this study focuses on three workplace supportive initiatives: childcare, job flexibilities, and personal day.

Notice (bruning, 2008)

Kim (2001) developed a scale to measure relationship quality by incorporating information gleaned from the interpersonal communication, relationship marketing, and public relations literatures. Kim (2001) initially hypothesized that 10

relationship dimensions – including trust, mutuality, commitment, satisfaction, communal relationship openness, community involvement, affective intimacy, relationship termination cost, and reputation – were central to organization–public relationships. The results from this investigation showed that four dimensions emerged from the analysis – trust, commitment, local or community involvement, and reputation. Although tests have examined the validity and reliability of the scale, application of the scale in a variety of contexts has not taken place.

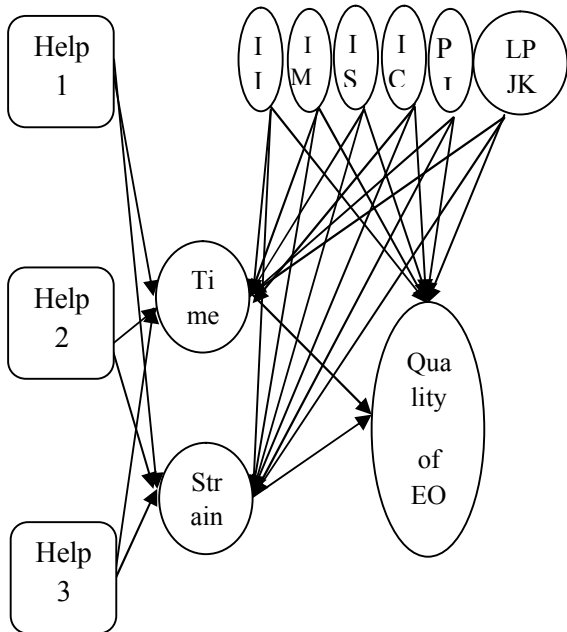


Fig. 1. The finalized theoretical model for the study. Time: time-based work–life conflict; strain: strain-based work–life conflict; II: idealized influence (behavior); IM: inspirational motivation; IS: intellectual stimulation; IC: individualized consideration; PJ: procedural justice in general; WLPJ: procedural justice referencing work–life conflict policies, decisions, and procedures; Help1: helpfulness of childcare initiatives; Help2: helpfulness of job flexibilities initiatives; Help3: helpfulness of personal day initiatives

Assumptions underlying the EOR

Who are the parties in the EOR? The implicit conjecture in most studies is that the individual employee and the organization enter into a relationship. However, since the organization is made up of multiple potential exchange partners (i.e., agents), it is not clear who the employee considers when answering questions about this relationship. This is partially a methodology problem since research on the EOR has almost exclusively used

surveys, and asks participants questions about the “organization”. In fact, if the organization is represented by agents as well as coalitions and groups, and depends on the individual employee's perception, it could be argued that each employee works for a different organization! Underlying the examination of the employee–organization relationship are two assumptions: (a) the employee attributes the organization with human like qualities, a process referred to as anthropomorphization (Levinson, Price, Munden, Mandl, & Solley, 1962) and (b) from the organization's perspective, organizational agents pursue the organization's interests in the employment relationship with employees. The anthropomorphism of the organization (currently visible in Organizational Support Theory and Psychological Contract Theory) can be traced to Levinson et al. (1962) who argued that employees view actions by agents of the organization as actions by the organization itself. This personification of the organization is facilitated by the fact that organizations have legal, moral and financial responsibilities for the agents of the organization (Eisenberger, Huntington, Hutchinson, & Sowa, 1986). Therefore, in EOR research, the assumption is made that employees view all possible agents and contract makers (even administrative contract makers such as human resource policies and mission statements) bundled into one “human like” contract maker in such a way that the employee has a relationship with a single entity (i.e., the organization)

Sample

Information comes from professional and academic literature about relationships. Also included are the results from a survey about relationships conducted by graduate students relationships at management school in Iran. For this study we have used questionnaires and 121 students, teachers and staff in school management in Iran, we have worked to fill out questionnaires.

Results

The AHP, developed by Saaty (1980) is designed to solve complex multi-criteria decision problems. It is a flexible and powerful tool for handling both qualitative and quantitative multi-criteria problems. The AHP is aimed at integrating different measures into a single overall score for ranking decision alternatives. Its main characteristic is that it is based on pair wise comparison judgements. AHP has been applied to a wide variety of decisions such as car purchasing (Byun, 2001), vendor selection (Tam & Tummala, 2001), IS project selection (Muralidar & Santhanam, 1990; Schniedejans & Wilson, 1991), and software selection (Kim & Yoon, 1992; Mamaghani, 2002). Although

there have been some studies on using AHP for software selection, each of the studies has focused on software with a different nature and function, such as antivirus and content filtering software, executive IS, simulation software, expert systems, multimedia authoring systems, logistics IS and AHP software. It is necessary to design and develop a generic AHP model to help Quality of employee–organization relationships (EORs) practitioners of their organization.

This approach is found to be very useful in collecting data. This determination is performed through using pair- wise comparisons. The function of the pair - wise comparisons is by finding the relative importance of the criteria and sub criteria which is rated by the nine - point scale proposed by Saaty (1980) , as shown in Table 1, which indicates the level of relative importance from equal, moderate, strong, very strong, to extreme level by 1, 3, 5, 7, and 9, respectively. The intermediate values between two adjacent arguments were represented by 2, 4, 6, and 8.

Table 1. “Measurement scales”. Source: Saaty (1980)

Verbal judgment	Numerical rating
Extremely preferred	9
Very strongly preferred	7
Strongly preferred	5
Moderately preferred	3
Equally preferred	1
Intermediate values	2, 4, 6, and 8

Analysis

Prioritize interpersonal relationships outcome

By help of AHP model, interpersonal relationships outcomes have priorities and the following weights we can be compared interpersonal relationships together.

Prioritize Quality of interpersonal relationships based on Control mutuality

As you can see In fig(3) Quality of interpersonal relationships based on the model, have been prioritized in the following figure. The first priority, these relationships are based on the Control mutuality , the highest quality have been obtained sequence 1.personal relationship, 2.community relationship, 3.professional relationship. If you want to have more Control mutuality in interpersonal relationships use of personal relationship.



Fig. 2. Prioritize interpersonal relationships outcome

Prioritize Quality interpersonal relationships based on Trust

As you can see In fig(4) Quality of interpersonal relationships based on the model, have been prioritized in the following figure. The first priority, these relationships are based on the Trust , the highest quality have been obtained sequence 1. professional relationship 2.community relationship , 3.personal relationship. If you want to have more Control mutuality in interpersonal relationships use of professional relationship.

Prioritize Quality interpersonal relationships based on Commitment

As you can see In fig(5) Quality of interpersonal relationships based on the model, have been prioritized in the following figure. The first priority, these relationships are based on the Commitment , the highest quality have been obtained sequence 1. professional relationship 2.community relationship , 3.personal relationship. If you want to have more Commitment in interpersonal relationships use of professional relationship.



Fig. 3. Prioritize Quality of interpersonal relationships based on Control mutuality

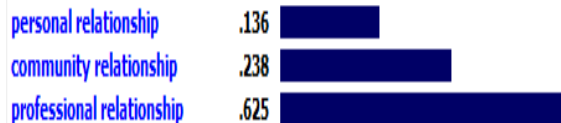


Fig. 4. Prioritize Quality interpersonal relationships based on Trust

Prioritize Quality interpersonal relationships based on Satisfaction

As you can see In fig(4) Quality of interpersonal relationships based on the model, have been prioritized in the following figure. The first priority, these relationships are based on the Satisfaction, the highest quality have been obtained sequence 1. professional relationship 2.community relationship , 3.personal relationship. If you want to have more Satisfaction in interpersonal relationships use of professional relationship.

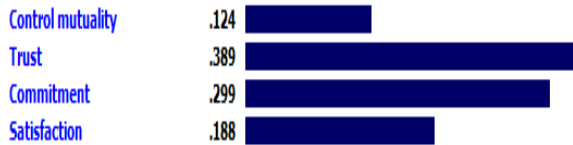


Fig. 5. Prioritize Quality interpersonal relationships based on Commitment

Prioritize Quality interpersonal relationships based on outcomes

Thus, If you're looking for a quality of organizational relationships based on relationships that has the highest quality to order. In order to achieve the highest quality in the entire organization . in fig 7. We show that the best interpersonal relationships is professional relationships and has the most Quality.

Discussion

The relative interpretability of the different transformational leadership dimensions explains the differential predictions of idealized influence (behavior), inspirational motivation, and individualized consideration for quality of EORs (see Van den Bos, Lind, Vermunt, & Wilke, 1997). Compared to interpreting the ability of their supervisors to motivate them to accomplish a common vision and get them committed to it, it may be easier and more direct for employees to perceive how much their immediate supervisors care about their individual needs and attend to their unique potentials and aspirations. Therefore, this study identified a statistically significant positive relationship between individualized consideration and quality of EORs.

The significant negative association between time-based work–life conflict and quality of EORs is consistent with what was hypothesized theoretically. It is worthwhile to speculate about why strain-based work–life conflict had a much weaker effect upon quality of EORs. Attribution theory (Brockner & Wiesenfeld, 1996) suggests that employees may view their behaviors as either internally driven or externally motivated. When employees perceive their jobs challenging but ultimately rewarding, they may devote great effort to their jobs and therefore can easily feel stressed out when the amount of work is great and the job requirements are demanding. Nevertheless, facing such a great strain-based interference between work and nonwork , employees might hold themselves rather than their organizations responsible, especially when they are internally motivated to work hard and achieve a lot at work (Folger & Cropanzano, 1998). Another possible interpretation is that time- based work–life conflict is a relatively more tangible measure in terms of whether

an organization has taken too much out of its employees' personal life.

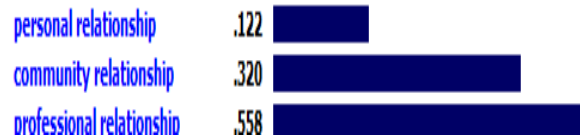


Fig. 6. Prioritize Quality interpersonal relationships based on Satisfaction



Fig. 7. Prioritize Quality interpersonal relationships based on outcomes

Relationship management theory holds that organization–public relationships can be analyzed by relationship types (personal, community, and professional) and by the actors in the relationship. relationship management which holds that the continuation of the organization and public relationship depends on the degree to which expectations are met. everyone who is employed in any capacity by organization is in a position of authority over customer and must not abuse that authority in any way to initiate or develop a close personal relationship with a customer. It is an obligation on all members of staff and employees to ensure that their behavior is beyond reproach. In the event that a close personal relationship develops between members of staff, it is incumbent on those concerned to ensure that the essential standards of professionalism and impartiality are maintained. Where such a personal relationship exists, the members of staff must inform their Head(s) of organization, so that considerations can be made to avoid situations, which may prejudice professionalism and integrity.

References

5. Jiang H,(2011),"A model of work–life conflict and quality of employee–organization relationships (EORs): Transformational leadership, procedural justice, and family-supportive workplace initiatives ", Public Relations Review ,PUBREL-978; No. of Pages 15.

6. Hung C.F,Chen Y.R,(2009),"Types and dimensions of organization–public relationships in greater China", Hong Kong Baptist University, Kowloon Tong, Hong Kong, *Public Relations Review* (35)181–186
7. Ledingham, J. A. (2003). Explicating relationship management as a general theory of public relations. *Journal of Public Relations Research*, 15, 181–198.
8. Huang, Y.-H. (2001). OPRA: A cross-cultural multiple-item scale for measuring organization–public relationships. *Journal of Public Relations Research*, 13, 61–90.
9. Hon, L. C., & Grunig, J. E. (1999). Guidelines for measuring relationships in public relations . Gainesville, FL: Institution for Public Relations.
10. Hornung, S., Rousseau, D. M., & Glaser, J. (2008). Creating flexible work arrangements through idiosyncratic deals. *Journal of Applied Psychology*, 93, 655–664.
11. McCown, N. (2007). The role of public relations with internal activists. *Journal of Public Relations Research*, 19, 47–68.
12. Freitag, A. R., & Picherit-Duthler, G. (2004). Employee benefits communication: Proposing a PR-HR cooperative approach. *Public Relation Review*, 30, 475–482.
13. Kim, H.-S. (2007). A multilevel study of antecedents and a mediator of employee–organization relationships. *Journal of Public Relations Research*, 19, 167–197.
14. Mills, J., & Clark, M. S. (1982). Communal and exchange relationships. *Review of Personality and Social Psychology* , 3, 121–144
15. Mills, J., & Clark, M. S. (1986). Communications that should lead to perceived exploitation in communal and exchange relationships.*Journal of Social and Clinical Psychology* , 4, 225–234
16. Mills, J., & Clark, M. S. (1994). Communal and exchange relationships: Controversies and research. In R. Erber, & R. Gilmour (Eds.), *Theoretical Frameworks for personal relationships* . Hillsdale, NJ: Lawrence Erlbaum Associations, pp. 29–42
18. Jo, S. (2006). Measurement of organization–public relationships: validation of measurement using a manufacturer relationship. *Journal of Public Relations Research*, 18(3), 225–248.
19. Hon, L., & Grunig, J. E. (1999). Guidelines for measuring relationships in public relations . The Institute for Public Relations.
20. Hung, C. J. F. (2002).The interplays of relationship types , relationship cultivation , and relationship outcomes: How multinational and Taiwanese companies practice public relations and organization–public relationship management in China . Unpublished doctoral dissertation, University of Maryland, College Park.
22. Hung, L., & Grunig, J. E. (2003 October). How to develop a quality relationship?: Types of relationships and their affects on relationship cultivation strategies.
23. In Paper presented at the Educator’s Academy of the Annual Conference of Public Relations Society of America New Orleans, LA.
24. Hung, C. J. F. (2005). Exploring types of organization–public relationships and their implication for relationship management in public relations. *Journal of Public Relations Research*, 17, 393–426.
25. Clark, M. S. (1984). Record keeping in two types of relationships. *Journal of Personality and Social Psychology* , 47, 549–557.
26. Clark, M., & Mills, J. (1979). Interpersonal attraction in exchange and communal relationships. *Journal of Personality and Social Psychology* , 37, 12–24.
27. Clark, M. S., & Mills, J. (1993). The difference between communal and exchange relationships: What it is and is not. *Personality and Social Psychology Bulletin* , 19, 684–691.
28. Clark, M. S., Mills, J., & Corcoran, D. (1989). Keeping track of needs in communal and exchange relationships.*Journal of Personality and Social Psychology* , 51, 333–338.
29. Clark, M. S., Ouellette, R Powell, M. C., & Milberg, S. (1987). Recipient’s mood, relationship type, and helping.*Journal of Personality, and Social Psychology* , 53, 94–113.
30. Clark, M. S., Powell, M. C., & Mills, J. (1986). Keeping track of needs in communal and exchange relationships.*Journal of Personality and Social Psychology* , 51, 333–338.
31. Clark, M. S., & Taraban, C. B. (1991). Reactions to and willingness to express emotions in communal and exchange relationships.*Journal of Experimental Social Psychology*, 27, 324–336.
32. Clark, M. S., & Waddell, B. (1985). Perception of exploitation in communal and exchange relationships. *Journal of Social and Personal Relationships* , 2, 403–413.
33. Luo, Y. (2001). Toward a cooperative view of MNC–host government relations: Building blocks and performance implications. *Journal of International Business Studies*, 32, 401–419.
34. Luo, Y. (2002). *Multinational enterprises in emerging markets*. Copenhagen, Denmark: Copenhagen Business School Press
35. Reynolds, J. (2005). In the face of conflict: Work–life conflict and desired work hour

- adjustments. *Journal of Marriage and Family*, 67, 1313–1331
36. Pleck, J. H., Staines, G. L., & Lang, L. (1980). Conflicts between work and family life. *Monthly Labor Review*, 103(3), 29–32
37. Grant-Vallonea, E. J., & Ensherb, E. A. (2001). An examination of work and personal life conflict, organizational support, and employee health among international expatriates. *International Journal of Intercultural Relations*, 25, 261–278
38. Bass, B. M., & Avolio, B. J. (2004). *Multifactor leadership questionnaire: Manual and sampler set* (3rd ed.). Palo Alto, CA: Mindgarden.
39. Lapierre, L. M., & Allen, T. D. (2006). Work-supportive family, family-supportive supervision, use of organizational benefits, and problem-focused coping:
40. Implications for work–family conflict and employee well-being. *Journal of Occupational*
41. Wadsworth, L. L., & Owens, B. P. (2007, January/February). The effects of social support on work–family enhancement and work–family conflict in the public
42. Jacqueline A-M. Coyle-Shapiro, Lynn M. Shore (2007), "The employee–organization relationship: Where do we go from here?", *Human Resource Management Review* 17 (2007) 166 – 179
43. Bruning S.D, Dials M, Shirka A,(2008),"Using dialogue to build organization–public relationships, engage publics, and positively affect organizational outcomes", *Public Relations Review* 34 (2008) 25–31
44. Banning . S.B, Schoen.M(2007), " Maximizing public relations with the organization–public relationship scale: Measuring a public’s perception of an art museum", *Public Relations Review* 33 (2007) 437–439
45. Ledingham, J. A., & Bruning, S. D. (1998). Relationship management and public relations: Dimensions of an organization-public relationship. *Public Relations Review* , 24, 55–65
46. Bruning, S. D., & Galloway, T. (2002, May). Expanding the organization-public relationship scale: Exploring the role that structural and personal commitment play in organization-public relationships. *Public Relations Review* , 29, 309–319.
47. Jakol, D.S (2011)"Good Volunteer-Professional Relationships: A Strategic Issue for Professionals", available in scouting.org/filestore/commissioner/pdf/513-145.pdf
48. Nokava (2010), <http://www.professional-resumes.com/build-a-strong-professional-relationship-with-your-employer.html>
49. Gallicano,T.D , (2008), "Personal Relationship Strategies and the Outcomes of Personal Relationships in a Multi-Tiered Membership Organization " ,School of Journalism and Communication ,University of Oregon
50. Toth, E. L. (2000). From personal influence to interpersonal influence: A model for relationship management. In J. A. Ledingham & S. D. Bruning (Eds.), *Public relations as relationship management: A relational approach to the study and practice of public relations* (pp. 205-219). Mahwah, NJ: Erlbaum.
51. Broom, G. M., Casey, S., & Ritchey, J. (2000). Concept and theory of organization- public relationships. In J. A. Ledingham & S. D. Bruning (Eds.), *Public relations as relationship management: A relational approach to the study and practice of public relations* (pp. 3-22). Mahwah, NJ: Erlbaum.
52. Grunig, J. E., & Huang, Y.-H. (2000). From organizational effectiveness to relationship indicators: Antecedents of relationships, public relations strategies, and relationship outcomes. In J. A. Ledingham & S. D. Bruning (Eds.), *Public relations as relationship management: A relational approach to the study and practice of public relations* (pp. 23-53). Mahwah, NJ: Erlbaum.
53. Huang, Y.-H. (1997). *Public relations strategies, relational outcomes, and conflict management strategies*. Unpublished doctoral dissertation, University of Maryland, College Park.
54. Thomlison, T. D. (2000). An interpersonal primer with implications for public relations. In J. A. Ledingham & S. D. Bruning (Eds.), *Public relations as relationship management: A relational approach to the study and practice of public relations* (pp. 177-203). Mahwah, NJ: Erlbaum.

11/12/2011

Upper Cretaceous Planktonic Foraminiferal Biostratigraphy of East Dorfak Area (Guilan – North of Iran)

Mohammad Modaresnia^{1*}, Khosro Khosrotehrani², Iraj Momeni³, Seyed Ahmad Babazadeh⁴

^{1*}Islamic Azad University – Science and Reserch Branch,Geology department, Tehran, Iran. ²Islamic Azad University – Science and Reserch Branch,Geology.department, Tehran, Iran. ³Shahid Beheshti University– Geology department, Tehran, Iran. ⁴Tehran Payamenour University–Geology department , Tehran , Iran .

Email: Modaresiraza@Yahoo.Com

Abstract: East Dorfak(studied area) are located in Nothern Iran(within Gorgan-Rasht region). The Upper Cretaceous sequence in this region comprises three lithostratigraphic unites (K_2^{SLm} , K_2^1 , K_2^{mL}). Two stratigraphic sections have been investigated in this area and outcrope samples collected in the measured sections. Previous studies have been very sparse and general.Consider of prepared thin sections and analysis the Late Cretaceous planktonic foraminifera content have presented detailed data. Identification of fifty-two index species belonging to the genera Dicarinella, Whitenella, Gansserina, Globotruncana, Globotruncanita, Globotruncanella, Contusotruncana, Macroglobigerinelloides, Marginotruncana, Radotruncana, Rugoglobigerina, Racemiguembelina, Heterohelix, Abathamphalus and Kuglerina has led to the recognition of nine (eight in Gurag section) biostratigraphic zones in this study. The biozones ranged in age from Coniacian to Late Maastrichtian.The Campanian and Early Maastrichtian demonstrated the largest diversity faunal. Sedimentary characteristics and planktonic foraminiferal content illustrated that deposition is done in deep marine environment. Moreover the study showed a little difference in the two sections under study.

[Mohammad Modaresnia, Khosro Khosrotehrani, Iraj Momeni, Seyed Ahmad Babazadeh. **Upper Cretaceous Planktonic Foraminiferal Biostratigraphy of East Dorfak Area (Guilan – North of Iran)**. Life Science Journal 2012; 9(1):242-253] (ISSN: 1097-8135). <http://www.lifesciencesite.com>. 34

Keywords: Planktonic foraminifera; Biozone; Coniacian; Campanian; Maastrichtian; Cretaceous; Biostratigraphy; Iran.

1. Introduction

The area under investigation is situated in Northern Iran, in south eastern part of Guilan province within Alborz zone (Nabavi. M.H 1976). The studied area is located between $50^{\circ} 2'$ to $50^{\circ} 10'$ langitude and $36^{\circ} 47'$ to $36^{\circ} 51'$ latitude (Fig.1). Upper Cretaceous Planktonic foraminifera Of East Dorfak has been rarely studied in previous studies and comprehensive biostratigraphic works were not carried out.

In this paper, the biostratigraphy and micropalaeontology investigation of outcrop samples were collected in the measured sections from East Dorfak Area in the West Gorgan-Rasht Region are presented and discussed.

The aim of this paper is to present Upper Cretaceous biostratigraphic data that allows reconstruction of the micropalaeontology of this region during the Late Cretaceous.

2. Materials and Methods

Eighty-Six closely spaced outcrop samples were collected from two stratigraphic sections that were measured from East Dorfak Area (Fig.1). The samples were taken from medium to thin bedded hemiplegic limestone (K_2^1); and thin to meddium bedded clayey hemiplegic to plagic limestone (K_2^{ml}) and thin to medium bedded arenaceous limestone (K_2^{slm}) of Upper Cretaceous lithostratigraphic unites.

Because it was very difficult to disaggregate the limestones and process them with normal washing,thin sections were prepared and analyzed the planktonic foraminifera.

The position of apertures and presenc of supplementary and accessory structure that have been used to distinguish genera were not identifiable in thin sections (Caron 1985).

However most of the diagnostic criteria, including the size and shape of test, thickness of well, size, number and arrangement of chambers, form and position of aperture and ornamentation such as ridges, spines and position and number of peripheral thickenings or keels, could be recognized in axial and

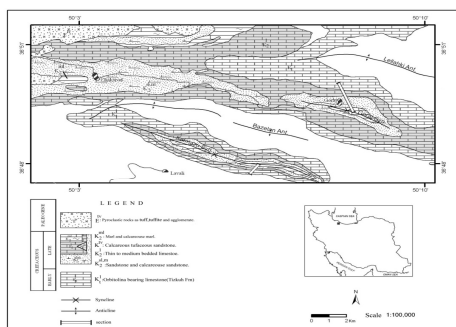


Fig. 1 . Geological map of studied area (East of Dorfak . Guilan . Iran)

subaxial sections (passing through or parallel to the axis of coiling (Sliter, 1989) (Fig.2).

A large number of specimens were encountered in the thin sections, but most of them were of no use for identification, because of partial or oblique cuts through the test. Accordingly axially oriented forms were picked to identify most taxa with a high degree of confidence.

The atlases of the European working group on Cretaceous Planktonic Foraminifera by Robaszynski and Caron (Coordinators 1979) and Robaszynski and others (1984) and the studies of Caron (1985) and Permulisilva and Sliter (1994) were the bases of the identification in this study. In addition Postoma (1971), Wonders (1979), Fleury (1980), Sliter (1989), Robaszynski and others (2000) and Permulisilva and Verga (2004) were usefull references, as they include illustrations of thin sections of Planktonic foraminifera.

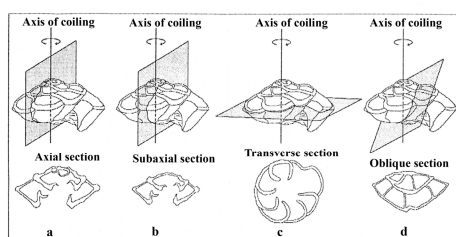


FIGURE 2. Principal sections through a planktonic foraminiferal test. a) Axial section: section passing through the axis of coiling. b) Subaxial section: section passing parallel to the axis of coiling but not passing through the proloculus. c) Transverse section: section passing perpendicular to the axis of coiling. d) Oblique section: section passing neither parallel nor perpendicular to the axis of coiling.

3. Regional Setting

The studied area (East Dorfak) which is approximately 80km long is oriented W-E and extends from East of Dorfak to West of Somamus in the North of Iran at East of Guilan province.

Iran is a part of short section of the Alpine orogenic belt that is located between the Arabian-African block (Gondwana margin) and the Asian Plate (Eurasia margin). It is interpreted as an assemblage of marginal Gondwana fragments that was detached from the Gondwanian-Arabian plate during the Late Palaeozoic (Permian) or Early Triassic (Stocklin, 1977). It was attached to Turanian plate (Eurasia) at the end of Middle or late Triassic (Stocklin, 1974, 1977; Sengor and Kidd, 1979; Wensink and Varekamp, 1980; Soffel and Forster, 1980; Davoudzadeh and Schmidt, 1982).

In the Late Cretaceous, Iran again enjoined with the Gondwanian Afro-Arabian plate, but the ocean area was not completely closed in some parts of Iran (Babazade, 2003). Three major tectonic units (Turanian, Iranian and Arabian plates) recognized by Lensch, et.al (1984) in Iran, are separated from each other by ophiolitic complexes (Stocklin, 1977) (Fig.3). These are subdivided in to smaller elements, such as kopet Dagh, Southern Caspian Sea, Zagros Thrust, Zagros. Folded belt, Alborz Mountain, Central Iran and

etc. Stocklin, 1977; Eftekharnajad, 1980; Alavi 1991; Nog-olsadat, 1993, Aghanabati, 2004).

Alborz in North of Iran and South of Caspian Sea is a great mountain chain that is oriented W-E and extend from Azarbaijan in West to Kopet Dagh in East. It is a part of Alpine-Himalayaian orogenic belt. This mountain is in the vicinity of Great Kavir fault in the east (Berberian, 1976; Nogol, 1977) and is connected to Pamir Mountain in west and is joined with Caucasus from Azarbaijan. Concerning tectonical and stratigraphical characteristics Alborz is subdivided in few subzones just like the: Eastern Alborz and Kopetdagh, Central Alborz; and Western Alborz & Azarbaijan (Stocklin, 1968; Stocklin and Nabavi, 1973; Nabavi, 1976). Central Alborz in width is subdivided in Gorgan-Rasht region and Southern & Western Alborz.

Gorgan-Rasht region the studied area is located in this region is situated between Caspian Sea in the north and Alborz fault in the south. Deposition of calcareous sediments is continued during Jurassic and Cretaceous. In the western part broadly Late Cretaceous volcanic rocks is presented. The Cenozoic is distinguished by absence of Paleocen-Eocen and Oligocen in a great compartment of this region and Miocen Sedimentary rocks directly but unconformable overly Cretaceous rocks. Yet in the studied area Cretaceous sedimentary rocks are covered by Eocen volcano- sediment and volcanic rocks.

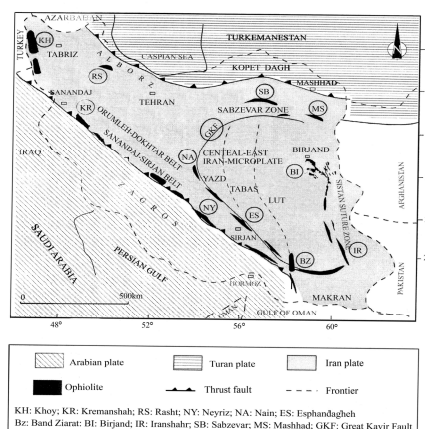


Fig. 3. Modified sketch map of Iran showing the major tectonic units, the inner nucleus and the positions of the main ophiolites (Lensch et al., 1984; Sengor et al., 1988; Stocklin, 1977; Dilek and Dilekoy, 1992; Fohrouz, 2003).

4. Lithology

Most sedimentary outcrops across the Upper Cretaceous in the studied area consist of three microfacies, clastic limestone such as calcareous microconglomerate and calcarenite with varying contents of coarse grains such as quartz and glauconite (up to 15 %) that is deposited in toe of slope, plagic limestone, (Plagic mudstone to wackstone with many intraclasts, (Dunham, 1962)) that deposited in deep

shelf marine and marly limestone to marlstone (Plagic wackstone to packstone, (Dunham, 1962)) include calcareous mud with varying amounts of influx of fine siliceous and mud materials together with planktonic rain that is deposited in a deep sea environment as basin.

All of these microfacies have bioclastic contents of planktonic fauna especially foraminifera.

In the middle part of Firuzkuh section among Upper Cretaceous sedimentary rocks volcanoclastic unite is presented too. In addition, Guraj section is thicker than Firuzkuh section (Fig.4)

4-1 Firuzkuh section

Upper Cretaceous sedimentary rocks in this section had 319m thickness and were subdividable into three parts:

The lower part with 131.5m thickness included an alternation of varying color and bedding fine grain limestone (Plagic mudstone to wackstone; Dunham, 1962) with a few chert nodules, (K₂¹). The middle part with 19.5m thickness included medium layer light calcareous tuffaceous sandstone, (K₂^{iv}). The upper part with 168m thickness included medium layer light marly limestone to marlstone (Plagic wackstone to packstone; (Dunham, 1962)), to upward chert nodules and two chert laminate were presented in this part, (K₂^{ml}).

In this section Upper Cretaceous sedimentary rocks covered Tizkuh Formation (Lower Cretaceous) with low angle angular unconformity, and Upper Cretaceous rocks were presented in a syncline core. For this reason upper boundary is uncertain, but in the west and north of Chakrud (South Malakut- North of studied area) is contacted with Paleogen volcanic and volcanoclastic rocks (Annels; Arthurton; Bazeley & Davis, 1972; in this study, 2010)

subdividable into three parts. The lower part was 47m in thickness and contained alternation of calcarenite and calcareous microconglomerate with variations in color and bedding (K₂^{slm}). The middle part was 367.9m in thickness and contained fine graine limestones of varying colors (Plagic mudstone to wackstone, (Dunham1962)) (K₂¹). The upper part was 64.8m and contained limestone, marly limestone to marlstone. (Plagic wackstone to packstone, (Dunham, 1962)) (K₂^{ml}).

In Guraj section, Upper Cretaceous rocks overlay Tizkuh Formation (Lower Cretaceous). This boundary is a low angle angular unconformity. In this section, Upper Cretaceous rocks are presented in a syncline core for this reason, the upper boundary is uncertain, but in the West and North Chakrud (South Malakut-North of studied area) Upper Cretaceous rocks is contacted with Paleogen volcanic and volcanoclastic rocks (Annels; Arthurton; Bazeley & Davis, 1972, in this study, 2010).

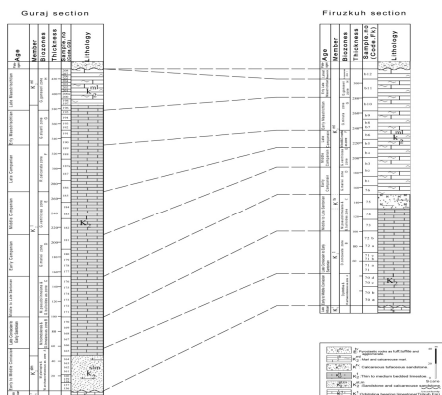


Fig. 4. correlation chart for the two studied section in the East Dorfak .

4-2 Guraj section

In the Guraj section, thickness of Upper Cretaceous sedimentary rocks was 433.3m and was

Age	Member	Biozones	Thickness	Sample no	Lithology
					1.1
					1.2
					1.3
					1.4
					1.5
					1.6
					1.7
					1.8
					1.9
					1.10
					1.11
					1.12
					1.13
					1.14
					1.15
					1.16
					1.17
					1.18
					1.19
					1.20
					1.21
					1.22
					1.23
					1.24
					1.25
					1.26
					1.27
					1.28
					1.29
					1.30
					1.31
					1.32
					1.33
					1.34
					1.35
					1.36
					1.37
					1.38
					1.39
					1.40
					1.41
					1.42
					1.43
					1.44
					1.45
					1.46
					1.47
					1.48
					1.49
					1.50
					1.51
					1.52
					1.53
					1.54
					1.55
					1.56
					1.57
					1.58
					1.59
					1.60
					1.61
					1.62
					1.63
					1.64
					1.65
					1.66
					1.67
					1.68
					1.69
					1.70
					1.71
					1.72
					1.73
					1.74
					1.75
					1.76
					1.77
					1.78
					1.79
					1.80
					1.81
					1.82
					1.83
					1.84
					1.85
					1.86
					1.87
					1.88
					1.89
					1.90
					1.91
					1.92
					1.93
					1.94
					1.95
					1.96
					1.97
					1.98
					1.99
					2.00

5. Biostratigraphy

The Upper Cretaceous sequence is deposited in a deep marine enviroment and it is accurately dated with succession of index planktonic foraminifera.

Moreover the presence of a well preserved index species Globotruncanid assemblage , makes this region is very important for study.

5-1 Zonal subdivisions

The resercher has identified nine biozones based on the occurrence of index planktonic foraminifera in the studied area. (Fig.5 & Fig.6).These biozones are recognized from lower Coniacian to Upper most Maastrichtian in Firuzkuh section (Fig.5) and eight biozones are distinguished in the Guraj section (Fig.6). Identification of specimens is based on microscopic observation of thin sections (Plates, 1 to 4).

The definition of the biozones is given, following the works of Caron (1985) Sliter (1989), Permulsilva and Sliter (1994) Robaszynski and Caron (1995) and Permulsilva and Verga (2004)

1. **Biozone A:** Dicarinnella primitiva and Whiteinella archacocretacea assemblage zone.

Age: Early to Middle coniacian.

Definition: This zone in the two studied sections is a assemblage zone.

Remarks: The diversification of Marginotruncana and presence of two very index Dicarinnella fall within this zone.

In the Firuzkuh section this zone includes: Dicarinnella primitiva (Dalbiez, 1995) Dicarinnella imbricate (Monard, 1950) Whiteinella archacocretacea Pessagno, 1967, Murichohedbergella planispira (Tappan, 1940), Marginotruncana marginata (Reuss, 1850), Marginotruncana pseudolinneiana Pessagno, 1967, Marginotruncana coronata (Bolli, 1945).

This zone in the Guraj section is called Murichohedbergella planispira and Whiteinella archacocretacea assemblage zone and includes: M.planispira, Heterohelix globulosa (Ehrenberg, 1840), Macroglobigerinelloides bolli (Pessagno, 1967), and M. pseudolinneiana.

2. **Biozone B:** Dicarinnella concavata zone.

Age: Late Coniacian to Early Santonian

Definition: Interval zone between first occurrence (FO) of Contusotruncana fornicata (Plummer, 1931) and last occurrence, (LO) of Dicarinnella concavata, (Brotzen 1934). Remarks: This zone contains the last occurrence (LO) of Murichohedbergella simplex (Morrow, 1934), first occurrence (FO) of Globotruncana lapparenti Brotzen, 1936, and first occurrence (FO) of Murichohedbergella holmdolensis (Olsson, 1964). In this zone the dominant taxa belong to the genera Marginotruncana (e.g. M.pseudolinneiana, M.marginata, M.coronata) and Murichohedbergella, (e.g. M. planispira, and M. holmdolensis).

The species Dicarinnella assymetrica (Sigal, 1952) and D. concavata exist but are rare.

In Firuzkuh section, this zone includes: Archacoglobigerina cretacea (d'Orbigny, 1840), H.globulosa, Loeblichella hessi, (Pessagno, 1962). Equivalent this zone in Guraj section is recognized as M. holmdolensis and Globotruncana linneiana zone. This zone is characterized by the presence of first occurrence (FO) of C. fornicata and first occurrence (FO) of G. linneiana.

This zone in Guraj section is called Murichohedbergella holmdolensis and Globotruncana linneiana assemblage zone and contains, first occurrence (FO) of G. lapparenti, first occurrence (FO) of G.linneiana and first occurrence (FO) of M.

holmdolensis, and includes: M. planispira, H. globulosa, M. pseudolinneiana, M. bolli.

3. **Biozone C:** Marginotruncana pseudolinneiana and Globotruncana bulloides assemblage zone.

Age: Middle to Late Santonian.

Definition: This zone is characterized by the assemblage of first occurrence (FO) of Globotruncana bulloides Vogler, 1941 and last occurrence (LO) of M.pseudolinneiana and in the Firuzkuh section includes: H. globulosa, M. bolli, A. cretacea, C. fornicata, M.holmdolensis too.

Remarks: In this zone, the dominant taxa belongs to the genus, Globotruncana (e.g. G.bulloides, G.linneiana, G. lapparenti) and so this zone contains last occurrence (LO) of M.planispira, and M.coronata and first occurrence (FO) of Globotruncana hilli (Pessagno, 1967).

In the Firuzkuh section, upper part of biozone consists of 19.5m tuffaceous calcareous sandstone (K₂^{IV}) does not exist any fossils.

In the Guraj section from bed nos. C G 171 to C G 176, this assemblage zone contains first occurrence (FO) of G. bulloides and last occurrence (LO) of M.pseudolinneiana, and so includes: M. planispira, L. hessi, H. globulosa, A. cretacea, C. fornicata, M. holmdolensis, G. lapparenti, G.linneiana.

4. **Biozone D:** Globotruncana mariei zone.

Age: Early Campanian.

Definition: Interval zone between first occurrence (FO) of Globotruncana mariei (Banner & Blow, 1960) and first occurrence (FO) of Rugoglobigerina rugosa (Plummer, 1926).

Remarks: In this zone, dominant taxa are from genus Globotruncana (e.g. Globotruncana lapparenti, Globotruncana linneiana, Globotruncana bulloides and Globotruncana hilli) and so this zone in Firuzkuh section includes: C.fornicata, M. holmdolensis, H. globulosa, M.bolli, A.cretacea,

In the Guraj section, from bed nos. C G 177 to C G 181 this interval zone is between first Occurrence (FO) of Globotruncana stuartiformis (Dalbiez, 1955) and first Occurrence (FO) of R. rugosa. This zone in Guraj section and so contains first Occurrence (FO) of G. hilli and first Occurrence (FO) of G. mariei, and includes: M. planispira, C. fornicata, G. arca, M. holmdolensis, G.lapparenti, G. linneiana, G. bulloides.

5. **Biozone E:** Globotruncana ventricosa zone.

Age: Middle Campanian.

Definition: Interval zone between first occurrence (FO) of Globotruncana ventricosa White, 1928, and first occurrence (FO) of Murichohedbergella monmothensis (Olsson, 1960).

Remarks: This zone contains first occurrence (FO) of Macroglobigerinelloides prairihilensis (Pessagno 1967), first occurrence (FO) of Globotruncana rosetta (Carsey, 1926) and first occurrence (FO) of

Macroglobigerinelloides alvarezii (Eternod Olvera 1959). In this zone, dominant taxa belongs to the genus *Globotruncana* (e.g. *G. linneiana*, *G. hilli*, *G. bulloides*, *G. mariei* and *G. lapparenti*) and so this zone in Firuzkuh section includes: *M. holmdolensis* and *R. rugosa*.

In the Guraj section it is interval zone between first occurrence (FO) of *G. ventricosa* and first occurrence (FO) of *M. alvarezii*. In this section first occurrence (FO) of *G. rosetta* is presented and dominant taxa are from genus *Globotruncana* (e.g. *G. linneiana*, *G. lapparenti*, *G. hilli* and *G. bulloides*) and so this zone in Guraj section includes: *M. holmdolensis*, *M. bolli*, *C. fornicata*, *R. rugosa*.

Faunal diversity and frequency in Guraj section is more than Firuzkuh section in this zone.

6. Biozone F: *Macroglobigerinelloides bolli* and *Globotruncana rosetta* assemblage zone.

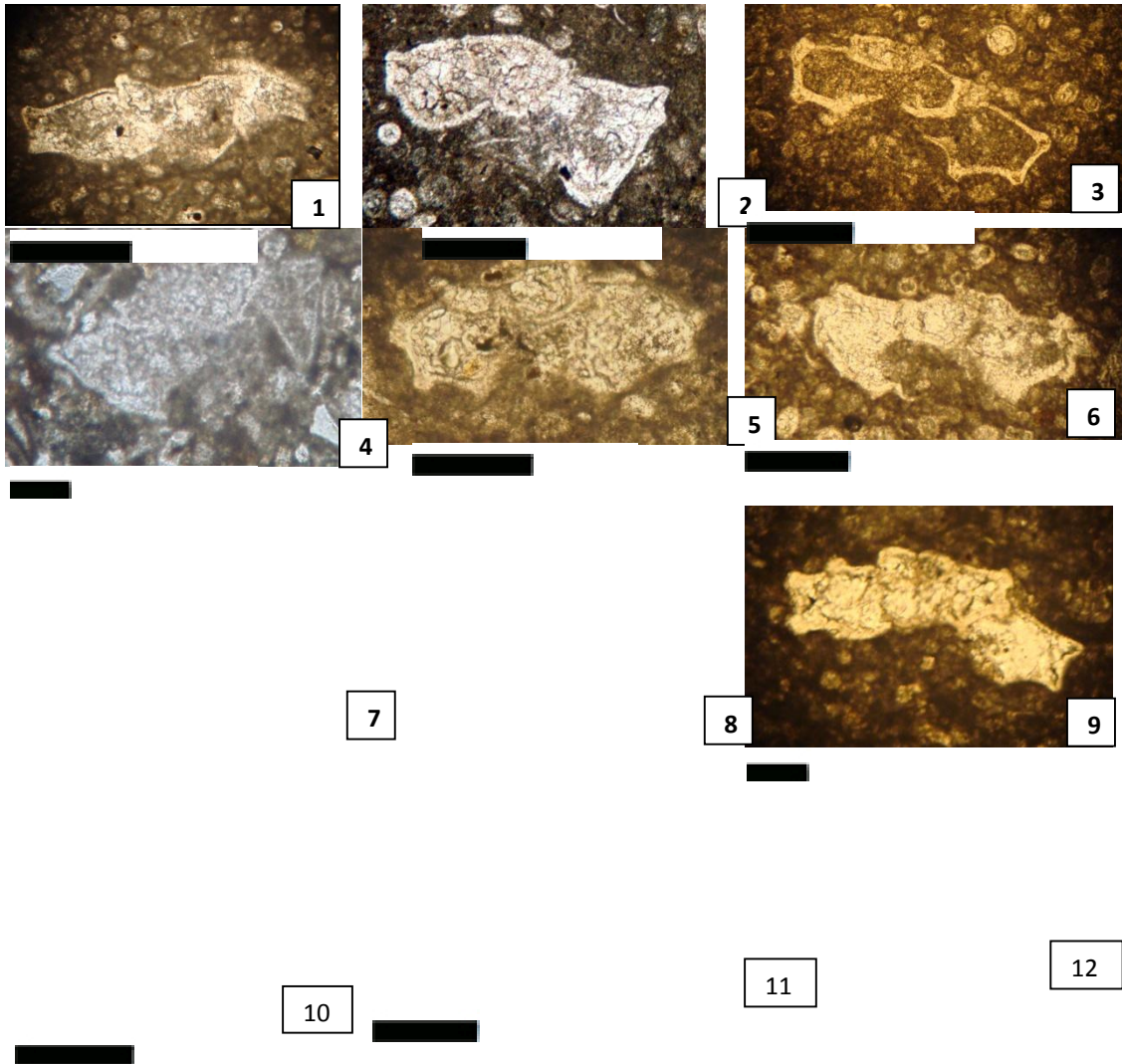
Age: Late Campanian.

Definition: This zone in Firuzkuh section is assemblage zone, includes: *G. rosetta*, *H. globulosa*, *A. cretacea*, *C. fornicata*, *M. holmdolensis*, *G. lapparenti*, *G. linneiana*, *G. bulloides* and *R. rugosa*. first occurrence of *M. prairihilensis* and last occurrence of *M. bolli* are presented in this zone.

Remarks: In the Firuzkuh section dominant taxa are belong to genus *Globotruncana* (e.g. *G. lapparenti*, *G. linneiana*, *G. bulloides*).

In the Guraj section this zone has been called *Radotruncana calcarata* zone.

Plate 1



13

14

15

Plate 1

1. *Marginotruncana coronata* (Bolli 1945), FK 7od, Middle Turonian–Early Campanian ×, 100. 2. *Dicarinella asymetrica* (Sigal 1952), FK 72a, Latest Coniacian–Earliest Campanian, ×, 80. 3. *Globotruncana linneiana* (d’Orbigny 1939), FK74, Santonian- Beginning of Late Maastrichtian, × 80. 4. *Globotruncanita peterssi* (Gondolfi 1955), CG198, Maastrichtian ×60. 5. *Marginotruncana marginata* (Reuss 1845), FK 71b, Late Turonian- Santonian, ×100. 6. *Dicarinella concavata* (Brotzen1934), FK 71b, Coniacian–Santonian, ×80. 7. *Murichohedbergella holmdolensis* (Olsson1964), CG 169, Coniacian- Maastrichtian to Paleocen, ×120. 8. *Murichohedbergella simplex*(Morrow1934), FK 73, Middle Albian, Early Santonian , ×200. 9. *Marginotruncana pseudolinneiana* Pessagno 1967, CG 173, Middle Turonian- Early Campanian, ×60. 10. *Kuglerina rotundata* (Broennimann 1952), bFK8, Latest Campanian- Maastrichtian, ×100. 11. *Dicarinella imbricate* (Monrod,1950), FK70d, Turonian- Coniacian, ×80. 12. *Loblichella hessi* (Pessagno 1962), CG176, Middle Albian- Turonian to Early Maastrichtian, ×120. 13. *Rugoglobigerina rugosa* (Plummer,1926), CG195, Campanian- Maastrichtian, ×100. 14. *Dicarinella primitiva*(Dalbiez 1955), CG176, Coniacian – Beginning of Santonian, ×80. 15. *Globotruncana hilli* (Pessagno 1967), CG182, Late Santonian- Maastrichtian ×160.

Plate 2

1

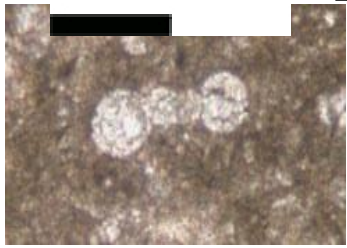
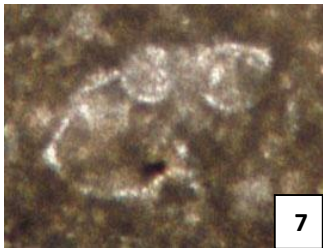
2

3

4

5

6



8

9

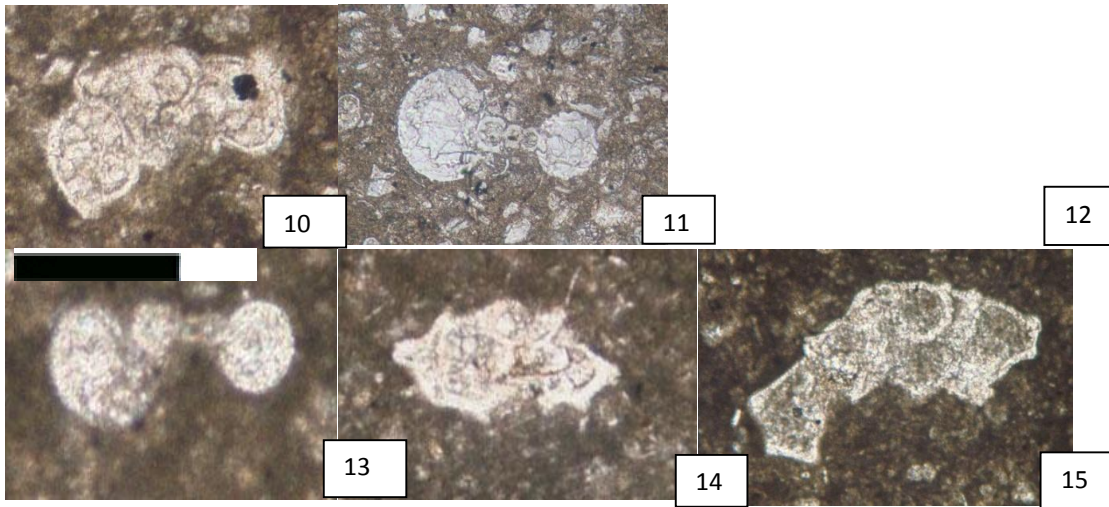
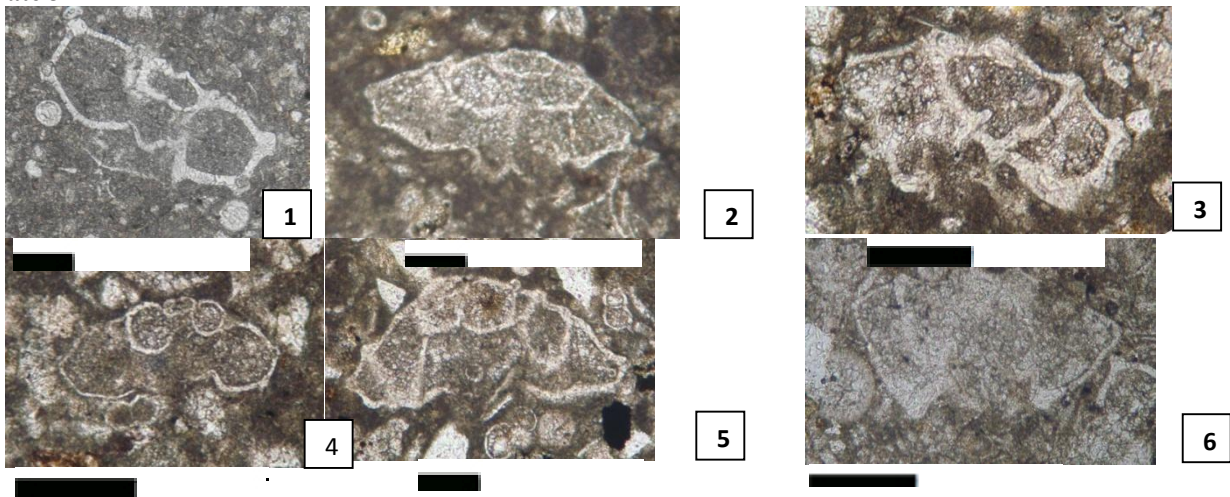
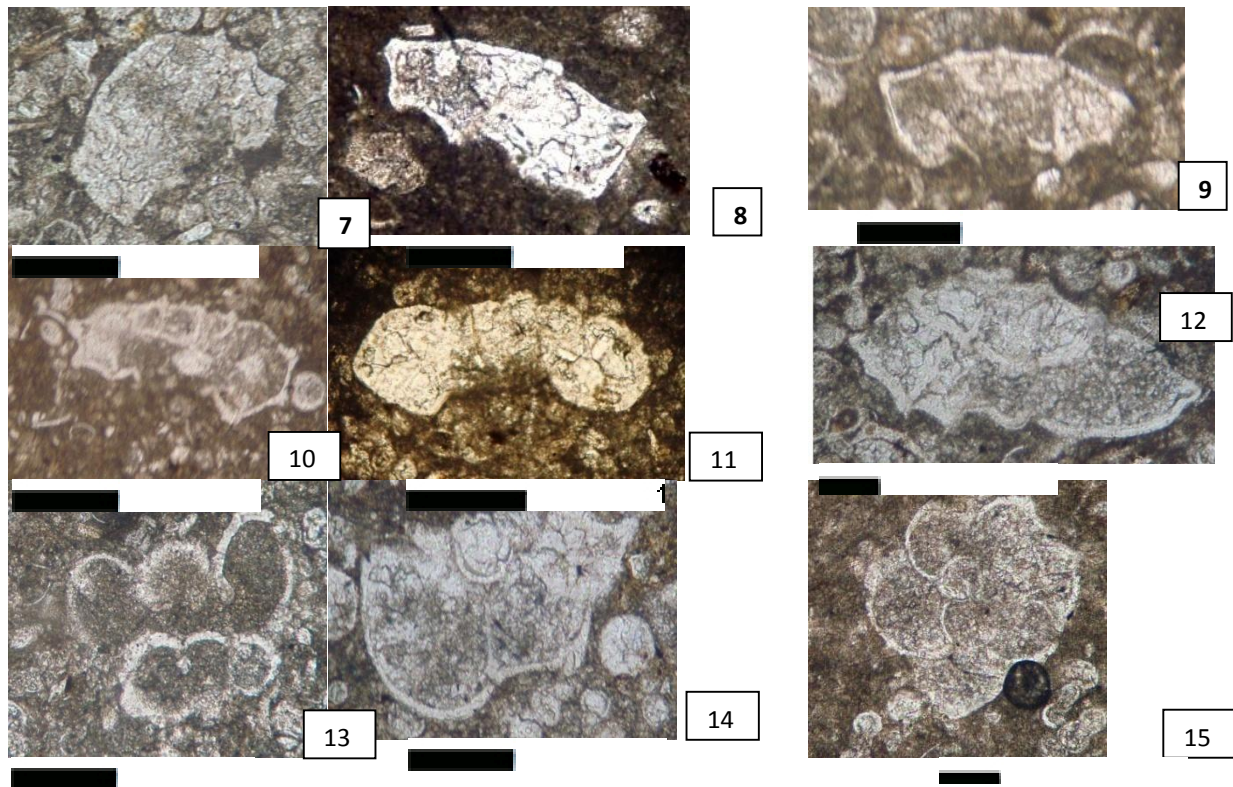


Plate 2

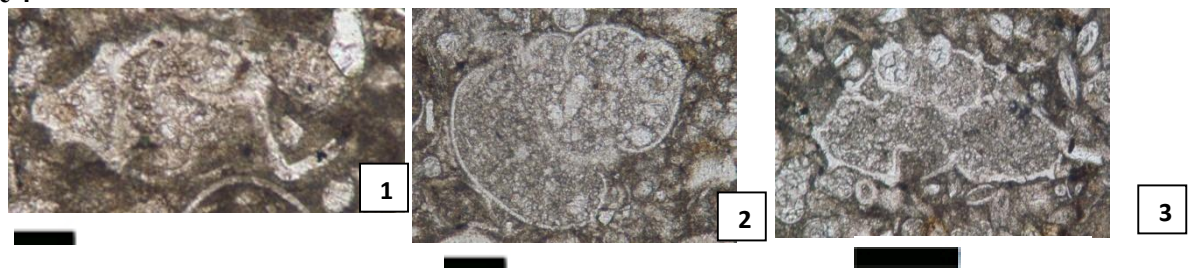
Rugotruncana aff subciromnodifer (Gandolfi1955), CG191, Late Campanian - Late Maastrichtian, X100. 2- Contusotruncana plummerae (Gandolfi1955), CG207, Late Campanian-Late Maastrichtian, X120.3. Globotruncanita stuarti (deLapparent 1918), CG192, Late Campanian-Maastrichtian, X 60.4. Macroglobigerinelloides bolli (Pessagno 1967), CG208, Coniacian-earliest Maastrichtian, X 120.5- Rugoglobigerina pennyi Broennimann 1952, bFK9, Late Campanian- Maastrichtian, X100.6- Globotruncana aegyptiaca Nakkady 1950 bFK12, Late Campanian –Maastrichtian, X80.7- Globotruncanella cf minuta Caron & Gonzalez Donoso 1984, CG189, Campanian- Maastrichtian, X160. 8- Macroglobigerinelloides messinae (Broennimann 1952), CG191, Campanian- Maastrichtian, X200. 9- Murichohedbergella aff monmouthensis (Olsson 1960), bFK, Middle Campanian- Maastrichtian to Paleocen, X200. 10- Globotruncanella havanensis (Voorwijk 1937), CG192, Late Campanian, Maastrichtian, X140. 11- Macroglobigerinelloides prairihilensis (Pessagno 1967), bFK9, Santonian – Late Maastrichtian, X120. 12- Macroglobigerinelloides subcarinatus (Bronnimann 1952) CG194, Latest coniacian- Maastrichtian, X200. 13- Murichohedbergella planispira (Tappan1940), CG167, Albian – Early Campanian, X200.14. Globotruncana mariei (d'Orbigny1839), CG194, Campanian- Late Maastrichtian, X160.15-Contusotruncana fornicata (Plummer 1931) CG194, Santonian-Middle Maastrichtian X80.

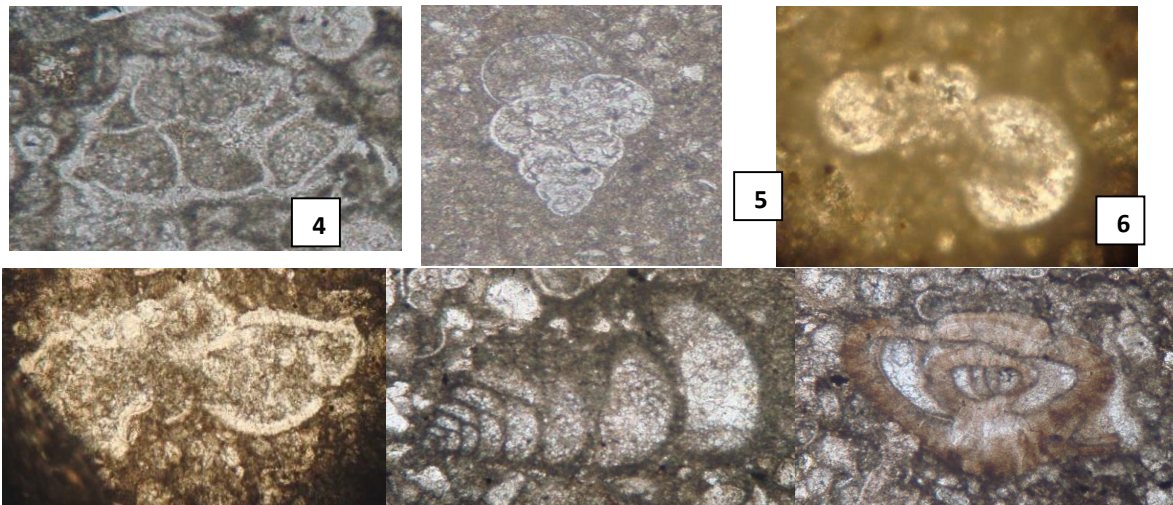
Plate 3



**Plate 3**

1- *Albathamphalus mayaronesis* (Bolli 1951), bFK12, Late Maastrichtian, X60. 2- *Globotruncana arca* (Cushman 1926), CG196, Middle Santonian- Maastrichtian, X60. 3- *Globotruncana ventricosa* White 1928, CG196, Middle Campanian- Middle Maastrichtian, X80. 4- *Archaeoglobigerina cretacea* (d'Orbigny 1840), CG196, Coniacian- Early Maastrichtian, X100. 5- *Contusotruncana contusa* (Cushman 1926) CG196, Late Maastrichtian, X60. 6- *Globotruncana dupeublei*, Caron et al. 1984, CG204, Latest Campanian- Maastrichtian, X80. 7- *Contusotruncana walfishensis* (Todd 1970), CG197, Latest Campanian- Maastrichtian, X80. 8- *Globotruncana lpparenti*, Brotzen 1936, Late Coniacian- Early Maastrichtian, X80. 9- *Globotruncana rosetta* (Carsey 1926), CG200, Middle Campanian- Maastrichtian, X80. 10- *Globotruncana bulloides* Vogler 1941, CG184, Latest Santonian- Middle Maastrichtian, X80. 11- *Whitienella archaeocretacea* Pessagno 1967, FK70b, Turonian- Middle Coniacian, X100. 12- *Globotruncana falsostuarti* Sigal 1952, CG189, Latest Campanian- Maastrichtian, X60. 13- *Racemigumembelina froctiosa*, Egger 1902, CG196, Late Maastrichtian, X80. 14- *Gansserina gansseri* (Bolli 1951) CG208, Late Maastrichtian, X80. 15. *Radotruncana calcarata* (Cushman 1927) CG186, Late Campanian, X60.

Plate 4

**Plate 4**

1- *Globotruncanita stuartiformis* (Dalbiez 1955), CG200, Campanian- Maastrichtian, X60. 2- *Rugoglobigerina macrocephala* Broennimann, 1952, Late Campanian- Maastrichtian, X60. 3- *Contusotruncana patelliformis* (Gandolfi, 1955), CG202, Middle Campanian- Late Maastrichtian, X80. 4- *Globotruncanita conica* (White 1928) CG201, Late Maastrichtian, X80. 5- *Heterohelix globulosa* (Ehrenberg 1840), CG188, Middle Turonian- Maastrichtian, X100. 6- *Murichohedbergella delroensis* (Carsey 1926) FK70b, Albian- Coniacian X140. 7- *Marginotruncana sigali* (Reichel, 1950), FK70d, Middle Turonian- Early Santonian X80. 8- *Laffiteina cf. marsicana* (Farinacci 1976), CG 205, Late Maastrichtian, X20. 9- *Marsonella oxycona* Reuss 1960, Early to Late Cretaceous, X20. 10- *Lenticulina* sp

Scale bar:**7. Biozone G** (in the Guraj section): *Radotruncana calcarata* zone.

Age: Late Campanian.

Definition: Interval zone between first occurrence (FO) of *Radotruncana calcarata* (Cushman, 1927) and first occurrence (FO) of *Globotruncanita stuarti* (de Laparent, 1918).

Remarks: In the Guraj section, this zone contains first occurrence (FO) of *Murichohedbergella monmothensis* (Olsson, 1960), first occurrence (FO) of *Rugoglobigerina macrocephala* Bronnimann, 1952, dominant taxa is from genera *Globotruncana* (e.g. *G. lapparenti*, *G. linneiana*, *G. bulloides*, *G. hilli*, *G. mariei*) and *Rugoglobigerina* (e.g. *R. rugosa*, *R. macrocephala*) and so, this zone in Guraj section includes: *L. hessi*, *H. globulosa*, *M. bolli*, *Globotruncana dupeblei*, *C. fornicata*, *M. alvarezii*, *M. holmdolensis*, *M. prairihilensis*.

8. Biozone H: *Globotruncanella minuta* zone.

Age: Early Maastrichtian.

Definition: Interval zone between first occurrence (FO) of *Globotruncanella minuta* Caron & Gozalez Donoso,

1984 and first occurrence (FO) of *Gansserina gansseri* (Bolli, 1951).

Remarks: This zone is characterized by the presence of *G. minuta*, *Kuglerina rotundata* (Bronnimann, 1952), *G. linneiana*, *G. arca*, *G. hilli*, *G. rosetta* and *M. monmothensis*.

In this zone dominant genus is *Globotruncana* (e.g. *G. linneiana*, *G. hilli*, *G. arca*, *G. rosetta* and *G. ventricosa*), last occurrence (LO) of *M. prairihilensis* and last occurrence of *Globotruncana lapparenti* is fall within this zone too.

This zone in Firuzkuh Section includes: *M. alvarezii*. And hence this zone in Guraj Section is called *Globotruncanita stuarti* zone that is interval zone between first occurrence (FO) of *G. stuarti* and first occurrence (FO) of *Globotruncanita conica* (White, 1928). This zone characterized by dominance of genus *Globotruncana* (e.g. *G. linneiana*, *G. arca*, *G. bulloides*, *G. hilli*, *G. mariei*, *G. ventricosa*, *G. rosetta*, *Globotruncana falsostuarti* Sigal, 1952 and *Globotruncana aegyptiaca* (Nakkady, 1950) and presence of *Contusotruncana patelliformis* (Gandolfi, 1955), *Contusotruncana plummerae* (Gandolfi, 1955)

,*M.monmothensis*, *M.holmolensis*, *Rugotruncana subcircumfer* (Gondolfi, 1955), *Globotruncanella havanensis* (Voorwijk, 1937), *R.macrocephala*, *G.falsostuarti*, *M.alvarezi* and *G.aegyptiaca* is seen in this zone too.

9. Biozone I: *Gansserina gansseri* zone.

Age: Early late Maastrichtian.

Definition: First occurrence (FO) of *G. gansseri* and first occurrence (FO) of *Contusotruncanacontusa* (Cushman, 1926) is fall within this zone.

Remarks: This zone in Firuzkuh section, is characterized by the disappearance of *G.linneiana*, *G. ventricosa* and *G. mariei* in the upper layer of section.

In this zone, dominant genus is *Globotruncana* (e.g. *G. linneiana*, *G. arca*, *G. bulloides*, *G. hilli*, *G. mariei*, *G. falsostuarti*, *G. rosetta*, *G. aegyptiaca*) and so includes: *H.globulosa*, *M.holmdolensis*, *R. rugosa*, *M. monmothensis*, *M. alvarezi*, *Racemiguembelina froctiosa* (Egger, 1902), *C. contusa*.

This zone in Guraj section represents diversity and has different characteristics from Firuzkuh section.

Last occurrence (LO) of *G.lapparenti*, last occurrence (LO) of *C. fornicata* and *M. prairihilensis* is observed in the beginning of this zone, and last occurrence (LO) of *G. ventricosa* in the middle part of this zone confirms that this zone in Guraj section has moved to the upper most of Maastrichtian.

Dominant genus in this zone in Guraj section is from *Globotruncana* (e.g. *G. linneiana*, *G. arca*, *G. bulloides*, *G. hilli*, *G. ventricosa*, *G. rosetta* and *G. falsostuarti*) and so, this zone in Guraj section includes: *H.globulosa*, *M.holmdolensis*, *G. stuartiformis*, *R.rugosa*, *C.patelliformis*, *C.plammerae*, *G.stuarti*, *M.monmothensis*, *R. macrocephala*, *Globotruncanitapeterssi* (Gandolfi, 1955), *G. havanensis*, *R. froctiosa*.

Further more, *Laffiteina mariosoni* is observed in this zone too.

10. Biozone JI: *Abathamphalus mayaroensis* zone.

Age: Latest Maastrichtian.

Definition: This zone in Firuzkuh section contain bed no bFk₁₂ at the top of section. Presence of first occurrence (Fo) of *Abathamphalusmayaroensis* (Bolli, 1951) and first occurrence of *R. froctiosa* are seen in this zone.

Remarks: This zone is not present in Guraj section and in the Firuzkuh section includes: *G. mariei*, *G. aegyptiaca*, *M. monmothensis*, *M. holmdolensis*, *M. alvarezi*, *G. gansseri*, *R. rugosa*.

The *Lenticulina* sp, *Oligosteginid* species such as *Calcisphaerula inominata lata* and *Pitonella ovalis* and so *Textularid* forms such as *Marsonella oxycona* and *Minoxia* sp have been seen in many samples in some part of two section.

Conclusions:

Planktonic foraminifera assemblage of Upper Cretaceous sedimentary rocks of studied area has been analyzed in detail and the following conclusions have been drawn:

1. Fifty-eight planktonic species belonging to twenty genera have yielded nine biozones. They are in ascending order: *Dicarinella primitiva* and *Whiteinella archacocretacea* assemblage zone, (Biozone A), *Dicarinella concavata* zone, (Biozone B), *Marginotruncana pseudolinneiana* and *Globotruncana bulloides* assemblage zone, (Biozone C), *Globotruncana marieizone*, (Biozone D) *Globotruncana ventricosa* zone, (Biozone E) *Macroglobigerinelloides bolli* and *Globotruncanarosetta* assemblage zone, (Biozone F) (In the Guraj section this biozone was called *Radotruncanacalcarata* zone) *Globotruncanella minuta* zone (Biozone G) (In the Guraj section this biozone was called *Globotruncanta stuarti* zone), *Gansserina gansseri* zone, (Biozone H) and *Abathamphalus mayaroensis* zone (Biozone I) (This zone was been presented just in Firuzkuh section).

2. The planktonic foraminifera from the Upper Cretaceous of studied area belong to the Tethyan bio province which is characterized by diverse keelled associations rich in thick-walled species. This assemblage is composed of representatives of the genera, *Marginotruncana*, *Dicarinella*, *Globotruncana*, *Globotruncanita*, *Contusotruncana*, *Rugoglobigerina* and etc.

3. The succession of planktonic foraminiferal assemblages in the East Dorfak area shows a continuity of the sedimentation during late cretaceous from coniacian to late Maastrichtian.

4. A distinct unconformity has been identified in lower boundary with Tizkuh formation (Barremian-Albian) This unconformity is here correlated with a major tectonic activity of the Austrian Orogeny.

5. Palaeogen volcanosediment and volcanic rocks overly late Cretaceous sedimentary rocks with unconformable contact. This unconformity is here correlated with a major tectonic activity of the Laramian Orogeny.

Acknowledgments

A part of the field work was supported by Islamic Azad University of Rasht branch, We are gratefully acknowledged for their help during the intense field work. Library works were supported by Islamic Azad University Science and Research Branch we are acknowledged for their helps. H.Babayi are thanked for their constructive editing of this paper.

*** Corresponding Author:**

¹ Mohammad Modaresnia

¹ Department of Geology

Science and Research Branch,

Islamic Azad University, Tehran, Iran.

Email: Modaresiraza@Yahoo.Com

References:

- Babazadeh, S.A. 2006. New biostratigraphic data from Cretaceous planktic foraminifera in Sahlabad province, eastern Iran.
- Carsey, D.O., 1926, Foraminifera of the Cretaceous of Central Texas: Texas University Bulletin, no. 26122, p. 1-56.
- Chungkham, P., and Caron, M., 1996, Comparative study of a Late Maastrichtian (A. mayaroensis zone) foraminiferal assemblage from two distant parts of the Tethys Ocean: Semsales Wildflysch Zone, Switzerland and Ukhrl Melange Zone, India: *Revue de Paleobiologie*, v. 15, no. p. 499-517.
- Davoudzadeh, M., Schmidt, K., 1981. Contribution to the paleogeography and stratigraphy of the Upper Triassic to Middle Jurassic of Iran. *Neues Jahrbuch für Geologie und Paläontologie, Abhandlungen* 162, 137-163.
- Davoudzadeh, M., Schmidt, K., 1982. Zur Trias des Iran. *Geologische Rundschau* 71, 1021-1039.
- Dilek, Y., Delaloye, M., 1992. Structure of the Kizildag ophiolite, a slow spread Cretaceous ridge segment north of Arabian promontory. *Geology* 20, 19-22.
- Dupeuble, P. A., 1969, Foraminifères planctoniques (Globotruncanidés et Heterohelicidae) du Maestrichtien Supérieur en Aquitaine occidentale, in Brönnimann, P., and Renz, H. H. (eds.), *Proceedings of the First International Conference on Planktonic Microfossils*, Geneva: E.J. Brill, Leiden, v. p. 153-161.
- Lensch, G., Schmidt, K., Davoudzadeh, M., 1984. Introduction to the geology of Iran. *Neues Jahrbuch für Geologie und Paläontologie, Abhandlungen* 165, 155-164.
- Loeblich, A. R., JR., and Tappan, H., 1988, *Foraminiferal Genera and Their Classification*: Van Nostrand Reinhold Company, New York, 970 p.
- Lowe, D.R., 1979. Sediment gravity flow: their classification and some problems of application to natural flows and deposits. *Society for Sedimentary Geology Special Publication* 27, 75-82.
- Meischner, K.D., 1964. Allogaptaxites, turbidite in reef-near sedimentation- basins. In: Bouma, A.H., Brouwer, A. (Eds.), *Turbidites*. Elsevier, Amsterdam, pp. 156-191.
- Nakkady, S. E., 1950, A new foraminifera fauna from the Esna shales and Upper Cretaceous Chalk of Egypt: *Journal of Paleontology*, v. 24, no. 6, p. 675-692.
- Özkan, S., 1985, Maastrichtian Planktonic Foraminifera and Stratigraphy of the Germav Formation, Gercüs Area, Southeast Turkey: unpublished M.Sc. Thesis, Middle East Technical University, Ankara, Turkey, 219 p.
- Özkan, S., and Koyluoglu, M., 1988, Campanian-Maastrichtian planktonic foraminiferal biostratigraphy of the Beydağları Autochthonous Unit, Western Taurids, Turkey: *Middle East Technical University Journal of Pure and Applied Sciences*, v. 21, p. 377-388.
- Pessagno, E. A., JR., 1962, The Upper Cretaceous Stratigraphy and Micropaleontology of South-central Puerto Rico: *Micropaleontology*, v. 8, no. 1, p. 349-368.
- Postuma, J. A., 1971, *Manual of Planktonic Foraminifera*: Elsevier Publishing Company, Amsterdam, 420 p.
- Permolli Silva, I., and Verga, D., 2004, *Practical manual of Cretaceous planktonic foraminifera*. International School on planktonic foraminifera, 3rd Course: Cretaceous, in Verga, D., and Rettori, R. (eds.), *Universities of Perugia and Milan, Tipografia Pontefelicina, Perugia (Italy)*, 283 p.
- Premulisilva, and Sliter, W. V., 1994, Cretaceous planktonic foraminiferal biostratigraphy and evolutionary trends from the Bottaccione section, Gubbio, Italy: *Palaenographia Italica*, v. 82, p. 1-89.
- Robaszynski, F. (coordinator), 1998, *Planktonic foraminifera- Upper Cretaceous, Chart of Cretaceous Biostratigraphy*, in de Graciansky, P.C., Hardenbol, J., and Vail, P. R. (eds.), *Mesozoic and Cenozoic Sequence Stratigraphy of European Basins*: Society For Sedimentary Geology (SEPM), Special Publication, no. 60, 782, p.
- Robaszynski, and Caron, M. (coordinators), 1979, *Atlas de Foraminifères planctoniques du Crétacé moyen. Parts 1-2: Cahiers de Micropaleontologie*, v. 1 and 2, p. 1-185, 1-181.
- Robaszynski, and Caron, M. 1995, Cretaceous planktonic foraminifera: comments on the Europe- Mediterranean zonation: *Bulletin de la Société Géologique de France*, v. 166, p. 681- 692.
- Robaszynski, and Caron, M., Gonzales Donoso, J. M., and Wonders, A.A.H. (eds.) 1984, *Atlas of Late Cretaceous Globotruncanids*: *Revue de Micropaleontologie*, v. no. 3-4, p. 145- 305.
- Rosales, I., Fernandez- Mendiola, P. A., and Garcia-Mondejar, J., 1994, Carbonate depositional sequence development on active fault blocks: the Albian in the Castro Urdiales area, northern Spain: *Sedimentology*, v. 41, p. 861-82.
- Sari, B. 2006. Upper Cretaceous planktonic foraminiferal biostratigraphy of the Beydağları autochthon in the Korkuteli area, western Taurides, Turkey. Sari, B. 1999, *Biostratigraphy of the Upper Cretaceous Sequences in the Korkuteli Area (Western Taurides)*: unpublished M. Sc. Thesis Doğuz Eylül University, Izmir, 162 p.
- Sengor, A.M.C., Altiner, D., Cin, A., Ustaomer, T, Hus, K.J., 1988. The origin and assembly of the Tethyside orogenic collage at the expense of Gondwana land. In: Audley- Charles, M.G.A. (Ed.), *Hallam Gondwana and Tethys*. Geological Society of London Special Publications 37, pp. 119-181.
- Sengor, A.M.C., Kidd, W.S.F., 1979. Postcollisional tectonics of the Turkish- Iranian plateau and a comparison with Tibet. *Tectonophysics* 55, 361-376.
- Sengor, A. M. C., and Yilmaz, Y., 1981, Tethyan evolution of Turkey: a plate tectonic approach: *Tectonophysics*, v. 75, p. 181-241.
- Sigal, J., 1977. Essai de zonation du Crétacé Méditerranéen à l'aide des foraminifères planctoniques. *Géologie Méditerranéenne* 4, 99-108.

29. Sliter, W.V., 1989. Biostratigraphic zonation for Cretaceous planktonic foraminifers examined in thin section. *Journal of Foraminiferal Research* 19, 1-19.
30. Sliter, W.V., 1992. Cretaceous planktonic foraminiferal biostratigraphy and paleoceanographic events in the Pacific Ocean with emphasis on indurated sediment, In: Ishizaki, K., Saito. T. (Eds.). *Centenary of Japanese Micropaleontology*. Terra Scientific Publishing Company, Tokyo, pp. 281-299.
31. Sliter, 1999, Cretaceous planktonic foraminiferal biostratigraphy of the Calera Limestone, Northern California, USA: *Journal of Foraminiferal Research*, v. 29, no. 4, p. 318-339.
32. Soffel, H., Forster, H., 1980. Apparent polar wander path of Central Iran and its Geotectonic interpretation . *Journal of Geomagnetism Geoelectricity* 32 (suppl. III), 117-135.
33. Stocklin, J., 1968. Structural history and tectonics of Iran: A review American Association of Petroleum Geologists Bulletin 52, 1229-1258.
34. Stocklin, J., 1974. Possible ancient continental margin in Iran. In: Burk, C.A., Drake , C.L. (Eds.) *The geology of continental margins*. Springer Verlag, Berlin, pp. 873-887.
35. Stocklin, J., 1977. Structural correlation of the Alpine ranges between Iran and Central Asia. *Memoire de la Société géologique de France hors série* 8, 333-353.
36. Stocklin, J., Eftekhar- nezhad, J., Hushmanzadeh. A., 1972. Central Lut reconnaissance, East Iran. *Geological Survey of Iran* 21, 1-62.
37. Wensink, H., Varekamp, J.C., 1980. Paleomagnetism of basalts from Alborz: Iran part of Asia in the Cretaceous. *Tectonophysics* 68, 113-129.
38. WHITE, M. P., 1928, Some index Foraminifera of the Tampico embayment area of Mexico, part 2: *Journal of Paleontology*, v. 2, no. 4, p. 280- 313.
39. Hallam Gondwana and Tethys. *Geological Society of London Special Publications* 37, pp. 119-181.
40. Sengor, A.M.C., Kidd, W.S.F., 1979. Postcollisional tectonics of the Turkish- Iranian plateau and a comparison with Tibet. *Tectonophysics* 55, 361-376.
41. Sengor, A. M. C., and Yilmaz, Y., 1981, Tethyan evolution of Turkey: a plate tectonic approach: *Tectonophysics*, v. 75, p. 181-241.
42. Sigal, J., 1977. Essai de zonation du Crétacé Méditerranéen à l'aide des foraminifères planctoniques. *Géologie Méditerranéenne* 4, 99-108.
43. Sliter, W.V., 1989. Biostratigraphic zonation for Cretaceous planktonic foraminifers examined in thin section. *Journal of Foraminiferal Research* 19, 1-19.
44. Sliter, W.V., 1992. Cretaceous planktonic foraminiferal biostratigraphy and paleoceanographic events in the Pacific Ocean with emphasis on indurated sediment, In: Ishizaki, K., Saito. T. (Eds.). *Centenary of Japanese Micropaleontology*. Terra Scientific Publishing Company, Tokyo, pp. 281-299.
45. Sliter, 1999, Cretaceous planktonic foraminiferal biostratigraphy of the Calera Limestone, Northern California, USA: *Journal of Foraminiferal Research*, v. 29, no. 4, p. 318-339.
46. Soffel, H., Forster, H., 1980. Apparent polar wander path of Central Iran and its Geotectonic interpretation . *Journal of Geomagnetism Geoelectricity* 32 (suppl. III), 117-135.
47. Stocklin, J., 1968. Structural history and tectonics of Iran: A review American Association of Petroleum Geologists Bulletin 52, 1229-1258.
48. Stocklin, J., 1974. Possible ancient continental margin in Iran. In: Burk, C.A., Drake , C.L. (Eds.) *The geology of continental margins*. Springer Verlag, Berlin, pp. 873-887.
49. Stocklin, J., 1977. Structural correlation of the Alpine ranges between Iran and Central Asia. *Memoire de la Société géologique de France hors série* 8, 333-353.
50. Stocklin, J., Eftekhar- nezhad, J., Hushmanzadeh. A., 1972. Central Lut reconnaissance, East Iran. *Geological Survey of Iran* 21, 1-62.
51. Wensink, H., Varekamp, J.C., 1980. Paleomagnetism of basalts from Alborz: Iran part of Asia in the Cretaceous. *Tectonophysics* 68, 113-129.
52. WHITE, M. P., 1928, Some index Foraminifera of the Tampico embayment area of Mexico, part 2: *Journal of Paleontology*, v. 2, no. 4, p. 280- 313.

12/12/2011

Multifunctionality of the Iranian Agriculture Sector in a Partial Equilibrium Framework

Zahra Kiani-Feyzabad ¹, Seyed-Ali Hosseini-Yekani ², Seyed-Mojtaba Mojaverian ²

¹. MS Student, Department of Agricultural Economics, Sari Agricultural Sciences & Natural Resources University, Sari, Iran; ². Assistant Professor, Department of Agricultural Economics, Sari Agricultural Sciences & Natural Resources University, Sari, Iran. s.a.hosseiniyekani@gmail.com

Abstract: One of the magnificent issues related to the trade liberalization and globalization is to consider this point that whether the governmental support, such as paying agricultural subsidy are definitely of deviated effects on the trade or these paying are necessarily categorized out of the alluded policies in the green-box. In this case-study, taking a multifunctional role for the Iranian agriculture sector in the realm of the partial equilibrium model in mind, this issue that the supporting such as granting subsidy to the agricultural sector can not at all be categorized among the policies of the green-box is evaluated, besides, without taking these roles, the positive effects at supporting such as granting subsidy to the agriculture sector, justify the utility. On the basis of this research, it is possible to simulate the consequences of joining to the world trade organization quantitatively.

[Zahra Kiani-Feyzabad, Seyed-Ali Hosseini-Yekani, Seyed-Mojtaba Mojaverian. **Multifunctionality of the Iranian Agriculture Sector in a Partial Equilibrium Framework**. Life Science Journal. 2012;9(1):254-264] (ISSN:1097-8135). <http://www.lifesciencesite.com>. 35

Keywords: Multifunctionality of Agriculture; Liberalization; Subsidy; Partial Equilibrium Model; Iran

1. Introduction

Globalization means the merger of the national economy with the global economy that causes the increase in the amount of the international trade, the globalization of the production and direct investment (Saffari, 2004). One of the ways to globalization is joining the World Trade Organization (WTO). The countries that import agricultural products and the ones exporting them try to support their agriculture sectors putting customs tariffs and paying the subsidy of the export of the agricultural products, respectively. Following the different countries efforts to liberalize the trade of the agricultural products, WTO decreed that the related to tariff and non-tariff obstacles of the trade be reduced and the subsidy of the export of the agricultural products be limited. The economic activities results in the increase in production, rivalry and efficiency (Mohammadi and Naghshinehfar, 2005). Edward (1991) believes that trade liberalization should result in the establishment of a trade system in which all the deviations market like the import tariff and the export subsidy are deleted. In the studies conducted by WTO, the internal supports are categorized into two classes: a) trade-deviator supports (yellow-box supports), which every country whose amount, for every product or the whole agriculture sector, should be determined and then gradually be decreased, and b) development supports (Green-box supports) that are allowed supports with the purpose of supporting the rural expansion, agriculture and landscape preservation (Bakhshi et al., 2009). Agricultural income results in becoming motivated in producing goods and creating

jobs and it insures the landscape preservation and food security. Natural landscapes, food security, rural employment, etc. are considered the marginal effects of the agricultural production. Many researchers have said that these effects are of two types: positive marginal effects like natural landscapes and negative marginal effects like soil corrosion. Recognizing the positive marginal effects has been known as the multifunctionality of agriculture (Pfeiffer, 2002). Many of high-cost countries, European Union countries, that are of a long-term background in conducting cost supports in the field of agricultural products higher than the global level, have utilized the multifunctionality as a means of insuring the positive marginal effects of the agricultural sector and justifying supporting their agriculture sectors (Brunstad et al., 2005). Supporting the agricultural sector in the field of the Green-Box policies i.e. the policies that do not result in the trade-deviation are acceptable. But are these supports, taking the multifunctional role of the agriculture and the production of the common goods the agricultural products, justifiable?

Brunstad et al. (1995), utilizing a numerical model in the form of partial equilibrium, established the level of the necessary support for the Norwegian agricultural sector assuming this issue that the only goal is to provide the food security. The results of this study, in comparison to the real activities in the Norwegian agriculture sector, indicated a 50 percent decrease in the employment and the optimal use of the land.

Brunstad et al. (1999) studied the landscape preservation as one of the common goods of the

agriculture sector utilizing the combinative information method in Norway. The researchers in this study calculated the optimized level of the products, employment and also supports in the situation that landscape preservation is considered the goal. On the basis of the different simulated experiments, the results of this study indicated that only a minor part of the broad conducted supports has been necessary.

Brunstad et al. (2005) determined the optimized level of supports, employment and production in Norway, and they considered the two objectives food security and landscape preservation in the objective function of the model. The results of their study proved this reality that only a minor part of the present supports considering common goods (food security and landscape preservation) has been necessary.

Prestegard (2004) using the partial equilibrium model showed that multifunctionality could hardly justify the supporting packages out of the Green-Box (supporting the market), whereas it might justify the governments support in the field of the production of the public goods.

Gelebe and Lohmann (2007) utilizes the function of the mercantile partial equilibrium model for analyzing the trade and environmental policies of the multifunctionality of agriculture. Although the issue of the multifunctionality might result in succoring the conduction of supporting the agriculture sector for criticizing the trade liberalization, it is not valid and cogent a reason when the trade liberalization paves the way for the initiation of the environmental policy.

Abler (2004) considered this problem that whether the supporting policies like income and cost supports could result in the increase in the functions of the agriculture sector or are the policies that directly target the functions of agriculture more effective than those targeting the cost and income of farmers? The answer to the first question was negative, and second one, too, depended on the policies targeting the land.

Donnellan and Hanrahan (2006) in a study evaluated the influence of the trade liberalization in the agriculture sector on the decrease of one of the negative external effects, greenhouse gases, utilizing the partial equilibrium model. The results indicated that for alleviating the effects of the greenhouse gases, there is needed a set of basis reforms in some parts that are under the agreement of the WTO.

In this study, for evaluating the effect of the liberalization of agriculture on the functions of this sector, Brunstad's partial equilibrium model (1995) has been utilized. In this study, it has been tried to assess the relationship between the multifunctionality

of the Iranian agriculture sector and the tariff and subsidy supports conducted in this sector. To do this, two functions, food security and the preservation of the family farms, as two the public goods produced in this sector, have been considered.

In order to evaluating the elimination of the supports provided by the government, such as tariff and the subsidies, considering two important functions of the agriculture sector i.e. food security and the preservation of the family farms, we test the following hypotheses:

H1: Not only elimination of each of the supports threatens the other functions of the agriculture sector, but also these functions are strengthened if the supports are decreased.

H2: The elimination of each of these supports will not end in the decrease in the labor force in the rural areas under the critical level and both functions of food security and family farms preservation will not be damaged at all.

2. Material and Methods

In this research, the relations between the major economic variables of the agriculture sector containing two sub-divisions, farming and gardening, and also animal-husbandry in the form of a partial equilibrium model whose initial structure has been proposed by Brunstad et al (1995), have been simulated. This model, according to two viewpoints, is considered a partial equilibrium one:

1- In a partial equilibrium model, the variables of income and cost are exogenous. Hence, it is different with the common equilibrium models such as Walras model (Burniaux et al., 1990).

2- In a partial equilibrium model, the prices of imports and exports of the products are considered exogenous. Taking the global price of the imports fixed has been adopted from the hypothesis of the small country.

Therefore, this model is different from those of the multi-market goods such as MTM (Huff and Moreddu, 1990) and GLS (Tyser and Anderson, 1987) models. The model utilized in this research is the same type as the programming models that have been introduced and designed McCarl and Spreen (1990). As it has been assumed in the long-term models, the assumption of the complete dynamism of labor-force and the capital is taken in mind. So the surplus of the labor-force and the capital, completely without friction, is absorbed by the other industries. In this model, the economic surplus (The consumer surplus and the producer surplus) of the agriculture sector has been maximized. This maximization has been done provided that there are relationships between the demand and supply of the sector. In this part, the considered relations and equations are

introduced. Relation 1 shows the production of each one of the sectors, agriculture and gardening and animal-husbandry in the form of Cobb-Douglas function. This is a function of the factor, for the generation of labor and capital.

$$(1) \quad y_j = ad_j \prod_{f \in F} v_{jf}^{\alpha_{ff}} \quad j \in J$$

In this function, the index j represents the products, y_j represents the production amount in every sub-division, ad_j is the parameter of the efficiency of the production function, the index f represents the production factors (labor and capital), α_{ff} is the elasticity of the production factor f in the production field j, and v is values of the production factors. On basis of relation 2, the amount of the family expenses is calculated deducting the family expenses in relation to other families, government (banks) and the external field from the total income of the family.

$$(2) \quad c_h = (1 - mps_h - ty_h) \cdot y_{h,h} - tr_{h,h} - tr_{gov,h} - tr_{row,h} \cdot exr$$

In this relation, h represents the families, mps_h represents the income of the family h for saving after paying the family tax, ty_h shows the direct tax rate for the family h, exr shows the rate of the exchange (Rials), $y_{h,h}$ shows the total income, $tr_{h,h}$ represents the family expenses, $tr_{gov,h}$ shows the government expenses, and $tr_{row,h}$ shows the expenses related to the external world. The demand for consumption of every income quintile in each one of the products of the following sub-divisions is calculated according to relation 3. In this relation β_{jh} is relation of the total family expenses that the consumer consumes for the goods j, and p_j is the average price of the goods j that is set by the producer.

$$(3) \quad c_{jh} = \frac{\beta_{jh} \cdot [c_h]}{p_j} \quad j \in J, h \in H$$

Relation 4, contains the scarcity restrictions of the production factor in terms of their present values. In this relation, \bar{v}_f is the maximum amount of the production.

$$(4) \quad \sum_j v_{jf} \leq \bar{v}_f \quad f \in F$$

The export rate is the rate that is calculated by the native producers when they sell their products in the global markets.

$$(5) \quad px_j = pwe_j \cdot exr \quad j \in J$$

As it was shown in relation 5, the export rate of each of the products is calculated by the

multiplication of the exchange rate in terms of the national country by the universal export cost of that product. px_j is the export cost (Rials), and pwe_j is the universal export cost (foreign exchange). The import price of every product is the price that consumers pay for the imported products in terms of the currency of their country. Because the consumers pay for the goods after the consumer tariff has been devised, the import price of every product is calculated according to relation 6.

$$(6) \quad pm_j = (1 + tm_j) \cdot exr \cdot pwm_j \quad j \in J$$

pwm_j is the import cost (Rials), tm_j is the import tariff rate, and pwm_j is the global cost of the imports (foreign exchange). Domestic consumers of every product use domestic and exterior goods (composite goods). The absorption price indicates the domestic cost according to the demanded price. Relation 7 shows the price of the composite goods that is a combination of the price the interior sold products and the price of the imported goods. The weights of the equation are the amount of the sold interior products and the amount of the imports. The absorption equation contains all the products that are sold in the country. In other words, contains all imported products or the products produced inside the country that are sold interiorly and it does not include the products that are completely exported.

$$(7) \quad pq_j = \frac{(pd_j \cdot yd_j + pm_j \cdot m_j)}{yq_j} (1 - sq_j) \quad j \in J$$

pq_j is the price of the composite goods, pd_j is the domestic price of the goods produced in the country, m_j is the amount of the imports, and sq_j is the subsidy rate per every product unit j. In addition, domestic producers either sell their products in their own country, or export them. Therefore, for every product that has been produced inside the country, the market production value (producer price) is calculated on the basis of relation 8 that shows the weight average of the goods produced in the country and export price of the products.

$$(8) \quad p_j = \frac{(pd_j \cdot yd_j + px_j \cdot x_j)}{y_j} \quad j \in J$$

y_d_j is the amount of the products sold in the country, and x_j shows the exports.

On the basis of relation 9, the composite products are consumed by the domestic demanders. The imperfect substitution between the imported goods and the domestic products that are consumed in the country are indicated by the constant elasticity

of substitution general function (CES). In this function, the supplied products are a composition of the goods produced in the country and the goods imported. In this function, the imported products and the ones produced in the country are used as "input". From economic viewpoint, it means that the demanders' preferences from amongst the imported and produced in the country products are expressed in the form of a CES function that is called Armington function. Constraints as $(-1 < \rho_j^q < \infty)$ in which ρ_j^q is the power $(-1 < \rho_j^q < \infty)$, the composite offer function (Armington), supply the assumption of the convexity of the above-mentioned function in proportion to the y-intercept. This characteristic equals the rate of technical descending substitution.

$$(9) \quad y_{qj} = a_{qj} \cdot \left(\delta_j^q \cdot m_j^{-\rho_j^q} + (1 - \delta_j^q) \cdot y_j^{-\rho_j^q} \right)^{\frac{-1}{\rho_j^q}} \quad j \in J$$

a_{qj} is the parameter of the translation of the composite supply function (Armington), and δ_j^q is the parameter of the ration of composite offer function(Armington). Also goods and services produced inside the country, either are sold in the country, or are exported whose specification is calculated by a constant elasticity of transformation (CET) function. CET function, according to relation 10, is used for the exported products. This function is like CES. The only difference between them is the existence of negative substitution elasticity. The isoquant curve related to the above equation, according to the constraints, is $(1 < \rho_j^t < \infty)$ per ρ_j^t in proportion to the concave origin of coordinates in which ρ_j^t is the power of $(1 < \rho_j^t < \infty)$, the product transformation function (CET). If it is demanded that the difference between Armington function and CET be presented via economic terms, it can be said that in CET, the variables of the relation are the production factors, whereas in the Armington function, the variables are the products.

$$(10) \quad y_{tj} = a_{tj} \cdot \left(\delta_j^t \cdot x_j^{-\rho_j^t} + (1 - \delta_j^t) \cdot y_j^{-\rho_j^t} \right)^{\frac{1}{\rho_j^t}} \quad j \in J$$

a_{tj} is the translation parameter of the production transformation function (CET), and δ_j^t is the ration parameter of the production transformation function(CET). On the other hand, the demand function for each of the products is equal to relation 11.

$$(11) \quad p_j = a_j - b_j c_j$$

The objective function in the model is the sum of economic surplus of the sector that has been defined as the sum of the surplus of the producers, the consumers and the importers. The producers benefit through selling the goods results from the domestic sales and the exports. Relation 12 shows the gained benefit from the domestic sales.

$$(12) \quad \sum_j p_j (y_j - x_j)$$

Relation 13 shows the gained benefit from the exports.

$$(13) \quad \sum_j p x_j x_j$$

Relation 14 shows the producers surplus

$$(14) \quad \sum_j (p_j - p m_j) m_j$$

Now if the cost T and relation 13 and 12 are deducted from each other, the sum of the surplus of the producer and the surplus of the importer will be as relation 15:

$$(15) \quad \sum_j (p_j c_j + p x_j x_j - p m_j m_j) - \sum_f r_f v_f - T + S$$

$p m_j$ is the price of the product j, s is the governmental supports, and r_f the price of the inputs.

On the basis of relation 16 the surplus of the consumer equals:

$$(16) \quad \sum_k \sum_j b_{kj} c_k c_j$$

According to the above relation and the relation number 11, the objective function of the model that contain the sum of the surplus of the consumer, producer and importer can be shown as follows:

$$(17) \quad \Pi = \sum_j (a_j c_j - \frac{1}{2} \sum_k b_{kj} c_k c_j + p x_j x_j - p m_j m_j) - \sum_f r_f v_f - T + S$$

The above-mentioned matrix was solved utilizing the macroeconomic data and the expressed numbers in the input-output matrix of the years 1380 of the Iranian central bank using GAMS software. But as it was stated in the introduction, in this research, the two functions, preserving family farms and food security, are evaluated as marginal and often ignored functions of the agriculture sector. Preserving family farms via supporting the small farmers (who usually exploit domestic non-specialist labor force) is conducted in accordance to preserving their producing units. Concerning food security, it deserves mentioning that the ability to provide food in every condition is called food security. Food security is defined in three levels, global, national and personal (Ballenger, 1992).

2.1. Global food security

$\text{Pr}[(\text{world production} + \text{world stocks}) \geq \text{world needs}] \geq \pi$

Where π is minimum acceptable likelihood.

This means that the sum of world production and stocks in every year must exceed the necessary consumption by a minimum acceptable likelihood.

2.2. National food security

$\text{Pr}[(\text{domestic production} + \text{domestic stocks} + \text{imports} + \text{aid}) \geq \text{domestic needs}] \geq \pi$

National food security is less restrictive, as consumption could be satisfied based on imports and aid from other countries. Therefore, even if global food security is below reasonable limits, rich countries will normally have enough purchasing power in world markets to secure a sufficient share of world production. The same logic applies to individual food security, which can be secured if a person has enough income or purchasing power, even if the nation's food supply is insufficient. It follows that if global food security is fulfilled, then national and individual food security is a matter of distribution or poverty relief. A special case is a blockade in connection with war, which rules out distribution between countries (infinite import prices). It seems unwise to dismiss totally the need for a minimum of activity within the agricultural sector to diminish the negative effects of unknown crises in the future. Import tariffs and production subsidies are not only costly, but may also impair the purchasing power and food security in countries with comparative advantage in food production. In this study, the production rate in every level of the decrease of supports has been used as an index to show food security.

3. Results and discussions

In this section, the results gained from the effect of different scenarios of the alleviation and ultimately eliminating tariff and subsidy supports on food security and preserving rural farms as the unproductive functions of the agriculture sector are evaluated. In the basis of the gained results, one can express their ideas on the relationship between the unproductive functions of the agriculture sector are the supports provided. In this article, three scenarios were followed.

1- The evaluation of the effect of the reduction of tariff (20, 40, 60, 80 and 100) on the unproductive functions of food security and the preservation of the rural farms.

2- The evaluation of the effects of the reduction the subsidies (20, 40, 60, 80 and 100) on

the functions of food security and the preservation of the rural farms.

3- The evaluation of the effects of the reduction of the total supports provided on the agriculture sector (20, 40, 60, 80 and 100) on the two functions food security and the preservation of the rural farms.

3.1. The Elimination of Tariff

3.1.1. The effect of the elimination of tariff on the food security

The numerical results gained from solving the model on the basis of the reduction of the tariff rate indicate an increase in the level of production in the stock breeding sector, so that the percentage of the changes in production in the first scenario in proportion to real values includes a rate of increase in production at 0.06%. Concerning this issue that it is feasible to know the production rate as the index of food security, the increase in production can affirm this fact that not only has not tariff (as one the supports provided on the agriculture sector) provided any supports on food security, but also by elimination it, the levels of production and even food security have increased; whereas, the level of production of the agriculture and gardening sector is of a slight gradual reduction, so that the percentage of the changes in production, in proportion to real values is 0.003%. This reduction is due to the bigger share of the agriculture and gardening sector in tariff. It is necessary to say that in the partial equilibrium models, every change in one sector will not affect the other sector; hence, the reduction in the level of production in the agriculture and gardening sector will not affect the stock breeding sector, and having a reduction in the level of production in the agriculture and gardening, food security will not be threatened. With the elimination of tariff, it seems logical that the imports increase, so that the results of this model prove this issue. The level of the exports in both sectors: agriculture and gardening, and stock breeding decreased, so that this reduction, with the complete elimination of tariff, reached at 2%. The increase in both sectors originates from the increase in consumption in both sectors. The highest level of the increase in consumption in the urban fourth quintile is 1.29%, and in the rural fifth quintile, it is 1.09% (Table2). The index of the price in the agriculture and gardening sector is of 1.14% increased, and in the stockbreeding sector, it is increased at 0.77%. The increase in price is due to the increase in consumption. This increase in agriculture and stockbreeding sector, because of the decrease in the production in the production in the agriculture and gardening sector, is more drastic (Table1).

Table 1: Effect of the elimination of tariff on production, imports, exports, prices and capital

Description		Actual values	First scenario	Second scenario	Third scenario	Fourth scenario	Fifth scenario
Production (billion rials)	Agriculture and gardening	76471	76470.4	76469.8	76469.2	76468.6	76467.99
	Stock breeding	54479	54515.6	54552.66	54590.2	54628.24	54666.79
Import (billion rials)	Agriculture and gardening	10689	10854.48	11025.59	11202.65	11385.98	11575.94
	Stock breeding	95	96.45	97.96	99.51	101.12	102.79
Export (billion rials)	Agriculture and gardening	6774	6744.07	6713.89	6683.45	6652.73	6621.74
	Stock breeding	680	678.41	676.8	675.17	673.52	671.85
Price (billion rials)	Agriculture and gardening	1	1	1	1.01	1.01	1.01
	Stock breeding	1	1	1	1	1.01	1.01
Capital (billion rials)	Agriculture and gardening	262	262.67	263.35	264.05	264.75	265.47
	Stock breeding	411	412.05	413.12	414.21	415.32	416.44

Source: research findings

Table 2: The effect of the elimination of tariff on consumption

Description		Actual values	First scenario	Second scenario	Third scenario	Fourth scenario	Fifth scenario
Agriculture and gardening	Consumption of the first urban quintile	2490	2491.86	2493.75	2495.67	2497.62	2499.6
	Consumption of the second urban quintile	3984	3987.18	3990.41	3993.69	3997.02	4000.41
	Consumption of the third urban quintile	4980	4984.67	4989.4	4994.21	4999.1	5004.07
	Consumption of the fourth urban quintile	5976	5989.08	6002.37	6015.86	6029.56	6043.49
	Consumption of the fifth urban quintile	7470	7444.45	7418.52	7392.17	7365.41	7338.22
	Consumption of the first rural quintile	1546	1546.55	1547.11	1547.68	1548.26	1548.84
	Consumption of the second rural quintile	2249	2250.12	2251.27	2252.42	2253.6	2254.8
	Consumption of the third rural quintile	2530	2532.03	2534.08	2536.17	2538.3	2540.45
	Consumption of the fourth rural quintile	3232	3235.45	3238.96	3242.51	3246.13	3249.81
	Consumption of the fifth rural quintile	4497	4506.55	4516.25	4526.1	4536.11	4546.28
Stock breeding	Consumption of the first urban quintile	122	122.09	122.18	122.28	122.37	122.47
	Consumption of the second urban quintile	195	195.16	195.31	195.47	195.64	195.8
	Consumption of the third urban quintile	244	244.23	244.46	244.7	244.94	245.18
	Consumption of the fourth urban quintile	293	293.64	294.29	294.95	295.63	296.31
	Consumption of the fifth urban quintile	366	364.75	363.48	362.19	360.88	359.54
	Consumption of the third rural quintile	1851	1852.48	1853.99	1855.52	1857.07	1858.65
	Consumption of the fourth rural quintile	2365	2367.53	2370.09	2372.69	2375.34	2378.03
Consumption of the fifth rural quintile	3290	3296.99	3304.08	3311.29	3318.61	3326.05	

Source: research findings

3.1.2. The effect of the elimination of tariff on the preservation of the family farms

By completely eliminating the tariff, employment, in all sectors, shows an increasing rate, so that the highest levels of the increase in employment in the fields of the rural skilled labor force and rural state unskilled labor force are 1011% and 0.55% respectively. Because the rural unskilled labor force work at the family farms, and, by eliminating the tariff, the job demand of the rural labor force has not decreased, and can insure the survival of the rural family farms.

In general, by eliminating the tariff, and of the supporting packages in the government's policy to back the agriculture sector, not only are not the other functions of the agriculture sector, such as food

security and the presentation of the rural farms, threatened, but also it is possible to justify the elimination of the supporting packages such as tariff, that results in the economic deviation (Table 3).

3.2. The Elimination of All the Subsidies

3.2.1. The effect of the reduction of the subsidies on security

In the scenario of the elimination of the subsidies, the level of production in the agriculture sector is of a slight decrease, where as that of the stockbreeding sector has decreased. The reduction in the production of the agriculture sector, according to the increase in the production cost, is reasonable. According to the sectional nature of the model, the transfer of the reduction in the agriculture and

gardening sector concerning the increase in the stock breeding sector indicates this fact that not only is not the function of food security threatened, but also it is an emphasis on keeping food security and the inefficiency of the supports provided on the agriculture sector. The imports, in the agriculture and stockbreeding sectors, have decreased at 0.3% and 3.34%, respectively. The decrease in the imports in the agriculture sector is due to the reduction in the production and consumption. The exports in the agriculture sector, because of the elimination of subsidies, have decreased at 1.5%, and those in the

stockbreeding sector have increased at 13.6% (Table4). The increase in the production in the stockbreeding sector along with the decrease in the demand for the surplus of the production of this sector has resulted a 13% growth in the exports. Also, the prices in the gardening sector, because of the decrease in the supply, have raised; because the decrease in the consumption has been compensated for with the decrease in the production and imports; and in the stockbreeding sector, due to the surplus of the supply, the price has decreased (Table5).

Table 3: The effect of the elimination of tariff on labor force

Description		Actual values	First scenario	Second scenario	Third scenario	Fourth scenario	Fifth scenario
Agriculture and gardening	Urban self-employed skilled labor force	84	84.06	84.12	84.19	84.25	84.32
	Urban state skilled labor force	16	16.01	16.02	16.03	16.05	16.06
	Urban self-employed unskilled labor force	5	5	5	5.01	5.01	5.01
	Urban state unskilled labor force	1143	1143.89	1144.79	1145.71	1146.64	1147.58
	Rural self-employed skilled labor force	105	105.23	105.46	105.69	105.93	106.17
	Rural state skilled labor force	80	80.11	80.21	80.32	80.44	80.55
	Rural self-employed unskilled labor force	7	7.01	7.02	7.03	7.04	7.05
	Rural state unskilled labor force	56912	56972.96	57034.86	57097.73	57161.62	57226.54
Stock breeding	Urban self-employed skilled labor force	131	131.1	131.19	131.29	131.39	131.5
	Urban state skilled labor force	25	25.02	25.04	25.05	25.07	25.09
	Urban self-employed unskilled labor force	8	8	8.01	8.01	8.01	8.02
	Urban state unskilled labor force	1791	1792.39	1793.81	1795.24	1796.7	1798.18
	Rural self-employed skilled labor force	164	164.35	164.71	165.08	165.45	165.83
	Rural state skilled labor force	125	125.17	125.33	125.51	125.68	125.86
	Rural self-employed unskilled labor force	11	11.01	11.03	11.04	11.06	11.07

Table 4: The effect of the elimination of the subsidies on production , export, price and capital

Description		Actual values	First scenario	Second scenario	Third scenario	Fourth scenario	Fifth scenario
Production (billion rials)	Agriculture and gardening	76471	76364.29	76253.62	76138.91	76020.05	75896.94
	Stock breeding	54479	54566.59	54662.27	54766.07	54878	54998.11
Import (billion rials)	Agriculture and gardening	10689	10681.03	10673.17	10665.39	10657.7	10650.07
	Stock breeding	95	94.34	93.69	93.04	92.41	91.77
Export (billion rials)	Agriculture and gardening	6774	6755.39	6735.58	6714.57	6692.34	6668.89
	Stock breeding	680	697.01	714.75	733.26	752.58	772.75
Price (billion rials)	Agriculture and gardening	1	1	1	1	1	1
	Stock breeding	1	0.99	0.98	0.97	0.95	0.94
Capital (billion rials)	Agriculture and gardening	262	256.81	251.63	246.47	241.31	236.17
	Stock breeding	411	402.86	394.74	386.63	378.55	370.48

Source: research findings

Table 5: The effect of the elimination of the subsidies on consumption

Description		Actual values	First scenario	Second scenario	Third scenario	Fourth scenario	Fifth scenario
Agriculture and gardening	Consumption of the first urban quintile	2490	2475.68	2461.39	2447.14	2432.92	2418.73
	Consumption of the second urban quintile	3984	3959.52	3935.1	3910.74	3886.44	3862.18
	Consumption of the third urban quintile	4980	4944.09	4908.27	4872.54	4836.88	4801.3
	Consumption of the fourth urban quintile	5976	5875.3	5774.86	5674.65	5574.68	5474.9
	Consumption of the fifth urban quintile	7470	7666.63	7862.76	8058.41	8253.63	8448.45
	Consumption of the first rural quintile	1546	1541.84	1537.68	1533.54	1529.41	1525.29
	Consumption of the second rural quintile	2249	2240.51	2232.05	2223.61	2215.18	2206.78
	Consumption of the third rural quintile	2530	2514.7	2499.45	2484.23	2469.05	2453.9
	Consumption of the fourth rural quintile	3232	3205.94	3179.95	3154.03	3128.17	3102.36
	Consumption of the fifth rural quintile	4497	4424.88	4352.96	4281.22	4209.65	4138.23
Stock breeding	Consumption of the first urban quintile	122	121.3	120.6	119.9	119.2	118.51
	Consumption of the second urban quintile	195	193.8	192.61	191.41	190.22	189.04
	Consumption of the third urban quintile	244	242.24	240.49	238.73	236.99	235.24
	Consumption of the fourth urban quintile	293	288.06	283.14	278.23	273.32	268.43
	Consumption of the fifth urban quintile	366	375.63	385.24	394.83	404.39	413.94
	Consumption of the first rural quintile	1131	1127.95	1124.92	1121.89	1118.86	1115.85
	Consumption of the second rural quintile	1645	1638.79	1632.6	1626.43	1620.26	1614.12
	Consumption of the third rural quintile	1851	1839.81	1828.65	1817.51	1806.41	1795.32
	Consumption of the fourth rural quintile	2365	2345.93	2326.92	2307.95	2289.02	2270.14
	Consumption of the fifth rural quintile	3290	3237.24	3184.62	3132.14	3079.77	3027.52

Source: research findings

3.2.2. The effect of the reduction of the subsidies on the preservation of the family farms

The numerical results of doing the model in the decrease of the subsidies indicates a falling trend in employment, so that the highest level of the reduction in the rural skilled labor force is 7%, that cannot be serious threat to the immigration of the

labor force. On the other hand, the index of the function of the preservation of the family farms is the rural unskilled labor force, and this index shows a negligible number. In general, the elimination the subsidies does not endanger the unproductive function of this sector (Table 6).

Table 6: The effect of the elimination of the subsidies on labor force

Description		Actual values	First scenario	Second scenario	Third scenario	Fourth scenario	Fifth scenario
Agriculture and gardening	Urban self-employed skilled labor force	84	83.58	83.16	82.74	82.32	81.91
	Urban state skilled labor force	16	15.92	15.85	15.77	15.7	15.62
	Urban self-employed unskilled labor force	5	4.99	4.97	4.96	4.95	4.94
	Urban state unskilled labor force	1143	1136.95	1130.91	1124.9	1118.9	1112.92
	Rural self-employed skilled labor force	105	103.45	101.91	100.38	98.84	97.32
	Rural state skilled labor force	80	79.27	78.55	77.83	77.11	76.39
	Rural self-employed unskilled labor force	7	6.94	6.88	6.82	6.75	6.69
	Rural state unskilled labor force	56912	56495.83	56081.12	55667.74	55255.56	54844.44
Stock breeding	Urban self-employed skilled labor force	131	130.34	129.69	129.04	128.39	127.74
	Urban state skilled labor force	25	24.88	24.76	24.64	24.53	24.41
	Urban self-employed unskilled labor force	8	7.98	7.96	7.94	7.92	7.9
	Urban state unskilled labor force	1791	1781.51	1772.06	1762.64	1753.24	1743.87
	Rural self-employed skilled labor force	164	161.58	159.18	156.78	154.38	152
	Rural state skilled labor force	125	123.86	122.73	121.61	120.48	119.36
	Rural self-employed unskilled labor force	11	10.9	10.81	10.71	10.61	10.52
	Urban self-employed skilled labor force	21326	21170.05	21014.65	20859.75	20705.3	20551.25

Source: research findings

3.3. The Elimination of Tariff and the Subsidies

3.3.1. The effect of the elimination of the tariff and the subsidies on food security

By eliminating all the provided supports on the agriculture sector, the level of production in the agriculture and gardening sector has transferred to the level of production in the stock breeding sector at %0.7. The level of import in the agriculture and stock breeding sectors shows %7.9 and %4.5 increases, respectively (Table 7). The percentage of the changes in export in the agriculture sector, in the scenario of the complete elimination of tariff is -3%, whereas it,

in the stock breeding sector, because of the surplus of the supply, has increased. Because of the rise of the price in the agriculture sector, and the stability of the price in the stockbreeding sector in different scenarios, not only has not the level of consumption in creased, but also it has decreased. The level of consumption in all quintiles has been of a falling rake of 7%, as well, whereas in the urban fourth quintile, it has been of an 11% growth, so that this level of growth is compensated for by an increase in imports, and there is no surplus stuff for exports in the gardening sector (Table 8).

Table 7: The effect of the elimination of tariff ,and the subsidies on production , export, price and capital

Description		Actual values	First scenario	Second scenario	Third scenario	Fourth scenario	Fifth scenario
Production (billion rials)	Agriculture and gardening	76471	76363.57	76251.95	76136.06	76015.8	75891.08
	Stock breeding	54479	54603.66	54737.82	54881.51	55034.74	55197.55
Import (billion rials)	Agriculture and gardening	10689	10846.38	11009.23	11177.84	11352.52	11533.59
	Stock breeding	95	95.78	96.61	97.47	98.37	99.32
Export (billion rials)	Agriculture and gardening	6774	6725.5	6675.65	6624.43	6571.85	6517.92
	Stock breeding	680	695.39	711.43	728.15	745.59	763.79
Price (billion rials)	Agriculture and gardening	1	1	1.01	1.01	1.01	1.02
	Stock breeding	1	0.99	0.98	0.97	0.96	0.95
Capital (billion rials)	Agriculture and gardening	262	257.47	252.94	248.41	243.88	239.35
	Stock breeding	411	403.89	396.79	389.68	382.58	375.47

Table 8: The effect of the elimination of tariff ,and the subsidies on consumption

Description		Actual values	First scenario	Second scenario	Third scenario	Fourth scenario	Fifth scenario
Agriculture and gardening	Consumption of the first urban quintile	2490	2477.51	2465.02	2452.52	2440.03	2427.53
	Consumption of the second urban quintile	3984	3962.65	3941.3	3919.95	3898.59	3877.23
	Consumption of the third urban quintile	4980	4948.68	4917.36	4886.04	4854.72	4823.38
	Consumption of the fourth urban quintile	5976	5888.17	5800.35	5712.53	5624.69	5536.82
	Consumption of the fifth urban quintile	7470	7641.51	7812.98	7984.46	8155.98	8327.56
	Consumption of the first rural quintile	1546	1542.38	1538.76	1535.14	1531.52	1527.9
	Consumption of the second rural quintile	2249	2241.62	2234.24	2226.86	2219.49	2212.11
	Consumption of the third rural quintile	2530	2516.7	2503.4	2490.1	2476.8	2463.5
	Consumption of the fourth rural quintile	3232	3209.34	3186.68	3164.03	3141.38	3118.73
	Consumption of the fifth rural quintile	4497	4434.28	4371.59	4308.9	4246.22	4183.52
Stock breeding	Consumption of the first urban quintile	122	121.39	120.78	120.16	119.55	118.94
	Consumption of the second urban quintile	195	193.95	192.91	191.86	190.82	189.77
	Consumption of the third urban quintile	244	242.47	240.93	239.4	237.86	236.33
	Consumption of the fourth urban quintile	293	288.69	284.39	280.08	275.78	271.47
	Consumption of the fifth urban quintile	366	374.4	382.8	391.21	399.61	408.02
	Consumption of the first rural quintile	1131	1128.35	1125.7	1123.06	1120.41	1117.76
	Consumption of the second rural quintile	1645	1639.6	1634.2	1628.81	1623.41	1618.02
	Consumption of the third rural quintile	1851	1841.27	1831.54	1821.81	1812.08	1802.35
	Consumption of the fourth rural quintile	2365	2348.42	2331.84	2315.27	2298.69	2282.11
	Consumption of the fifth rural quintile	3290	3244.11	3198.25	3152.39	3106.53	3060.66

Source: research findings

3.3.2. The effect of the reduction of tariff and the subsidies on the preservation of the family farms

In different scenarios, employment, too, is of a falling rate, so that the highest level of reduction is at 6%, and in the field of the rural unskilled labor

force it is at 3%, that is not considerable an amount with the critical level of these numbers. This reduction dose not result in the immigration of the rural labor force, and the function of the preservation of the family farms will not be threatened (Table 9).

Table 9: The effect of the elimination of tariff ,and the subsidies on labor force

Description		Actual values	First scenario	Second scenario	Third scenario	Fourth scenario	Fifth scenario
Agriculture and gardening	Urban self-employed skilled labor force	84	83.64	83.28	82.92	82.56	82.2
	Urban state skilled labor force	16	15.93	15.87	15.8	15.74	15.67
	Urban self-employed unskilled labor force	5	4.99	4.98	4.97	4.96	4.94
	Urban state unskilled labor force	1143	1137.82	1132.65	1127.49	1122.33	1117.17
	Rural self-employed skilled labor force	105	103.68	102.36	101.04	99.72	98.4
	Rural state skilled labor force	80	79.38	78.76	78.14	77.52	76.9
	Rural self-employed unskilled labor force	7	6.95	6.89	6.84	6.79	6.74
	Rural state unskilled labor force	56912	56555.9	56200.42	55845.4	55490.7	55136.19
Stock breeding	Urban self-employed skilled labor force	131	130.44	129.88	129.32	128.76	128.2
	Urban state skilled labor force	25	24.9	24.8	24.69	24.59	24.49
	Urban self-employed unskilled labor force	8	7.98	7.96	7.95	7.93	7.91
	Urban state unskilled labor force	1791	1782.88	1774.78	1766.69	1758.61	1750.53
	Rural self-employed skilled labor force	164	161.93	159.87	157.81	155.75	153.69
	Rural state skilled labor force	125	124.03	123.06	122.09	121.12	120.15
	Rural self-employed unskilled labor force	11	10.92	10.83	10.75	10.67	10.59
	Urban self-employed skilled labor force	21326	21192.56	21059.36	20926.32	20793.41	20660.57

Source: research findings

4. Summary and Concluding Remarks

In the negotiations of the WTO on the trade liberalization, the elimination of the supports provided by government that result in trade deviation in the agriculture sector is crucial. The elimination of many of these supporting packages without considering the functions of the agriculture sector seems completely unreasonable. In this study, it has been tried that, taking two important functions of the agriculture sector i.e. Food security and the preservation of the family farms, in to consideration, the elimination of the supports provided by the government, such as tariff and the subsidies be evaluated. The result of the model indicated that not only dose not the elimination of each of the supports threaten the other functions of the agriculture sector, but also these functions are strengthened if the supports are decreased. The elimination of each of these supports will not end in the decrease in the labor force in the rural areas under critical level and both functions of food security and family farms preservation will not be damaged at all. Considering the other functions of the agriculture sector such as the preservation of the landscapes, keeping population in faraway areas, rural development, etc.,

it is possible to justify the complete elimination of the governments backing policies.

Corresponding Author:

Dr. Seyed-Ali Hosseini-Yekani
Department of Agricultural Economics
Sari Agricultural Sciences & Natural Resources
University, Sari, Iran
E-mail: s.a.hosseiniyekani@gmail.com

References

1. Abler, D., 2004. Multifunctionality, Agricultural Policy, and Environmental Policy. *Agricultural and Resource Economics Review* 33/1.
2. Bakhshi, M., Z. Mullai and A. Bakhtiyari, 2009. Ways to support rural communities by the World Trade Organization Agreement on Agriculture and provide guidance for Iran. Planning Research Institute, agricultural economics, rural development.
3. Ballenger, N. and C. Mabbs-Zeno, 1992. Treating food security and food aid issues at the GATT. *Food Policy*, pp. 264–276.
4. Brunstad, R.J., I. Gaasland and E. Vaørdal, 1995. Agriculture as a provider of public goods: a case

- study for Norway. *Agricultural Economics* 13, pp. 39–49.
5. Brunstad, R.J., I. Gaasland and E. Vaørdal, 1995. A Model for the Agricultural Sector in Norway. Working Paper No. 25/95. Bergen: Foundation for Research in Economics and Business Administration (SNF).
 6. Brunstad, R.J., I. Gaasland and E. Vaørdal, 1999. Agricultural production and the optimal level of landscape preservation. *Land Economics* 75, pp. 538–546.
 7. Brunstad, R.J., I. Gaasland and E. Vaørdal, 2005. Multifunctionality of agriculture: an inquiry into the complementarity between landscape preservation and food security. *European Review of Agricultural Economics* 32(4), pp. 469–488.
 8. Burnieaux, J., F. Delorme, I. Lienert and J.P. Martin, 1990. WALRAS-A Multi-sector, Multi-Country applied general equilibrium model for quantifying the economy-wide effects of agricultural policies. OECD Economic studies. No. 13/ winter, pp. 69-1020.
 9. Donnellan, T., K. Hanrahan, 2006. Potential WTO trade reform multifunctionality impacts for Ireland. Working Paper No. 16.
 10. Edward, S., 1991. “Monetarism and liberalization” Chicago University Press, Chicago.
 11. Glebe, T. and U. Lohmann, 2007. Agricultural multifunctionality and trade liberalization. *Cahiers d’économie et sociologie rurales*, pp. 82-83.
 12. Huff, B.H. and C. Moreddu, 1990. The Ministerial Trade Mandate Model. OECD Economic studies. No. 13/ winter, pp. 45-67.
 13. McCarl, B.A. and T.H. Spreen, 1980. Price Endogenous Mathematical Programming As a Tool for sector Analysis. *American Journal of Agricultural Economics* 62(1), pp. 87-107.
 14. Mohammadi, H. and M. Naghshinehfar, 2005. Effects of trade liberalization on the supply, demand, imports and exports of wheat and pistachio in Iran. *Iranian Agricultural Sciences*, Year XII, No. 1.
 15. Pfeiffer, G., 2002. Multifunctionality and Trade, Agricultural Economics Department, University of Nebraska – Lincoln.
 16. Prestegard, S.S., 2004. Multifunctional agriculture, policy measures and the WTO: the Norwegian case. *Acta Agric. Scand., Sect. C, Food Economics* 1, pp. 151-162.
 17. Safari, S., 2004. Investigating the relationship between globalization and economic growth - trade, globalization, multi-country analysis of selected. Doctoral Thesis, Faculty of Economics, Allameh Tabatabaei University, Tehran.

1/5/2012

Association between CC16 Polymorphism and Bronchial Asthma

Nisreen M.El Abiad¹, Hisham Waheed², William M. Morcos², Samar M. Salem², and Hala Ataa³, Olfat G. Shaker⁴

Departments of: ¹Pediatric, ⁴Medical Biochemistry, Faculty of Medicine, Cairo University, ²Child Health, NRC. and ³Al Galaa Teaching Hospital, Cairo, Egypt.

hishamwb@yahoo.com

Abstract: Background: Asthma is one of the most common chronic pediatric diseases, and is responsible for a significant proportion of school day losses. Asthma is influenced by genetic and environmental factors. The inheritance pattern of asthma demonstrates that it is a complex genetic disorder. Clara cell secretory protein (CC16) is an ideal candidate for involvement in an inherited predisposition to asthma owing to its chromosomal location, nature and function. Objective: to screen exons of CC16 gene on chromosome 11 for detection of sequence variation in families to determine whether these allelic polymorphism are associated with clinical asthma or not and to detect the relation between type of genetic polymorphism and asthma severity. Patients and Methods: This study included 20 stable asthmatic children with 21 of their atopic family members, also 11 healthy non atopic subjects were included as control group, all cases were subjected to genetic study methods including pedigree construction, PCR and detection of allelic polymorphism. Results: Significant correlation (90%) between homozygous CC16, 38 (AA) (75%) and 38 (AG) (15%) allelic polymorphism and increased prevalence of asthma was detected in families but there was no correlation between CC16 allelic polymorphism and asthma severity. Conclusion: There was a correlation between CC16 allelic polymorphism and increased prevalence of asthma and this gene is present also in normal subjects who are not triggered by environmental factors.

[Nisreen M.El Abiad, Hisham Waheed, William M. Morcos, Samar M. Salem, and Hala Ataa, Olfat G. Shaker. **Association between CC16 Polymorphism and Bronchial Asthma.** Life Science Journal 2012; 9(1):265-270]. (ISSN: 1097-8135). <http://www.lifesciencesite.com> 36

Key words: CC16- Gene polymorphism – PCR- Asthma

1. Introduction:

Asthma is a chronic pulmonary disorder characterized by air way inflammation and bronchial hypereactivity (Hersberger et al., 2010). The etiology of asthma is complex. The dynamics that contribute to disease pathogenesis are multifactorial and involve overlapping molecular and cellular mechanisms, particularly the immune response to respiratory virus infection or allergen sensitization. Several factors may contribute to the development or exacerbation of asthma including age, host factors, genetic polymorphisms, and altered immune responses (Tauro et al., 2008).

Several genetic loci have been associated with asthma, and some of these associations have been replicated in independent studies. Several quantitative traits associated with asthma phenotype have been linked to markers on chromosome 11q13, the gene of Clara cell secretory protein (CC16) is an ideal candidate for involvement in an inherited predisposition to asthma owing to its chromosomal location, nature and function. CC16 gene is located on long arm of chromosome 11 within a region linked to atopy and increase airway responsiveness (Laing et al., 2000). The uniform increase of CC16 after swim exercise indicates that CC16 is of importance in epithelial stress, and may as such be an

important pathogenic factor behind asthma development (Rombeg et al., 2010). High level of CC16 protein produced in the airway appears to function as an anti-inflammatory agents.

The assessment of respiratory risks in vulnerable population has thus for a long time relied on spirometric tests and self-reported symptoms which are relatively late and inaccurate indicators of lung damage. Blood tests measuring lung-specific proteins (pneumo proteins) such as Clara cell protein and surfactant – associated proteins are now available to evaluate the permeability and / or the cellular integrity of pulmonary epithelium (Bernard et al., 2004).

Aim of the study:

To screen exons of CC16 gene on chromosome 11 for detection of sequence variation in families to determine whether these allelic polymorphism are associated with clinical asthma or not and to detect the relation between type of genetic polymorphism and asthma severity.

2. Patients and Methods:

The present study included 20 stable asthmatic children during their regular follow up at Allergy Clinic, Pediatric Hospital, Cairo University. Their

ages ranged from 5-15 years. 21 subjects of their affected atopic family members were included in the study as well after a detailed questionnaire. Patients were classified according to National Asthma Education and Prevention Program (NAEPP) updated (2002): Intermittent asthma: 9 cases; persistent asthma: Mild: 19 cases, Moderate 12 cases, Severe: 1 case. Another 11 healthy subjects with no personal or family history of asthma or other atopic manifestations were included as a control group. All cases were subjected to the following: A detailed history taking for asthma and other atopic manifestations using the standard sheet of allergy clinic, thorough clinical examination; peak expiratory flow rate (PEFR) for diagnosis of air way obstruction; routine laboratory investigations including CBC, urine and stool analysis; total serum IgE. by enzyme – linked immunosorbent assay (ELISA), and genetic study for all cases and control including pedigree construction and molecular study by PCR. Subjects were genotyped by restriction digestion of PCR products with *Sau* 961 endonuclease. The DNA was isolated from 3 ml whole blood using wizard genomic DNA purification Kit (Promega, Madison WI, USA). The sequence was obtained from published data (Hayward, 1995). These primers were supplied by Pharmacia . (Figures 1, 2, and 3)

Exon 1: 5 CAGTATCTTATGTAGAGCCC3`
5CCTGAGAGTTCCTAAGTCCAGG3`

Statistical methods:

All the above data were collected and analyzed using SPSS win statistical package version 11 by analysis of variance or students t-test. Correlations were studied by simple pearsons coefficient. Significance was defined as $P < 0.05$. Comparison

between 3 groups was done using non-parametric ANOVA test.

3. Results:

The study included 20 stable asthmatic children and 21 subject of their affected atopic family members. Twenty one subjects (51%) were males and twenty subjects (49%) were females. Another 11 healthy subjects were included as control cases, 4 subjects (37%) were males and 7 subjects (63%) were females.

Table (1): shows comparison of selected data (age, sex, other atopic manifestations, asthma severity, absolute eosinophilic count (AEC), allelic detection of CC16 gene) in asthmatic group and control group. Table (2) shows comparison between selected data (sex, asthma severity, other atopic manifestations passive smoking, serum Ig E and inhaled corticosteroids) and types of allelic polymorphism either homozygous, heterozygous, or not detected genetic polymorphism. our results show that 31 cases were homozygous AA; 14 males (45.2%) and 17 females (54.8%), 6 cases were heterozygous AG; 5 males (83.3%) and 1 female (16.7%), while not detected allelic polymorphism GG in 4 cases; 2 males (50%) and 2 females (50%).

In homozygous allelic polymorphism (31 cases); 16 (51.6%) were atopic and 15 (48.4%) were non atopic, while heterozygous cases (6), 5 were atopic and 1 (16.7%) was non atopic and not detected allelic polymorphism in 4 cases all were atopic (100%). There was a history of passive smoking in 35 cases (85.3%) of them 27 cases were homozygous, 4 cases were heterozygous and 4 cases with not detected allelic polymorphism.

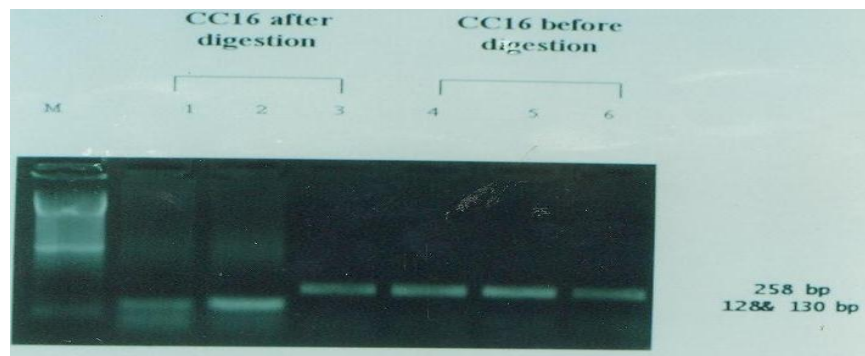


Figure 1. An agarose gel electrophoresis 2% stained with ethidium bromide showing three cases before and after digestion with restriction enzyme *Sau* 961.

M : Molecular DNA Marker (100 bp each)

Lanes 1,2 : 2 cases with homozygous alleles giving bands at 128 and 130 bp.

Lanes 3 : Case with undefined allele after digestion with bands at 258 bp.

Lanes 4-6 : Are the same 3 cases before digestion with bands at 258 bp.

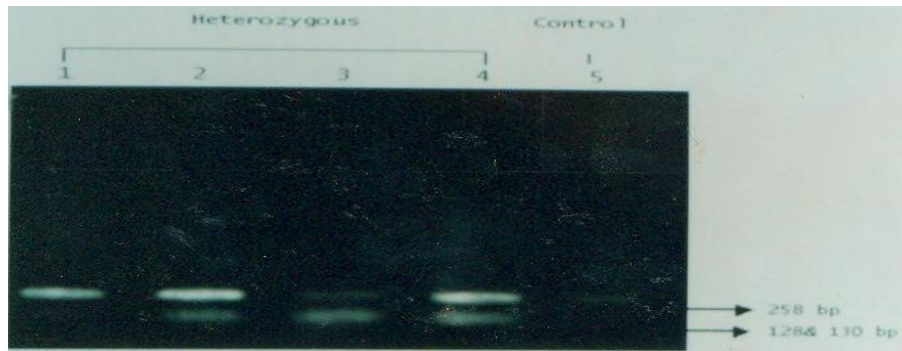


Figure 2. PCR products of CC16 gene after digestion with restriction enzyme *Sau* 961 showing cases with heterozygous alleles at 258, 128, and 130 bp.

Lanes 1-4 : heterozygous alleles.

Lane 5 : control case.

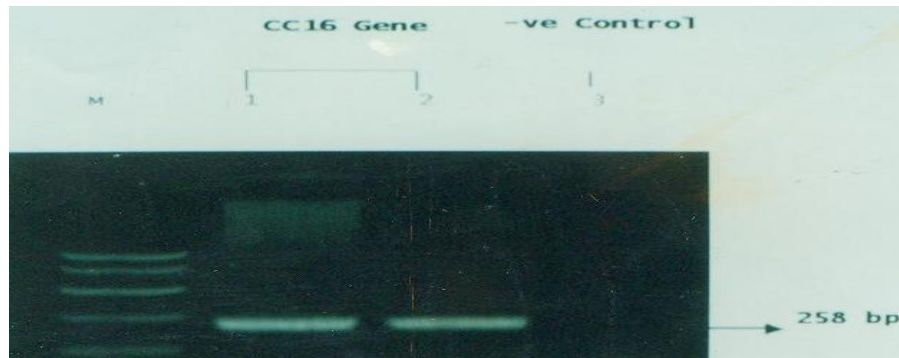


Figure 3. Agarose gel electrophoresis 2% stained with ethidium bromide showing strong gene expression of CC16 gene at 258 (Lanes 1,2) and negative control (Lane 3), M is PCR marker (1000, 750, 500, 300, 150, 50 bp).

Table 1. Characteristics of study and control groups .

Characteristics		Study group n=41	Control group N=11
Age (yr.)	Median \pm SD Range	7 \pm (13.86) (5-53)	6 \pm (4.4) (4-35)
Sex	Male Female	21 (51.2%) 20 (48.8%)	4(36.4%) 7 (63.6%)
Other atopic manifestations	Atopic Non atopic	25 (61%) 16 (39%)	- 11 (100%)
* Asthma severity	* Intermittent * Persistent - Mild - Moderate - Severe	9 (22%) 19 (46.3%) 12 (29.3%) 1 (2.4%)	- -
Serum IgE (IU/L)	Median \pm SD Range	116.5 \pm (179.14) (0-850.4)	81.7 (167.86) (17.40-508.2)
Absolute eosinophilic count (AEC) (cell/mm ³)	Median \pm SD Range	385.35 \pm (364.71) (.00 – 1470.00)	165.00 \pm (184.41) (9-621.00)
Allelic Polymorphism	Homozygous Heterozygous Not detected	31 (75.6%) 6 (14.6%) 4 (9.8%)	1 (9.1%) - 10 (90.9%)

* Asthma severity based on guidelines of NAEPP (1997) update (2002).

Table 2. Comparison between selected data and types of allelic polymorphism

Genetic Group	Homozygous	Heterozygous	Not detected gene
Data	(n=31)	(n=6)	(n=4)
Sex			
Male	14 (45.2%)	5 (83.3%)	2 (50%)
Female	17 (54.8%)	1 (16.7%)	2 (50%)
Severity of asthma			
* Intermittent	5 (16.1%)	2 (33.3%)	2 (50%)
* Persistent			
- Mild	15 (48.4%)	4 (66.6%)	-
- Moderate	11 (35%)	-	1 (25%)
- Severe	-	-	1 (25%)
Other atopic Manifestations			
Atopic n= 25 (61%)	16 (51%)	5 (83%)	4 (100%)
Non atopic n= 16 (39%)	15 (48.4%)	1 (16.7%)	-
Passive smoking			
Yes (n=35)	27 (87.1%)	4 (66.7%)	4 (100%)
No (n=6)	4 (12.9%)	2 (33.3%)	-
IgE			
Median	118.6	26.3	96.8
Inhaled corticosteroids			
n= 13 (31.7%)	11 (35%)	-	2 (50%)

Table 3. Comparison between asthma severity and allelic polymorphism

Genetic Group	Homozygous	Heterozygous	Not detected	Total
Asthma Severity	(n = 31)	(n= 6)	(n=4)	(n=41)
Intermittent	5 (16.1%)	2 (33.3%)	2 (50%)	9 (22%)
Mild	15 (48.4%)	4 (66.6%)	-	19 (46.3%)
Moderate	11 (35.5%)	-	1 (25%)	12 (29.3%)
Severe	-	-	1 (25%)	1 (2.4%)

Based on guidelines provided by asthma education and prevention program, 1997 (NAEPP) (update to 2002).

Table 4. Comparison between serum IgE and allelic polymorphism

Genetic Groups	Homozygous	Heterozygous	Not detected gene
Serum IgE (IU/L)			
Maximum	850.4	201.9	508.2
Minimum	0	0	17.4
Median	118.6	26.3	96.8
S.D.	± 19.74	± 76.59	± 153.83

Table 5. Comparison between AEC and asthma severity

Asthma severity	Intermittent	Mild	Moderate and Severe
AEC			
Maximum	1470	990	1276
Minimum	27	0	20
Median	456.5	192	308.5
S.D.	± 505.4	± 284.4	± 3030.6

Table (3) shows comparison between asthma severity and allelic polymorphism, where no correlation could be found. Table (4) shows comparison between total serum Ig E and allelic polymorphism, where median serum IgE was higher in homozygous group followed by heterozygous group while in not detected allelic polymorphism median serum IgE was the least.

Table (5) shows statistical comparison between AEC and asthma severity, where AEC was higher in intermittent asthma followed by moderate and severe

asthma and the least levels were those of mild asthma.

4. Discussion:

Asthma is a major health problem, it is the most common childhood disease and it is responsible for a significant proportion of school day loss. Asthma affects an estimated 5 to 15% of children in different populations and as such it is a major health care issue in most countries (Krowiec and Lemanske, 2004).

Because of the expression, pattern and function of CC16, it is an intriguing candidate gene for

chronic inflammatory lung diseases such as asthma. It is located on long arm of chromosome 11 q 13, a region occupied by several genes involved in the regulation of allergy and inflammation (Madsen et al., 2008).

In our work, genetic study was done to detect possible association between single nucleotide polymorphism (SNP) of CC16 gene exon 1 38 (AG) and asthma, and correlate between it and asthma severity. As regards asthma severity we followed NHLBI classification. The most common type of asthma was mild persistent asthma which represented 46.3% of cases, moderate persistent asthma represented 29.3%, intermittent asthma 22% and the least common was severe persistent asthma which represented 2.4%. The present work demonstrated that 53% came from urban area in comparison to 47% of patients came from rural areas. This is in accordance with the work of Reidler et al. (2001), who demonstrated that growing upon a farm confers protection against the development of atopy and asthma, also Von Mutius (2000), emphasized the importance of environmental factors in the pathogenesis, precipitation and aggravation of asthma and other allergic diseases. This could be explained by outdoor pollutants especially industrial smog that are responsible for the higher incidence of asthma in urban areas.

We found 61% of cases having other atopic manifestation which is consistent with Jane et al. (2000), who suggested a strong association between asthma and atopy. High incidence of smoking (85.4%) was found among the parents of our patients agreeing with the result of Norris et al. (2000), who showed higher incidence of parental smoking (62%). Also Shijubo et al. (1999), and Herman et al. (1998), suggested that tobacco smoking has been associated with 30% decrease in serum CC16 protein.

Atopy is a genetic susceptibility to produce IgE directed towards common environmental allergen. This laboratory finding together with elevated blood eosinophils with the presence of respiratory symptoms aid in the clinical diagnosis (Howard et al., 2000). AEC in our patients was significantly high (385.35 ± 364 cells/cmm) than in control (165.09 ± 184.4 cells/cmm) which is consistent with Micheal et al. (2005), who stated that eosinophilia greater than 4% or 300-400/ μ L supports the diagnosis of asthma but an absence of this finding is not exclusionary. High serum IgE level was detected in our cases compared with control which is consistent with the study of Micheal et al. (2005), they reported that total serum IgE levels greater than 100 IU are frequently observed in patients experiencing allergic reactions but it is not specific for asthma and may be observed in other allergic conditions.

PEFR is a useful measure of pulmonary function and is frequently utilized in asthma management, it also correlates with the degree of asthma severity (Van Helden et al., 2001) which is consistent with the present study.

We have observed a strong association between CC16 polymorphism and asthma. Thirty-one subjects (75%) of asthmatic patients were found to be homozygous for the gene 38 (AA), 6 subjects (15%) were heterozygous 38 (AG) and only 4 subjects (9.7%) were negative for genetic polymorphism 38 (GG), which were strongly different than control group where we found 10 cases (91%) negative for polymorphism and only one case (9%) was homozygous for polymorphism 38 (AA). This was consistent with Laing et al. (1998), who concluded significant relationship between genotype differences at position 38 of exon 1 of the CC16 gene and the risk of asthma which was increased 6.8 fold in homozygous subjects 38 (AA) and 4.2 fold in heterozygous 38 (AG). Also Ingrid et al. (2000), found that homozygous 38 (AA) subjects had reduced plasma levels of CC16 protein compared with 38 (AG) and (GG) subjects and stated that each additional 38 A allele was estimated to produce a 15% decrease in geometric means of plasma level of CC16 protein and associated with 63% increased risk of asthma.

Regarding control cases, one case was detected to be homozygous for polymorphism 38 (AA) which was consistent with Laing et al. (1998), who found 10.2% of participants homozygous for polymorphism 38 (AA). This may be due to lack of exposure to triggering factors of asthma. On the other hand, Mansur et al. (2002), observed no significant difference in the distribution of positive bronchial reactivity to metacholine across the three gene types.

Homozygous polymorphism 38 (AA) was detected in 48% of mild asthma cases, in 35% of moderate asthma cases and in 16.1% of intermittent asthma which is consistent with Sengler et al. (2003). Heterozygous polymorphism 38 (AG) was detected in 66.7% of mild asthma cases and in 33.3% of intermittent asthma. While not detected gene polymorphism was present in 25% of moderate asthma cases, 50% of intermittent asthma and in 25% of severe asthma cases. We could not correlate between the percentage of allele polymorphism and the severity of asthma due to small size of the sample.

Sengler et al. (2003), found that in asthmatic multicenter asthma study participant, FEV₁ value differ significantly between CC16 phenotypes, the lowest value were observed in children homozygous 38 (AA) followed by heterozygous 38 (AG). On the other hand Zhonghua et al. (2004), didn't reveal any

association between the genotype and allele frequencies of gene and severity of asthma. These contradictory results may be explained by race difference as it is possible that there is significant degree of genetic difference between populations.

5. Conclusion:

There is a correlation between CC16 allelic polymorphism and increased prevalence of asthma and this gene is present also in normal subjects who are not triggered by environmental factors. On the other hand no relation between CC16 allelic polymorphism and asthma severity could be detected in our study.

Corresponding author

Hisham Waheed

Child Health Department, National Research. Center
Cairo, Egypt

hishamwb@yahoo.com

References:

- Bernard A, Carbonnelle S, Nick milder M, De Burbure C. Non-invasive biomarkers of pulmonary damage and inflammations. Application to children exposed to ozone and trichloramine. *J. Toxicol. And Applied Pharm.* 2004, 206 (2): 185-90.
- Hayward A. Who's to blame asthma. *Lancet.* 1995, 346:1343.
- Herman C, Aly B, Nyberg C, et al. Determinants of Clara cell protein (CC16) concentration in serum: a reassessment with two different immunoassay. *Clin. Chem. Acta.* 1998; 272: 101-10.
- Hersberger M, Thun G, Imboden M, Brandstatter A, et al. Association of STR polymorphism in CMA 1 and IL-4 with asthma and atopy: The SAPALDIA Cohort. *J. Human Immun.* 2010; 71 (11): 1154-60.
- Howard T, Meyers D, Bleecker E, et al. Mapping susceptibility genes for asthma and allergy. *J. Allergy Clin. Immunol.* 2000; 105 (suppl): 5477-81.
- Ingrid A, Laing I, Cedric H, et al. Association between plasma CC16 levels, the 38 (AG) polymorphism, and asthma. *Am. J. Respir. Crit. Care. Med.* 2000 ; 161: 124-27.
- Jane R, Clark I, John L, et al. Evidence for genetic association between asthma and atopy. *Am. J. Respir. Crit. Care. Med.* 2000 ; 162 (6): 2188-93.
- Krowiec M and Lemanske R. Wheezing in infants in : Behrman R., Kliegman R., Jenson H. : Nelson text book of Pediatrics. 2004 (17th ed) WB : Saunders com. 3 (379): 1417-19.
- Laing I, Al-fred B, Paul R, et al., Association between CC16 levels, 38 (AG) polymorphism and asthma *Am. J. of Resp. and Crit. Care Med:* 2000, 161: 124-27.
- Laing I, Goldbalatt J, Eber E, et al. A polymorphism of the CC16 gene is associated with an increased risk of asthma. *J. Med. Genet.* 1998, 35: 463-67.
- Madsen C, Durand K, Nafstad P, et al. Association between environmental exposure and serum concentration of Clara cell protein among elderly men in Oslo, Norway *J. Environmental Research.* 2008, 108 (3) : 354-60.
- Mansur A, Fryer A, Hepple M, et al. An association study between the Clara cell secretory protein (CC16) 38 (AG) Polymorphism and asthma phenotypes. *Clin. Exp. Allergy.* 2002, 323: 994-99.
- Micheal J, Morris P, Perkins H. et al. Asthma. *J. Medicine .* 2005, 6: 1-11.
- National Heart, Lung and Blood Institute. Global strategy for asthma management and prevention. Bethesda, M:D:National Institute of Health. 2002, 02-3659.
- Norris G, Larson T, Koeing J, et al. Asthma aggravation, passive smoking, combustion, and stagnant air. *Thorax.* 2000, 55: 466-70.
- Reidler J, Von E, MaCaubas C, et al. Exposure to farming in early life and development of asthma and allergy a cross sectional survey. *Lancet.* 2001, 385: 1129-33.
- Romberg K, Bjermer L, Tufvesson E. Exercise but not mannitol provocation increase urinary Clara cell protein (CC16) in elite swimmers. *J. Resp. Med.* 2010, 105 (1): 31-36.
- Sengler C, Heinzmann A, Jerkic S, et al. Clara cell protein 16 (CC16) gene polymorphism influences the degree of air way responsiveness in asthmatic children. *J. Allergy Clin. Immunol.* 2003, 3 : 515-19.
- Shijubo N, Itoh T, Yamaguchi Y, et al. Serum BAL Clara cell 10 DK a protein CC10 levels and CC10 positive bronchiolar cells are decreased in smokers. *Eur. Respir. J.* 1999, 10: 1108-14.
- Tauro S, Su Y, Thomas S, et al. Molecular and cellular mechanisms in the viral exacerbation of asthma. *J. Microbes and Infection.* 2008, 10 (9): 1014-23.
- VanHelden S, Hoal E, Van Helden P, et al. Factors influencing peak expiratory flow in teenage boys. *S. Afr. Med.* 2001, 91 (4): 996-1000.
- Von Mutius E. The environmental predictors of allergic disease. *J. Allergy Clin. Immunol.* 2000, 105: 9-19
- Zhonghuo Y, Xue Y, Xue Z. Study an association between CC16 gene 38 (AG) mutation and asthma in patients of Han population in Chong qung, China. *Chinese J. of Medical Genetics.* 2004, 94: 1003-06.

1/5/2012

Laparoscopic / Thoracoscopic Ivor Lewis Esophageal Resection for Cancer (Report of Two Cases and Review of the Literature)

Saleh M. Aldaqal

Department of Surgery; Faculty of Medicine, King Abdulaziz University, Jeddah, Kingdom of Saudi Arabia
Arabia. sdaqal@yahoo.com

Abstract: Open esophagectomy may be associated with significant morbidity and mortality. With the increasing experiences in laparoscopic and thoracoscopic techniques, minimal invasive approaches to esophagectomy are being explored to determine the feasibility, results, and potential advantages.

We will present our experience in two cases of laparoscopic / thoracoscopic Ivor Lewis esophageal resection for carcinoma of the lower esophagus. The presentation of the two cases, their surgical approach and postoperative course will be discussed in addition to literature review of similar cases.

[Saleh M. Aldaqal. **Laparoscopic / Thoracoscopic Ivor Lewis Esophageal Resection for Cancer (Report of Two Cases and Review of the Literature)**. Life Science Journal 2012; 9(1):271-276]. (ISSN: 1097-8135). <http://www.lifesciencesite.com>. 37

Keywords: Laparoscopic, Thoracoscopic, Ivor Lewis, Esophageal

Introduction

Although minimal invasive esophagectomy have been reported since 1992^[1], it is still considered to be investigative in most institutions. It has the potential to improve mortality, morbidity, hospital stay, and functional outcome when compared to the open methods^[2]. It is expected that with further improvements in instrumentation and experience, these difficult procedures may become more accessible and widely practiced.

Case 1

A 55-year-old male was presented with a history of progressive dysphagia to liquid and solid foods for six months. In addition, the patient also reported generalized fatigability, loss of appetite and weight loss of about 10 kg over a period of three months before seeking medical advice. He was diabetic and smoker for 30 years. There was no significant family history of cancer.

Physical examination was unremarkable apart from significant weight loss.

Routine blood investigations were normal. Plain chest films were unremarkable. Upper gastrointestinal endoscopy revealed a malignant stricture at the lower part of esophagus starting at 35 cm below the dental arch which could not be passed by the endoscope. Multiple biopsies were taken which showed adenocarcinoma of the lower esophagus.

Computerized tomography (CT) scan of the thorax and abdomen with oral and intravenous contrasts revealed a circumferential thickening at the distal end of the esophagus with a mass extending to the gastric fundus with no mediastinal and para aortic lymphadenopathy nor distant organ metastases.

The patient was operated in February 2009 where laparoscopic / thoracoscopic Ivor Lewis esophagectomy with mini right thoracotomy was performed. The duration of the abdominal dissection was 4.5 hours, and the thoracic dissection was 3.5 hours. Total blood loss was 240 ml (Table 1). The patient stayed overnight in the Intensive Care Unit (ICU) and were transferred to the ward the following day. A gastrograffin study was done on the third postoperative day and showed intact anastomosis (Fig. 10). Oral nutrition was started on fourth postoperative day, and was discharged on fifth postoperative day. Histopathology was showed a well to moderately differentiated adenocarcinoma, and both gastric and esophageal margins were negative for tumor involvement. The tumor involved full thickness of muscularis propria, 3 mm away from the deep margin; the maximum tumor size was 9 cm with no lymphovascular invasion. There was intestinal metaplasia in the adjacent esophageal mucosa. Two out of ten mediastinal lymph nodes were positive for tumor metastasis. Consequently we evaluated the tumour in stage III, pT3pN1M0. The patient was submitted to adjuvant chemo radiotherapy, which was well tolerated and is still alive up to this report .

Case 2

A 53-year-old male was presented with a history of progressive dysphagia to liquid and solid foods for 5 months. The patient also reported loss of appetite and weight of about 15 kg over a period of two months before seeking medical advice. He had no significant past medical or surgical history. He was a smoker for more than 30 years. There was no significant family history of cancer.

Physical examination was unremarkable apart from significant weight loss.

Routine blood investigations were normal. Plain chest films were unremarkable. Upper gastrointestinal endoscopy revealed esophageal mass at 30 cm below the dental arch and extended to the cardia of the stomach. Multiple biopsies were taken which showed adenocarcinoma of the lower esophagus.

CT scan of the thorax and abdomen with oral and intravenous contrasts revealed a circumferential thickening at distal part of the esophagus extending to the fundus of the stomach with one sub diaphragmatic lymph node, there was no mediastinal lymph node enlargement.

The patient was operated in June 2009 where laparoscopic / thoracoscopic Ivor Lewis esophagectomy with mini right thoracotomy was performed. The duration of the abdominal dissection was 3.5 hours, and the thoracic dissection was 2.5 hours. Total blood loss was 200 ml (Table 1). The patient stayed overnight in the Intensive Care Unit (ICU) and was transferred to the ward the following day. A gastrograffin study was done on the third postoperative day and showed intact anastomosis. Oral nutrition was started on fourth postoperative day, and was discharged on fifth postoperative day. Histopathology was showed a well differentiated adenocarcinoma, and the tumor size was 6 cm. Both gastric and esophageal margins were negative for tumor deposit. The tumor involved full thickness of the muscularis propria, 3 mm away from the deep margin with no lymphovascular invasion. Fourteen lymph nodes were identified and all were negative for tumor deposition (Tumor in pathologic stage II b,pT3pN0M0). The patient was submitted to adjuvant chemo radiotherapy, which was well tolerated and is still alive up to this report .

Operative Technique

1) Abdominal part:

The operative procedures done for both patients were the same. Patient was placed in supine position with legs apart. Five ports were inserted at the upper abdomen as shown in figure (1). One 11-mm port is used in right epigastrium for access for stapling devices to create the gastric tube. The left lobe of the liver was retracted upward to expose the esophageal hiatus using self-retaining system. The laparoscopic dissection starts by dividing the hepatogastric ligament toward the right crus of the diaphragm. The right crus was exposed and dissected from the top of the hiatus to the decussation with the left crus. This plane was developed then cephalad along the left crus to develop a retro-esophageal window and a penrose drain was passed around the esophagus and used for

retraction (Fig. 2). The dissection was directed toward the mid to upper great curve just outside of the gastroepiploic arcade and was directed cephalad toward the short gastrics were all divided. The plane along the greater curve was developed and continued distally, care was taken to avoid injury to the major gastroepiploic arcade as it constitutes the major source of blood flow to the gastric tube (Fig. 3). Dissection was continued along this plane dividing the connecting vessels to the omentum. Care should be taken to preserve enough tissue to keep a healthy arcade without leaving too much tissue that will result in excessive bulk of tissue on the gastric tube lead to tension on the arcade or make it difficult for the gastric tube to ascend through the hiatus along the left crus. The dissection along the greater curve continues toward the hepatoduodenal attachments. These were divided along the lateral duodenum and gallbladder area to complete the Kocher maneuver. The greater curve is lifted and all the retro-gastric attachments were divided, the left gastric vascular complex including vein, artery, and lymph nodes were dissected, and the vessels were divided using an endoscopic vascular stapler (Endo-GIA II, U.S. Surgical). An area just above the first 2 to 3 arcades of the right gastric artery into the pyloro-antral area was chosen for firing the first stapler (Fig. 4). The vascular load was used here to minimize bleeding. The first few arcades of the right gastric vessels into the pyloroantral area were spared and the stapler is fired in a perpendicular orientation to the lesser curve. As the construction of the gastric tube continues, care was taken to align the stapler parallel to the greater curve arcade. we continue to apply gentle stretching of the stomach as the tube was constructed. Once the gastric conduit was completed, a pyloroplasty was performed. The muscle was divided open along the length of the pyloric channel. The pyloric incision was closed transversely using nonabsorbable 2-0 sutures. Next, mobilization at the hiatus into the thoracic cavity, in a circumferential manner was performed. The tip of the gastric tube was sewn to the lower end of the lesser curve staple line on the side of the specimen. The gastric tube was assessed for viability and adequate tension-free length.

2) Thoracic part:

The patient was positioned on the operating table in a left decubitus after he was intubated with double lumen endotracheal tube. Four ports were inserted in the right hemithorax as shown in figure (5). Following port placement, a thorough thoracoscopic exploration was performed. For the dissection, we used the ultrasonic dissecting instrument with a relatively sharp tip (U.S. Surgical); which was an

excellent dissecting tool. The inferior pulmonary ligament was divided to the inferior pulmonary vein and a plane between the pericardium and periesophageal area was developed (Fig. 6). All lymph nodes and periesophageal fat were taken en bloc with the esophagus. The dissection plane continued along the pericardium and airway, contralateral pleura, aorta, azygos vein, and thoracic duct. The mediastinal pleura along the esophagus was opened toward the azygos vein and extended from the azygos vein to the diaphragm. A penrose drain was passed around the esophagus and used for retraction. The azygos vein was divided (Fig. 7) using a vascular stapler (Endo-GIA II, U.S. Surgical). Above the level of the azygos vein, the dissection plane was maintained directly onto the esophageal wall (Fig. 8). This plane was continued cephalad toward the thoracic inlet. The subcarinal lymph node packet and all surrounding peri-esophageal nodes, fat, and hiatal hernia sac was dissected en-block with the esophagus down to the diaphragmatic crus. The distal dissection continues until visualization of the crus has occurred. The assistant or surgeon can retract the esophagus anterior to posterior

periodically to allow a circumferential view as the dissection was performed. Careful dissection and visualization of aorto-esophageal vessels should be performed and larger branches clipped before division to minimize bleeding.

The esophagus was transected and a 25-mm EEA anvil was inserted into the esophageal stump; then the purse string was tied. The fundic tip was opened and a 25-mm end-to-end stapler (EEA, U.S. Surgical) was passed through the chest and this opening and the exit point of the EEA was through the posterior gastric tube, avoiding the area of the short gastrics posteriorly and avoiding too close a proximity to the lesser curve staple line (Fig. 9). The EEA device was docked with the anvil and fired. A nasogastric tube was inserted under direct visualization across the anastomosis and the tip should lie in the gastric tube above the pyloroplasty. The opening in the tip of the gastric tube was closed with a linear stapling instrument. A 4-5 cm mini thoracotomy was performed to remove the specimen and two chest tubes were inserted and all the port sites were closed by sutures.

Table 1. Summary of the perioperative findings of Cases 1 and 2

	Age (year)	Sex	Operative Time (hour)		Blood Loss (ml)	ICU Stay	Total Hospital Stay (Day)
			Abdominal Dissection	Thoracic Dissection			
Case 1	55	Male	4.5	3.5	240	1	5
Case 2	53	Male	3.5	2.5	200	1	5
Mean	54		4	3	220	1	5

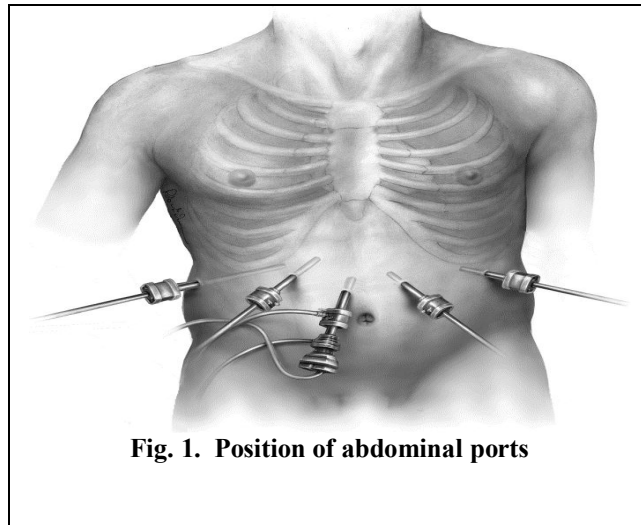


Fig. 1. Position of abdominal ports

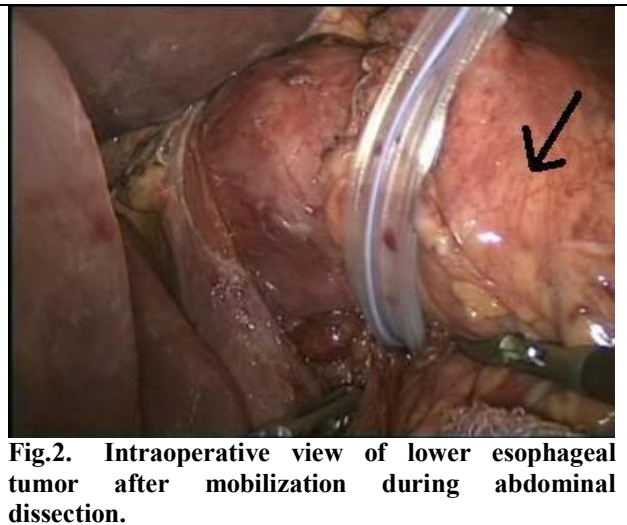


Fig.2. Intraoperative view of lower esophageal tumor after mobilization during abdominal dissection.



Fig. 3. Dissection of gastroepiploic arcade

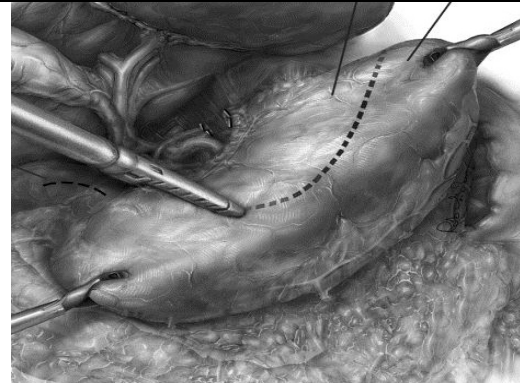


Fig. 4. Creation of gastric tube

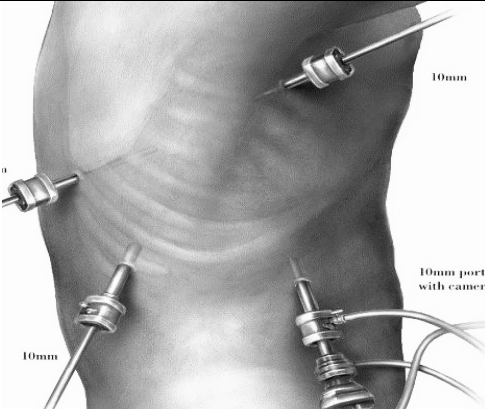


Fig. 5. Position of thoracic ports

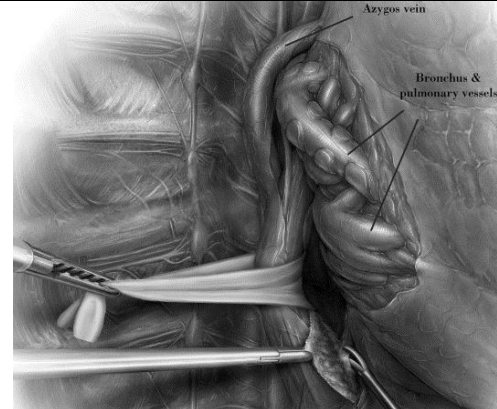


Fig. 6. Dissection of thoracic esophagus



Fig. 7. Transection of azygos vein

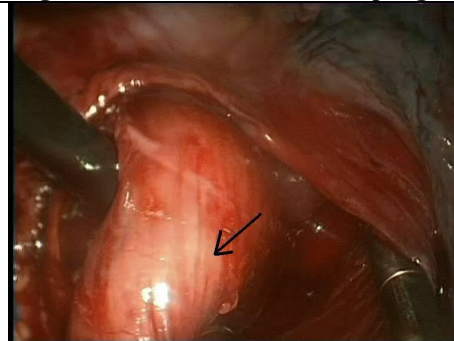


Fig. 8. Intraoperative view of upper esophagus after mobilization during thoracic dissection

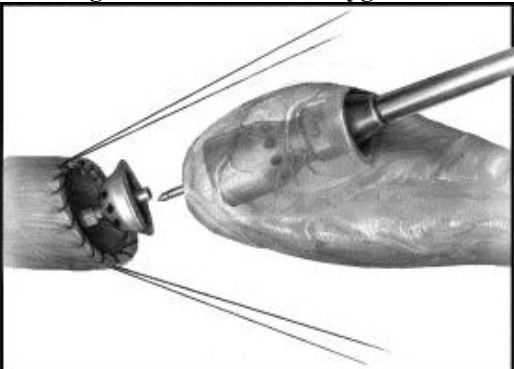


Fig. 9. Gastroesophageal anastomosis in the upper part of the thorax

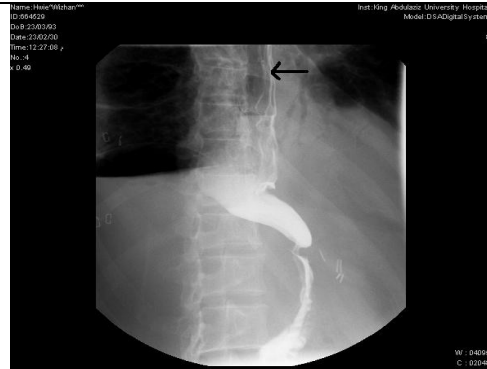


Fig. 10. Postoperative gastrograffin swallow of the same patient.

Discussion

In an attempt to lower morbidity of the open esophageal resection for cancer, some centers have explored Minimally Invasive Esophagectomy (MIE). The potential benefit of this technique is to improve the pain control and pulmonary function by avoiding synchronous thoracotomy and laparotomy incisions. Recently, several series have described the feasibility and safety of minimally invasive Ivor Lewis oesophagectomy. The extent of minimally invasive techniques has ranged from a laparoscopic abdominal component with a thoracotomy or mini-thoracotomy, to a thoracoscopic thoracic component and an open abdominal procedure^[3,4].

We used a minimally invasive abdominal and thoracoscopic technique with mini thoracotomy component in both of our patients during minimally invasive Ivor Lewis oesophagectomy. MIE using combined laparoscopic and thoracoscopic approach has the potential to offer an oncologically complete operation, while taking advantage of the benefits of minimally invasive surgery, which may translate into less overall morbidity. Recent data from other publications also suggests that lymph node yields may be improved, although insufficient data exist at this time to comment on oncologic results or outcomes with this technique^[5,6]. On the other hand, MIE is technically a very challenging operation with a very steep learning curve and is only performed in few centers across the world.

The published experience with minimally invasive Ivor Lewis esophagectomy has been limited to case reports and small case series. The use of thoracoscopy and/or laparoscopy for esophageal resection was introduced in 1992 by **Cushieri et al**^[7]. The first report of laparoscopy combined with thoracotomy was published in 1996 by **Jagot et al**^[8]. In this serie, six patients underwent laparoscopic mobilization of the stomach combined with a right thoracotomy and intrathoracic anastomosis. There were no conversions to an open procedure and all patients had an uneventful recovery. The first description of a complete minimally invasive approach was reported in 1999, when **Watson et al.**^[9] described two patients where a hand-assisted laparoscopic approach was combined with a thoracoscopic anastomosis. There was no report of complications. Recently, **Nguyen et al.** described a total of three patients who had completely laparoscopic procedure combined with a thoracoscopic anastomosis^[10]. All the three patients had an uneventful postoperative course.

To date, there is no controlled comparative trial between open esophagectomy and MIE. **Nguyen et al.**^[10] compared 18 thoracoscopic and laparoscopic resections with their historical experience on open

resections. Operative times, blood loss, transfusion requirements, ICU and hospital stays were shorter after MIE but without any difference in fistula or respiratory complication rates.

Review of the literature from 1992 to 2007 showed 609 patients underwent laparoscopic and thoracoscopic esophageal resection for cancer^[11,12]. Conversion rate was 4.7%, operative time was between 220 and 550 minutes (mean 350), hospital stay was between 6.5 and 16 days (mean 9), mortality 2.4 to 18% (mean 14%), over all morbidity 43%, respiratory complication 16.7%, re-operative rate 8.3%, vocal cord paralysis 3.1%, anastomotic leaks 9%, number of lymph nodes retrieved were between 9 and 48 (mean 16.5), and duration of follow up was between 3 and 32 months (mean 23)^[12,13]. Other reported complications of MIE were chylothorax, tracheo-bronchial tears or necrosis, massive bleedings, splenectomies, visceral injuries (pancreas, colon). As many of the studies stated that they reported only "major" complications, the incidence of common surgical complications such as surgical site infections or thromboembolic complications was not mentioned by most of the series and thus no reliable incidences could be calculated^[14,15].

There was no morbidity or mortality in our two patients. The mean operative time was 4 hours for the abdominal dissection and 3 hours for the thoracic dissection and anastomosis, mean blood loss was 220 ml, mean ICU stay was 1 day, mean hospital stay was 5 days, and mean follow up was 1 year (Table 1).

In conclusion, laparoscopic / thoracoscopic Ivor Lewis esophagectomy is feasible. It reduces hospital stay and perioperative morbidity with quick postoperative recovery. There is a need for more prospective studies to compare the open esophagectomy with laparoscopic esophageal resection regarding the overall morbidity, mortality and the oncological outcome. We have found that it is a safe technique with preliminary results. Although very feasible, it should not be attempted without sufficient training and should be carried out only in specialized medical centers and by surgeons with adequate experience with open esophagectomy.

Acknowledgment

I would like to thank Professor Mohammed Alharbi for his review of the manuscript, and Mrs. Nora N. Yusuf and Mrs. Joy De Silva for their secretarial help.

Corresponding author

Saleh M. Aldaqal

Departments of Surgery, Faculty of Medicine, King Abdulaziz University, Jeddah, Kingdom of Saudi Arabia.

sdaqal@yahoo.com**References**

- [1] Nguyen NT, P.R. Schauer, J.D. Luketich. (1999): Combined laparoscopic and thoracoscopic approach to esophagectomy. *J Am Coll Surg*; 188(3): 328–332.
- [2] Law S, J. Wong (2002): Use of minimally invasive oesophagectomy for cancer of the oesophagus. *Lancet Oncol*; 3(4): 215–222.
- [3] Atkins B, Shah A, Hutcheson K, (2004), Reducing hospital morbidity and mortality following esophagectomy. *Ann Thorac Surg*; 1170–1176.
- [4] Sutton CD, White SA, Marshall LJ, Berry DP, Veitch PS., (2002), Endoscopic assisted intrathoracic oesophagostomy without thoracotomy for tumors of the lower oesophagus and cardia. *Eur J Surg Oncol* : 46–48.
- [5] Yamamoto S, Kawahara K, Maekawa T, (2005), Minimally invasive esophagectomy for stage I and II esophageal cancer. *Ann Thorac Surg*; 80(6): 2070–2075.
- [6] Gossot D, Cattani P, Fritsch S, (1995), Can the morbidity of esophagectomy be reduced by the thoracoscopic approach? *Surg Endosc*; 9(10): 1113–1115.
- [7] Cuschieri A, Shimi S, Banting S. (1992), Endoscopic oesophagectomy through a right thoracoscopic approach. *JR Coll Surg Edinb*; 37:7–11.
- [8] P. Jagot, A. Sauvanet, L. Berthoux and J. Belghiti, (1996), Laparoscopic mobilization of the stomach for oesophageal replacement, *Br J Surg* 83; 540–542.
- [9] Watson DI, Davies N, Jamieson GG. (1999), Totally endoscopic Ivor Lewis esophagectomy. *Surg Endosc*; 13:293–7.
- [10] Nguyen NT, Hinojosa MW, Smith BR, Chang KJ, Gray J, Hoyt D., (2008), Minimally invasive esophagectomy: lessons learned from 104 operations. *Ann Surg* ; 248(6): 1081-91.
- [11] Bernabe KQ, Bolton JS, Richardson WS., (2005), Laparoscopic hand-assisted vs. open transhiatal esophagectomy. A case-control study. *Surg Endosc* : 334–337.
- [12] Decker G, Coosemans W, De Leyn P, Decaluwé H, Nafteux P, Van Raemdonck and et al., (2009), Minimally invasive esophagectomy for cancer. *Eur J Cardiothorac Surg* ; 35(1): 13-21.
- [13] Santillan AA, Farma JM, Meredith KL, Shah NR, Kelley ST., (2008), Minimally invasive surgery for esophageal cancer. *J Nation Compr Canc Netw*; 6(9): 879-84. Review.
- [14] Sunpaweravong S, Chewatanakornkul S, Ruangsri S., (2008), Initial experience and result of thoracoscopic and laparoscopic esophagectomy. *J Med Assoc Thai*; 91(8): 1202-5
- [15] Fabian T, Martin JT, McKelvey AA, Federico JA., (2008), Minimally invasive esophagectomy: a teaching hospital's first year experience. *Dis Esophagus*; 21(3): 220-5.

1/5/2012

Determinants of Patient Satisfaction in the Surgical ward at a University Hospital in Saudi Arabia

Saleh M. Aldaqal¹; Hattan Alghamdi¹; Hassan AlTurki¹; Basem S. El-deek² and Ahmed A. Kensarah¹

¹Department of Surgery; Faculty of Medicine, King Abdulaziz University, Jeddah, Kingdom of Saudi Arabia

²Department of Community Medicine, Faculty of Medicine, King Abdulaziz University, Jeddah, Kingdom of Saudi Arabia

sdaqal@yahoo.com

Abstract: Objectives, to determine the factors that affect patient satisfaction in the surgical ward of a university hospital and provide useful information for the hospital management, wishing to improve patient satisfaction in Saudi Arabia. Methods: A cross-sectional study was conducted from June 2011 till to August 2011 in the surgical ward at King Abdulaziz University Hospital in Jeddah, Saudi Arabia. A patient satisfaction questionnaire was administered to the first 95 patients ready for discharge from the hospital during the study period, and we obtained data from patients who rated their satisfaction with care provided. We analyzed the data to identify potentially modifiable factors associated with dissatisfaction. Results: The patients included 55 males (58.5%) and 39 females (41.5%). The average age of patients was 45.9 years (range 15-83 years) and the average length of stay was 6.43 days (range 1–50 days). The overall satisfaction rate was 89.6%. The level of satisfaction was high regarding the explanation of the on call doctor about the operation in the emergency department (75.5%), Doctor's reception in the clinic (81.25%), surgical team reception in the ward (79.75%), Response of the team about the patient's questions (71.75%), and Safety level in the hospital (74.75%). The lowest level of satisfaction was for the waiting time in the emergency (40%), the waiting time in the clinic (62%), the response of consulting doctors of the other departments (60.75%), the explanation of the surgical team about the life style after operation (53%), and the quality of food in the hospital (56.75%). There was a strong relation between the patient dissatisfaction and patient's age (P value: 0.003), gender (P value: 0.001, with more female satisfaction), and duration of hospital stay (P value: 0). Conclusion: In a studied area, the factors that influence patient satisfaction are old age (> 50 years old), male gender, waiting time in emergency department and out-patient department (clinic), quality of food, quick response of consulting doctors of other departments, explanation of surgical team about lifestyle after surgery (eating habits, wound management, having shower and exercise), and length of hospital stay. We recommend the hospital management to address these factors to improve patient satisfaction.

[Saleh M. Aldaqal; Hattan Alghamdi; Hassan AlTurki; Basem S. El-deek and Ahmed A. Kensarah. **Determinants of Patient Satisfaction in the Surgical ward at a University Hospital in Saudi Arabia.** Life Science Journal 2012; 9(1):277-280]. (ISSN: 1097-8135). <http://www.lifesciencesite.com>. 38

Key Words: Patient satisfaction, Questionnaire, Surgical ward, Hospital management

1. Introduction

Patient satisfaction is a critical health care outcome indicator and should be given focus by the hospital administrators. From a management perspective, patient satisfaction with health care is important for several reasons ⁽¹⁾. First, satisfied patients are more likely to maintain a consistent relationship with a specific provider. Second, by identifying sources of patient dissatisfaction, an organization can address system weaknesses, thus improving its risk management. Third, satisfied patients are more likely to follow specific medical regimens and treatment plans. Finally, patient satisfaction measurement adds important information on system performance, thus contributing to the organization's total quality management ⁽²⁾. The Department of Surgery at King Abdulaziz university hospital (KAUH) in Jeddah, which is a 750-bed, tertiary care hospital with all types of medical

services; has developed and implemented a surgical quality improvement plan in 2009 that aimed to improve the health care provided to the patients. Patient satisfaction was one of the important indicators of this plan in which our study was designed. The objective of the study is to determine the factors which affect patient satisfaction in surgical ward of our hospital and provides important information for hospital management to improve patient satisfaction.

2. Patients and Methods:

After obtaining the ethical approval from the local Ethical Committee, a cross-sectional study was conducted from 14th of June 2011 till 1st of August 2011 in the surgical ward at KAUH. It is a patient-centered on socio-demographic factors and patient expectation. Questionnaires were distributed to the first 125 patients ready for discharge from the

hospital during the study period. However, only 95 patients returned a completely filled form. No individual identifying information was included on the surveys and participants were given no incentive to participate. Patients were excluded if they had hospital stays of less than 1 day to ensure that they had adequate time to interact with the hospital. The questionnaire was designed based on factors came from examination of the literature review on patients satisfaction. It is a patient-centered on socio-demographics factors as age, gender, social status and patient health status and the patient expectations. The questionnaire has 5 indices; Emergency index which has 7 questions; Outpatient and admission office index which has 12 questions; Service before operation with 8 questions; Service after operation with 12 questions and finally, Hospital service in general included 12 questions. Each question has five responses from "strongly agree" to "strongly disagree" in the form of a Likert scale of items. Patient satisfaction was measured by asking participants to rate: overall, how satisfied they were with their care, 1 = very dissatisfied to 5 = very satisfied; whether they would be willing to return to

the hospital for future care, 1 = not willing to 5 = very willing; and whether their needs had been met by the services at the hospital, 1 = not at all to 5 = very much so.

The data were entered and analyzed using the statistical package for social sciences (SPSS Inc, Chicago, IL, USA), version 17. Statistical significance was determined when the p value was < 0.005 , by using paired T-test for comparison.

3. Results:

Patients included 55 males (58.5%) and 39 females (41.5%). The average age of patients was 45.9 years (SD = 2, range = 15-83 years). Nineteen percent of patients had completed primary school, 24% had completed high school, 39% had completed undergraduate studies, and 13% had completed postgraduate degrees. Five percent did not provide their education level. The average length of stay was 6.43 days (SD = 2.88, range = 1-50 days). Fifty patients (53.2%) were admitted from emergency department while 44 patients (46.8%) were admitted from out-patient department (table 1).

Table 1 socio-demographic factors of the patients

Variable	Number	%
Total No. of patients	94	100
• Gender		
○ Male	55	58.5
○ Female	39	41.5
• Age Group		
○ <30 yr	23	24.5
○ 30-40 yr	16	17
○ 40-50 yr	12	12.8
○ 50-60 yr	17	18.1
○ >60 yr	17	18.1
• Type of Surgery		
○ General Surgery	78	83
○ Other Subspecialities	10	11.3
• Level of Education		
○ High	31	33
○ Low	37	39.4
• Admission		
○ Emergency Admission	50	53.2
○ Elective Admission	44	46.8
• Duration of the Hospital Stay		
○ 1-5 days	31	33
○ 6-15 days	35	37.2
○ 16-30 days	18	19.1
○ 31-50 days	5	5.3

The overall satisfaction rate was 89.6%, male satisfaction rate was 83.4% while female satisfaction rate was 88.7%. The overall level of satisfaction in emergency service was high for explanation of on-call doctor to the surgical intervention (75.5%), while the lowest was for waiting time in Emergency for more than 3 hours (40%). On Outpatient department and admission office service, the highest value was

for doctor's reception in the clinic (81.25%), while the lowest index was for waiting time in the clinic for more than one hour (62%). On the service before the operation, the highest value was for surgical team reception in the ward (79.75%), while the lowest value was for the Response of consulting doctors of other departments (60.75%). On the Service after the operation, the highest value was for the Response of

the Team about the Patient's questions (71.75%), while the lowest value was for the explanation of the surgical team about lifestyle after surgery (eating habits, wound management, having shower and exercise, 53%). On the Service of the hospital in general, the highest value was for the safety level in the hospital (74.75%), while the lowest index was for the quality of the food in the hospital (56.75%) (table

2). All other entities in all services were above 60%. After adjustment for patient and surgical factors, there was a strong relation between patient dissatisfaction and patient's age (P value: 0.003) (table 3), gender (P value: 0.001) with more female satisfaction, and duration of hospital stay (P value: 0), (table 4).

Table 2 Comparison between Male and Female Satisfaction

Index	Question	Male Mean	Female Mean	Significance Value
• Emergency	○ Are you satisfied about how quick is the response of the surgical on call team?	2.71 *	2.66	0.033
	• OPD and Admission Office			
○ Are you satisfied about the explanation of the doctor about the nature of your operation?	2.7	3.16	0.028	
• Service Before the operation	○ Are you satisfied about the explanation of the surgical team about the nature of your operation?	2.61	3.17	.02
	○ Are you satisfied about the explanation of the surgical team about the dangers and the complications of the operation?	2.54	3.05	.044
	○ Are you satisfied about the radiological investigations' appointment?	2.85	2.74	.033
	• Service After the operation			
○ Are you satisfied about the explanation of the surgical team about the medications that should be used after the operation?	2.25	2.89	.009	
○ Are you satisfied about the response of the team for your questions?	2.74	3.05	.029	
○ Are you satisfied about how quick is the response of the team for your demands?	2.58	2.87	.046	
• Service in General	○ Are you satisfied about the nursing team?	3	2.89	.035
	○ Are you satisfied about the nursing team performance?	3.05	2.87	.032
	○ Are you satisfied about the cleaning of the inpatient room?	2.96	2.61	.001
	○ Are you satisfied about your bathroom cleaning?	2.89	2.28	.002
	○ Are you satisfied about the food in the hospital?	2.27	2.28	.031

*Mean satisfaction rate

Table 3 Correlation between the Age of the patients and the Satisfaction

Index	Question	Significance Value
• Emergency	○ Are you satisfied about how quick is the response of the surgical on call team?	.003
	• OPD/Admission Office	
○ Are you satisfied about admission office employer?	.022	
• Service Before the Operation	No Significance	
• Service After the Operation	No Significance	
• Service in General	○ Does the inpatient room satisfy your needs?	.02

Table 4 Correlation between Hospital Stay and Patient Satisfaction

Index	Question	Significance Value
Emergency		No Significance
OPD/Admission Office		No Significance
Service Before the Operation		No Significance
• Service After the Operation	○ Are you satisfied about the explanation of the surgical team about the daily habits after the operation?	.036
	• Service in General	
○ Are you satisfied about the nursing team performance?	0	
○ Are you satisfied about the inpatients room?	.005	

4. Discussion:

The health service quality has three dimensions: client quality, professional quality and management quality. Client quality is the dimension that receives most attention in discussions of quality of health care-based on how satisfied clients are with their care^(3,4). In Saudi Arabia, the health care infrastructure is reasonable in terms of facilities and personnel. The real challenge is to improve staff performance and patient satisfaction, in order to minimize rework, wastage, delay and costs. Today, we recognize that quality as perceived by the health care recipient is vitally important. As a result of this new focus, measurement of customer satisfaction has become equally important^(5,6).

In the Surgery Department at our hospital (KAUH), we developed a surgical quality improvement plan (KAUH-SQIP) in 2009. The objectives of this plan are to increase patient satisfaction, reduce postoperative morbidity and mortality, reduce the median length of stay and participate in national and international audits and research. In this plan, we collect data on a variety of variables as patient satisfaction, morbidity and mortality then we analyze, review and act on the finding. As part of this plan we conducted our study, and it has provided an important first step in our understanding of patient satisfaction.

In our study, the overall satisfaction rate was 89.6%, while Myles *et al.*, in 1999 reported 96.8%^(7,8). A significant relation was found between old age (more than 50 years) and male gender and the patient dissatisfaction, which can give information about the group of patient that the hospital has to take more care of them during their management. Another important factor for patient dissatisfaction is the length of the hospital stay. Many studies showed that using laparoscopic surgery, single port surgery, robotic surgery and out-patient and day care surgery associated with early recovery of the patient and less hospital stay which will result in more patient satisfaction⁽⁹⁻¹¹⁾. For that reason we recommend the surgeons and the hospital to use these surgical techniques when indicated and to be as part of the surgical residency training program.

Other factors which influence patient dissatisfaction are waiting time in the Emergency Department (more than 3 hours) and the out-patient department (more than 1 hour), quality of food, quick response of consulting doctors of other departments, explanation of surgical team about lifestyle after surgery (eating habits, wound management, having shower and exercise), and length of the hospital stay.

We recommend hospital management to address these factors to improve patient satisfaction.

We recommend other health care organizations in our country to measure patient satisfaction as we have limited studies about this in Saudi Arabia. This will give us a better understanding of the factors that influence patient satisfaction and to elaborate the mechanisms through which the organizational environment impacts on client satisfaction.

Corresponding author

Saleh M. Aldaqal

Departments of Surgery, Faculty of Medicine, King Abdulaziz University, Jeddah, Kingdom of Saudi Arabia. sdaqal@yahoo.com.

References

1. Ancarani, A, Di Mauro, C., Giammanco, M.D. How are organizational climate models and patient satisfaction related? A competing value framework approach. *Social Science and Medicine*, 2009; 69: 1813–1818.
2. Braunsberger, K., Gates, R.H. Patient/enrollee satisfaction with health care and health plan. *Journal of Consumer Marketing*, 2002; 19:575–590.
3. Chang, E., Hancock, K., Chenoweth, L., Jeon, Y., Glasson, J., Gradidge, K., Graham, E. The influence of demographic variables and ward type on elderly patients' perceptions of needs and satisfaction during acute hospitalization. *International Journal of Nursing Practice*, 2003; 9:191–201.
4. Crow, R., Gage, H., Hampson, S., Hart, J., Kimber, A., Storey, L., Thomas, H. The measurement of satisfaction with health care: implications for practice from a systematic review of the literature. *Health Technology Assessment*, 2002; 6 (32):1–245.
5. Donahue, K.E., Ashkin, E., Pathman, D.E. Length of patient–physician relationship and patients' satisfaction and preventive service use in the rural south: a cross-sectional telephone study. *BMC Family Practice*, 2005; 6:40–48.
6. Hill, M.H., Doddato, T. Relationships among patient satisfaction, intent to return, and intent to recommend services provided by an academic nursing center. *Journal of Cultural Diversity*, 2002; 9:108–112.
7. Jaipaul, C.K., Rosenthal, G.E. Are older patients more satisfied with hospital care than younger patients? *Journal of General Internal Medicine*, 2003; 18: 23–30.
8. Jha, A.K., Orav, J., Zheng, J., Epstein, A.M. Patients' perception of hospital care in the United States. *The New England Journal of Medicine*, 2008; 359:1921–1931.
9. Mangelsdorff, A.D., Finsteun, K. Patient satisfaction in military medicine: status and an empirical test of a model. *Military Medicine*, 2003; 168:744–749.
10. Nguyen-Thi, P.L., Briancon, S., Empeur, F., Guillemin, F. Factors determining inpatient satisfaction with care. *Social Science and Medicine*, 2002; 54:493–504.
11. Schneider, B., Ehrhart, M.G., Mayer, D.M., Saltz, J.L., Niles-Jolly, K. Understanding organization–customer links in service settings. *Academy of Management Journal*, 2005; 48: 1017–1032.

1/2/2012

Transformational Leadership Role of Principals in Implementing Informational and Communication Technologies in Schools

Mojgan Afshari*, Simin Ghavifekr, Saedah Siraj and Rahmad Sukor Ab. Samad

Department of Educational Management, Planning and Policy, Faculty of Education, University of Malaya
mojganafshari@yahoo.com

Abstract: The implementation of information and communication technologies is very important to schools. Transformational leaders provide greater contributions to implement technology in education. This paper examines the relationship between two independent variables (computer competence and computer use) and transformational leadership role of principals in implementing ICT in schools. This paper based on responses from 320 school leaders in Iran, reports that computer competence and ICT usage are key factors that influence technology leadership behaviors. It is suggested that decision makers should provide professional development for principals to become proficient in all the competency areas.

[Mojgan Afshari, Simin Ghavifekr, Saedah Siraj, & Rahmad Sukor Ab.Samad. **Transformational Leadership Role of Principals in Implementing Informational and Communication Technologies in Schools.** Life Science Journal 2012; 9(1):281-284]. (ISSN: 1097-8135). <http://www.lifesciencesite.com>.

Keywords: ICT competence, ICT use, transformational leadership, school principals

1. Introduction

Investments in information and communication technology (ICT) for enhancing formal and non-formal education systems are essential for schools improvement (Tong & Trinidad, 2005). According to Betz (2000), information technology will only be successfully implemented in schools if the principal actively supports it, learns as well, provides adequate professional development and supports for his/her staff in the process of change. In fact, school principals have a main responsibility for implementing and integrating ICT in schools (Schiller, 2003). Anderson and Dexter (2005) carried out a study on technology leadership behaviors of school principals and found that "although technology infrastructure is important, technology leadership is even more necessary for effective utilization of technology in schools" (p.49). Moreover, various other research studies support the literature that leadership is an important key factor in effective use of technology in education (Schiller, 2003; Anderson & Dexter, 2005). Therefore, it can be said that technology leadership behaviors are important to successful implementation of educational technology plans (Chang, Chin & Hsu, 2008).

It is widely accepted that the transformational leadership behaviors of principals play a crucial role in technology integration into the curriculum and promoting students' learning (Betz, 2000). In fact, transformational leaders pay attention to the needs and desires of their followers and help them get their highest potential (Crawford, 2005). According to

Schepers, Wetzels and Ruyter (2005), transformational leaders often exhibit strong values and ideals and can motivate people to act in ways that support the organization above their own interest. Based on transformational theory, principals should be innovative, competent, and role models to those that they lead. This declaration was supported by Dawon and Rakes (2003), who stated that principals as transformational leaders play a critical role in the successful implementation of school initiatives and they act as a role model. Therefore, it is important to identify the factors that impact the transformational leadership role of principals in implementing ICT in schools. "Principals as transformational leaders of school improvement, should have competence in using computers (Schiller, 2003), realize the importance of the new technologies and model the use of technology to show how technology can positively impact the school environment (Stuart, Mills & Remus, 2009).

"However, although school leaders may have formally mandated technology leadership responsibilities this can be problematic since they often do not have the training or background to feel confident in dealing with technology" (Stuart et al., 2009, p.733). Previous research studies indicated that using computer and ICT competence are important factors that influence role of principals in implementing ICT in schools. However, despite the importance role of the principals in supporting technology integration, there has been little research on using of ICT by principals and their transformational leadership role in implementing ICT

in Iranian schools. The current study is based on this pressing need and addresses the following questions:

- 1) What is the relationship between level of computer use by secondary school principals and their transformational leadership role in implementing ICT in schools?
- 2) What is the relationship between principals' perceptions of their level of computer competence and their transformational leadership role in implementing ICT in schools?

2. Methodology

A descriptive study of an exploratory nature was used in this study. In fact, exploratory studies are most useful when "not much has been written about the topic or the population being studied" (Creswell, 2003). Based on the secondary principals Directory, the total number of Iranian secondary school principals in the province of Tehran was 1312 during the 2007-2008 school years. This Directory is maintained and updated on a quarterly basis by Tehran Department of Education. To obtain the required data for this study, three questionnaires were used. They were distributed among 320 sample principals selected randomly from the population. Stratified sampling was utilized in this study. In fact, Tehran is the biggest cities in Iran and consists of 19 educational areas. In each area, the population of secondary school principals is not homogeneous. When sub-populations vary significantly, it is advantageous to sample each subpopulation (stratum) independently. So, we used stratified sampling method to have less variability in selection.

In addition, a panel of expert established face and content validity of these instruments. Also, internal consistency of them was obtained by Cronbach's alpha that was calculated by the SPSS 16 statistical package. The Cronbach's alpha coefficients for these scales were: Computer Competence Scale=0.97, Transformational leadership style Scale=0.812 and Level of computer use Scale=0.917. To conduct this study, permission was gained from the Ministry of Education and the research department of Tehran's Ministry of Education. They permitted us to attend the principals' meeting in each educational area of the Ministry of Education. A total of 350 questionnaires were distributed among all members of the sample in these sessions. The completed questionnaires were collected at the end of these sessions. Principals who could not fill their questionnaires completely were given approximately three weeks from that date to return the questionnaires by mail. In all, 350 surveys were distributed, 320 were returned, resulting in a return rate of 91.4%. All of the returned surveys, a total of

320, were used in the analysis. In this study descriptive statistics were used to describe and summarize the properties of the mass of data collected from the respondents (Airasian & Gay, 2000). Correlation analysis was used to determine the relationship between each of the independent variables and transformational leadership role of principals in implementing ICT in school.

3. Findings and Discussion

Study results showed that about 48.4% of the respondents were female and about fifty point three percent of the respondents were within the 45-54 age range. Approximately forty five percent of the respondents had more than 21 years of experience. About fifty three percent of the principals worked in private schools, and sixty point three percent held bachelor's degrees. Most of the principals stated that they had attended computer training programs (95.5%). Regarding the type of training, about fifty three percent of them stated that they received their training through in-service training.

3.1. The Association between Transformational Leadership and Independent Variables

The relationship between Transformational leadership and independent variables (level of computer use and computer competence) were explored by using the Pearson Product-moment correlation. This analysis was used to find the strength and direction of the linear relationship between two variables (independent variable and dependent variable).

Table 1: Summary of the Correlation Matrix of Independent Variables and Transformational Leadership

Variable	Pearson Correlation	Sig. (2-tailed)
Transformational Leadership	1	
Computer Competence	0.61**	0.000
ICT use	0.70**	0.000

According to Table 1, computer competence was significantly linked to transformational leadership [$r=0.61$, $n=320$, $p < 0.01$]. Moreover, we found that there was a strong and positive correlation between computer use and transformational leadership [$r =0.70$, $n=320$, $p<0.05$]. Based on these results, we can conclude that principals who use computer frequently in their administrative and instructional tasks and have higher levels of skill and

knowledge in ICT use will exhibit more transformational leadership behaviors in their schools and acted as strong role models for the effective use of technology in support of teaching and learning. Such principals can transmit a vision or a sense of mission for comprehensive integration of technology, foster an environment and culture conducive to the realization of that vision and create enthusiasm in followers, applied technology to enhance their professional practice and to increase their own productivity. This finding was supported by Stuart et al.' (2009) study. They found that school leaders who are ICT competent and use computer in their administrative and instructional tasks are effective technology leaders. Also, study result is consistent with Schiller's (2003) proposition that ICT competence is a key factor that influence technology leadership role of principals. Therefore, principals should understand the role of ICT in their work life and learn appropriate skills to use this knowledge (Stuart et al., 2009) in order to encourage teachers to use technology in their teaching and learning process.

3. Conclusion

Role of principals in influencing, empowering and supporting teachers in successful ICT implementation in schools is very important (Yuen, Law & Wong, 2003). In fact, principals who act as transformational leaders can encourage creativity, open-mindedness and facilitate conditions and events that create a positive environment for technology adoption (Frambach & Schillewaert, 2002; Schillewaert et al., 2005).

According to Rogers (2003), such principals play an essential role in the diffusion and adoption of innovations. The leadership style exhibited by the leader could help or hinder technology infusion. Findings of this study showed that principals spent a few times a week working on their computers and they had moderate competence in using computer. Also, study results indicated that principals' computer competence and level of computer use by principals have a significant association with transformational leadership style. It is suggested that Iranian principals should be active learners in this fast changing arena. They should never stop learning and honing their skills but they must maintain a personal plan for self-improvement and continuous learning (Bennis, 1990). Principals should improve their style of leadership and be familiar with current research and best practices. Furthermore, they should use new technologies and model the use of them to change and improve the environment in which educators function. School leaders should be enthusiastic to model the transformational components of charisma (idealized influence),

inspirational motivation, intellectual stimulation and individualized consideration in order to implement ICT effectively in their schools. According to Bass and Riggio (2006), transformational leadership can be taught. Therefore, decision makers should provide professional development for principals to learn the skills and knowledge they need to use technology tools and also to learn the components of transformational leadership to implement and integrate technology into their schools effectively.

Corresponding Author:

Dr. Mojgan Afshari

Department Educational Management, Planning and Policy, Faculty of Education, University of Malaya

E-mail: mojganafshari@yahoo.com

References

1. Tong M, Trinidad S. Conditions and Constraints of Sustainable Innovative Pedagogical Practices Using Technology. *IEJLL: International Electronic Journal for Leadership in Learning* 2005; 9(3).
2. Betz M. Information Technology and schools: the principal's role. *Educational Technology & Society* 2000; 3 (4).
3. Schiller J. Working with ICT: Perceptions of Australian principals. *Journal of Educational Administration*, 2003; 41(2): 171-185.
4. Anderson R, Dexter S. School technology leadership: An empirical investigation of prevalence and effect. *Educational Administration Quarterly* 2005; 41(1): 49.
5. Chang I, Chin J, Hsu C. Teachers' Perceptions of the Dimensions and Implementation of Technology Leadership of Principals in Taiwanese Elementary Schools. *Educational Technology & Society* 2008; 11(4): 229-245.
6. Crawford C. Effects of transformational leadership and organizational position on knowledge management. *Journal of knowledge management* 2005; 9(6): 6-16.
7. Schepers J, Wetzels M, de Ruyter K. Leadership styles in technology acceptance: do followers practice what leaders preach? *Managing Service Quality* 2005; 15(6):496-508.
8. Dawson C, Rakes G. The influence of principals' technology training on the integration of technology into schools. *Journal of Research on Technology in Education* 2003; 36(1): 29-49.
9. Stuart C, Mills A, Remus U. School leaders, ICT competence and championing innovations. *Computers & Education* 2009; 53(3): 733-741.
10. Flanagan L, Jacobsen M. Technology leadership for the twenty-first century principal. *Journal of*

- Educational Administration 2003; 41(2): 124-142.
11. Creswell W. Research design: Sage Publications. 2003.
 12. Airasian P, Gay LR, Mills GE. Educational research: Competencies for analysis and application. New Jersey, Upper Saddle: Prentice Hall, 2000.
 13. Stuart LH, Mills AM, Remus U. School leaders, ICT competence and championing innovations. Computers & Education 2009; 53(3): 733-741.
 14. Yuen AHK, Law N, Wong KC. ICT implementation and school leadership: Case studies of ICT integration in teaching and learning. Journal of Educational Administration 2003; 41(2): 158-170.
 15. Frambach RT, Schillewaert N. Organizational innovation adoption: a multi-level framework of determinants and opportunities for future research. Journal of Business Research 2002; 55(2): 163-176.
 16. Schillewaert N, Ahearne MJ, Frambach RT, Moenaert RK. The adoption of information technology in the sales force. Industrial Marketing Management 2005; 34(4): 323-336
 17. Rogers EM. Diffusion of innovations (5th ed.). New York: Free Press, 2003.
 18. Bennis WG. Why leaders can't lead: The unconscious conspiracy continues. Francisco: Jossey-Bass, 1990.
 19. Bass BM, Riggio RE, Transformational leadership: Lawrence Erlbaum, 2006.

Effect of the Strengthened Ribs in Hybrid Toughened Kenaf/ Glass Epoxy Composite Bumper Beam

M.M. Davoodi¹, S.M. Sapuan¹, Aidy Ali¹, D. Ahmad²

¹Department of Mechanical and Manufacturing Engineering, Universiti Putra Malaysia, 43400 UPM Serdang, Selangor, Malaysia

²Department of Biological and Agricultural Engineering, Universiti Putra Malaysia, 43400 UPM Serdang, Selangor, Malaysia
makinejadm2@asme.org

Abstract: The growth of car production governs new environmental regulations “End-of Life Vehicles” (ELV) to enforce car manufacturer to substitute synthetic material to bio based materials. Low mechanical properties of natural fibre composite confine their application in automotive non-structural components. Hybridizations of kenaf with glass fibre along with epoxy PBT toughening did not completely fulfill the required impact property of the developed bio-composite bumper beam to substitute with typical material of the bumper beam glass mat thermoplastic (GMT). Therefore, in the first stage of the geometrical improvement “concept selection” concluded that the double hat profile (DHP) is the most suitable concept out of eight bumper beam concepts when six parameters with different weight (strain energy, deflection, weight, cost, manufacturing and rib possibility) are determined. In second trial, the usage of strengthen rib is employed to improve the impact property and performance of the bumper beam for utilization of hybrid kenaf/glass fibre as a car bumper beam. The low-speed impact test based on the (ECE R42) regulation is modeled. Eight vertical ribs with thickness 4 mm are located along the bumper beam. The pendulum hit to the middle of the bumper, while it is fixed to the vehicle chassis through two energy absorbers. The strain energy and deflection were determined and compared with the same profile, but in un-ribbed condition. It is concluded that the ribbed bumper beam decrease the deflection of the bumper beam by 11% and strain energy by 11.3%. The ribbed bumper beam increases the structural safety factor and its reliability for utilization in automotive structural components.

[Majid Davoodi Makinejad, Mohammad Sapuan Salit, Aidy Ali, Desa Ahmad. **Effect of the Strengthen Ribs in Hybrid Toughened Kenaf/ Glass Epoxy Composite Bumper Beam**. Life Science Journal.2012;9(1):285-289]. (ISSN:1097-8135). <http://www.lifesciencesite.com>. 40

Keywords: Bumper beam; Finite element analysis; Hybrid material; Natural fibre composite

1. Introduction

Strengthen ribs are exploited to improve the structural strength of hybrid kenaf/glass epoxy composite bumper beam in second trial of geometrical improvement in order to enhance the performance of the developed material in structural component's applications. Strengthen ribs increase distortion resistance and structural stiffness with fewer materials in slender wall (Al-Ashaab, Rodriguez, 2003). It can decrease the bumper beam deflection, elongation and increase impact energy (Brydson, 1999, Hosseinzadeh, Shokrieh, 2005, Marzbanrad, Alijanpour, 2009). The previous result showed that the toughened hybrid kenaf/glass fibre epoxy composite cannot fulfill the GMT impact strength. The geometry improvement commenced with bumper concept selection within six criteria with different weight. It is concluded that the bumper beam concept, double hat profile (DHP), as a best one out of eight concepts (Davoodi, Sapuan, 2011). This study focused on geometry improvement by adding the vertical ribs to the selected concept and

compares the strain energy and deflection with the un-ribbed bumper beam.

There are different parameters that effect in the rib strength (pattern, thickness, top and bottom fillet, weld line area, position) (Harper, 2006, Smith and Suh, 1979, Zhang, Liu, 2009). Besides, load direction, load position, material and manufacturing process should be considered in rib design (Samaha, Molino, 1998). Hosseinzadeh, Shokrieh 3) compare the bumper beam made from sheet molding compound (SMC) and GMT with and without ribs. It is resulted that the rib in the GMT bumper beam can decrease the deflection of the beam 13% and slightly increases the impact force; however, the ease of manufacturing should be focused. Marzbanrad, Alijanpour 4) showed that the ribbed bumper increase the rigidity and enhance the impact force by 7% in steel bumper beam. Murata, Shioya 10) used the high density EPP with rib structure to increase the energy absorption capacity. He showed that the fine tuning of the rib design (thickness, height, spacing) while combine with EPP can optimize the energy absorption.

This study focused on the bumper beam structure under low speed impact test with vertical strengthening thin-walled ribs and analyzing the energy absorption improvement of the selected concept. It emphasize on the structural performance of the ribbed bumper beam with developed toughened hybrid kenaf/glass epoxy. The material model of the developed hybrid bio-composite was extracted from the previous study experimental test and checked with the same simulated impact condition. The parameters of the model such as type and size of the element and meshes were modified to match the results together. Then the exact low speed impact test condition (ECE R42) was simulated by finite-element software, ABAQUS Ver16R9. The impact loads defined while the impactor with 1000 kg hit to the bumper beam, which is fixed from both end sides while attached to a solid block, which represent the car weight in center of mass at $x=530$. The meshes, steps, interactions and jobs are defined. Strain energy and deflection of double hat profile (DHP) is analyzed when the vertical ribs are added. The ribbed bumper stands more effective against the impact load and increases the reliability of the developed hybrid bio-composite material for utilization in the car bumper beam.

2. Material and Methods

The ingredients of the hybrid bio-composite material consist of kenaf fiber, glass fibre, epoxy and polybutylene terephthalate (PBT) respectively were provided from Institute of Tropical Forestry and Forest Products (INTROP) (Malaysia), Fibreglass Enterprise (China), LECO Corporation (USA), CBT® 160 (PBT) from CYCLICS Corporation (USA). Three plies of glass fibers, and two plies of stretched twisted long kenaf with orientation (0, 90, 0, 90, 0) are prepared. The PBT 5% (w/w) is added under structure-less method to the epoxy and sprayed to the prepared plies and compressed by a preheated mold $T=85^{\circ}C$ under controlled conditions ($P=80$ bars and $T=85^{\circ}C$) (See Figure 2). The property of the material which is conducted from the previous study was imported to the ABAQUS V16R9 (Davoodi, Sapuan, 2012).

The low-speed impact (ECE R42) was simulated in ABAQUS Ver16R9. A pendulum with unladen weight (1000 kg for normal car) and speed 4 km/h at the contact point, hit to the middle of the bumper beam, while is fixed to the chassis (block present the car weight, center of mass at $X=530$) through two traverse energy absorbers. Figure 2 shown pendulum and boundary conditions.

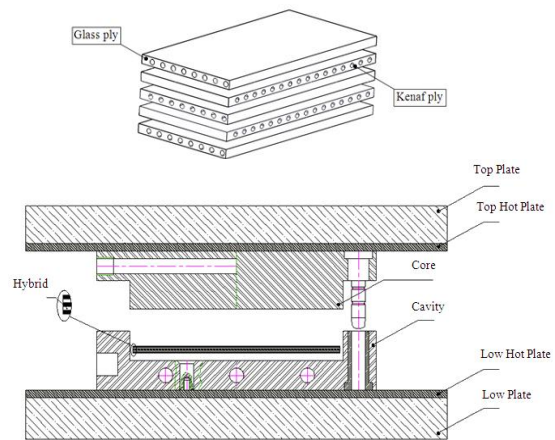


Figure 1. Compression mould for hybrid bio-composite

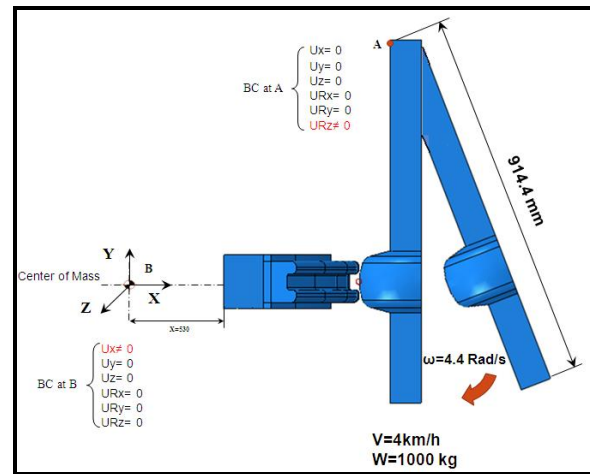


Figure 2. Low impact test simulation and boundary condition

The whole of the simulated components elements characteristics are introduced in Table 1.

Table 1. Elements characteristics in FEA

No	Part Name	Element type	Element No.	Node	Element Name
1	Barrier	C3D4	2196	620	tetrahedral
2	Mass	C3D8R	16510	19712	hexahedral
3	Left Holder	S4R	513	509	quadrilateral
4	Right Holder	S4R	520	517	quadrilateral
5	Beam	S3	1228	1328	triangular
Total			20967	22686	

Every plies of the hybrid composite are defined separately in ABAQUS with thickness 0.8 mm and 0° (glass fibre), 90° (kenaf fibre) direction. The main properties extracted from experimental test and defined in ABAQUS. Since impact property is the

main interested objective in this study, the same impact condition was simulated to match the compatibility between experimental by changing the parameters such as type and number of element and method of meshing (Figure 3).

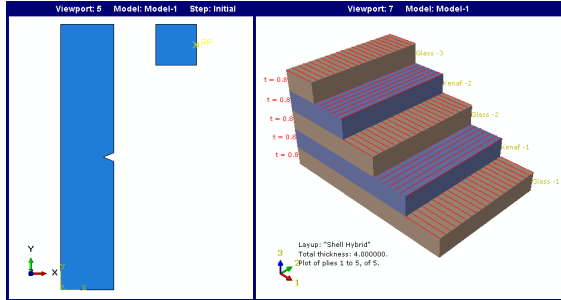


Figure 3. Hybrid kenaf/glass modeling for verification with impact test condition

The low-impact test condition is defined for elastic deformation of the bumper beam (AISI, 2006). Since the bumper beam is fixed from both traverse sides, the applied impact load tends it to bend. In bending, the composite failure initiates with matrix cracking followed by debonding between layers, delamination and finally fibre fracture. In ABAQUS, the progressive damage and failure prediction of both fibre and matrix failure determine based on Hashin theory (Hashin, 1980). The Hashin introduced four criteria modes: fibre tension, fibre compression, matrix tension and matrix compression. In this study, the bending of the hybrid composite bumper beam in the outer layers causes the matrix tension and cracking. So, matrix tension is considered as an initiation step of failure.

$$F_{mt} = \left[\frac{\sigma_{22}^o}{Y^T} \right]^2 + \left[\frac{\sigma_{12}^o}{S^L} \right]^2 = 1$$

- F_{mt} = Failure in matrix tension
- d_f, d_m, d_s = Damage variables
- σ = True stress
- σ^o = Effective stress
- $\sigma_{22} \geq 0$
- Y^T = Traverse tensile strength
- S^L = Longitudinal shear strength

The effective stress can determine from product of the following matrix to the true stress.

However, in the software just should input the requested parameters for Hashin criteria consideration.

$$\sigma^o = \begin{bmatrix} \frac{1}{1-d_f} & 0 & 0 \\ 0 & \frac{1}{1-d_m} & 0 \\ 0 & 0 & \frac{1}{1-d_s} \end{bmatrix} \sigma$$

Eight vertical ribs (200 mm distance between adjacent ribs and end cap) with 4 mm thickness are located in longitudinal direction of the bumper beam. The ribs are placed along the X direction for ejection purposes except end caps (Figure 4).

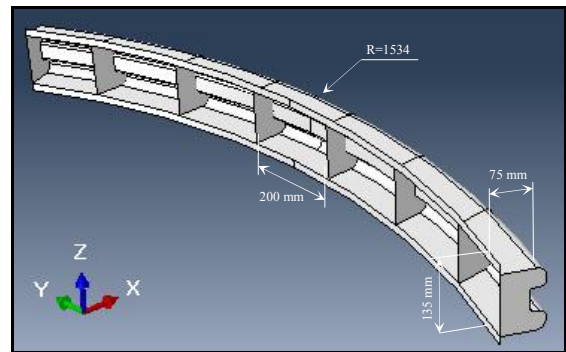


Figure 4. The strengthen ribs of bumper beam

3. Results

Deflection of the both bumper beams during the impact is shown in figure 5.

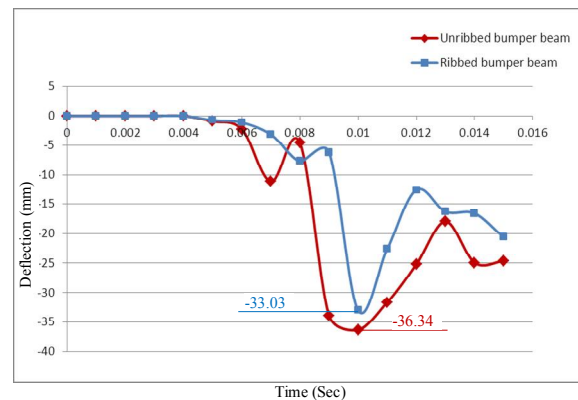


Figure 5. Deflection of ribbed and unribbed bumper beam

From the graph, it is evident that the maximum deflection of the unribbed bumper is 3.31 mm more than the ribbed bumper. In other words, the

vertical ribs decreased deflection of the bumper beam by 11%. Moreover, the unribbed bumper beam deflection commenced earlier than ribbed one, since it has less solidified.

Figure 6 shows the strain energy of both ribbed and unribbed bumper beam. It is evident that the strain energy in the ribbed bumper beam commenced earlier than unribbed one because of more stability of the ribbed bumper beam in energy absorption, cause faster response to the external impact load. Moreover, it is presented that the maximum amount of strain energy in the ribbed bumper beam increased by 11.3% compare with unribbed bumper beam because of rigidity enhancement of the structure. The strain energy undulation of the ribbed bumper beam cause by the rib zone strain energy removal and unsteady load distribution from the rigid pendulum to the beam and side energy absorbers.

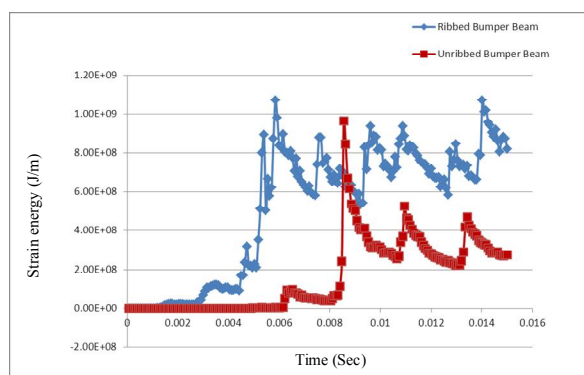


Figure 6. Strain energy of ribbed and unribbed bumper beam

It is evident, there are eight pick points in strain energy graph, which might be because of the energy dissipation of the ribs during the energy damping process.

4. Discussions

The accurate design of the strengthened ribs and its effective parameters such as features, spacing, thickness, height, can increase the energy absorption capacity (Murata, Shioya, 2004) as well as decrease the shrinkage and thermal expansion in the bumper beam. The unribbed bumper beam makes less-rigid sections and may absorb more impact energy by elastic deformation without damage (Rosato and Murphy, 2004).

The additional ribs slightly increase strain energy and decrease deflection in bumper beam, but cause weight rises and manufacturing difficulty (Hosseinzadeh, Shokrieh, 2005, Marzbanrad, Alijanpour, 2009). Besides, it requires more pressure to flow the material to the ribbed cavities and cause

bumper beam denser and more solid. The vertical ribs with thickness 4 mm prevent the deflection of the lateral beam surfaces. Making ribs in the beam needs specific cavities in the die, which makes a difficulty in mold making and production. It causes higher compressive pressure to flow the material to the thin cavity for forming the ribs. The author recommends the experimental approach in order to verify the developed toughened hybrid kenaf/glass epoxy composite to control various parameters for a reasonable replacement solution of new developed material. Moreover, since the strength improvement of the ribbed bumper beam is not quite significant, fabrication of the whole bumper beam in real processing method can show the manufacturing difficulty by the developed material for making the ribbed bumper beam.

Acknowledgements:

The principal author wishes to thank the Universiti Putra Malaysia for supporting this research financially through the Research University Fellowship Scheme.

Corresponding Author:

M.M. Davoodi

Department of Mechanical and Manufacturing Engineering, Universiti Putra Malaysia, 43400 UPM Serdang, Selangor, Malaysia

E-mail: makinejadm2@asme.org

References

1. Al-Ashaab, A., et al., Internet-based collaborative design for an injection-moulding system. *Conc. Eng.*, 2003; 11(4): 289.
2. Brydson, J.A., *Plastics Materials*. New Delhi: Butterworth-Heinemann; 1999.
3. Hosseinzadeh, R., Shokrieh, M., and Lessard, L., Parametric study of automotive composite bumper beams subjected to low-velocity impacts. *Compos. Struct.*, 2005; 68(4): 419-427.
4. Marzbanrad, J., Alijanpour, M., and Kiasat, M., Design and analysis of an automotive bumper beam in low-speed frontal crashes. *Thin. Walled. Struct.*, 2009; 47(8-9): 902-911.
5. Davoodi, M., Sapuan, S., Ahmad, D., Aidy, A., Khalina, A., and Jonoobi, M., Concept Selection of Car Bumper Beam with Developed Hybrid Bio-Composite Material. *Mat. Desig.*, 2011.
6. Harper, C.A., *Handbook of plastic processes*: Wiley-Interscience; 2006.

7. Smith, K.L. and Suh, N.P., An approach towards the reduction of sink marks in sheet molding compound. *Polym.Eng.Sci.*, 1979; 19(12): 829-834.
8. Zhang, Z., Liu, S., and Tang, Z., Design optimization of cross-sectional configuration of rib-reinforced thin-walled beam. *Thin. Walled. Struct.*, 2009; 47(8-9): 868-878.
9. Samaha, R.R., Molino, L.N., and Maltese, M.R. Comparative performance testing of passenger cars relative to FMVSS 214 and the EU 96/EC/27 side impact regulations: phase I. 1998.
10. Murata, S., Shioya, S., and Suffis, B., Expanded Polypropylene (EPP): A Global Solution for Pedestrian Safety Bumper Systems. 2004.
11. Davoodi, M.M., Sapuan, S.M., Ahmad, D., Aidy, A., Khalina, A., and Jonoobi, M., Effect of polybutylene terephthalate (PBT) on impact property improvement of hybrid kenaf/glass epoxy composite. *Mat. Lett.*, 2012; 67(1): 5-7.
12. Hashin, Z., Failure criteria for unidirectional fiber composites. *Journal of applied mechanics*, 1980; 47: 329.
13. Rosato, D.V. and Murphy, J., Reinforced plastics handbook: Elsevier Advanced Technology; 2004.

1/5/2012

Investigation of the Structural and Optical Properties of Bismuth Telluride (Bi_2Te_3) Thin Films

F. S. Bahabri

Physics. Department, Science of Faculty for Girls, King AbdulAziz University- KSA

f_s_bahabri@hotmail.com

Abstract: In the preparation of Bismuth Telluride thin films are reported in the present work. Measurements of the structural and optical properties of Bi_2Te_3 thin films were studied by X-ray diffraction, transmission (TEM) and scanning (SEM) electron microscope and electron diffraction techniques. Bi_2Te_3 thin films were "polycrystalline" Hexagonal form. The crystallite size was determine .The optical energy gap was evaluated. The study was carried out under vacuum., These properties has been reported to date. It was found from the optical properties studies that the type of transition of Bi_2Te_3 is an indirect transition.

[F. S. Bahabri. **Investigation of the Structural and Optical Properties of Bismuth Telluride (Bi_2Te_3) Thin Films.** Life Science Journal 2012; 9(1):290-294]. (ISSN: 1097-8135). <http://www.americanscience.org>. 41

Key words: Thermal evaporation, Structure , Bismuth Telluride – Thin Films

1. Introduction

Bismuth chalcogenides materials such as Bi_2Te_3 and Bi_2Se_3 comprise some of the best performing room temperature thermoelectric with a temperature-independent thermoelectric effect.^[1] Nano structuring these materials to produce a layered super lattice structure of alternating Bi_2Te_3 and Bi_2Se_3 layers produces a device within which there is good electrical conductivity but perpendicular to which thermal conductivity is poor.^[2]

Bismuth telluride compounds are usually obtained with directional solidification from melt or powder metallurgy processes. Materials produced with these methods have lower efficiency than single crystalline ones due to the random orientation of crystal grains, but their mechanical properties are superior and the sensitivity to structural defects and impurities is lower due to high optimal carrier concentration.

The required carrier concentration is obtained by choosing a nonstoichiometric composition, which is achieved by introducing excess bismuth or tellurium atoms to primary melt or by dopant impurities. Some possible dopants are halogens and group IV and V atoms. Due to the small band gap (0.16 eV) Bi_2Te_3 is partially degenerate and the corresponding Fermi-level should be close to the conduction band minimum at room temperature. The size of the band-gap means that Bi_2Te_3 has high intrinsic carrier concentration.^[3]

Narrow-gap semiconductors have attracted considerable interest due to their wide application in infrared optoelectronics^[4]. Bi_2Te_3 is a narrow gap semiconductor^[5]. Belonging to the family of V-VI compounds of the general type Bi_2X_3 ($X = \text{Te}, \text{Se}, \text{S}$). Nevertheless some of the transport properties of Bi_2Te_3 have been scarcely reported, especially no

detailed study of the electrical conductivity and Hall coefficient in a wide range of temperature has been performed^[6-8].

The shape of the absorption edge in the semiconductor Bi_2Te_3 has been determined from transmission measurements on cleavage sections. The edge is of the form expected for indirect transitions, but an interpretation in terms of phonons characterized by a single energy is not applicable. A brief study of anisotropy effects is included. The energy gap at room temperature is close to 0.13 eV.^[9,10]

2. Experimental and Measurement technique :

The preparation for structural and optical properties of Bismuth Telluride Bi_2Te_3 with a purity of 99.999%, thin films are reported in the present work. Bi_2Te_3 thin films were grown by a vacuum thermal evaporation technique which deposited on a flat cleaned glass substrates for the structural properties and quartz substrates for the optical properties with a thermal evaporation method. The structural properties of Bi_2Te_3 samples of 170 nm , 235 nm, 275 nm and 342nm thicknesses, have been analyzed using X – ray Diffraction (Philips, PW 1700) in the degrees range of $10^\circ - 100^\circ$, and the wavelength $\lambda_{\text{CuK}\alpha} = 1.5418 \text{ \AA}$. Measurements of these samples were performed at the room temperature. The effect of thicknesses are studied. The optical properties of Bi_2Te_3 samples with 45 nm, 130 nm, 154 nm, 202 nm, 245 nm thicknesses, have been analyzed using a spectrophotometer (Jasco V570) in the wavelength range of 200–2500 nm.

3. Results and Discussion:

The Bi_2Te_3 powder Fig.1 and as-grown at room^[1-3] temperature samples with a different thicknesses of 170nm , 235nm, 275nm and 342nm,

Fig.2.were investigated by X-ray diffraction "Bragg's Law", which describes the condition for constructive

interference from successive crystallographic planes.

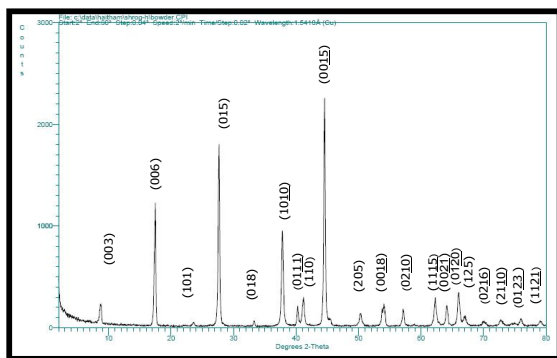


Fig. 1. X-ray diffraction of powder Bi_2Te_3 .

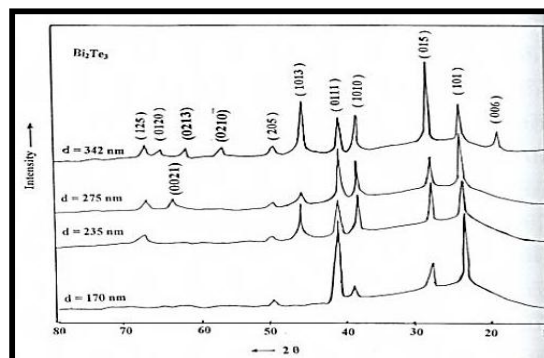


Fig. 2. X-ray diffraction of Bi_2Te_3 of different thicknesses thin films.

The pattern indicated that both as – deposited and annealing films in vacuum at 443K for 1h Fig.3, were polycrystalline with a Hexagonal structure and the calculated lattice constant are a =

4.43Å , c = 30.55Å, highly oriented crystallographic growth of Bi_2Te_3 thin films of 342nm thickness as shown in Fig.3.

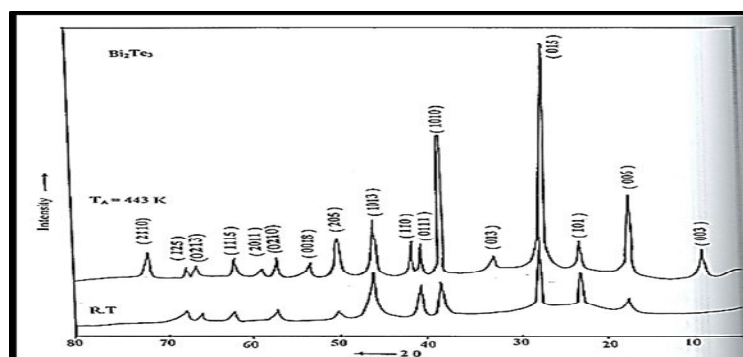


Fig. 3. X-ray diffraction of Bi_2Te_3 thin film of 342 nm thickness before and after annealing $T= 443\text{K}$, for 1h .

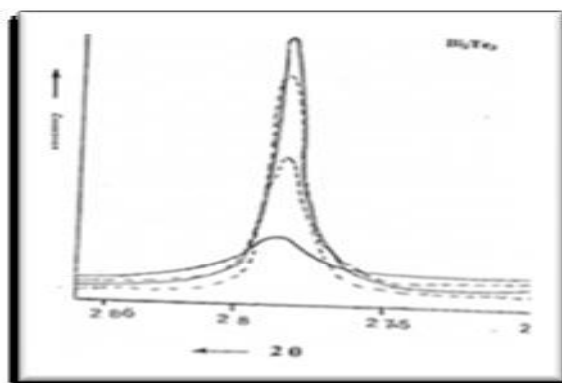


Fig.4. The full width of (015) peaks of a maximum intensity of different thicknesses.

The crystal size "Grain Size " D, Fig.4, was determined by inspecting its effect on the broadening

of the X-ray line profiles by step scan, using Scherrer's formula.^[11]

$$D = \frac{KA}{\beta \cos \theta} \quad (1)$$

where: λ is the X-ray wavelength, $\lambda_{CuK\alpha} = 1.5418 \text{ \AA}$, K: is the shape factor "constant" = 0.95, β : is the (015) full width at half maximum intensity = 9.89×10^{-3} and θ : is the scattering angle or the Bragg's angle . This leads to Bragg's law, which describes the

condition for constructive interference from successive crystallographic planes, From the calculated the values of the grain size D, are listed in table [1].

Table [1]: The relation between the crystal size "Grain Size " D with the film thicknesses of Bi_2Te_3 .

Film Thickness d (nm)	Grain Size D (nm)
170	60
235	110
275	150
342	160

This technique showed that the crystallite size increase as the film thickness increase. In addition, studies on the structural properties of Bi_2Te_3 thin films of 60 nm thickness, involved both electron diffraction technique, scanning electron microscope (SEM) Fig.5 and transmission electron microscope (TEM) Fig.6 were used to check the

crystallinity of the films. These studies revealed that the crystallite size was relatively larger for annealed samples. Electron diffraction was used to obtain information about the structure of Bi_2Te_3 of 60 nm thickness. An electron diffraction pattern are shown in Fig.7.

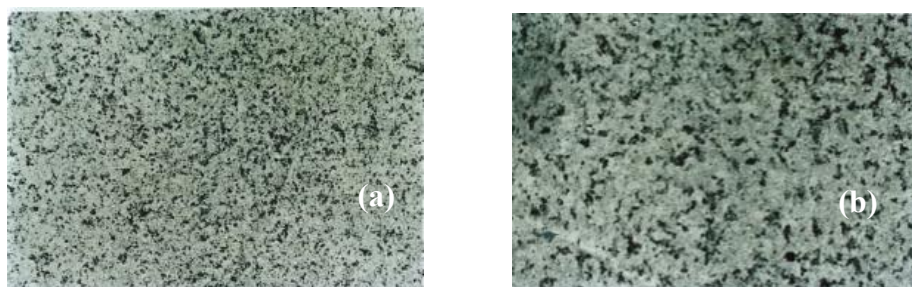


Fig. 5. SEM diffraction pattern of Bi_2Te_3 thin film indicating (a) before (b) after annealing.

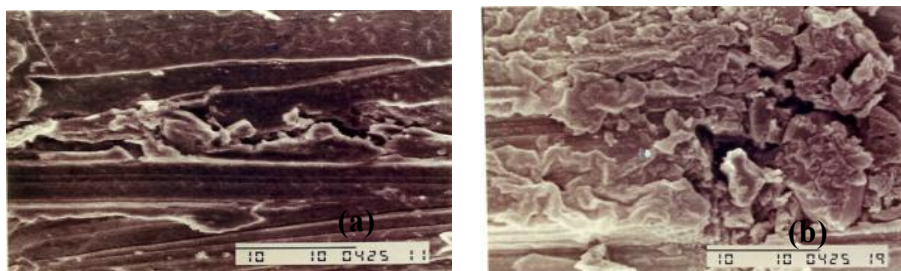


Fig. 6. TEM diffraction pattern of Bi_2Te_3 thin film indicating (a) before (b) after annealing.



Fig. 7. An electron diffraction pattern indicating (a) before (b) after annealing Bi_2Te_3 thin films.

The results show that annealing does not change the polycrystalline, but it affects the size and shape of the coordination compound nanoparticles corresponding with the size and shape of the samples, suggesting that the presented system increases the crystallite size.

The optical properties of Bi_2Te_3 samples, which have been analyzed using a spectrophotometer

at room temperature from the Transmission and Reflection spectra of Bi_2Te_3 thin films of various thicknesses are shown in Fig.8. The optical constants (refractive index n , absorption index k and absorption coefficient α) were determined for both n and k , which are independent on the film thickness in the range of 105- 503 nm.

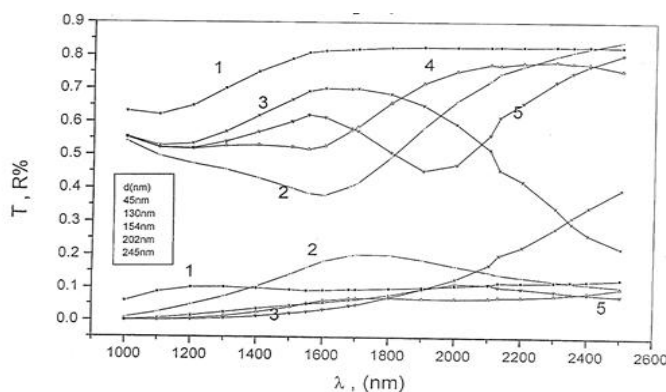


Fig. 8. Transmission and Reflection spectra of Bi_2Te_3 thin films of various thicknesses.

From the analysis of spectral distribution of n and k , shown in Fig.9.

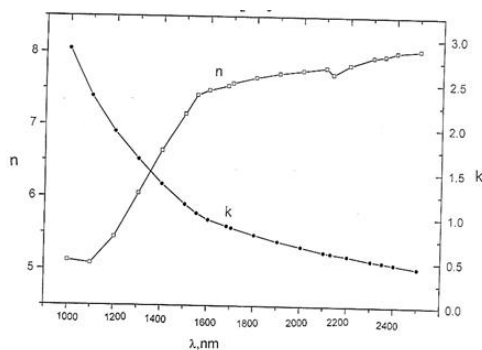


Fig.9. The analysis of Bi_2Te_3 spectral distribution of n and k .

It was found that the type of transition of Bi_2Te_3 is an indirect transition. The shape of the absorption edge in the semiconductor Bi_2Te_3 , Fig.10,

has been determined from transmission measurements on cleavage sections.

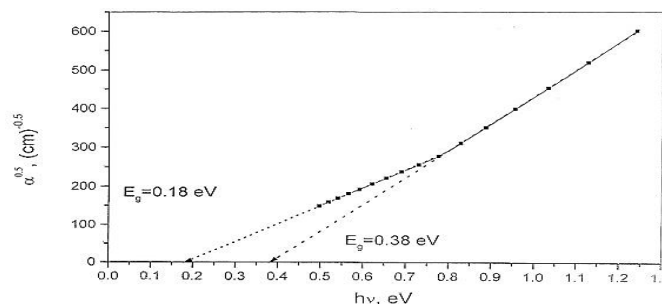


Fig.10.Relation of $(\alpha h\nu)^{1/2}$ vs $h\nu$ plot for the Bi_2Te_3 thin films.

The edge is of the form expected for indirect transitions, but an interpretation in terms of phonons characterized by a single energy is not applicable. It was found two edges with energy gap $E_1^{ind} = 0.18$ eV and the other one is $E_2^{ind} = 0.38$ eV.

4- conclusion:

The structural and optical properties of Bismuth Telluride Bi_2Te_3 were studied for Bi_2Te_3 thin films of various thicknesses. These samples were investigated by X-ray diffraction, it's a polycrystalline thin films with " Hexagonal structure. Also the studies involved both electron diffraction technique , scanning electron microscope (SEM) , transmission electron microscope (TEM) and electron diffraction to check the crystallinity of the films. It was found from the optical properties studies that the type of transition of Bi_2Te_3 is an indirect transition.

References

- Dresselhaus, M. S., (2007); New directions for low-dimensional thermoelectric materials. Adv. Mater. 19, pp. 1043–1053
- Chung Hogan. D.Y, Schindler T, Iordarridis. J , Brazis. L., Kanneurf. P, Baoxing Chen Uher. C.R and Kanatzidis. C., (1997); 16th International Conference on Thermoelectrics , pp. 459-462.
- Venkatasubramanian. R., Silvoia. E., Colpitts. T, and O'Quinn. B., (2001); Nature, pp.413, 597.
- Dheepa. J, Sathyamoorthy. R and Velumani. S, (2007); "Characterization of Bismuth Telluride Thin Films – Flash Evaporation Method". J. Mate. Cha. Vol. 58, Issu 8-9, pp.782 – 785.
- Gaetskaya and Smorodina V. A., (1982); INORG. Mater (USA)18,11, pp.1820.
- Desalegne Teweldebrhan, VivekGoyal, Muhammad Rahman, and Alexander A. Balandin, (2010); "Atomically-thin crystalline films and ribbons of bismuth telluride". J.Appl. Phys. Lett. 96, Issue 5- 053107; doi:10.1063/1.3280078.
- Austin.I. G., (1958); Proc. Phys. Soc, No. 72, No.4, pp. 545 -doi:10.1088/0370-1328/72/4/309
- Santosh. G., Arora. M, Sharma. R. K., and Rastogi. A. C., (2003); J. current Applied Physics. Vol.3 . Issu 2-3, pp.195 – 197.
- Auugustin. S, Ampili. S, Kang. J and Mathai. E, (2005); Materials Research Bulletin 40, pp. 1314-1325.
- Saji. A, Ampili. S, Yang. S-H., Ju . K.J., and Elizabeth. M (2005); J. Phys. Condens. Matter 17, pp.2873
- Pejova . B, Grozdanov. I, (2002) ; Thin Solid Films 408 - 6.

1/5/2012

Molecular characterization of *Cotugnia polycantha* (Cestoda, Cyclophyllidea, Davaineidae) infecting doves (*Streptopelia senegalensis*) and pigeons (*Columba livia Domestica*) from Egypt

Sabry E. Ahmed

Department of Zoology, Faculty of Science, Zagazig University
drsabryahmed11@gmail.com

Abstract: The genomic DNA was extracted from cestode parasites, *Cotugnia polycantha* from two different hosts, doves (*Streptopelia senegalensis*) and pigeons (*Columba livia domestica*). The random amplified polymorphic DNA-polymerase chain reaction (RAPD-PCR) was applied to differentiate between *C. polycantha* infecting doves and pigeons. Eight primers of arbitrary sequences were used in the PCR reactions. The eight primers screened gave total amplified fragment markers 133.

The total number of unique bands was 25 and the highest polymorphism percentage (63.63%) was obtained among the two specimens. Molecular analysis of the present data, showed that *C. polycantha* infecting doves (*S. senegalensis*) differs from that infecting pigeons (*C. livia domestica*).

So, *C. polycantha* infecting doves could be named *C. polycantha streptopeli* and *C. polycantha* infecting pigeons, *C. polycantha columbi*.

[Sabry E. Ahmed **Molecular Characterization of *Cotugnia polycantha* (Cestoda, Cyclophyllidea, Davaineidae) Infecting Doves (*Streptopelia senegalensis*) and Pigeons (*Columba livia Domestica*) from Egypt**] Life Science Journal 2012; 9(1):295-301]. (ISSN: 1545-1003). <http://www.lifesciencesite.com>

Key Words: Doves – Pigeons – Cestode- Genomic DNA – DNA fragments.

1. Introduction

The phylogeny of Eucestoda has been a matter of controversy for a century (Mariaux, 1996; Hoberg et al., 1997). Initial cladistic studies based on morphological characters (Brooks et al., 1991) were attempted to identify and specify the relationships among the major lineages of Eucestoda. This represents the first modern phylogenetic study of these parasites and constitutes a foundation on which to base more detailed analysis (Justine, 1998). Subsequently, using a revised and greatly augmented morphological data base, and for the first time, including spermatological characters, Hoberg et al. (1997) reported that the addition of any new characters of cestodes might increase the accuracy of phylogenetic inference.

Molecular techniques have become widely accepted all over the world. They provide a more specific method than methods conventionally employed in epidemiological studies (Coote, 1990; Erlich et al., 1991; Barker, 1994; Rognlie et al., 1994; Kramer and Schnieder, 1998; Heckerroth and Tenter, 1999; Mostafa et al., 2003 and Aldemir, 2006). Molecular techniques such as PCR and its variants are used for the diagnosis of

parasitic diseases and identification of parasites (Aldemir, 2006).

Molecular approaches are the most effective and accurate means for the detection of many organisms and for screening of genetic variation among populations (Wongsawad and Wongsawad, 2010).

The RAPD technique is based on amplification of a random DNA segment with a single primer of arbitrary nucleotide sequence and using polymerase chain reaction (Welsh and McClelland, 1990; Williams et al., 1990; Mohammedzadeh et al., 2007 and Nuchprayoon et al., 2007).

Molecular techniques based on genomics are very useful for epidemiological and diagnostic tools as well as for research on genetic variation of parasitic organisms (Mas-Coma et al., 2005 and Meshgi et al., 2008)

DNA Polymorphism assay based on random amplified Polymorphic DNA polymerase chain reaction (RAPD-PCR) has been proved useful for analyzing the inter- and intra-specific genetic variations and phylogenetic relationships (Gasser, 2005; Mas-Coma et al., 2005; Nuchprayoon et al., 2007 and Rokni et al., 2010).

The technique is very rapid, simple and generates reproducible fingerprints of the

PCR products. In addition, it neither depends on previous knowledge or availability of the target DNA sequences nor requires DNA hybridization (Mohammedzadeh *et al.*, 2007; Nuchprayoon *et al.*, 2007 and Sripalwit *et al.*, 2007).

Ahmed and Abdel-Moaty (2011) reported that *C. polycantha* infecting doves, *S. senegalensis*, differs from that infecting pigeons, *C. livia domestica*. Sperm ultrastructure was used as a new tool for identification.

In the present study, *C. polycantha* infecting two different hosts, doves *Streptopelia senegalensis* and pigeons *Columba livia domestica*, were compared using random amplified polymorphic DNA (RAPD) analysis for differentiation between them.

2. Materials and Methods

Parasite preparation

Adult tape-worms were collected alive from the small intestine of naturally infected and recently killed doves, *Streptopelia senegalensis*, and pigeons, *Columba livia domestica*, from Sharkia Province, Egypt. The collected parasites were rinsed several times with 0.65% saline solution. Some were mounted as a whole and prepared as permanent slides for investigation and identification. The remaining flukes were kept in 70% ethyl alcohol at -20°C for DNA extraction.

Genomic DNA extraction

Genomic DNAs were isolated on a small scale from 1ml of adult worms using multisource genomic DNA, Mini-Prep Kit, Axgene Biotechnology, U.S.A Cat. No.110420-25, according to manufacture manual.

RAPD analysis

Primers for RAPD were tested in parasite specimens and eight of them were selected due to successful amplification for two specimens. Names and sequences of primers are as shown in table (1).

Table (1): RAPD primers

Name	Sequence
OPA-10	GTGATCGCAG
OPB-O3	CATCCCCCTG
OPA-14	GCTGGTCTGT
OPB-19	ACCCCCGAAG
OPC-01	TTCGAGCCAG
OPC-13	AAGCCTCGTC
OPD-01	ACCGCGAAGG
OPD-13	GGGGTGACGA

PCR analysis was performed in 25 μl volume containing 2.5 mM MgCl₂, 0.2 mM of dNTPS, 20 μM primer, 50 ng genomic DNA and 1.0 unit Taq DNA polymerase (Bioren, Germany). All reactions were performed in a Perkin Elmer 2400 Thermal cycler. RAPD program was performed as 1 cycle of 94°C for 4 min (primary denaturation), 40 cycles of 94°C for 1 min (denaturation), then 35°C for 1 min. (annealing), 72°C for 1 min (extension) and a final extension step of 72°C for 10 min.

Detection of PCR products

The products of both RAPD based PCR analyses were detected using agarose gel electrophoresis (1.2% in 1X TBE buffer), stained with ethidium bromide (0.3 $\mu\text{g}/\text{ml}$), visually examined with UV transilluminator and photographed using a CCD camera (UVP, UK).

Data analysis

Clear, unambiguous and reproducible bands recovered through different techniques were considered for scoring. Each band was considered as a single locus. Data were scored as '1' for the presence and '0' for the absence of a given DNA band. Band size was estimated by comparing it with 1-kb ladder (Invitrogen, USA) using Totallab, TL120 1D v2009 (nonlinear Dynamics Ltd, USA).

3. Results

Parasitic genomic DNA extracted from *C. polycantha* recovered from two different hosts, *S. senegalensis* and *C. livia domestica* was amplified using 8 primers provided distinct patterns. The RAPD profiles of the two parasites with every primer are shown in figure 1 and table 2. The analysis of RAPD profiles indicated the presence of genetic variation between the two specimens as there

was considerable variation in the RAPD profiles among them using on the basis of number and intensity of bands. The 8 primers selected produced clearly distinguishable band patterns and yielded a total of 133 scoreable RAPD fragments. The 133 bands ranged between 143 and 1367 bp (base pair) in length by comparison with a 1-kb ladder. The number of bands generated by every primer, number of polymorphic bands and number of bands of the two specimens are shown in table 2. The higher number of bands was generated by primer B19 and A14, amplifying the two specimens. The parasitic specimen preparation from *S. senegalensis* produced a higher number of DNA fragments (69 DNA fragments) than that from specimen 2 from *C. livia domestica* (64 DNA fragments) as shown in table 2.

All primers except primer C13 generated specific DNA fragments markers for the both two specimens or one of them. The total

number of unique markers was 25 [15 for (1) and 10 for (2)] as shown in Fig. 1 and table 2.

All primers produced 54 monomorphic bands for the two specimens (1 and 2), while polymorphic ones without unique bands were negative (0) (table 3). All primers produced unique bands and polymorphic with unique (25). The total number of bands was (79) and the highest percentage of polymorphism was (63.63) as shown in (table 3 and Fig. 1).

Seven primers produced DNA unique bands for two specimens.

Primer A10 produced seven unique bands 352, 362, 536, 628, 653, 717 and 968 bp, primers B03 and A14 produced one unique band for each of 672 and 816 bp respectively. Primer B19 produced six bands, 347, 373, 411, 829, 1168 and 1367 bp. Primers C01 and D01 produced three unique bands for each (272, 383 and 1256 bp) and 299, 364 and 1003 bp, respectively. Primer D13 produced four unique bands 143, 254, 343 and 932 bp.

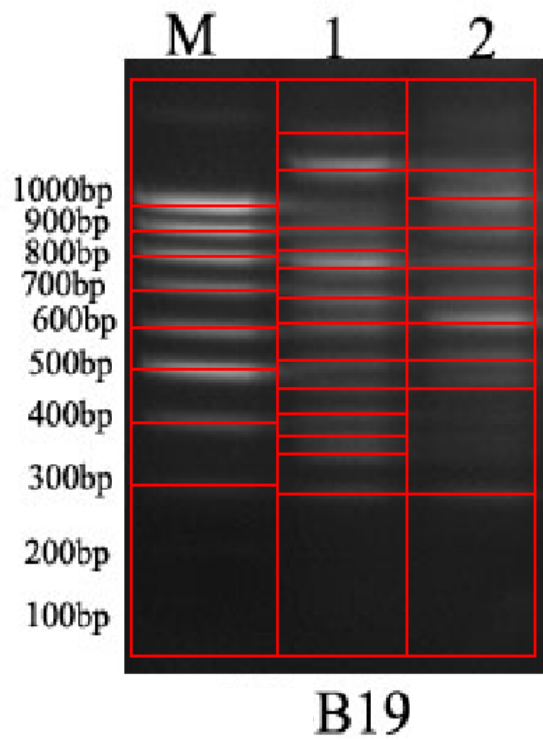
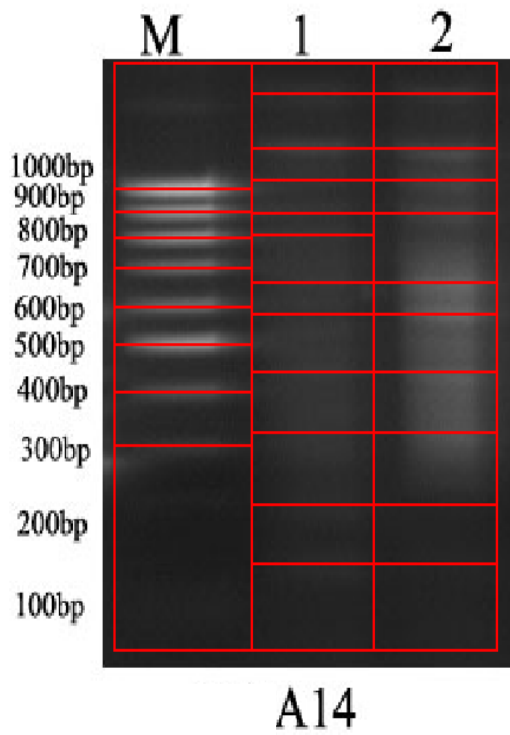
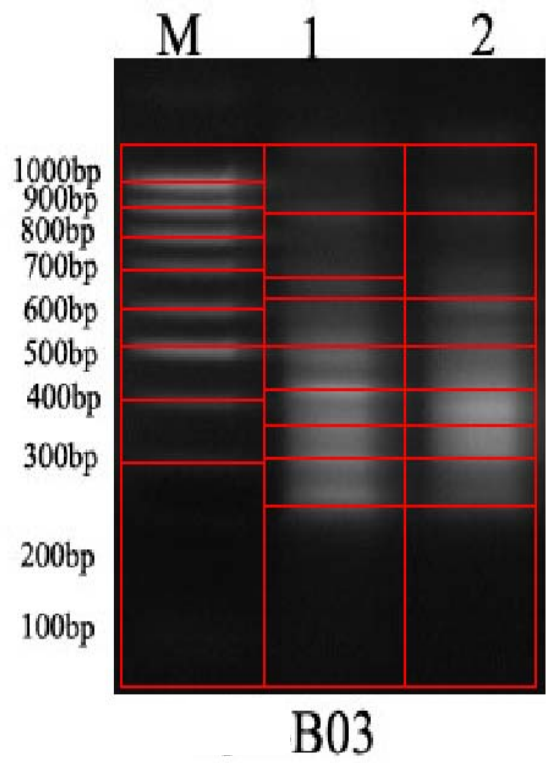
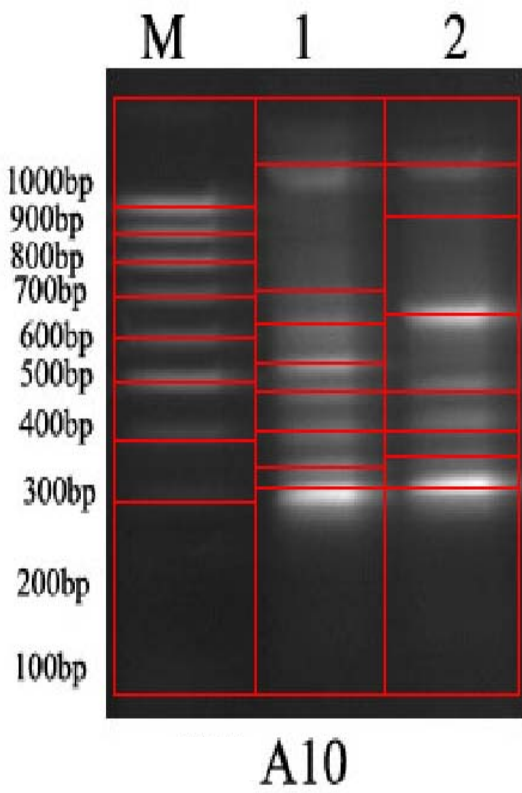
Table (2): Number of amplified fragments marker of *C. polycantha* from two specimens based on RAPD-PCR analysis

<i>C. polycantha</i> from		RAPD Primers								Total
		A10	B03	A14	B19	Col	C13	D01	D13	
<i>S. senegalensis</i> (1)	AF	8	8	11	13	7	7	9	6	69
	SM	4	1	1	5	1	0	3	0	15
<i>C. livia domestica</i> (2)	AF	7	7	10	9	8	7	6	10	64
	SM	3	0	0	1	2	0	0	4	10
Total TSM		7	1	1	6	3	0	3	4	25
Total TAF		15	15	21	22	15	14	15	16	133

AF: amplified fragment; SM: marker including either the presence or absence of a band; TAF: total amplified fragment; TSM: total number of specific marker across a each specimen.

Table (3): Polymorphism data for 8 primers using Gel Images for the two specimens

Gel image \ Primers	A 10	B 03	A14	B19	Col	C13	D 01	D13	Total
	Monomorphic bands	4	7	10	8	6	7	6	6
Polymorphic (without unique)	0	0	0	0	0	0	0	0	0
Unique bands	7	1	1	6	3	0	3	4	25
Polymorphic (with unique)	7	1	1	6	3	0	3	4	25
Total number of bands	11	8	11	14	9	7	9	10	79
Polymorphism %	63.63	12.5	9.09	42.86	33.33	0%	33.33	40.0	33.53



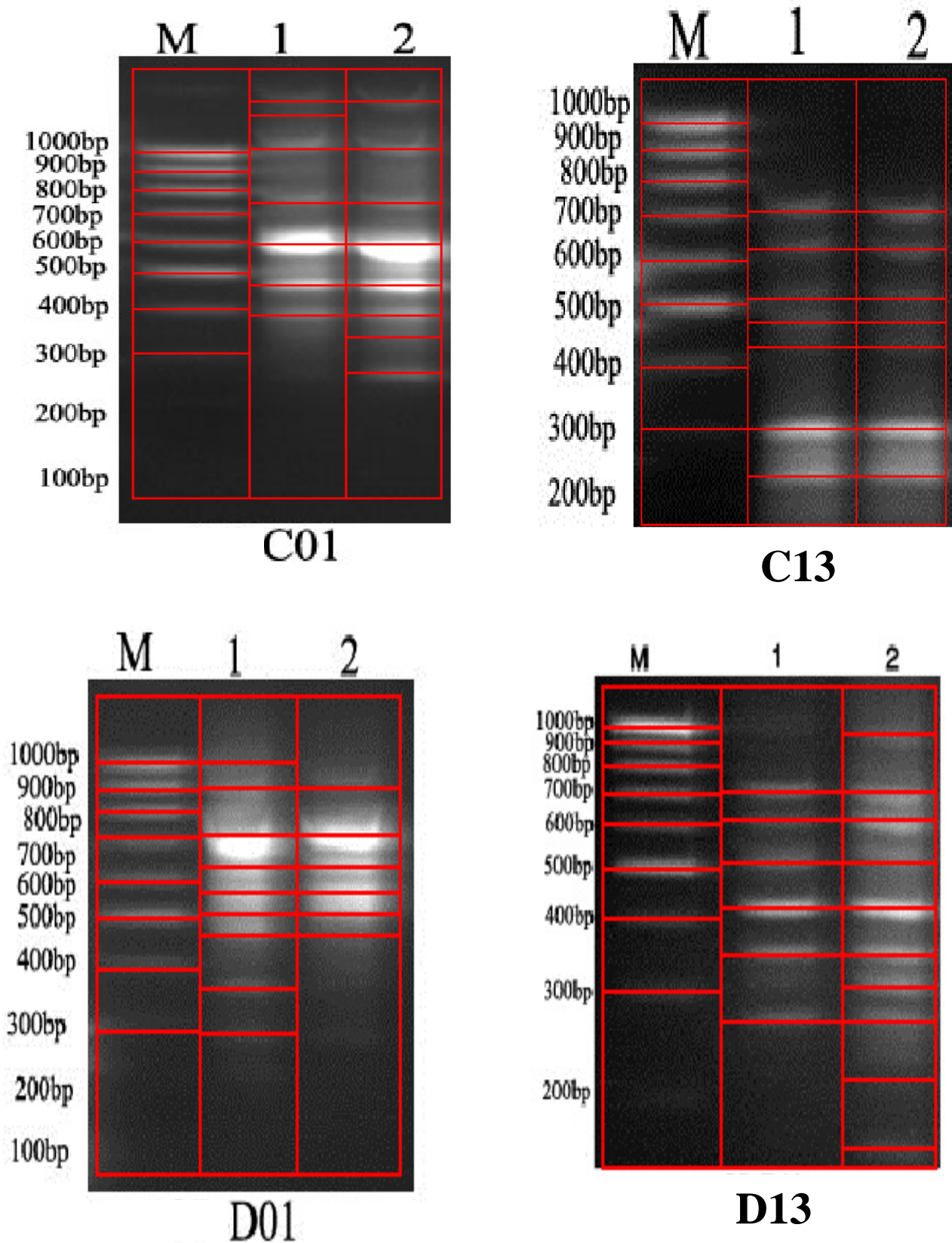


Fig. (1): Agarose gel electrophoresis showing the RAPD profiles of *C. polycantha* infecting doves, *S. senegalensis* (1) and pigeons, *C. livia domestica* (2) generated by 8 primers. 1-kb DNA ladder.

4. Discussion

The taxonomy of different species of cestodes represents insufficiently solved task and the reliable identification of many taxa by classic taxonomic methods is problematic. This is particularly the case for soft bodies animals such as cestodes. However, detailed studies of morphological and genetic variation of different cestode groups have been performed using morphological, biometrical, cytogenetic and isoenzyme approaches (Kralová and Spakulová, 1996; Eom *et al.*, 2002; Maravilla *et al.*, 2003).

However, recent advances in molecular biology, in particular the amplification of specific DNA regions via the polymerase chain reaction (PCR) and the improvement of direct deoxy sequencing techniques may allow to distinguish closely related species by comparing their DNA (Coote, 1990; Erlich *et al.*, 1991; Barker, 1994; McManus and Bowles, 1996 and Mostafa *et al.*, 2003).

Previous studies on molecular phylogenetic analysis using CO1 and 28S rDNA proposed a phylogenetic relationship and the position of 3 taxa, *Taenia solium*, *T. saginata* and *T. asiatica* (Queiroz and Alkire, 1998) suggested that *T. saginata* and *T. asiatica* represent one host-colonization, whereas *T. solium* represents another independent colonization event. This conclusion is further supported by cladistic analysis employing morphological characters in which *T. saginata* and *T. asiatica* were sister species and distantly related to *T. solium* (Hoberg *et al.*, 2001).

Polymerase chain reaction (PCR)-based molecular techniques, such as random amplified polymorphic DNA (RAPD), have been used for differential diagnosis of species and strains and to gain knowledge of the genetic diversity in parasite populations (Bandi *et al.*, 1993; Kaukas *et al.*, 1994; Tighe *et al.*, 1994; Kralová and Spakulová, 1996; Brouwer *et al.*, 2001; Eom *et al.*, 2002).

Simpson *et al.* (1993) proved that RAPD-PCR is undoubtedly a powerful approach for the analysis of genetic variation and identification of genetic markers. So, RAPD is of particular value in the study of the genetic variation of cestodes. The amplified products can be broadly classified into variables (polymorphic) and contents (monomorphic) which can be used as diagnostic markers (Hadrys *et al.*, 1992). The RAPD-PCR was applied to discriminate between three cestode parasites infecting domesticated birds, *Railletina vinagoi*, *Cotugnia polycantha* infecting pigeons and *R. sinensis* infecting chicken (Taha *et al.*, 2006).

Ahmed and Abdel-Moaty (2011) found that *Cotugnia polycantha* infecting doves, *Streptopelia senegalensis* differed from *C. polycantha* infecting pigeons, *Columba livia domestica*, by the ultrastructure of spermatozoa which is considered as a new tool for identification.

In the present study, the (RAPD-PCR) confirm that *C. polycantha* infecting doves, *S. senegalensis*, differ from *C. polycantha* infecting pigeons *C. livia domestica*.

So, *C. polycantha* infecting doves could be named *C. polycantha streptopeli* and *C. polycantha* infecting pigeons, *C. polycantha columbi*.

Conclusion

The members of some genera or some species of cestode parasites may exist as a number of phenotypes and genotypes that are closely similar and can not be recognized morphologically, but can be, identified using molecular assays.

The RAPD-PCR technique has proved to be a reliable technique in detecting intra-specific genetic variation between closely similar and closely related parasitic members of the same species.

Acknowledgement

The author wishes to thank deeply Prof. Dr. Khaled Soliman. Department of Genetics, Faculty of Agriculture, Ain-Shams University, Egypt, for processing parasitic samples for DNA extraction, DNA amplification, and gel electrophoresis and for his support in (RAPD-PCR) analysis.

Corresponding author

Sabry E. Ahmed

Department of Zoology, Faculty of Science, Zagazig University
drsabryahmed11@gmail.com

References

- Ahmed, S.E. and Abd El-Moaty, S.M. (2011): Comparative ultrastructural study of spermatozoa of *Cotugnia polycantha* (Cestoda, Cyclophyllidae, Davaineidae), the intestinal parasites of pigeons (*Columba livia domestica*) and doves (*Streptopelia senegalensis*) from Egypt. Journal of American Science. Vol.7(12): 1016-1024.
- Aldemir, O.S. (2006): Differentiation of cattle and sheep originated *Fasciola hepatica* by RAPD-PCR. Revue Méd. Vét., 157(2):65-67.
- Bandi, C.; La Rosa, G.; Bardin, M.G.; Damiani, G.; de Carneri, I. and Pozio, E. (1993): Arbitrary primed polymerase chain reaction of individual *Trichinella* specimens. J.Parasitol., 79: 437-440.
- Barker, R.H. (1994): Use of PCR in field.Parasitol. Today, 10:117-119.
- Brooks, D. R; Hoberg, E. P. and Week, P. J. (1991). Preliminary phylogenetic systematic analysis of major lineages of Eucestoda (Platyhelminthes: *Cercomeria*). Proc. Biol. Soc. Washington, 104: 561-668
- Brouwer, K. C. P.; Ndhlovu, A. Maunatsi, and Shiff, C. (2001): Genetic diversity of a population of *Schistosoma haematobium* derived from school children in East Central Zimbabwe. J. Parasitol., 78: 762-769.
- Coote, U.G. (1990): Amplification of nucleic acids by the Polymerase Chain Reaction. Article, 4:57-59.
- Eom, K. S., H. K. Jeon, Y. Kong, U. W. Hwang, X. Li, L. Xu, Z. Feng, Z. S. Pawlowski, and Rix, H. J.

- (2002): Identification of *Taenia asiatica* in China: Molecular, morphological, and epidemiological analysis of a Luzhai isolate. *Parasitol.*, 88: 758–764.
- Erlich, H.A.; Gelfand, D. and Sninsky, J.J. (1991): Recent advances in the Polymerase Chain Reaction. *Science*, 252:1643-1651.
- Gasser, R.B. (2005): Molecular tools-advances, opportunities and prospects. *Vet. Parasitol.*, 136: 69-89.
- Hadrys, H.M.; Balick, M. and Schierwater, B. (1992). Applications of random amplified polymorphic DNA (RAPD) in molecular ecology. *Mol. Ecology*, 1: 55-63.
- Hedrick, P. (1992). Shooting the RAPDs. *Nature*, 355: 679-680.
- Heckerroth, A.R. and Tenter, A.M. (1999): Development and validation of 6 species-specific nested PCR for diagnosis of acute Sarcocystosis in sheep. *Int. J. Parasitol.*, 29: 1331-1349.
- Hoberg, E. P., Alkire, N. L., DE Queiroz, A. & Jones, A. (2001): Out of Africa: origins of the *Taenia* tapeworms in humans. *Proc. Roy. Soc. London, B*, 268: 781-787.
- Hoberg, E.P.; Mariaux, J.; Justine, J. L.; Brooks, D.R. and Weeks, P.J.(1997): Phylogeny of the orders of the Eucestoda (Cercarioromorphae) based on comparative morphology: Historical perspectives and a new working hypothesis. *J. Parasitol.*, 83: 1128-1147.
- Justine, J.L. (1998): Spermatozoa as phylogenetic characters for the Eucestoda. *J. Parasitol.*, 84(2): 385-408.
- Kaukas, A.E.; Neto, E.D.; Simpson, A.J.; Southgate, V.R. and RoHinson, D. (1994): A phylogenetic analysis of *Schistosoma haematobium* group species based on randomly amplified polymorphic DNA. *Int. J. Parasitol.*, 24: 285-290.
- Král'ová, I. and Spakulova, M. (1996): Intraspecific variability of *Proteocephalus exiguus* La Rue, 1911 (Cestoda: Proteocephalidae) as studied by the random amplified polymorphic DNA method. *Parasitol. Res.*, 82(6): 542-54.
- Kramer, F. and Schnieder, T. (1998): Sequence heterogeneity in a repetitive DNA element of *Fasciola*. *Int. J. Parasitol.*, 28: 1923-1929.
- Mas-Coma, S.; Bargues, M.D. and Valero, M.A. (2005): Fasciolosis and other plantborne trematode zoonoses. *Int. J. Parasitol.*, 35:1255-78.
- Maravilla, P.; Souza, V.; Valera, A.; Romero-Valdovinos, M.; Loez-Vidal, Y.; Dorniguez-Alpizar, J.L.; Ambrosio, S.; Kawa, S. and Fusser A. (2003): Detection of genetic variation in *Taenia solium*. *J. Parasitol.*, 89(6): 1250-1254.
- Mariaux, J. (1996): Cestode systematics: Any progress? *Int. J. Parasitol.*, 26: 231-243.
- Mc Manus, D. and Bowles, J. (1996): Molecular genetic approaches to parasite identification: their value in diagnostic parasitology and systematics. *Int. J. Parasitol.*, 26: 687-704.
- Meshgi, B.; Karimi, A. and Shayan, P. (2008): Genetic variation of *Fasciola hepatica* from sheep, cattle and buffalo. *Res. J. Parasitol.*, 3(2) 71-78.
- Mohammadzadeh, T.; Sadjjadi, S.M.; Motazedian, M.H. and Mowdavi, G.R. (2007): Study on the genomic diversity of *Hymenolepis nana* between rat and mouse isolates by RAPD-PCR. *Iran. J. Vet. Res.*, 8(1): 16-22.
- Mostafa, O.M.; Taha, H.A. and Ramadan, G. (2003): Diagnosis of *Fasciola gigantica* in snail using the polymerase chain reaction (PCR) assay. *J. Egypt. Soc. Parasitol.*, 33:733-742.
- Nuchprayoon, S.; Jupnee, A. and Poovorawan Y. (2007): Random Amplified polymorphic DNA (RAPD) for differentiation between Thai and Myanmar strains of *Wuchereria bancrofti*. *Filaria J.*, 6(6): 4-8.
- Queiroz, A., and Alkire, N. L. (1998): The phylogenetic placement of *Taenia* cestodes that parasitize humans: *J. Parasitol.*, 84: 379-383.
- Rognlie, M.; Dimke, K. and Knapp, S. (1994): Detection of *Fasciola hepatica* in infected intermediate hosts using RT-PCR. *J. Parasitol.*, 80, 748-755.
- Rokni, M.B.; Mirhendi, H.; Behnia, M.; Haranol, M.F. and Jalalizand, N. (2010): Molecular characterization of *Fasciola hepatica* isolates by RAPD – PCR and ribosomal ITS1 sequencing. *Iran. Red Crescent Med. J.*, 12(1): 27-32.
- Simpson, A.J.G.; Neto, E.D.; Steindel, M. et al. (1993): The use of RAPDs for the analysis of parasites. In: Penna, S.D.I.; Chakraborty, R.; Epplen, J.T. and Jeffreys, J. (eds.) "DNA Fingerprinting: State of Sciences". Boston, Birkhauser, p: 331-337.
- Sripalwit, P.; Wongsawad, C.; Wongsawad, P. and Anuntalabhochai, S. (2007): High annealing temperature – random amplified polymorphic DNA (HAT-RAPD) analysis of three Paromphistome flukes from Thailand. *Exp. Parasitol.*, 115: 98-102.
- Taha, H.A.; Mostafa, O.M.S. and Soliman M.I. (2006): Study of three cestode parasites infecting domesticated birds using RAPD-PCR analysis. *Egypt. J. Zool.*, 46: 1-10.
- Tighe, P.J.; Goyal, P.K.; Wilson, Z.A.; Wakelin, D. and Pritchard, I. (1994): Analysis of genetic variation in isolates of *Trichinella* using random amplified polymorphic DNA. *Mol. Biochem. Parasitol.*, 63: 175-178.
- Welsh, J. and McClelland, M. (1990): Fingerprinting genomes using PCR with arbitrary primers. *Nucleic Acids Res.*, 18:7213-7218.
- Williams, J.G.; Kubelik, A.R.; Livak, K.J.; Rafalski, J.A. and Tingey, S.V. (1990): DNA polymorphisms amplified by arbitrary primers are useful as genetic markers. *Nucleic Acids Res.*, 18:6531-6535
- Wongsawad, C. and Wongsawad, P. (2010): Molecular markers for identification of *Stellantchasmus falcatus* and a phylogenetic study using the HAT-PAPD method. *Korean J. Parasitol.*, 48(4): 303-307

Risk Factors for the Development of Ventilator – Associated Pneumonia in Critically-III Neonates

Mona Afify*, Salha AI-Zahrani* and Maha A Nouh**

Department of Biology and Microbiology, Science College for Girls, King Abd-Elaziz University* and Pediatrics
 Department, Royal Commission Hospital in Yunbu** - Kingdom of Saudi Arabia.

drmonaafify@hotmail.com

Abstract: Ventilator-associated pneumonia (VAP), viewed as an inevitable consequence of critical illness, is increasingly accepted as an avoidable adverse health care incident. Whereas morbidity and mortality from VAP is well-documented in adults, it is poorly studied in children. This investigation was conducted to determine characteristics and possible risk factors for VAP, in critically ill neonates admitted to the neonatal intensive care unit (NICU). According to clinical pulmonary infection score (CPIS), 33 neonates were selected as having VAP and 24 neonates who did not develop VAP were assigned as non-VAP group. All neonates were subjected to case history, clinical examination, ABG, chest X-ray, and laboratory investigations (CBC, serum albumin, serum CRP, and blood culture). Neonates with VAP were subjected to broncho-alveolar lavage (BAL) sampling. The BAL samples were subjected to macroscopic and microscopic examination, as well as quantitative cultures. Obtained results revealed that indications for mechanical ventilation (MV) included respiratory distress syndrome (RDS), congenital pneumonia, meconium aspiration syndrome (MAS), and hypoxic ischemic encephalopathy (HIE), with nonsignificant differences between VAP group and non-VAP group. VAP rates were significantly increased with decreased body weight and gestational age and with increased duration of NICU admission, duration of MV and use of invasive maneuvers. VAP was significantly associated with hypothermia, mucopurulent endotracheal tube (ETT) secretions, and radiological findings. The use of inotropes and corticosteroids was significantly noted among neonates with VAP than that among non-VAP neonates. Raised serum C-reactive protein (CRP), hypoalbuminemia and positive blood cultures were significantly associated with increased VAP rates. Cultures of BAL samples revealed *Klebsiella pneumoniae* (in 33%), *Pseudomonas aeruginosa* (in 21%), *Staphylococcus aureus* (in 15%), *Escherichia coli* (in 15%), *Pneumococci* (in 6%) and *Candida albicans* (in 9%). There was nonsignificant similarity in the type of organisms cultivated from either blood or BAL. In conclusion risk factors for the development of VAP include; 1) decreased body weight and gestational age, 2) increased duration of NICU admission, MV, and use of invasive maneuvers, 3) hypothermia, mucopurulent ETT secretions and the use of inotropes/ corticosteroids, 4) raised serum CRP, hypoalbuminemia and positive blood cultures and 5) nosocomial infection by *Klebsiella*, *Pseudomonas*, *Staph aureus*, *E coli* and *Candida*.

[Mona Afify, Salha AI-Zahrani and Maha A Nouh. **Risk Factors for the Development of Ventilator – Associated Pneumonia in Critically-III Neonates.** Life Science Journal. 2012;9(1):302-307] (ISSN:1097-8135). <http://www.lifesciencesite.com>. 43

Key words: nosocomial infection-neonatal pneumonia-mechanical ventilation.

1. Introduction

Nosocomial infections are a major cause of patient illness and death (Chen et al., 2005). Device-associated infections, such as catheter-associated urinary tract infections, and ventilator-associated pneumonia (VAP) pose the greatest threat to patient safety in intensive care units (ICUs), (Kwak et al., 2010). VAP is the most common nosocomial infection in general ICUs, and represents 31% of all ICU-acquired infections (Rello et al., 2002). It is also a leading cause of morbidity with rates of associated mortality ranging from 20% to 70% (Bouza et al., 2006).

Ventilator-associated pneumonia, the second most common healthcare-associated infection in pediatric intensive care units, accounts for 20% of nosocomial infections (Elward, 2003). Defined as pneumonia developing later than 48h after intubation

and initiation of mechanical ventilation (MV), VAP is associated with morbidity and mortality (Langley and Bradley, 2005). Significant morbidity is reported between 3.7 and 10.0 additional ventilation days in neonates and children, resulting in prolonged admission and hospital costs (Richardson et al., 2010).

An established relationship exists between VAP and aspiration of colonized oropharyngeal secretion, due to inadequate glottic closure around ETTs, especially in those nursed supine. Suctioning has also been implicated in VAP through direct contamination due to inadequate hand washing (Berdal et al., 2007). This work aimed to study characteristics and possible risk factors for the development of VAP, in critically ill neonates.

2. Patients and Methods:

The present study was carried at the NICU, during years 2010 to 2011, on 57 neonates who received MV, for more than 48h, because of different illnesses, Table 1.

Inclusion criteria:

A new radiographic infiltrate (> 24 h) or progressive infiltrates, 48h after initiation of ventilation till 48 h after extubation, with worsening of gas exchange, in the form of frequent desaturations, increased oxygen requirements, or increased ventilator demands and at least three of the following criteria:

1. Temperature instability of unknown etiology.
2. Increased respiratory secretions, or increased suctioning requirements.
3. Apnea, tachycardia, nasal flaring, with retraction of chest wall, wheezes or rales.
4. Bradycardia (<100 beats/ min) or tachycardia (> 170 beats/min).

The diagnosis of VAP was established, using the CPIS. A CPIS of more than six was associated with a high likelihood of pneumonia (Fartouidi et al., 2003).

Methods:

All neonates were subjected to the following:

1. Case history and clinical examination, including:
 - a) Vital signs and assessment of the gestational age, using modified Ballard scoring system. (Ballard et al., 1991)
 - b) Clinical evidence of sepsis and pneumonia, assessed with a sepsis score which included the following symptoms and signs; lethargy, diarrhea, vomiting, fever, jaundice, pyoderma, hypothermia, cyanosis, abdominal distention, seizures, conjunctivitis, significant apnea, tachypnea, and poor capillary refill. If the infant had 3 or more of the above signs and symptoms, septicemia was suggested (Tollner, 1982).
 - c) Determination of postnatal age at which VAP developed.
2. Laboratory evidences of sepsis on study entry:
 - a) Complete blood count (CBC) by counter apparatus.
 - b) Quantitative serum C-reactive protein (CRP) by turbidimetry (Sanata, 2001).
 - c) Blood culture on sulphonated broth media (Vandepitte, 1991).
3. Arterial blood gases (ABGs) and chest radiographs, done daily (or more frequently if indicated).
4. Non-bronchoscopic broncho-alveolar lavage (NB-BAL) sampling (Aly et al., 2008):

Neonates diagnosed as having VAP were subjected to NB-BAL procedure, for bacteriological confirmation of the clinical diagnosis.

Contraindications to the procedure included; high oxygenation requirement ($FiO_2 > 0.85$), pneumothorax, bradycardia, hypotension, and/or platelet count of $< 30.000/mm^3$.

A complete clinical examination and a chest radiograph were performed one hour after completion of sampling. Additional sedation was required if the baby was fighting the ventilator and FIO₂ was increased just before the procedure (pre-oxygenation). The baby was positioned supine with the head turned 90° to the left to ensure that the suction catheter is advanced down the trachea and enters the right main bronchus. The obtained fluid was then collected in the sterile mucous trap and sent to the microbiology laboratory, for:

- a) Macroscopic examination: The appearance of the specimen was described regarding volume, color, consistency and aspect.
- b) Microscopic examination: The number of white cells was estimated, using Gram stain.
- c) Qualitative cultures of BAL.

Statistical analysis:

Data were entered, checked and analyzed using Epi-info (2000). Data were expressed as mean \pm standard deviation ($X \pm SD$), in quantitative variables, number and percentage for qualitative variables. Values of $P < 0.05$ were considered statistically significant (Dean et al., 2000).

3. Results:

As shown in table (1), indications for MV, in all neonates included RDS (40%), congenital pneumonia (30%), MAS (17.5%) and HIE (12.3%), with nonsignificant differences between VAP group and non-VAP group, ($p=0.83$).

Table (2) presents the demographic characteristics of both study groups. The mean gestational age and body weight were significantly lower among neonates with VAP than that in neonates with non-VAP ($p = 0.04$ & 0.01 , respectively) with nonsignificant difference regarding sex ($p=0.75$). The mean duration in NICU and on MV were significantly higher among VAP group than that among non-VAP group of neonates ($p=0.03$ & 0.001 , respectively). Meanwhile, the use of invasive maneuvers (chest tubes/UVC) was significantly noted among the neonates with VAP ($p=0.001$).

As shown in table (3), hypothermia, mucopurulent ETT secretions, radiological findings with progressive infiltrates were significantly observed in neonates with VAP than that in non-VAP neonates ($p=0.04$, 0.001 and 0.001 , respectively). The use medications (inotropes and corticosteroids) was significantly noted among neonates with VAP than that among non-VAP

neonates (p=0.02 & 0.03, respectively), with nonsignificant differences, regarding the use of surfactant and antacids (p> 0.05).

Table (4) shows that there were significant differences between VAP and non-VAP groups regarding the mean serum CRP, serum albumin levels and positive blood cultures (p= 0.03, 0.02 & 0.018, respectively), with nonsignificant differences of other laboratory findings (p> 0.05). Positive blood cultures were detected in 49% (16/33) of neonates with VAP versus 29% (7/24) in neonates without VAP.

As shown in table (5), cultures of BAL obtained from 33 neonates with VAP revealed Gram negative organisms (*klebsiella pneumoniae*, *pseudomonas aeruginosa*, and *E.coli* in 23 (69.7%) neonates, Gram positive organisms (*staphylococcus aureus* and *pneumococci*) in 7 (21.2%) neonates, and *candida albicans* in 3 (9.1%) neonates. Cross tabulation and correlation between blood cultures and BAL cultures, among VAP neonates shows nonsignificant similarity in the type of organisms cultivated from either blood or BAL (P = 0.49).

Table (1) Indications of mechanical ventilation in 57 neonates admitted to NICU, presented as number (n) and percent (%)

	Total n = 57	Patients (VAP) n = 33	Control(non-VAP) n = 24	χ^2	P value
RDS	23 (40.4%)	13 (39.4%)	10 (41.7%)	0.86	0.83 (NS)
Congenital pneumonia	17 (29.8%)	9 (27.3%)	8 (33.3%)		
MAS	10 (17.5%)	7 (21.2%)	3 (12.5%)		
HIE	7 (12.3%)	4 (12.1%)	3 (12.5%)		

NICU: neonatal intensive care unit
 RDS: respiratory distress syndrome
 MAS: meconium aspiration syndrome.
 χ^2 : Chi²
 NS: nonsignificant
 HIE: hypoxic ischemic encephalopathy.

Table (2) Demographic characteristics of 33 neonates with VAP versus 24 neonates without VAP.

Characteristic (s)	VAP n = 33	Non-VAP n = 24	Test of significance	P- value
Gestational age (wks), X ±SD	33.6±3.2	35.7±1.6	"t" = 2.1	0.04 (S)
Body weight (g)	1500 ±870	2650±380	"t" = 24	0.01 (S)
Gender, n (%)			χ^2 = 0.1	0.75 (NS)
Males	18 (54.5%)	11 (45.8%)		
Females	15 (45.5%)	13 (54.2%)		
Mode of delivery, n (%)			χ^2 = 0.49	0.48 (NS)
NVD	19 (57.6%)	13 (54.1%)		
C/S	14 (42.4%)	11 (45.8%)		
Duration in NICU (days), X ±SD	10.9 ±5.2	8.4 ±2.0	"t" = 2.19	0.03 (S)
Duration on MV (days), X ±SD	6.3 ± 1.67	4.7 ± 1.1	"t" = 4.1	0.001(S)
Invasive maneuvers, n (%)			χ^2 = 14.56	0.001 (S)
Chest tubes	9 (27.3%)	2 (8.3%)		
UVC	25 (75.8%)	6 (25%)	χ^2 = 13.87	0.001 (S)

VAP: ventilator associated pneumonia
 wks: weeks
 S: significant
 C/S: cesarean section
 n: number
 X ±SD: mean ±standard deviation
 NS: nonsignificant
 NVD: normal vaginal delivery
 %: percentage
 χ^2 : Chi²
 g: gram
 UVC: umbilical vein catheter

Table (3) Clinical characteristics and medications of 33 neonates with VAP versus 24 neonates without VAP, presented as number (n) and percent (%)

Characteristic (s)	VAP n = 33	Non-VAP n = 24	χ^2	P- value
Hypothermia (temperature < 36.5°C)	19 (57.6%)	7 (29.1%)	1.26	0.04 (S)
Mucopurulent ETT secretions	24 (72.7%)	3 (12.5%)	21.4	0.001 (S)
Radiological findings	33 (100%)	- (-)	56.0	0.001 (S)
Medications:				
Inotropes (vasopressors)	29 (87.9%)	12 (50%)	6.32	0.02 (S)
Corticosteroids	13 (39.4%)	3 (12.5%)	4.37	0.03 (S)
Surfactant	6 (18.2%)	4 (16.6%)	0.02	0.88 (NS)
Antacids (H2 blocker)	27 (81.8%)	16 (66.7%)	3.5	0.06 (NS)

VAP: ventilator associated pneumonia
 ETT: endotracheal tube.
 χ^2 : Chi²

Table (4) Laboratory data of 33 neonates with VAP versus 24 neonates without VAP.

	VAP n = 33	Non- VAP n = 24	Test of significance	P- value
TLC (x10 ³ /mm ³), X±SD	19.1±7.8	16.55±3.4	"t" = 1.66	0.06 (NS)
Hb (g/dl), X ±SD	9.73±2.96	8.66±2.13	"t" = 1.57	0.11 (NS)
Platelet count (x10 ³ /mm ³), X±SD	148.7±61.2	185.7±89.4	"t" = 1.83	0.06 (NS)
C-reactive protein (mg/dl), X±SD	54.5±40.57	28.0±4.92	"t" = 1.18	0.03(S)
Serum albumin (g/dl), X±SD	2.6±0.53	3.06±0.49	"t" = 2.92	0.02 (S)
Blood culture, n (%)				
Sterile	17 (51.5%)	17 (70.8%)	$\chi^2 = 5.58$	0.018(S)
Positive	16 (48.5%)*	7 (29.2%)**		

VAP: ventilator-associated pneumonia. n: number χ^2 : Chi2 %: percent

X±SD: mean ± standard deviation mm³: cubic millimeter mg: milligram g: gram

dl: deciliter TLC: total leucocytic count.

*: *klebsiella pneumoniae* 5 (15.2%), *staph aureus* 4(12.1%), *pseudomonas aeruginosa* 3 (9.1%), *E-coli* 3(9.1%) and *candida albicans* 1 (3%).

** : *klebsiella pneumoniae* 2(8.3%), *staph aureus* 2(8.3%), *pseudomonas aeruginosa*, *E-coli* and *Candida albicans*, each in 1 neonate (4.2%).

Table (5) Cross correlation between blood cultures and BAL cultures among 33 VAP patients.

Blood culture	Organism	BAL culture						
		<i>Klebsiella pneumoniae</i>	<i>Candida albicans</i>	<i>Staph aureus</i>	<i>Pseudomonas aeruginosa</i>	Pneumococci	E-coli	total
No growth		7	2	3	4	0	1	17
<i>Klebsiella pneumoniae</i>		0	1	1	1	0	2	5
<i>Candida albicans</i>		1	0	0	0	0	0	1
<i>Staph aureus</i>		1	0	0	1	2	0	4
<i>Pseudomonas aeruginosa</i>		1	0	1	0	0	1	3
E – coli		1	0	0	1	0	1	3
Total		11	3	5	7	2	5	33

BAL: broncho-alveolar lavage

Pearson $\chi^2 = 4.39$

VAP: Ventilator-associated pneumonia

P-value = 0.49 (nonsignificant)

4. Discussion:

Mechanical ventilation (MV) is an essential feature of modern NICU care. Unfortunately, MV is associated with a substantial risk of VAP (Aly et al., 2008), which represents the second most common nosocomial infection among patients in ICU and has the highest mortality rate (Shalini et al., 2009; Rebmann and Linda, 2010).

Two important processes are thought to be involved in the pathogenesis of VAP; bacterial colonization of the aero-digestive tract and the aspiration of contaminated secretions into the lower airway. The ETT is thought to play a prominent role in the development of these processes, not only by introducing oropharyngeal contents into the airway at the time of ETT placement in the airway, but also by serving as a "bridge" for bacteria to travel from the oropharynx to the lower airway. In addition, there is increasing evidence showing that the biofilm formed on the ETT surface may serve as a reservoir from which bacteria are continuously seeded into the lower respiratory tree (Pacheco-Flower et al., 2004).

Defining the infective organism causing VAP increases the accuracy of the clinical and radiological

diagnosis. Hence, it helps modifying the initial antibiotics according to the culture and sensitivity tests and so preventing the emergence of resistant strains. Subsequently, the duration of ventilation, length of NICU stay and hospital expenses are markedly decreased. NB-BAL is used in neonates as it is a safe technique with few adverse effects (Koksal et al., 2006).

In the current study, CPIS was used for the diagnosis of VAP which is a diagnostic algorithm relying on easily available clinical, radiological and laboratory data in a weighted manner that makes it a reliable alternative for diagnosing VAP (Teixeria et al., 2007).

In this study, the demographic characteristics of neonates with and without VAP did not differ significantly as regard sex, diagnosis at admission and modes of delivery. Similar results were obtained by Duke (2005). On other hand, VAP rates were significantly increased with decreased body weight and decreased gestational age. Nearly similar results were reported by other studies (Petdachai, 2004; Chastre, 2005; Foglia et al., 2007). Furthermore, VAP was significantly associated with increased

duration of NICU admission, duration of MV and increased use of invasive maneuvers. Koksall et al (2006) stated that prolonged duration of MV generally increases the risk of infection due to exposure to other devices including nebulizers, humidifiers, and ventilator circuits. Meanwhile, the risk of VAP increases by 11% for every additional ventilator week (Apisarnthanarak, et al., 2003).

In this study, VAP was significantly associated with the presence of hypothermia, mucopurulent ETT secretions, radiological findings with progression of lung infiltrates, and use of inotropes and/or corticosteroids. Nearly similar results were obtained by Apisarnthanarak et al (2003), who reported that hypothermia and tachypnea are the most clinical symptoms associated with the development of VAP, and by Fischer et al (2000) who found that inotropic support is significantly more required in the VAP group. Furthermore, the use of corticosteroids is associated with the development of VAP (Foglia et al., 2007).

Out of the laboratory findings in our study neonates, increased mean serum CRP and hypoalbuminemia are significantly associated with the development of VAP. Failure of CRP levels to fall suggests infectious complication or ineffective or inappropriate treatment (Povoa et al., 2005). Alp et al (2004) stated that the inflammatory cascade leads to a common pathway, causing generalized increase in the vascular permeability (capillary leak syndrome), which leads to leakage of protein rich fluid into the interstitium. This appears to be the primary cause of hypoalbuminemia in sepsis.

In this study, microorganisms associated with blood stream infection in neonates with VAP, were *klebsiella pneumoniae* (15.2%), *staph aureus* (12.1%), *pseudomonas aeruginosa* (9.1%), *E-coli* (9.1%) and *candida albicans* in 3% of positive blood cultures. Meanwhile, blood culture was sterile in (51.5%) of neonates. NB-BAL cultures reported that gram negative bacteria were isolated from the majority of neonates with VAP (69.7%), with *klebsiella pneumoniae* predominating the positive cultures (33.3%). On the other hand, gram positive infection comprised (21.2%) of the total cultures, with *staph aureus* predominating the positive cultures, while *candida albicans* was positive in 9% of samples. Nearly similar results were reported by other studies (Koksall et al., 2006; Petdachai, 2004; Apisarnthanarak, et al., 2003). However, the reported species isolated differed from a study to another. This can be explained by the fact that the distribution of microorganisms differs from a NICU to another and also differs within same place from one period of time to another.

In this study, non of the studied neonates who developed VAP had the same organism that caused their blood stream infection. This is in agreement with other studies (Apisarnthanarak, et al., 2003; Yuan et al., 2007).

Infection preventionists play a key role in a hospital VAP prevention programme. Their role includes policy development, consultation on best practices, surveillance, risk assessment, education, communication, and facilitation of quality improvement projects to lower VAP rates in their facility (Rebmann & Linda, 2010).

Recommendations:

- 1) Strict training and supervision of infection control protocols, 2) suctioning guidelines should be strictly followed in the NICU, 3) the use of disposable ventilator circuits should be encouraged, and 4) unnecessary invasive procedures should be limited.

Corresponding Author:

Dr. Mona Afify

Department of Biology and Microbiology, Science College for Girls, King Abd-Elaziz University, Kingdom of Saudia Arabia.

E.mail: drmonaafify@hotmail.com

References:

1. **Chen Y.Y. Chou Y.C. and Chou P. (2005):** Impact of nosocomial infection on cost of illness and length of stay in intensive care units. *Infect Control Hosp Epidemiol*; 26: 281-287.
2. Kwak Y.G, Lee S.O. Kim H.Y, et al (2010): Risk factors for device –associated infection related to organizational characteristics of intensive care units: Findings from the Korean Nosocomial Infections Surveillance System. *J Hosp Infect*; 75: 195-199.
3. **Rello J. Ollendorf D.A. Oster G., et al. (2002):** Epidemiology and outcomes of ventilator-associated pneumonia in a large US database. *Chest*; 122: 2115-2121.
4. **Bouza E. Hortal J. Munoz P., et al. (2006):** Postoperative infections after major heart surgery and prevention of ventilator-associated pneumonia: a one-day European Prevalence Study (ESGNI-008). *J Hosp Infect*; 64: 224-230.
5. **Elward A.M. (2003):** Pediatric ventilator-associated pneumonia. *Pediatr Infect Dis J*; 22:445-446.
6. **Langley J.M. Bradley J.S. (2005):** Defining pneumonia in critically ill infants and children. *Pediatr Crit Care Med*; 6(suppl): S9-S13.
7. **Richardson M. Hines S. Dixon G. Highe L. Brierley J. (2010):** Establishing nurse-led ventilator-associated pneumonia surveillance in

- paediatric intensive care. *J Hosp Infect*; 75: 220-224.
8. **Berdal J.E., Bjornholt J., Blomfeidt A. Smith-Erichsen N. and Bukholm G. (2007):** Patterns and dynamics of airway colonization in mechanically-ventilated patients. *Clin Microbiol Infect*; 13: 476-480.
 9. **Fartouidi M., Maritupe B., Honore S., Ceri C., Zahar J.R. and Brun-Bussion C. (2003):** Diagnosing pneumonia during mechanical ventilation: the clinical pulmonary infection score revisited. *Am J Respir Crit Care Med*; 168: 173-179.
 10. **Ballard J.L., Khoury J.C. and Wedig K., et al. (1991):** New Ballard score, expanded to include extremely premature infants. *J Pediatr*; 119: 417-423.
 11. **Tollner U. (1982):** Early diagnosis of septicemia in the newborn. *Clinical studies and sepsis score. Eur J Paediatr*; 138 (4): 331-337.
 12. **Sanata C. (2001):** Cord blood levels of cytokines as predictors of early neonatal sepsis. *Acta Paediatrica*; 90: 1176-81.
 13. **Vandepitte J. (1991):** Basic laboratory procedures in clinical bacteriology. Geneva, World Health Organization, 1991.
 14. **Aly H., Badawy M., and El-Kholy A. (2008):** Randomized, controlled trial on tracheal colonization of ventilated infants: can gravity prevent ventilator-associated pneumonia? *Pediatrics*; 122(4): 770-774.
 15. **Dean A.G., Dean J.A., and Coulombier D., et al. (2000):** Epi-info (version 6.1): a word processing, database and statistical program for epidemiology and micro-computer office center of disease control Atlantia, Georgia USA.
 16. **Shalini T., Malik G., Amita J., and Neera K. (2009):** Study of ventilator-associated pneumonia in neonatal intensive care unit: characteristics, risk factors and outcome. *Intenet J Medical update*; 5(1): 12-19.
 17. **Rebmann T. and Linda R. Greene. (2010):** Preventing ventilator-associated pneumonia: an executive summary of the Association for Professionals in Infection Control and Epidemiology, Inc, Elimination Guide. *J Infect Control*, 38: 647-649.
 18. **Pacheco-Fowler V., Gaonkar T., Wyer P.C. and Modak S. (2004):** Antiseptic impregnated endotracheal tubes for the prevention of bacterial colonization. *J Hosp Infect*; 57: 170-174.
 19. **Koksal N., Hacimustafaoglu M., Celebi S. and Ozakin C. (2006):** Nonbronchoscopic bronchoalveolar lavage for diagnosis of ventilator associated pneumonia in newborn. *Turkish J Pediatrics*; 48: 213-220.
 20. **Teixeria P.J.Z., Seligman R., Hertz F.T., Cruz D.B. and Fachel J.M.G. (2007):** Inadequate treatment of ventilator-associated pneumonia: risk factors and impact on outcomes. *J Hosp Infect*; 65: 361-367.
 21. **Duke T. (2005):** Neonatal pneumonia in developing countries. *Arch Dis fetal Neonatal Ed*; 90: 211-219.
 22. **Petdachai W. (2004):** Ventilator associated pneumonia in newborn intensive care unit in Prachomklao Hospital Thailand. *Southeast Asian Trop Med Pub Health J*; 3:724-729.
 23. **Chastre J. (2005):** Conference summary: ventilator-associated pneumonia. *Respir Care*; 50 (7): 975-983.
 24. **Foglia E., Meier M. and Elward A. (2007):** Ventilator-associated pneumonia in pediatric and neonatal intensive care unit patients. *Clin Microbiol*; 20(3): 409-425.
 25. **Apisarnthanarak A., Hozmann – Pazgal G., Hamvas A. and Olsen M. (2003):** Ventilator associated pneumonia in extremely preterm neonates in neonatal intensive care unit: Characteristics, risk factors, outcomes. *Pediatrics*; 112: 1283-1289.
 26. **Fischer J.E., Ramser M. and Fanconi S. (2000):** Use of antibiotics in pediatric intensive care and potential savings. *Intens Care Med*; 26: 959-966.
 27. **Povoa P., Coelho L. and Almedia E. (2005):** C-reactive protein as a marker of infection in critically ill patients. *Clin Microbiol Infect*; 11:101-108.
 28. **Alp E., Guven M. and Yildiz O., et al (2004):** Incidence, risk factors and mortality of nosocomial pneumonia in intensive care units: a prospective study. *Annals Clin Microbiol Antimicrob*; 3:1-17.
 29. **Yuan T.M., Chen L.H. and Yu H.M. (2007)** Risk factors and outcomes for ventilator-associated pneumonia in neonatal intensive care unit patients. *J Perinat Med*; 35 (4): 334-338.

1/8/2012

Life Science Journal

(Acta Zhengzhou University Overseas Edition)

Call for Papers

The academic journal “*Life Science Journal*” (ISSN: 1097-8135) is inviting you to publish your papers.

Life Science Journal, the Acta Zhengzhou University Oversea Version registered in the United States, is an international journal with the purpose to enhance our natural and scientific knowledge dissemination in the world under the free publication principle. The journal is calling for papers from all who are associated with Zhengzhou University-home and abroad. Any valuable papers or reports that are related to life science-in their broadest sense-are welcome. Other academic articles that are less relevant but are of high quality will also be considered and published. Papers submitted could be reviews, objective descriptions, research reports, opinions/debates, news, letters, and other types of writings. Let's work together to disseminate our research results and our opinions.

Please send your manuscript to editor@sciencepub.net.

Address:

Life Science Journal - Acta Zhengzhou University Overseas Edition

Marsland Press

PO Box 180432, Richmond Hill, New York 11418, USA

Telephone: (347) 321-7172

Emails: editor@sciencepub.net; sciencepub@gmail.com; lifesciencej@gmail.com;

Website: <http://www.sciencepub.net>; <http://www.lifesciencesite.com>

Volume 9, Number 1, (Cumulative No.28) Part 2 March 25, 2012 ISSN:1097-8135

Life Science Journal

Marsland Press

PO Box 180432, Richmond Hill, New York 11418, USA

Website:
<http://www.sciencepub.net>

Emails:
editor@sciencepub.net
sciencepub@gmail.com

Phone: (347) 321-7172

Copyright © 2005-2012 Marsland Press / Zhengzhou University

